

Role of kynurenine on platelet's function and beyond

This research has been conducted at The School of Pharmacy and
Pharmaceutical Sciences, Trinity College Dublin, The University of Dublin as
fulfilment of philosophy degree in Pharmaceutical Sciences and Pharmacology

by

Nadhim Kamil Hante AL-Shiblawi

2020

Under the direction and supervision of

Supervisor: Dr. Maria J. Santos-Martinez

Co-supervisor: Dr.Lidia Tajber

Declaration

I declare that the work described here is entirely the candidate's own work

I declare that this thesis has not been submitted as an exercise for a degree at this or any other university and it is entirely my own work.

I agree to deposit this thesis in the University's open access institutional repository or allow the Library to do so on my behalf, subject to Irish Copyright Legislation and Trinity College Library conditions of use and acknowledgement.

I consent to the examiner retaining a copy of the thesis beyond the examining period, should they so wish (EU GDPR May 2018).

Nadhim Kamil Hante

To the Holly shrine of Imam Ali bin Abi-Talib in Najaf-Iraq.....

To the beloved ones whose bodies left this life, but their spirits are still filling it with love and hope.....

To my wife and children.....

To my father and mother; brothers and sisters.....

To all who support me throughout my life.....

Acknowledgements

First and foremost, I would like to extend a huge thank you to my supervisors Dr. Maria J. Santos Martinez and Dr. Lidia Tajber for the advices, support and encouragement. Dr. Maria Santos Martinez has a major role not only in my professional but also in my personal development throughout the last 4 years and without her help this project would not have been possible.

A very special thank you to Dr. John Gilmer, Dr. Carlos Medina, Dr. Richard Porter, Dr. Vanesa Martinez and Dr. Ali Al-Tamimi (School of Pharmacy RCSI). Your knowledge, advice and support were always invaluable and greatly appreciated.

In addition, I'd like to thank my colleagues and postdocs lab members past and present Vanesa Martinez, Sadbh O'Neil, Caoimhe Clerkin, Melissa Daly, Maria Pigott, Michelle Lowry, Mohammedali Selo, Carmen Coll Merino, Luiza Dos Santos, Mariadelva Catalano, Jessie Santoro, Niamh McNamee, Johannes Sake, Róisín Daly, Anindya Mukhopadhyaya and Dimitrios Tsiapalis for their friendship and making the work environment very enjoyable.

Huge thanks to Helen Thornbury from the Dean of Graduate Studies office in Trinity College Dublin for her help and support.

Special thanks and gratefulness to all blood donors as without their contributions, this work would not have been done and huge thanks to the technical and working staff in the School of Pharmacy, Trinity College Dublin especially Brian Talbot who are always available for help.

Deep thanks to the Dean's Research Initiatives Fund to Dr. Maria Santos and the Ministry of Higher Education (MoHER) in Iraq and the Iraqi Cultural Attache' in London, especially Dr. Hassan Al-Alak and the current counsellor of Iraqi Cultural

Attache' in London Proffessor Nahi Al-Rikabi, for their support and funding this project.

Finally, Deep thanks to the staff in the Iraqi cultural attache' in London especially Mr. Ali Al-Rubae for their help and support along the past 4 years

Abbreviations

12-HETE	12-hydroxy eicosatetraenoic acid
5-HT _{2A}	Hydroxytryptamine 2A
6-MCDF	6-methoxy-1,3,8-trichlorodibenzofuran
AA	Arachidonic acid
AC	Adenylyl cyclase
ADP	Adenosine diphosphate
AhR	Aryl hydrocarbon receptor
AML	Acute myeloid leukemia
α -NF	Alpha-naphthoflavone
Arnt	AhR nuclear translocator
bFGF	Basic fibroblast growth factor
BSA	Bovine serum albumin
Btk	Bruton tyrosine kinase
C.media	Conditioned media
cAMP	Cyclic adenosine monophosphate
cGMP	Cyclic guanosine monophosphate
COX	Cyclooxygenase enzyme
cPLA ₂	Cytosolic phospholipase A ₂
c-src	Cytosolic src-family kinase
DAC	Diacyl glycerol
DCs	Dendritic cells
DMSO	Dimethyl sulfoxide
DREs	Dioxin-responsive elements
DVT	Deep venous thrombosis
EGF	Endothelial growth factor
eNOS	Endothelial nitric oxide synthase

ERK	Extracellular stimuli-responsive kinase
FBS	Fetal bovine albumin
FcR γ	Fc receptor gamma signaling chain
FGF-2	Fibroblast growth factor-2
FICZ	6-formylindolo [3, 2-b] carbazole
FITC	Fluorescein isothiocyanate
GAS	IFN- γ activation sequence
GP	Glycoprotein
GPCR	G-protein coupled receptor
GTP	Guanosine 5'-triphosphate
HMBG1	High-mobility group box 1
HPLC	High performance liquid chromatography
IDO	Indoleamine 2,3-dioxygenase
IDO-1	Indolamine dioxygenase-1
IFN- γ	Interferón-gamma
iNOS	Inducible nitric oxide synthase
IP ₃	Inositol triphosphate
IP-R	Prostacyclin receptor
ISRE	Interferon-stimulated response element
ITAM	immunoreceptor tyrosine activation motif
JAK	Janus kinase
JNK	c-Jun NH ₂ -terminal kinase
LDH	Lactate dehydrogenase
L-NAME	L-N ^G -Nitroarginine methyl ester
LOD	Limit of detection
LOQ	Limit of quantification

LTA	Light Transmission aggregometer
MAPK	Mitogen activated protein kinase
MMP	Matrix metalloproteinases
MNF	3'-methoxy-4'-nitroflavone
NAD	Nicotinamide adenine dinucleotide
NK cells	Natural killer cells
NO	Nitric oxide
NSCLC	Non-small-cell lung cancer
ODQ	1H-[1,2,4] oxadiazolo [4,3-a]quinoxalin-1-on
PBS	Phosphate buffer saline
PBST	Phosphate buffer saline-tween
PDE	Phosphodiesterase enzyme
PDGF	Platelet derived growth factor
PE	Phycoerythrin
PGH ₂	Prostaglandin H ₂
PI3K	Phosphatidylinositide 3-kinase
PKA	cAMP-dependent protein kinase
PKC	Protein kinase C
PKG	cGMP-dependent protein kinases
PLC	Phospholipase C
PLC β	Phospholipase C β
PLC γ 2	Phospholipase C gamma
PLT-4	Platelet factor-4
PRP	Platelet rich plasma
PSGL-1	P-selectin glycoprotein ligand-1
PVDF	Immunoblot polyvinylidene fluoride
RDS	Relative standard deviation
RIAM	Rap1-GTP-interacting adaptor molecule

ROS	Reactive oxygen species
Rp-8-pCPT-cGMP	Para-Chlorophenylthioguanosine- 3', 5'- cyclic monophosphate
Rp-cAMP	Adenosine- 3', 5'- cyclic monophosphorothioate, Rp- isomer
SCLC	Small-cell lung cancer cell lines
SFKs	Src family kinases
sGC	soluble guanylyl cyclase
SNAP	S-Nitroso-N-acetyl-DL-penicillamine
STAT1	Signal transducer and activator of transcription 1
TBS	Tris-buffered saline
TCDD	Tetrachlorodibenzo-p-dioxin
TCIPA	Tumour cell-induced platelet aggregation
TDO	Tryptophan 2,3-dioxygenase
TF	Tissue factor
TGF- β 1	Transforming growth factor- β 1
TIMP-4	Tissue inhibitor of metalloproteinase-4
TLR4	Toll-like receptor 4
TMF	Trimethoxyflavone
TPH	Tryptophan hydroxylase enzyme
Treg	Regulatory T cells
TRPC6	Transient receptor potential channel
TSP1	Thrombospondin-1
TXA2	Thromboxane A2
TXS	Thromboxane synthase
VASP	Vasodilator stimulated phosphoprotein
VEGF	Vascular endothelial growth factor
VTE	Venous thromboembolism
Vwf	Von Willebrand factor
WP	Washed platelets

Summary

Kynurenine is a metabolite of the amino acid tryptophan by the action of the tryptophan dioxygenase enzyme in the liver and the ubiquitous indolamine dioxygenase enzyme in other tissues. Although it has been shown that kynurenine participates in different processes involving the central nervous-, immune- and cardiovascular- systems, its effect on platelet function has not been yet investigated. In this study, it is shown for the first time that kynurenine inhibits collagen-, adenosine diphosphate-, thromboxane- and arachidonic acid- induced platelet aggregation. The mechanism by which kynurenine modulates platelet function involves the activation of the adenylyl cyclase (AC) enzyme and of the reduced and oxidized heme forms of the soluble guanylyl cyclase (sGC) enzyme. Activation of those enzymes leads to an increase of cyclic guanosine monophosphate (cGMP) and cyclic adenosine monophosphate (cAMP) respectively. Kynurenine phosphorylates the vasodilator stimulated phosphoprotein (VASP) by cAMP- and cGMP-dependent protein kinases. VASP participates in cytoskeleton redistribution during platelet shape change and in GPIIb/IIIa activation. Kynurenine may represent a natural endothelial derived inhibitor of platelet aggregation that can activate both, adenylyl cyclase and guanylyl cyclase. Kynurenine may activate the soluble guanylyl cyclase enzyme when the enzyme is refractory to NO and therefore may represent a physiological back up system for NO and a new therapeutic approach in pathological conditions where oxidative stress inactivates platelet response to NO. In fact, studying the binding site of kynurenine to both forms of soluble guanylyl cyclase may open the door for the development of novel therapeutic compounds that could activate both forms of the enzyme.

Having found that kynurenine have the ability to inhibit platelet aggregation induced by collagen, ADP, the thromboxane analogue U46619 and arachidonic acid. The effect of kynurenine on platelet function resulted to be cGMP and cAMP dependent, meaning that the effect of this tryptophan metabolite can be linked with most of the major pathways involved in platelet aggregation. Those findings, together with the already known participation of kynurenine in cancer biology, led us to investigate its potential effect on TCIPA. TCIPA refers to the

ability of cancer cells to aggregate platelets and constitutes a crucial step during cancer cell invasion, angiogenesis and during the development of metastatic foci. It has been shown that tumour cell lines differ in their capability to induce platelet aggregation and that the mechanism by which TCIPA takes place can also vary from one cell line to another.

Kynurenine (100-500 μM) significantly inhibited TCIPA induced by A549, Hela, HT-29, SW-480 and HCC-1954 cells. However, the amount of kynurenine produced by the different cell lines *in vitro* did not justify and did not correlate with the differences in their capability to induce platelet aggregation.

Pharmacological modulation of kynurenine generation by the induction and/or inhibition of the indoleamine 2,3-di-oxygenase (IDO) enzyme in HCC-1954 and A549 cells (the most and the least potent cell line inducing TCIPA) did not modify their potency towards TCIPA indicating that, at the induced concentrations, kynurenine was not able to inhibit this interaction.

A new approach preparing platelets suspension using conditioned media to look at platelet function was also investigated. The ability of platelets re-suspended in conditioned media from A549 cells, to aggregate in the presence of collagen, HCC-1954 and A549 cells was found to be significantly reduced when compared to platelets re-suspended in fresh media. On the other hand, when platelets suspensions were prepared in HCC-1954 conditioned media, platelets aggregated spontaneously in the absence of any stimuli.

This research demonstrates, for the first time, that 1) kynurenine is able to inhibit platelet aggregation induced by a wide range of cancer cell lines although at higher concentrations than the ones produced by the cells *in vitro* conditions 2) conditioned media from tumour cell lines that have the ability to aggregate platelets, and therefore to induce TCIPA, can exert opposite effects on platelet function. This novel approach has the potential to provide a better insight for looking at the effect of cell derived mediators that could inhibit or induce platelet aggregation within the tumour microenvironment and deserves more attention and to be further investigated.

Table of Contents

Role of kynurenine on platelet's function and beyond.....	1
Declaration	2
Acknowledgements.....	i
Abbreviations	iii
Summary	vii
1. Introduction	21
1.1. Blood platelets	21
1.1.1. Platelet Adhesion	22
1.1.2. Platelet activation	22
1.1.3. Platelet aggregation.....	28
1.2. L-Tryptophan metabolism.....	31
1.3. Kynurenine and NO; the potential platelet connection.....	36
1.4. Blood platelets and cancer.....	37
1.5. Mechanisms involved in tumour cell-induced platelet aggregation and cancer progression.....	38
1.5.1. Platelet receptors	38
1.5.2. Tumour cells and platelets released mediators	40
1.6. Pharmacological modulation of tumour cell-induced platelet aggregation....	44
1.7. Involvement of kynurenine in cancer biology.....	47
2. Aims of the project	49
3. Materials and Methods	50
3.1. Reagents.....	50
3.2. Blood Collection	50
3.3. Cell culture	51
3.4. Light Transmission Aggregometry (LTA)	52
3.5. Cytotoxicity assay.....	54
3.6. Optical microscopy.....	54
3.7. Immunoblotting	55
3.7.1. Sample preparation	55
3.7.2. Protein quantification	55
3.7.3. Electrophoresis	56

3.7.4.	Protein expression detection	56
3.8.	Flow cytometry.....	57
3.9.	Intraplatelet cGMP and cAMP measurement	58
3.10.	HPLC	59
3.10.1.	Kynurenine measurements	59
3.10.2.	Tryptophan measurements	62
3.11.	Statistical analysis	63
4.	Results and discussion	64
4.1.	Effect of kynurenine on platelet function	64
4.1.1.	Thromboxane analogue (U46619)	64
4.1.2.	Arachidonic acid	66
4.1.3.	Adenosine diphosphate (ADP)	68
4.1.4.	Serotonin	69
4.1.5.	Collagen	71
4.1.6.	Effect of kynurenine on the expression of platelet receptors	73
4.2.	Potential mechanisms of action of kynurenine on human platelets	75
4.2.1.	Kynurenine and the aryl hydrocarbon receptor.	75
4.2.2.	Effect of FICZ on collagen-induced platelet aggregation	76
4.2.3.	Effect of TCDD on collagen-induced platelet aggregation	77
4.2.4.	Effect of TMF on collagen-induced platelet aggregation.....	78
4.2.5.	Effect of FICZ and TCDD on ADP-induced platelet aggregation.....	79
4.2.6.	The effect of TMF on ADP-induced platelet aggregation	82
4.2.7.	Effect of kynurenine in PRP pre-incubated with TMF in the presence of collagen or ADP	85
4.2.8.	Effect of FICZ and TCDD preincubated with kynurenine in PRP stimulated with collagen or ADP.....	87
4.3.	Does Kynurenine act through a platelet surface receptor or intraplatelet compartment?.....	89
4.4.	Kynurenine platelet uptake study	91
4.5.	Potential relationship between nitric oxide and kynurenine.....	93
4.5.1.	Our first hypothesis.....	93
4.5.2.	Effect of kynurenine on L-NAME treated platelets.....	95
4.5.3.	Effect of Kynurenine on platelet's soluble guanylyl cyclase	96
4.5.4.	Effect of ODQ on platelet expression of GPIIb/IIIa and P-selectin.....	97
4.5.5.	updated hypothesis.....	102
4.5.6.	Activation of platelet sGC.....	103

Effect on intraplatelet cGMP	103
4.5.7. Activation of platelet adenylyl cyclase	106
Effect on intraplatelet cAMP	106
4.5.8. Phosphorylation of VASP by kynurenine	107
4.5.9. Effect of sGC inhibitor and PKG inhibitor on Kynurenine VASP phosphorylation	238
4.5.10. Effect of AC and PKA inhibitors on Kynurenine induced VASP phosphorylation at serine 157.	110
4.6. Pharmacological modulation of kynurenine on collagen-induced platelet aggregation-by PKG and PKA inhibitors.	116
4.6.1. Pharmacological modulation of adenylyl cyclase- cAMP- protein kinase A pathway.	116
4.6.2. Pharmacological modulation of guanylyl cyclase- cGMP- protein Kinase G pathway.	117
4.7. Soluble guanylyl cyclase enzyme activators and stimulators	119
4.7.1. Kynurenine pharmacophores and their potential effect on soluble guanylyl cyclase	119
4.7.2. Effect on platelet cGMP concentration	122
4.7.3. Pharmacological effect	123
4.8. Role of kynurenine in TCIPA.....	126
4.8.1. Tumour cell-induced platelet aggregation (TCIPA) study.....	126
4.8.2. Effect of kynurenine on TCIPA	133
4.8.3. Kynurenine – Lag phase relationship.....	164
4.8.4. Pharmacological modulation of Kynurenine production and its effect on TCIPA	171
4.8.5. Effect of the pharmacological manipulation of IDO on HCC-1954 and A549 on TCIPA.....	191
4.8.6. Effect of conditioned media on TCIPA.....	197
4.8.7. Effect of media pH on platelet aggregation.....	207
5. Conclusions	210
Appendix 1- Reagents	214
Appendix-2 Electrophoresis gel preparation reagents	217
6. References	219

List of figures

<i>Figure 1-1: Signalling pathway of collagen, von willebrand and integrins induced platelet aggregation</i>	24
<i>Figure 1-2: G-protein coupled receptors activation pathways</i>	26
<i>Figure 1-3: Tryptophan metabolic pathway</i>	31
<i>Figure 1-4: Aryl hydrocarbon receptor(AhR) genomic pathway</i>	35
<i>Figure 1-5: Aryl hydrocarbon receptor (AhR) non-genomic pathway</i>	36
<i>Figure 1-6: Common agents used to control TCIPA in experimental models</i>	47
<i>Figure 3-1: Schematic illustration of light transmission aggregometry</i>	53
<i>Figure 3-2: Standard curve for measuring kynurenine concentrations by HPLC</i>	60
<i>Figure 3-3: Linear regression relationship of Tryptophan concentrations and the mean peak area</i>	62
<i>Figure 4-1: Effect of kynurenine on thromboxane analogue (U46619) induced platelet aggregation</i>	65
<i>Figure 4-2: Effect of kynurenine on thromboxane analogue (U46619) induced platelet aggregation</i>	65
<i>Figure 4-3: Effect of kynurenine on arachidonic acid- induced platelet aggregation</i>	66
<i>Figure 4-4: Effect of Kynurenine on arachidonic acid induced platelet aggregation</i>	67
<i>Figure 4-5: Effect of kynurenine on ADP- induced platelet aggregation</i>	68
<i>Figure 4-6: Effect of Kynurenine on ADP- induced platelet aggregation</i>	69
<i>Figure 4-7: Effect of serotonin on platelet aggregation</i>	70
<i>Figure 4-8: Effect of kynurenine on collagen- induced platelet aggregation</i>	71
<i>Figure 4-9: Micrographs from optical microscopy showing the effect of kynurenine on platelet aggregation induced by collagen</i>	72
<i>Figure 4-10: Effect of kynurenine on collagen- induced platelet aggregation</i>	72
<i>Figure 4-11: Representative gates from flow cytometry showing the effect of kynurenine on platelet expression of GPIIb/IIIa and P-selectin</i>	74
<i>Figure 4-12: Effect of kynurenine on platelet expression of GPIIb/IIIa and P-selectin by flow cytometry</i>	74

<i>Figure 4-13: Immunoblotting showing the expression of AhR receptor in platelets</i>	76
<i>Figure 4-14: Effect of FICZ on collagen-induced platelet aggregation</i>	77
<i>Figure 4-15: Statistical analysis of the effect of TCDD on collagen-induced platelet aggregation</i>	78
<i>Figure 4-16: Effect of TMF on collagen-induced platelet aggregation</i>	78
<i>Figure 4-17: Statistical analysis of the effect of FICZ and TCDD on ADP-induced platelet aggregation</i>	80
<i>Figure 4-18: Statistical analysis of the effect of incubation over-time of FICZ and TCDD on ADP-induced platelet aggregation</i>	81
<i>Figure 4-19: Statistical analysis of the effect of DMSO on ADP- induced platelet aggregation</i>	82
<i>Figure 4-20: Effect of TMF on ADP-induced platelet aggregation</i>	83
<i>Figure 4-21: Statistical analysis of the effect of incubation overtime of DMSO (vehicle) and TMF with platelet rich plasma in ADP-induced platelet aggregation</i>	84
<i>Figure 4-22: Light transmission aggregometry traces showing the effect of 2 minutes incubation time of TMF (10μM) and DMSO on ADP- (10μM) induced platelet aggregation. TMF 10μM inhibited platelet aggregation in the presence of ADP when compared to DMSO</i>	84
<i>Figure 4-23: Effect of collagen and ADP on platelets preincubated with TMF 10μM and Kynurenine</i>	86
<i>Figure 4-24: Effect of TCDD and FICZ on the inhibitory effect of Kynurenine in collagen and ADP induced- platelet aggregation</i>	87
<i>Figure 4-25: Cytotoxicity assay.Effect of Kynurenine, FICZ, TMF, TCDD and DMSO on platelets</i>	88
<i>Figure 4-26:Statistical analysis of the effect of collagen on washed platelets (WP) prepared from kynurenine treated platelet rich plasma (PRP)</i>	90
<i>Figure 4-27: Representative traces from light transmission aggregometry showing the effect of BCH 25mM on the inhibition of collagen induced platelet aggregation by kynurenine</i>	92
<i>Figure 4-28: Effect of BCH on kynurenine inhibitory effect</i>	92
<i>Figure 4-29: Proposed relationship between nitric oxide and kynurenine</i>	94
<i>Figure 4-30 : Effect of kynurenine on L-NAME treated platelets collagen</i>	96

Figure 4-31: Effect of Kynurenine on ODQ treated platelets _____	97
Figure 4-32: Effect of ODQ on platelet's expression of activated GPIIb/IIIa and P-Selectin _____	98
Figure 4-33: Representative gates from flow cytometry showing the effect of ODQ on collagen induced platelet aggregation in the presence of kynurenine _____	99
Figure 4-34: Soluble guanylyl/guanylate cyclase (sGC) domain structure _____	100
Figure 4-35: Activation of soluble guanylyl cyclase by nitric oxide and BAY58-2667 _____	101
Figure 4-36: Updated proposed relationship between nitric oxide and Kynurenine _____	102
Figure 4-37: Downstream of soluble guanylyl cyclase enzyme (sGC) _____	103
Figure 4-38: Effect of kynurenine on intraplatelet cGMP when sGC in the reduced heme form _____	104
Figure 4-39: Effect of kynurenine on intraplatelet cGMP when sGC in the oxidised heme form _____	105
Figure 4-40: Activation of reduced and oxidised heme moiety of sGC by kynurenine _____	105
Figure 4-41: Effect of kynurenine on intraplatelet cAMP _____	106
Figure 4-42: VASP phosphorylation (at serine 238) by Kynurenine _____	108
Figure 4-43: Effect of Kynurenine on platelet VASP (at serine 157) phosphorylation _____	108
Figure 4-44: Effect of Kynurenine vehicle (DMSO) on VASP phosphorylation _____	109
Figure 4-45: Diagram showing soluble guanylyl cyclase (sGC) inhibitor (ODQ) and adenylyl cyclase (AC) inhibitor (SQ 22536) enzymes ; and the correspondent protein kinases inhibitors (RP-8-Pcpt-cGMP) and (Rp-cAMP) _____	110
Figure 4-46: Effect of ODQ and cGMP inhibitor on SNAP and Kynurenine induced VASP phosphorylation at serine 238 _____	111
Figure 4-47: Effect of adenylyl cyclase inhibitor and cAMP inhibitor on Forskolin and Kynurenine induced VASP phosphorylation at serine 157 _____	113
Figure 4-48: Mechanism of action of Kynurenine on platelet aggregation _____	115
Figure 4-49: Pharmacological modulation of Kynurenine activation of platelet's adenylyl cyclase and protein kinase A in collagen induced platelet aggregation _____	117
Figure 4-50: Effect of PKG inhibitor on Kynurenine in collagen- induced platelet aggregation _____	118
Figure 4-51: Structures of common soluble guanylyl enzyme activators and stimulators. _____	120

<i>Figure 4-52: Chemical structure of compounds that have structural and metabolic relationship with kynurenine</i>	121
<i>Figure 4-53: Effect of compounds structurally or metabolically related to kynurenine on intraplatelet cGMP</i>	123
<i>Figure 4-54: Effect of picolinic acid, quinaldic acid, melatonin and kynuramine on collagen induced platelet aggregation</i>	124
<i>Figure 4-55: Representative traces from LTA showing the effect of picolinic acid, quinaldic acid, melatonin and kynuramine on collagen induced platelet aggregation in PRP</i>	125
<i>Figure 4-56: Effect of cell number on tumour cell-induced platelet aggregation (TCIPA) by different cell lines</i>	128
<i>Figure 4-57: Effect of cell number on lag phase of tumour cell-induced platelet aggregation (TCIPA) by different cell lines</i>	129
<i>Figure 4-58: Representative traces from light transmission aggregometer showing the differences in the lag phase of A549-induced platelet aggregation</i>	130
<i>Figure 4-59: Representative traces from light transmission aggregometer showing the variation in lag phase of TCIPA induced by HT-29 cells when various number of cells were used</i>	130
<i>Figure 4-60: Representative traces from light transmission aggregometer showing the difference in lag phase but not in maximal platelet aggregation induced by HT-29 cells when various number of cells were tested</i>	131
<i>Figure 4-61: Representative traces from light transmission aggregometer showing the short lag phase of TCIPA induced by various cell number of SW-480 colon cancer cells</i>	132
<i>Figure 4-62: Representative traces from light transmission aggregometer showing the potency of HCC-1954 inducing platelet aggregation regardless of cell number used</i>	132
<i>Figure 4-63: Statistical analysis showing the differences in the duration of the lag phase induced by 1000 cells for the different cell lines</i>	133
<i>Figure 4-64: Effect of Kynurenine on tumour cell-induced platelet aggregation (TCIPA) by A549 lung carcinoma cells</i>	135
<i>Figure 4-65: Effect of Kynurenine on lag phase duration induced by A549</i>	136

<i>Figure 4-66: Representative traces from light transmission aggregometer showing the effect of kynurenine on maximal aggregation and lag phase of A549-induced platelet aggregation.</i>	136
<i>Figure 4-67: Effect of Vehicle (DMSO) on A549 induced platelet aggregation</i>	137
<i>Figure 4-68: Potential mechanism of TCIPA by A549</i>	138
<i>Figure 4-69: Effect of kynurenine on A549-induced platelet expression of activated GPIIb/IIIa and P-selectin</i>	139
<i>Figure 4-70: Representative gates from flow cytometry showing the effect of kynurenine on A549-induced platelet expression of GPIIb/IIIa activated (PAC 1) and P-selectin</i>	139
<i>Figure 4-71: Effect of Kynurenine on HeLa cells-induced platelet aggregation</i>	141
<i>Figure 4-72: Effect of kynurenine on lag phase of HeLa -induced platelet aggregation</i>	142
<i>Figure 4-73: Effect of vehicle (DMSO) on TCIPA induced by HeLa cells</i>	142
<i>Figure 4-74: Representative traces from light transmission aggregometer showing the effect of kynurenine on maximal aggregation and lag phase induced by HeLa cells</i>	143
<i>Figure 4-75: Hela cells induced TCIPA</i>	144
<i>Figure 4-76: Effect of kynurenine on HT-29 cells-induced platelet aggregation</i>	146
<i>Figure 4-77: Representative micrographs showing the effect of kynurenine on TCIPA by 10000 HT-29 cells</i>	147
<i>Figure 4-78: Effect of kynurenine on the duration of the lag phase of HT-29 induced platelet aggregation</i>	147
<i>Figure 4-79: Representative traces from light transmission aggregometer showing the effect of kynurenine on HeLa cells induced platelet aggregation</i>	148
<i>Figure 4-80: Effect of the vehicle (DMSO) on TCIPA by HT-29</i>	148
<i>Figure 4-81: Mechanism of HT-29 cells induced platelet aggregation</i>	149
<i>Figure 4-82: Effect of kynurenine on SW-480-induced platelet aggregation</i>	151
<i>Figure 4-83 : Effect of kynurenine on lag phase during SW-480induced platelet aggregation</i>	152
<i>Figure 4-84: Representative traces from light transmission aggregometer showing the effect of kynurenine on SW-480 cells induced platelet aggregation</i>	153
<i>Figure 4-85: Effect of vehicle (DMSO) on TCIPA by SW-480</i>	153

<i>Figure 4-86: Mechanism of SW-480 induced TCIPA</i>	154
<i>Figure 4-87: Effect of Kynurenine on HCC-1954 cells induced platelet aggregation</i>	156
<i>Figure 4-88: Representative traces from the light transmission aggregometer showing the concentration dependent inhibitory effect of kynurenine on TCIPA induced by HCC-1954 cells</i>	157
<i>Figure 4-89: : Representative micrographs showing the effect of Kynurenine on HCC-1954 induced platelet aggregation</i>	157
<i>Figure 4-90: Effect of Kynurenine on Lag time of HCC-1954 induced platelet aggregation</i>	158
<i>Figure 4-91: Effect of Vehicle (DMSO) on SW-480 TCIPA</i>	159
<i>Figure 4-92: Mechanism of HCC-1954 induced TCIPA</i>	160
<i>Figure 4-93: Effect of kynurenine on platelet expression of GPIIb/IIIa and P-selectin during TCIPA induced by HCC-1954</i>	161
<i>Figure 4-94: Representative gates from flow cytometry showing the effect of kynurenine on platelet expression of GPIIb/IIIa activated (PAC1) and P-selectin</i>	162
<i>Figure 4-95: Platelet pathways controlled by kynurenine</i>	163
<i>Figure 4-96: Basal concentration of kynurenine produced by the different cell lines as measured by HPLC</i>	165
<i>Figure 4-97: Traces from HPLC showing the area under the curve and peak height of kynurenine produced by each cell line in conditioned media after 48 hours of incubation.</i>	166
<i>Figure 4-98: Traces from HPLC showing the area under the curve and peak height of the remaining concentration of tryptophan in the in conditioned media of A549, HELA, HT-29, SW-480 and HCC-1954 after 48 hours of incubation with FBS free media.</i>	167
<i>Figure 4-99: Relationship between kynurenine produced by each cell lines and their lag phase</i>	168
<i>Figure 4-100: Effect of platelets on kynurenine production and tryptophan consumption in A549 cells</i>	169
<i>Figure 4-101: Effect of platelets on kynurenine production and tryptophan consumption in HCC-1954 cells</i>	170
<i>Figure 4-102: Induction of IDO and kynurenine production by A549 cells</i>	172

<i>Figure 4-103: Representative HPLC traces showing the area under the curve and peak height of kynurenine in conditioned media from A549 cells incubated with epacadostat 1μM or IFN-γ (50-400 ng/mL)</i>	173
<i>Figure 4-104: Representative HPLC traces showing the area under the curve and peak height of tryptophan measured in conditioned media from A549 cells after inhibition or induction of indoleamine dioxygenase-2 with epacadostat 1 μM or IFN-γ</i>	174
<i>Figure 4-105: Induction of IDO and kynurenine production in HCC-1954 cells</i>	175
<i>Figure 4-106: Representative HPLC traces showing the area under the curve and peak height of kynurenine produced in conditioned media by HCC-1954 cells incubated with epacadostat 1 μM or IFN-γ (50-400 ng/mL) for 48 hours</i>	176
<i>Figure 4-107: Representative HPLC traces showing the area under the curve and peak height of tryptophan in conditioned media following incubation of HCC-1954 cells with epacadostat 1 μM or IFN-γ (50-400 ng/mL)</i>	177
<i>Figure 4-108: Induction of IDO and kynurenine production in SW-480 cells</i>	178
<i>Figure 4-109: Representative HPLC traces showing the area under the curve and peak height of kynurenine produced by SW-480 cells in conditioned media after incubation with Epacadostat 1 μM or IFN-γ (50-400 ng/mL)</i>	179
<i>Figure 4-110: Representative HPLC traces showing the area under the curve and peak height of tryptophan in conditioned media from SW-480 cells incubated with epacadostat 1μM or IFN-γ (50-400 ng/mL)</i>	180
<i>Figure 4-111: Effect of Epacadostat on kynurenine production and tryptophan consumption in IFN-γ treated A549 cells</i>	182
<i>Figure 4-112: HPLC traces showing the effect of epacadostat 1 μM on kynurenine production by A549 cells incubated with IFN-γ (50-400 ng/mL).</i>	183
<i>Figure 4-113: HPLC traces showing the effect of epacadostat 1μM on tryptophan in conditioned media from A549 cells treated with IFN-γ (50-400ng/mL)</i>	184
<i>Figure 4-114: Effect of Epacadostat on kynurenine production and tryptophan consumption in IFN-γ treated HCC-1954 cells</i>	185
<i>Figure 4-115: HPLC traces showing the effect of epacadostat 1μM kynurenine production by HCC-1954 cells incubated with IFN-γ (50-400 ng/mL).</i>	186
<i>Figure 4-116: HPLC traces showing the effect of epacadostat 1μM on tryptophan in conditioned media from HCC-1954 cells treated with IFN-γ (50-400ng/mL)</i>	187

<i>Figure 4-117: Effect of epacadostat on kynurenine production and tryptophan consumption in IFN-γ treated SW-180 cells</i>	188
<i>Figure 4-118: HPLC traces showing the effect of Epacadostat 1 μM on kynurenine production by SW-480 cells incubated with IFN-γ (50-400ng/mL)</i>	189
<i>Figure 4-119: HPLC traces showing the effect of epacadostat 1 μM on tryptophan in conditioned media from SW-180 cells treated with IFN-γ (50-400ng/mL)</i>	190
<i>Figure 4-120: Effect of A549 cells incubated with INF-γ on platelet aggregation</i>	192
<i>Figure 4-121: Representative traces from light transmission aggregometer showing the effect of IFN-γ on A549 TCIPA</i>	192
<i>Figure 4-122: Effect of epacadostat on IFN-γ incubated A549 TCIPA</i>	193
<i>Figure 4-123: Representative traces from light transmission aggregometer showing the effect of epacadostat on the increment in lag phase of A549 induced by IFN</i>	193
<i>Figure 4-124: Effect of L-NAME on TCIPA induced by IFN-γ incubated A549 cells</i>	196
<i>Figure 4-125: Representative traces from light transmission aggregometer showing the effect of L-NAME on the increment in lag phase of A549 induced by IFN-γ</i>	196
<i>Figure 4-126: Effect of conditioned media from A549 on TCIPA induced by HCC-1954</i>	199
<i>Figure 4-127: Representative traces from light transmission aggregometer showing the effect of A549 depleted conditioned media on 1000 HCC-1954 cells TCIPA</i>	199
<i>Figure 4-128: Effect of conditioned media from A549 on HCC-1954 induced platelet expression of GPIIb/IIIa and P-selectin</i>	200
<i>Figure 4-129: Representative gates from flow cytometry analysis for GPIIb/IIIa and P Selectin expression</i>	200
<i>Figure 4-130: Effect of conditioned media from A549 on TCIPA induced by A549.</i>	201
<i>Figure 4-131: Representative traces from light transmission aggregometer showing the effect of A549 depleted conditioned media on A549 cells TCIPA</i>	202
<i>Figure 4-132: Effect of conditioned media from A549 on A549 induced platelet expression of GPIIb/IIIa and P-selectin</i>	202
<i>Figure 4-133: Representative gates from flow cytometry showing the effect of A549 conditioned media on GPIIb/IIIa and P Selectin expression induced by A549 cells</i>	203
<i>Figure 4-134: Effect of conditioned media from A549 cells on collagen-induced platelet aggregation</i>	204

Figure 4-135: Representative traces from the light transmission aggregometer showing the effect of A549 conditioned media on collagen induced platelet aggregation ____ 205

Figure 4-136: Representative micrographs showing showing the effect of A549 conditioned media on collagen induced platelet aggregation _____ 205

Figure 4-137: Effect of collagen on platelet expression of GPIIb/IIIa and P-selectin of platelets suspended in A549 conditioned media _____ 206

Figure 4-138: Representative flow cytometry gates showing GPIIb/IIIa and P Selectin expression of platelets suspended in A549 conditioned media _____ 207

Figure 4-139: Effect of pH on collagen-induced platelet aggregation _____ 208

1. Introduction

1.1. Blood platelets

Platelets are small, 2 μm in size, discoid anucleated blood elements derived from megakaryocytes that play an important role in haemostasis and thrombosis [1]. Once platelets mature, they are viable from 7 to 10 days in the blood stream. If they are not consumed during haemostatic responses within this time, they undergo apoptosis and are cleared by the liver and the spleen [2]. The average blood count in healthy individuals ranges between 150,000 to 400,000 platelets/ μL [3].

Platelet's plasma membrane contains glycoproteins and integrins essential in critical steps during platelet-mediated haemostasis and thrombosis. In fact, Glycoproteins (GP) like GPIb-IX-V; GPVI or GPIIb-IIIa (also known as integrin $\alpha\text{IIb}\beta\text{3}$), and other receptors like protease-activated receptors (PAR), and P2Y receptors, are crucial for mediating platelet adhesion and aggregation [4, 5].

Platelets contain lysosomes, mitochondria, endoplasmic reticulum [3] and three types of granules in their cytoplasm:

- (i) Dense granules: rich in platelet agonists such as serotonin and adenosine diphosphate (ADP) that amplify platelet activation [6]
- (ii) α -granules: abundant in platelet receptors including GPIIb/IIIa and P-selectin and proteins that enhance the platelet activation process and coagulation [7]
- (iii) Lysosomal granules that mainly contain glycosidases and proteases [6]

Under physiological conditions, the shear stress in the blood vessel makes platelets to remain close to the endothelium [8], where the production of nitric oxide (NO), prostaglandin I_2 (PGI_2 or prostacyclin) and the ADP-ase CD39 enzyme are in charge of keeping them in an inactivated state [3]. However, at sites of vascular injury, immobilized adhesive proteins become exposed and platelets respond in three consecutive and integrated phases that involve adhesion, activation and platelet aggregation [9]

1.1.1. Platelet Adhesion

After vascular injury, platelets interact with the subendothelial extracellular matrix which contains adhesive macromolecules including collagen and von Willebrand factor (vWF) [9, 10].

At low shear stress, platelet adhesion involves the binding of platelet receptors to fibrillar collagen, fibronectin and laminin. Under high shear stress, the binding to the subendothelium is mediated primarily by the interaction of vWF with the GPIb/IX/V complex [11] required to decelerate platelets and to allow the collagen receptors to bind to collagen and to firmly adhere to the endothelial surface [9].

1.1.2. Platelet activation

Activation of platelets comprises multiple, complex and imbricated signalling processes (figures 1-1 and 1-2) that involve rearrangement of the platelet cytoskeleton, platelet shape change, granule secretion, mobilization of calcium and the recruitment of more platelets for the formation of the definitive platelet plug [12].

Briefly, platelet activation takes place mainly through:

(1) The interaction of the platelet agonists (thrombin, thromboxane A₂, ADP and serotonin), with their specific receptors and the subsequent receptor-mediated platelet activation signalling pathway.

(2) The confluence of the complex signalling network on common signalling pathways that involve activation of phospholipase C (PLC) and the subsequent formation of inositol trisphosphate (IP₃) and diacyl glycerol (DAG); increase of cytosolic Ca⁺² and protein kinase C (PKC), mitogen-activated protein kinase (MAPK) and Rap1 (critical mediator of integrin activation) activation.

(3) The activation of the integrin αIIbβ₃ (GPIIb-IIIa) by the 'inside-out' signalling pathways.

Platelets have two main collagen receptors, GPVI and GPIa/IIa. Activation of platelets by collagen requires the engagement of both receptors [13]. The GPIa/IIa receptor is responsible for the 'physical' attachment of platelets to the collagen fibrils. The GPVI is considered as a 'signalling molecule' as it is responsible for the activation of integrins, [14], PLCγ₂ and PLCβ₂ [15, 16], TXA₂ synthesis and granule secretion (Figure 1-1) [17].

The interaction of vWF with its receptor (GPIb-IX), induces an increase of intracellular cyclic guanosine monophosphate (cGMP) levels [18, 19] and, in turn, activation of cGMP-dependent protein kinase (PKG) and mitogen activated protein kinases (MAPKs) (figure 1-1) [18, 20, 21]. Although NO may be important for vWF- induced cGMP elevation [18, 19], a NO-independent soluble guanylyl cyclase (sGC) activation has also been proposed [22].

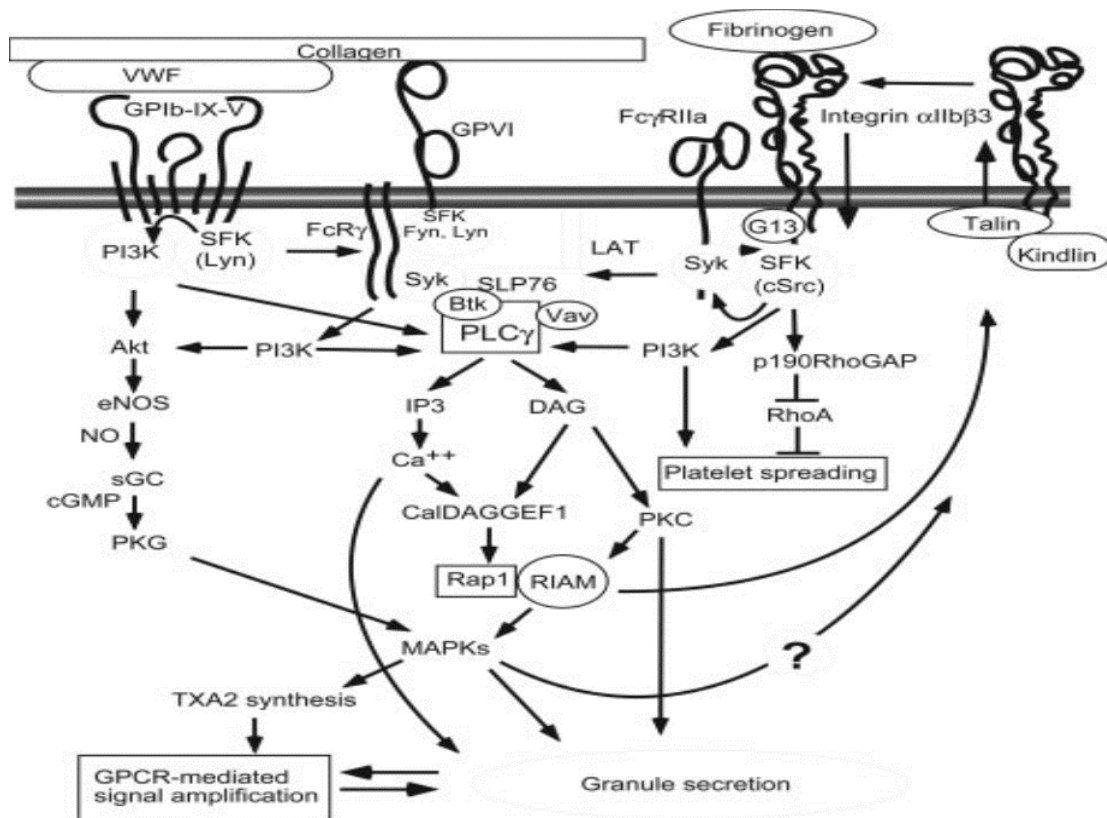


Figure 1-1: Signalling pathway of collagen, von Willebrand factor and integrin($\alpha_{IIb}\beta_3$) receptors.[12]

Activation of collagen and von Willebrand factor receptors initiates a cascade of events that culminate in granule secretion, thromboxane generation and inside out signalling pathway of platelet integrins which is triggered by Rap1 and MAPK through talin and kindlin. Integrin activation causes outside in signalling pathway leading to platelet spreading and activation. VWF: von Willebrand factor; GPIb-IX-V: glycoprotein GPIb-IX-V; PI3K: phosphatidylinositol-3 kinase; SFK: Src-family kinase (Lyn, Fyn), AKT: protein kinase B, eNOS: Endothelial nitric oxide synthase, NO: nitric oxide, sGC: soluble guanylyl cyclase, cGMP: Cyclic guanosine monophosphate, PKG: cGMP-dependent protein kinase, MAPKs: Mitogen activated protein kinases, TXA2: Thromboxane A2, SLP-76: Src homology (SH) 2 domain-containing leukocyte phosphoprotein of 76 kDa, BTK: tyrosine kinase, IP3: Inositol tri-phosphate, DAG: diacyl glycerol, CalDAGGEF1: Calcium and DAG-regulated guanine nucleotide exchange factor 1, Rap1 (a small guanosine triphosphatase), RIAM: Rap1-GTP-interacting adaptor molecule, VAV (guanine nucleotide exchange factor), cSrc: cytosolic src-family kinase, RhoGAP: Rho GTPase activating protein, PKC: protein kinase C, GPCR: G-protein coupled receptor, FcγRIIa: Fc receptor gamma

The recruitment of additional platelets is mediated by platelet agonists that are produced or released locally once some level of platelet activation, following platelet adhesion, has already occurred. All those mediators have in common that they act via G protein-coupled receptors (GPCRs) (figure 1- 2). In fact, through the activation of G protein-mediated signalling pathways, the generation and release of further mediators amplifies the initial signals to ensure the recruitment of more platelets into a growing thrombus [5]

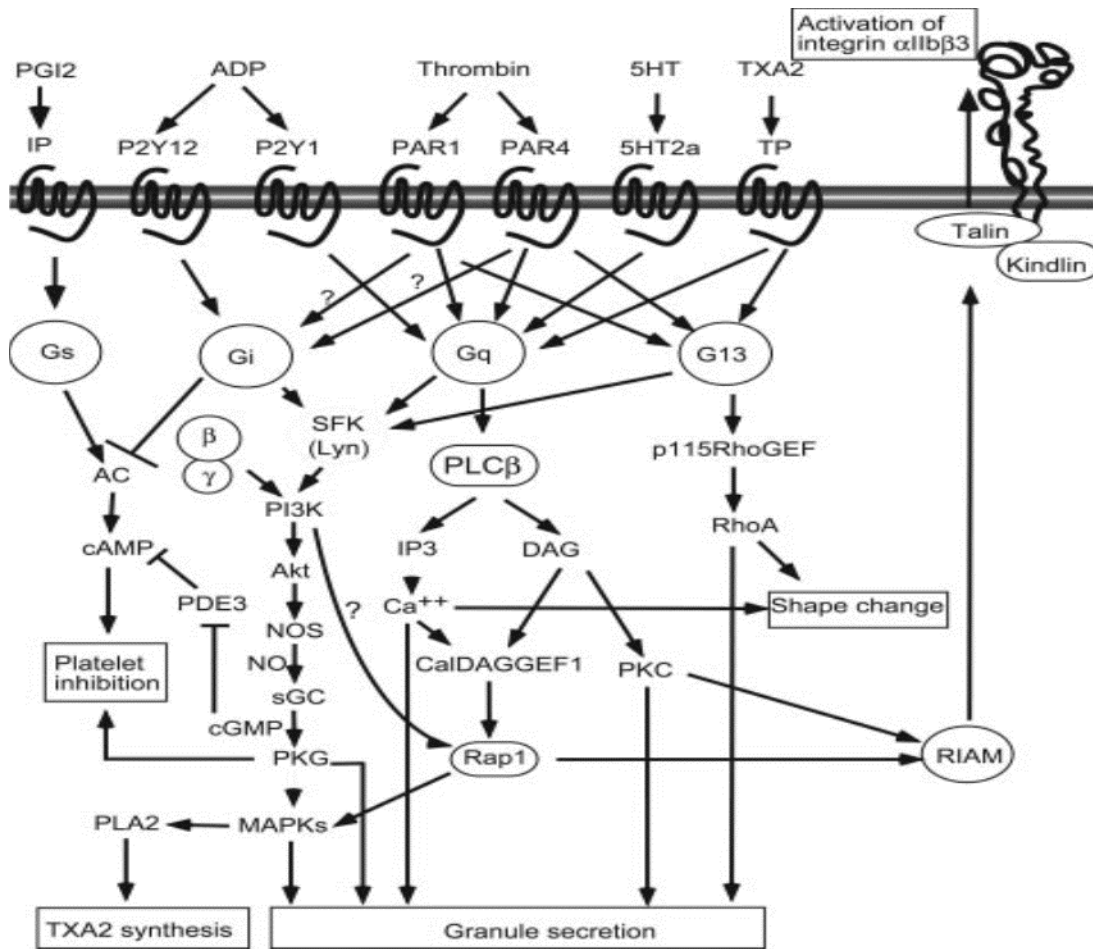


Figure 1-2: G-protein coupled receptors activation pathways [12]. Gq signalling pathway involves activation of PLC β resulting in the formation of IP₃ and diacyl glycerol leading to elevation of free cytoplasmic [Ca²⁺] and activation of protein kinase C (PKC). G13 signalling pathway involves activation of RhoA which induces platelet shape change and stimulates granule secretion. Gi-type G proteins inhibit adenylyl cyclase (AC) enzyme that catalyse the conversion of ATP to cAMP and are also a major source of β/γ complexes, that regulate phosphatidylinositol 3-kinases (PI3Ks) and the subsequent activation of Rap1 while Gs G-proteins activate AC enzyme leading to platelet inhibition.

Platelets express Gq, G12/G13, Gi/Gz, and Gs proteins. Those G proteins are associated with agonist receptors, with the exception of Gs which is coupled to the prostacyclin receptor (IP) and inhibits platelet function by stimulating cyclic adenosine monophosphate (cAMP) synthesis (figure 1-2) [23].

Thrombin is the most important-serine protease effector of the coagulation system and one of the most effective activators of platelets. Thrombin formation is launched by the exposure of tissue factor (TF) to the blood stream after the disruption of the vascular endothelium and it takes place on the surface of activated platelets [24]. Thrombin- induced platelet activation is mediated in humans via a dual system of G-protein-coupled protease-activated receptors (PARs), PAR1 and PAR4 [25, 26], that directly couple to Gq, G12/G13 and, in some cases, also to the Gi family of G proteins [27, 28] (figure 1-2).

TXA₂ is a platelet agonist synthesized from arachidonic acid (AA) by the action of the enzymes cyclooxygenase-1 (COX-1) and thromboxane synthase in platelets. The action of TXA₂ is locally restricted due to its short half-life (around 30 seconds). For that reason, a stable analogue of the endoperoxide prostaglandin H₂ (U46619) that also activates TXA₂ receptor (TP) is widely used instead during pharmacological studies. TP receptor mainly acts through Gq and G12/G13 proteins (figure 1-2) [27].

ADP is stored at high concentrations in platelet's dense granules and it is also released from damaged cells at the site of vascular injury. Platelet activation by ADP is mediated by two G protein-coupled receptors, P2Y1 and P2Y12 [29, 30]. While P2Y1 couples to Gq proteins [31, 32], P2Y12 is coupled to Gi- proteins [33]. The P2Y12 receptor is irreversibly inhibited by thienopyridines such as clopidogrel, which is currently used for the secondary prevention of cardiovascular events [34, 35].

Serotonin is taken up by platelets, stored in dense granules and released during platelet activation. It serves as a positive-feedback mechanism by activating 5-hydroxytryptamine 2A (5-HT_{2A}) receptors on platelets, which are also Gq-coupled [5].

1.1.3. Platelet aggregation

Platelet aggregation is mainly mediated by the platelet integrin receptor GPIIb/IIIa which allows the binding of fibrinogen to the receptors of adjacent platelets consolidating the platelet plug [36-38]. The effect of platelet agonists such as TXA₂ [39], ADP [40] and matrix metalloproteinase-2 (MMP-2) [41] trigger a biochemical cascade of events, known as 'inside-out' signalling, that ultimately leads to the activation of the GPIIb/IIIa mainly through the interaction of Rap1 with the Rap1-GTP-interacting adaptor molecule (RIAM) as shown in figures 1-1 and 1-2.

P-selectin, stored in α -granules of inactivated platelets and translocated to the platelet surface during platelet activation [42]. P-selectin mediates the initial platelet-leukocyte tethering and triggers leukocyte activation interacting with specific carbohydrate ligands on leukocyte called, P-selectin glycoprotein ligand-1 (PSGL-1) [43].

After activation of the GPIIb/IIIa, the 'outside-in' signalling also plays an important role in the amplification of the platelet response. Upon integrin ligation, the G protein subunit G α 13 binds to the cytoplasmic domain of β 3 [44] activating the Src family of the tyrosine kinase family [45, 46] [47] and initiating the SFK-dependent signals required for 'outside-in' signalling that it is critical for a stable platelet adhesion, spreading, and clot retraction [48].

The major endothelium-derived inhibitors of platelet activation are prostacyclin (PGI₂) and nitric oxide (NO) that exert their inhibitory effect raising the intra-platelet levels of the cyclic nucleotides cAMP and cGMP, respectively.

Prostacyclin acts through a G_s-coupled receptor (IP receptor) and stimulates the adenylyl cyclase enzyme (AC) [49]. Once PGI₂ binds to its receptor on the platelet surface, the activation of its intracellular receptor-linked stimulatory G-protein (G_s) is converted into its active form, binds to the enzyme and stimulates the synthesis of cAMP from ATP (figure 1-2). Cyclic AMP inhibits Ca⁺² mobilization, granule release, PLA₂ activity and TXA₂ production [50] and activates the cAMP-dependent protein kinase (PKA). In addition, cAMP is a co-

factor needed for the phosphorylation of the vasodilator-stimulated phosphoprotein (VASP) at the serine 157 [51-53].

VASP is an actin- and profilin- binding protein. VASP is expressed at high concentrations (approximately 25 μ M) in platelets [54]. VASP is crucial during platelet activation and participates in the cytoskeleton redistribution during platelet shape change and during GPIIb/IIIa activation. [55, 56].

The main phosphorylation sites in VASP are at Ser 157 and Ser 239 [57]. Analysis of phosphorylation kinetics has indicated that Ser 157 might be preferentially phosphorylated by PKA while Ser 239 by PKG [58].

Nitric oxide is mainly synthesized in endothelial cells through the action of the endothelial NO synthase (eNOS) [22, 59, 60] and diffuses into platelets where activates the sGC enzyme [5]. However, NO can also be produced in platelets. The presence of Ca^{+2} /NADPH dependent, L-arginine/NO constitutive NOS (eNOS) and Ca^{+2} independent induced NOS (iNOS) in human platelets was demonstrated by Radomski et al in the early nineties [61]. NO activates the cytosolic sGC resulting in a significant increase of cGMP levels in platelets (more than ten-fold increase). Although sGC can be also activated by vWF and calcium ionophore [18, 19, 22] and thrombin or collagen [62-64], the increase in cGMP level by these agents that induce platelet aggregation is more modest (about two-fold) than by NO.

For NO to activate the conversion of guanosine 5'-triphosphate (GMP) to cGMP by the enzyme [65], sGC heme group must be in reduced form, otherwise NO loses its ability to activate the enzyme. 1H-[1,2,4]oxadiazolo[4,3-a]quinoxalin-1-one (ODQ) is used in pharmacological studies to inhibit the effect of NO by oxidising the heme group contained in sGC, so that the enzyme becomes refractory to NO action [66]. cGMP exerts its effect through the activation of cGMP-dependent protein kinases (PKG) and cGMP-regulated ion channels [67]. cAMP activates PKA and phosphorylates VASP at the serine 157 while phosphorylation of VASP at serine 239 is PKG dependent [51]. NO/cGMP effect during platelet inhibition can be mediated by both, PKG- and PKA- dependent mechanisms [68] because cGMP can also inhibit phosphodiesterase 3 (PDE3) enzyme which hydrolyse cAMP leading to activation of PKA [69]. cGMP may also interfere with the transport of biogenic amines into platelets and may therefore,

down-regulate the uptake of serotonin by platelets via cGMP- induced protein phosphorylation [70]. cGMP modulates intra-platelet Ca^{+2} , increasing the activity of the Ca^{+2} ATPase extrusion pump and therefore increasing leakage across the plasma membrane [71]. Furthermore, cGMP inhibits Ca^{+2} mobilisation from intracellular stores [72], leading to a reduced availability of Ca^{+2} within and in the proximal vicinity of platelets [73]. Some of these effects are thought to be mediated by direct phosphorylation of IP3 [74]. Additionally, cGMP may affect the membrane phospholipid metabolism through the inhibition of PLC and PLA2 [72] and can also down-regulate the expression of GPIIb/IIIa and P-selectin platelet receptors [75-78].

1.2. L-Tryptophan metabolism

L-Tryptophan is an essential amino acid that accounts for 1-1.5% of the total amino acid content of the human body. It is the precursor of bioactive compounds including serotonin and kynurenine[79] (figure 1-3)

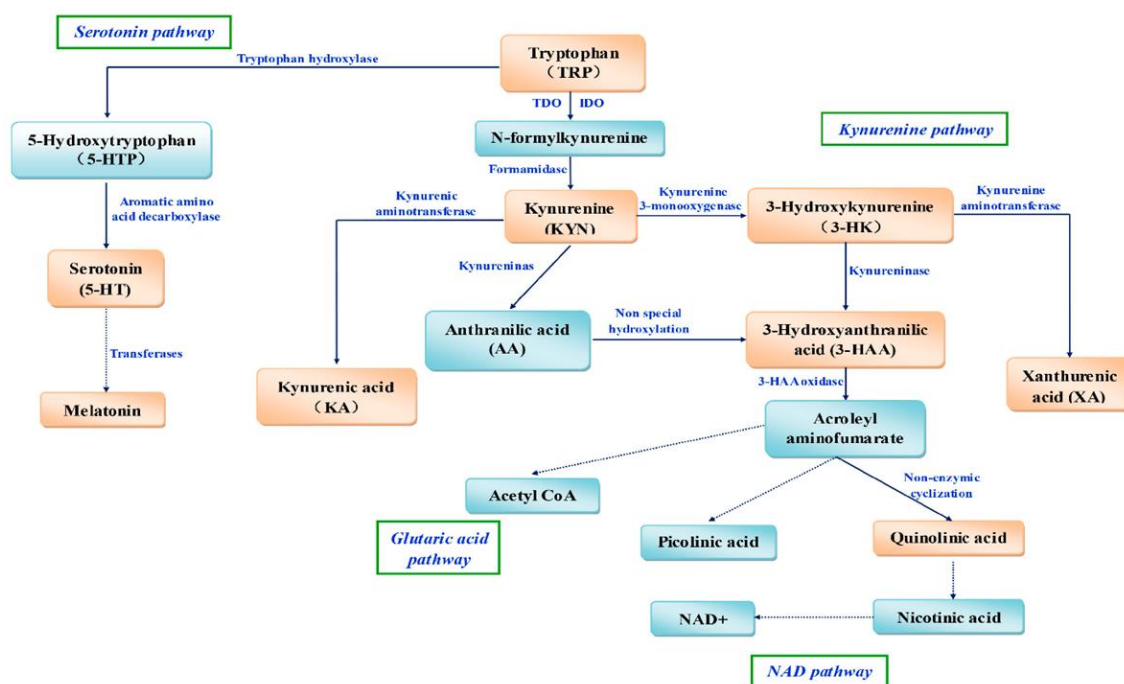


Figure 1-3: Tryptophan metabolic pathway [80]. Tryptophan is metabolised by tryptophan hydroxylase to serotonin and melatonin while tryptophan metabolism by tryptophan dioxygenase (TDO) and indolamine dioxygenase (IDO) leads to kynurenine formation which further metabolised through kynurenine pathway into various metabolites. TDO: tryptophan dioxygenase; IDO: indolamine dioxygenase; 3-HAA oxidase: 3-hydroxyanthranilic acid oxidase; NAD+: nicotine adenine dinucleotide.

Serotonin derives from tryptophan by the action of the tryptophan hydroxylase enzyme (TPH) [81]. The most abundant production of serotonin takes place in the gastrointestinal system by intestinal enterochromaffin cells and it is taken up by platelets and stored in their dense granules [82, 83]. In fact, about 99% of the total blood serotonin [5-HT] is accumulated in platelets due to their powerful uptake and storage mechanisms [84].

Serotonin has a broad impact as a neurotransmitter and neuromodulator and it has been implicated in numerous psychiatric conditions and psychological processes [85]. Upon platelet activation, serotonin is released from aggregated platelets and induces vasoconstriction and promotes platelet aggregation [86,

87]. Serotonin is also involved in inflammation as participates in the activation of monocytes and T lymphocytes, monocytes cytokine production, recruitment of neutrophils, extravasation of immune cells and regulation of type I interferon-gamma (IFN- γ) production through scavenging reactive oxygen species (ROS) [88-90]. Serotonin has been implicated as the 'driving force' in establishing intestinal inflammation and serotonin receptor antagonists have been shown to block the inflammatory process in animal models of intestinal inflammation [91, 92]. Serotonin-mediated inflammatory effects have also been documented in other diseases such as rheumatic disorders [93, 94].

L-kynurenine is another metabolite of L-tryptophan through the action of the constitutively expressed tryptophan 2,3-dioxygenase (TDO) enzyme in the liver and by the inducible indoleamine 2,3-dioxygenase (IDO) enzyme in other tissues [95]. Interestingly, increasing the tryptophan conversion into kynurenine, IDO can limit the synthesis of other tryptophan-dependent molecules, including serotonin [96, 97].

IDO is an intracellular heme-containing enzyme that catalyses the initial rate-limiting step in tryptophan degradation along the kynurenine pathway [98]. Purified IDO has been shown to require superoxide anion radical (O_2^-) as a substrate and co-factor for its maximal activity [99, 100].

IDO is expressed in endothelial cells, placenta, lungs, epithelial cells in the female genital tract and lymphoid tissues in mature dendritic cells (DCs) [101, 102]. IDO can be induced during infectious and inflammatory processes by inflammatory cytokines such as IFN- γ [103, 104] [105] and its role in preventing T cell-driven rejection of allogeneic foetuses has been also well documented [106]. Kynurenine has the ability to generate a 'tolerogenic situation' by controlling not only Th1, but also Th17 and Treg cells by different mechanisms, such as tryptophan depletion which induces cell cycle arrest in lymphocytes [107] driving these cells into apoptosis [108] [109-111] and/or by differentiation of naive CD4+ T cells into T regulatory cells (Treg) [112].

Modulation of IDO activity and/or kynurenine pathway provides a potential therapeutic approach for inflammatory diseases [113]. It has been found that IDO induces tolerance and immune-escape, fine-tunes inflammation, and it functions as a homeostatic mechanism that prevents excessive immune responses [114].

On the other hand, pharmacological inhibition of IDO results in disease aggravation in several models of inflammatory disease, including experimental autoimmune encephalomyelitis [115], collagen-induced arthritis [116], asthma [117] and colitis [118].

The ability of kynurenine to regulate the vascular tone has gained a lot of attention and debate. Degradation of tryptophan to kynurenine has been found to be strongly correlated with sepsis and the development of hypotension in humans [119]. Tryptophan-containing dipeptides act as selective inhibitors of human angiotensin-converting enzyme (ACE) which has an important role in controlling blood pressure and it is a well-known target for the treatment of hypertension [120]. Wang et al have found that kynurenine induces vascular relaxation and have suggested that this effect is mediated by activation of guanylate cyclase and adenylate cyclase [102]. It has been also reported that kynurenine induces arterio-dilatation via activation of voltage-dependent K⁺ channel encoded by the KCNQ gene family [121]. However, hypertensive patients with high concentrations of kynurenine in blood are more challenging to be pharmacologically controlled than those with lower kynurenine concentrations [122]. Moreover, kynurenine seems to be also involved in endothelial dysfunction and progression of atherosclerosis in patients with chronic kidney disease and kynurenine metabolites may be involved in the progression of hypertension [123, 124].

Kynurenine has neuroactive properties through two metabolites: kynurenic acid (neuroprotective) and quinolinic acid (neurotoxic). Kynurenic acid is an endogenous broad-spectrum antagonist of excitatory amino acid receptors, including the N-methyl-D-aspartate receptors (NMDAR). It can inhibit the over excitation of these receptors and reduce cell damage induced by excitotoxins. Moreover, kynurenic acid non-competitively blocks the $\alpha 7$ -nicotinic acetylcholine receptors, thereby permitting modulation of the cholinergic and glutamatergic neurotransmission. Quinolinic acid is a selective N-methyl-D-aspartate receptor agonist which can cause lipid peroxidation, generation of free radicals and apoptosis via the over excitation of these receptors. Changes in the relative or absolute concentrations of the kynurenine metabolites have been found in several neurodegenerative disorders, such as Huntington's disease and Parkinson's disease, stroke and epilepsy, in which the hyper activation of amino acid receptors could be involved.

Human platelets express NMDARs subunits that support activation and platelet aggregation. In fact, although NMDAR agonists do not induce platelet aggregation, do facilitate platelet aggregation while NMDAR antagonists inhibit platelet aggregation [125]

Kynurenine is considered an aryl hydrocarbon receptor (AhR) agonist [126]. AhR is a cytosolic receptor for low molecular weight molecules [127] mainly expressed in the liver, lungs, skin and gastrointestinal tract [128, 129]. There are two pathways associated with the AhR receptor, called the classical or genomic pathway and the non-genomic pathway. In the cytosol, AhR exists in a latent state as part of a multiprotein complex (figure 1-4). Once the receptor binds to its ligands like TCDD, the AhR-complex translocates to the nucleus and binds to the AhR nuclear translocator (Arnt). The resultant AhR-Arnt heterodimer binds to a specific motif called dioxin-responsive elements (DREs), in the promoter region of target genes leading to transcription of CYP1A1, CYP1A2 and CYP1B1 and other members of the cytochrome P450 family [130, 131].

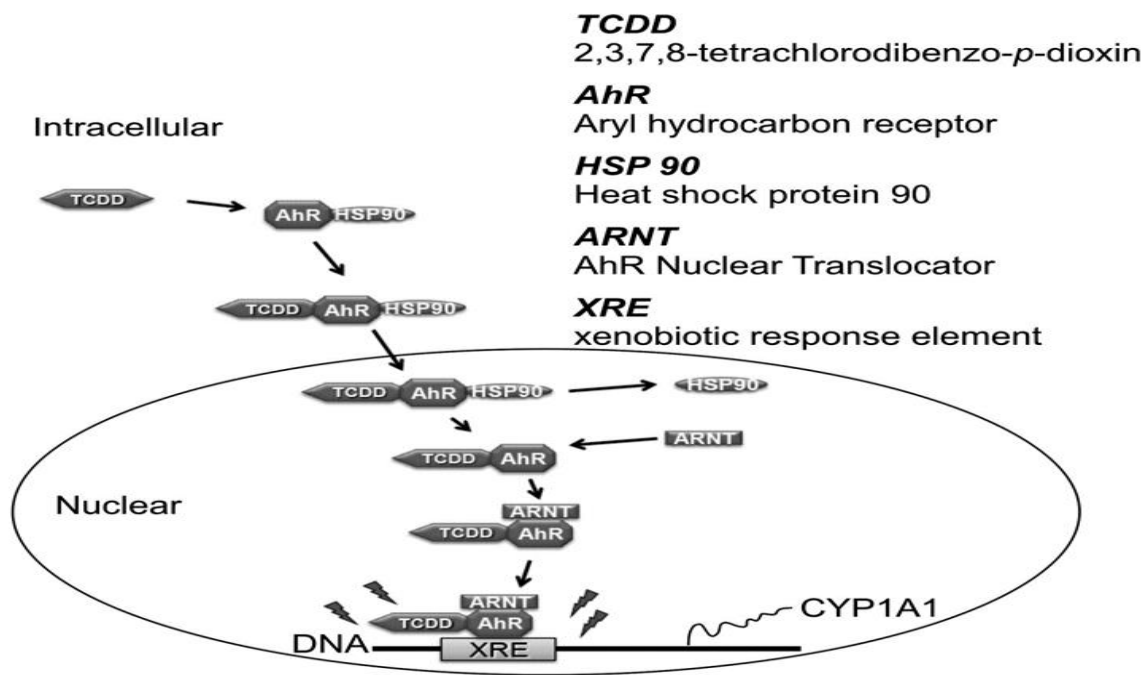


Figure 1-4: Aryl hydrocarbon receptor(AhR) genomic pathway[132]. Activation of AhR receptor by Tetrachlorodibenzo-*p*-dioxin (TCDD) leads to translocation of the receptor- agonist complex from cytoplasm to the nucleus leading to transcription and expression of cytochrome P-450 genes. TCDD: 2,3,7,8-tetrachlorodibenzo-*p*-dioxin; AhR: Aryl hydrocarbon receptor; HSP 90: heat shock protein 90; ARNT: AhR nuclear translocator; XRE: xenobiotic response element.

The AhR non-genomic pathway (Figure 1-5), does not involve translocation of the AhR to the nucleus, but instead results in a cascade of signalling events that include increase in intracellular Ca^{+2} , phosphorylation of MAPKs, cPLA2 activation, generation of AA and other inflammatory mediators [133].

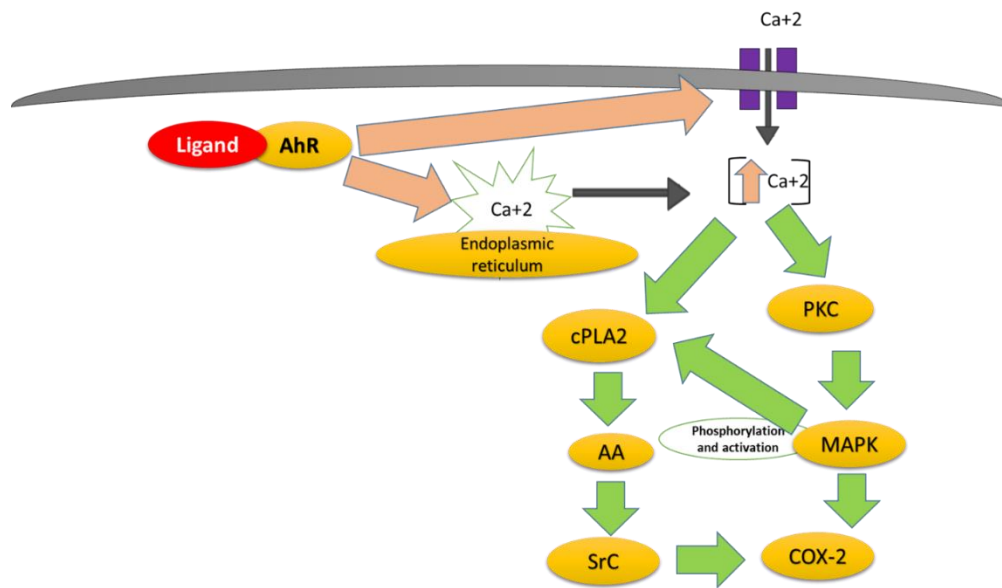


Figure 1-5: Aryl hydrocarbon receptor (AhR) non-genomic pathway. Upon ligand activation of AhR receptor, the increase in intracellular Ca^{+2} level activates both, the protein kinase C (PKC) and the cytosolic phospholipase A2(cPLA2) leading to the activation of the cyclooxygenase-2 (COX-2) enzyme through mitogen activated protein kinase (MAPK) and Src family kinases. Green arrow (activates).

AhR ligands include dioxins, furans, polychlorinated biphenyls, tryptophan metabolites and benzimidazoles [127]. The halogenated aromatic hydrocarbon 2,3,7,8-tetrachlorodibenzo-p-dioxin (TCDD) is the most potent AhR ligand [134]. A number of compounds are described as AhR antagonists, including the flavone derivatives alpha-naphthoflavone (α -NF) [135]; 6,2',4'-trimethoxyflavone (TMF) [136]; 3'-methoxy-4'-nitroflavone (MNF) [137] and 6-methoxy-1,3,8-trichlorodibenzofuran (6-MCDF) [138]. TMF, seems to act in a species-independent manner and does not appear to exhibit partial agonistic properties at all [136].

1.3. Kynurenine and NO; the potential platelet connection...

It has been shown that both, exogenous and endogenous NO, can inhibit IDO activity and that oxidative arginine and tryptophan metabolism in IFN- γ primed mononuclear phagocytes are functionally related [139]. The mechanism by which NO inhibits IDO seems to be related to its interaction with the heme-iron group present at the active site of the enzyme. NO has a high affinity for the heme-iron group and this interaction may interfere with the conversion of the ferrous form into the ferric form required for IDO catalysis[139]. Another mechanism by which

NO could inhibit IDO activity is through its ability to rapidly react with, and thereby eradicate, the superoxide anion proposed to be required also for IDO enzyme activity [139]. Although it is well known that kynurenine plays an important role in immune modulation [107, 109-112], kynurenine has been also shown to be an endothelium-derived relaxing factor involved in the regulation of blood pressure during systemic inflammation exerting its effect independently of NO [102] and to contribute to the regulation of vascular tone in atherosclerosis [140]. Those findings demonstrated that kynurenine is an endothelial-derived vasorelaxing factor with a demonstrated effect on blood pressure, and the connection between NO and IDO, led us to investigate the potential effect of kynurenine on platelet function.

1.4. Blood platelets and cancer.

The involvement of platelets in cancer was first reported by Armand Trousseau in 1865 and described as a recurrent migratory thrombophlebitis [141]. One hundred years later, Gasic et al observed that the number of metastasis induced by TA3 ascites tumour cells in mice could be significantly decreased when thrombocytopenia was induced by neuraminidase and enhanced by the infusion of platelet rich plasma (PRP) in the rodents [142]. Other researchers reported later that experimentally induced thrombocytopenia has been associated with reduction in the number of metastases in experimental models of cancer metastasis [143]. It is widely demonstrated that tumour cells have the capability to induce platelet aggregation and that this ability is correlated with the number of lung metastases in various animal models [144].

The ability of malignant cells to aggregate platelets is known as tumour cell-induced platelet aggregation or TCIPA [145]. The mechanisms by which tumour cells induce platelet aggregation may differ depending on the tumour type. However, when this interaction takes place multiple advantages are conferred to cancer cells. Platelets can protect tumour cells by coating them and thereby shielding them from the high shear stress within the vasculature and from immune system's effector cells. For example, platelet-derived factors, like transforming growth factor- β 1 (TGF- β 1), have demonstrated to protect tumour cells from immunosurveillance [146, 147]. Indeed, Platelet-derived TGF- β has been shown

to down-regulate the activating immunoreceptor NKG2D on natural killer cells (NK cells) impairing NK cell antitumor activity [148]. On the other hand, it has been also shown that platelets can pass their MHC class I molecules on to tumour cell membranes by direct contact, reducing in this way NK cell reactivity and cytotoxicity towards tumour cells [149]. Some malignant cells can gain a 'platelet-like phenotype', expressing similar adhesion molecules and receptors, like GPIb and integrin receptors on their surface, and this concept of "platelet-mimicry" has been suggested to be related to the lack of tumour-directed immune surveillance [150].

Platelets can also facilitate tumour cell extravasation to the local subendothelial matrix or distant organs via platelet P-selectin and its ligands or by activation of the endothelial P2Y2 receptor by the ATP released by platelets [89, 151]. Moreover, when platelets pcome in contact with cancer cells and aggregate, they release a number of growth factors that can be used by tumour cells for growth and for the development of new blood vessels within the tumour [152, 153].

The development of metastasis is responsible for more than 90% of all cancer-related deaths [154]. As discussed above, TCIPA correlates with the metastatic potential of tumour cells and platelets participate during critical steps in cancer metastasis including tumour cell attachment to the vessel wall [155, 156] facilitating invasion and tumour cell migration [157, 158]. Thrombocytosis is frequently observed in patients with metastatic malignant tumours [159, 160] and the risk of venous thromboembolism (VTE), including deep venous thrombosis (DVT) and pulmonary embolism (PE) are increased up to seven-fold in cancer patients when compared with non-cancer patients [161-163].

1.5. Mechanisms involved in tumour cell-induced platelet aggregation and cancer progression

1.5.1. Platelet receptors

Tumour cells can activate platelets by direct contact through major platelet receptors and ligands such as GPIb-IX-V and GPIIb/IIIa, which have been also identified on the surface of some human and animal cancer cells such as MCF7 (human breast carcinoma), B16 (murine melanoma) and 3LL (Lewis lung carcinoma cells), facilitating platelet adhesion and aggregation [164, 165]. The

interactions between cancer cells and platelets during TCIPA are reciprocal with regard to the network of platelet-cancer cell adhesion molecules involved in the process. For example, the expression of platelet GPIb-IX-V, GPIIb/IIIa and P-selectin on the tight inter-junction between platelets and cancer cells is crucial during TCIPA where not only cancer cells have the ability to stimulate the platelet receptor expression, but platelets upregulate GPIb and GPIIb/IIIa on the surface of MCF7 cells [164].

GPIb-IX-V Is expressed on platelets and megakaryocytes and it constitutes one of the most abundant receptors on platelets membrane. It mediates the first binding of platelets to subendothelial von Willebrand factor (vWf) under high shear force in arterioles and small arteries [166, 167]. Other ligands for GPIb-IX-V include thrombin [168], P-selectin [169], leukocyte integrin $\alpha_1\beta_2$ [170], high molecular weight kininogen and clotting factors XI and XII [171-173]. Binding of vWf to GPIb-IX-V results in platelet activation and GPIIb/IIIa expression by activation of phospholipase C (PLC), phospholipase A2 (PLA2), and phosphatidylinositide 3-kinases (PI3K) in cooperation with or independently of Fc receptors (FcγRIIA or FcRγ chain) [174]. GPIb has been proven to be expressed on the surface of platelets and MCF7 cells during TCIPA [164, 175, 176] and preincubation of platelets with antibodies against the GPIb receptor has demonstrated to inhibit platelet aggregation induced by glioblastoma, neuroepithelioma and breast cancer cells *in vitro* [177-179]. The addition of purified vWf during TCIPA by HT-1080 cells, has been shown to potentiate cell interactions with platelets [180]. On the other hand, specific antibodies for blocking the GPIb-IX-V receptor or vWf function have been used to successfully reduced cancer cells-platelets interactions [175, 181].

GPIIb/IIIa has shown to play a crucial role during TCIPA induced by cancer cells of various origins in both experimental settings: *in vitro* and *in vivo* [164, 175, 181-183]. Melanoma cells-induced platelet aggregation was found to be mediated through GPIIb/IIIa and inhibited by antibodies directed to the platelet receptor [184]. GPIIb/IIIa has also a predominant role on TCIPA by glioblastoma and neuroepithelioma cells as platelet aggregation can be totally abolished when antibodies against GPIIb/IIIa are employed [178]. The role of GPIIb/IIIa receptors during TCIPA is beyond its adhesion and bridging function as its involvement in

cancer metastasis has been also related to the release of proangiogenic factors (vascular endothelial growth factor-VEGF) or basic fibroblast growth factor (bFGF) from platelets activated by melanoma or breast cancer cells [185, 186]. Integrin $\alpha_v\beta_{III}$ is another adhesion molecule, expressed in low amounts on platelets but abundant on cancer cells, that may play a role in TCIPA connecting tumour cells to platelets by plasma proteins such as fibrinogen [187]. However, a direct binding between GPIIb/IIIa and the melanoma cell-expressed $\alpha_v\beta_{III}$ has been observed without the assistance of fibrinogen or other molecules [188].

P-selectin: P-selectin is primarily expressed in platelets and in endothelial cells [189, 190]. Upon platelet activation, P-selectin is translocated to the platelet surface from α -granules and mediates platelet binding to leukocytes and/or to endothelial cells [191]. Blocking or downregulating P-selectin expression has been associated with a reduction of the metastatic potential of colon cancer and the development of lung metastasis in mice accompanied by a significant reduction of platelets binding to cancer cells [192-194]. Activation of GPIIb/IIIa mediated by P-selectin has been linked to platelet's deposition in solid tumours and in turn, deficiency and blockage of P-selectin lead to a significant decrease of platelet deposition, tumour growth and angiogenesis in murine models of cancer [195]. Platelets and platelet-derived P-selectin have been also involved into the recruitment of monocytes to the metastatic microenvironment by the induction of inflammatory proteins from vascular endothelium as chemokine CCL5 (Rantes) [196]. Furthermore, in a variety of mucin-producing cancers, mucin seems to participate in a mutual activation mechanism between neutrophils and platelets by binding to P-selectin on platelets and L-selectin on neutrophils which induces the release of cathepsin G from neutrophils and platelet activation [197]. In fact, blocking P-selectin expression on platelets not only reduces TCIPA but also affects several pro-carcinogenic and cancer-related immunological mechanisms that contribute to tumour growth and metastasis [198].

1.5.2. Tumour cells and platelets released mediators

The release of platelet agonists such as ADP, thrombin, thromboxane A_2 and the local production of other tumour-associated proteins by cancer cells can result in platelet granules secretion and consequently end in platelet activation and

aggregation [199-202]. For example, tumour cells can release high-mobility group box 1 protein (HMGB1), which interacts with the toll-like receptor 4 (TLR4) in platelets leading to their activation *in vitro* and promoting metastasis *in vivo* [203]. Some tumour cells express tissue factor (TF) on their membrane which activates the coagulation cascade generating thrombin which in turn induces platelet activation and aggregation [204]. Therefore, a number of different mediators have been identified and demonstrated to contribute to tumour growth and to the potential development of haematogenous metastasis.

Tissue factor is a transmembrane glycoprotein that binds to factor VIIa (TF/VIIa) initiating the extrinsic coagulation pathway and leading to the conversion of prothrombin to thrombin. Overexpression of TF has been described in numerous tumour cells and has been correlated with the progression to invasive cancer [205]. In fact, TF not only seems to play a major role in TCIPA *in vitro* but it has been also strongly associated and recognised as the most important factor responsible for the pro-thrombotic state of cancer patients [206].

Adenosine diphosphate (ADP) contributes to TCIPA induced by neuroblastoma [207], a number of lung cancer [208], melanoma [209], breast cancer [210] and fibroelastoma [180] cell lines. It has been shown that during TCIPA by breast cancer cells MCF-7, platelets are aggregated by ADP via activation of the P2Y₁₂ purinergic receptor [210] which mediates platelet degranulation through inhibition of the AC enzyme and activation of PI3K [211, 212]. In a murine study, Cho et al. demonstrated the release of ADP at the interface between ovarian cancer cells and platelets and the significance of the platelet P2Y₁₂ receptor-ADP interaction during TCIPA for tumour growth of primary ovarian malignant tumours. [213]. Holmes et al have recently investigated the effect of Cangrelor (a P2Y₁₂ inhibitor) on platelet secretion and aggregation in patients suffering from breast cancer. In their work, they demonstrated, *ex vivo*, that the drug induced a higher percentage of platelet inhibition when platelets isolated from cancer patients were tested and compared to its effect on platelets from healthy controls. Cangrelor also led to a significant reduction of the amount of VEGF, thrombospondin-1 and TGF- β 1 (proteins known to play an important role in cancer progression and angiogenesis) secreted from platelets isolated from cancer patients when compared to platelets from the healthy controls [214].

Thromboxane A₂ (TXA₂) is also a potent inducer of platelet aggregation [39] and can promote the binding of platelet-tumour cells aggregates to endothelial cells [215]. Many types of cancer cells including colorectal, prostate, bladder, thyroid and non-small-lung carcinoma overexpress thromboxane synthase (TXS) [216-220]. Thromboxane synthase catalyzes the conversion of PGH₂ to TXA₂ and the release of TXA₂ from murine and human cancer cell lines has been associated with platelet aggregation by activation of the thromboxane receptors on platelets [221-224]. On the other hand, platelet activation induced by rat Walker 256 carcinosarcoma cells have been shown to be correlated to the production of thrombin and eicosanoid metabolites leading to TCIPA [225]. Inhibition of thromboxane synthase activity showed to reduce tumour proliferation and induced apoptosis, effect reversed by addition of TXA₂ [216]. Inhibition of TXA₂ synthesis also reduced the development of metastasis by Lewis lung carcinoma or B16a melanoma cells in a mice model of lung metastasis [226]

Various serine proteinases including **thrombin**, matrix metalloproteinases (MMPs) and cysteine proteinases like cathepsin B and cancer procoagulant (EC 3.4.22.26), have been also identified during TCIPA.

Thrombin is the main enzyme in the coagulation cascade and also the most potent platelet activator present in blood. Thrombin acts via G-protein-coupled proteinase-activated receptors (PARs) [26] [227] [228]. Human glioblastoma U87MG [229] , neuroblastoma [230] and pancreatic cancer [231] cells induce TCIPA by thrombin generation. Thrombin is also key for supporting both, tumour cell proliferation and therefore local colonic adenocarcinoma growth, and the development of metastasis, by activation of PAR-1 and fibrinogen [232]. *In vitro* studies of TCIPA using lung cancer cells have demonstrated that non-small-cell lung cancer (NSCLC) induce platelet aggregation by thrombin generation which was inhibited by the addition of the anticoagulant agent hirudin. However, TCIPA by small-cell lung cancer cell lines (SCLC), was fully abolished only when both an ADP scavenger (apyrase) and hirudin were used in combination, highlighting the fact that the release/production of ADP is also crucial for the activation of platelets under this specific circumstances [208]

Cathepsins, such as cathepsin B and K [233], can induce platelet aggregation when released from cancer cells [234-236] by the generation of oxygen-derived free radicals [237]. B16 and B16a melanoma cells are known to release a cathepsin B-like cysteine proteinase which is responsible for their metastatic potential [234]. On the other hand, the release of cathepsin K by breast cancer cells has been positively correlated with platelet aggregation [238].

Matrix metalloproteinases is a family of zinc- and calcium-dependent endopeptidases that can degrade most of the components of the extracellular matrix and play a role in the regulation of platelet function [239]. MMP-2 is constitutively secreted in most cell types, whereas the secretion of MMP-2 in platelets is initiated by platelet activation [41].

MMP-2 is released by both, platelets and cancer cells, during TCIPA induced by HT-1080 and MCF7 cells [180, 210, 240]. The aggregating effects of MMP-2 involve the activation of proMMP-2 to MMP-2 by MMP-14 [210]. The enhanced generation of MMP-2 may be responsible for the increased aggregability of platelets collected from patients with metastatic prostate cancer [241]. Caco-2 colonic cancer cells stimulate platelet aggregation through the release of MMP-2 and ADP. The pro-aggregatory effects of Caco-2 cells are associated with an increase of platelet GPIb, GPIIb/IIIa, and P-selectin receptors [242]. Fibrosarcoma HT-1080 cells have been found to be more aggressive than A549 lung cancer cells in their ability to induce TCIPA due to production more MMP-2. The release of MMP-2 during this interaction was reduced by NO and in turn TCIPA was inhibited in cGMP dependent mechanism [180].

Galectin-3 is a member of a carbohydrate-binding proteins family with a high affinity for beta galactoside-containing carbohydrates [243]. This protein is overexpressed in many types of tumours and it has been involved in cancer progression and metastasis [244]. Galectin-3 contains a collagen domain that it is thought to mediate TCIPA through its interaction with the platelet collagen receptor GPVI, inducing the release of growth factors from platelet granules like PDGF that it is known to play an important role in the aberrant expression of COX-2 in cancer cells. Overexpression of COX-2 in HT-29 cells has led, when co-incubated with platelets, to an increase in the generation of PGE₂ that in turn

can facilitate platelet aggregation [245]. In addition, COX-2 expression has been also associated to cancer progression and considered as a poor prognosis factor of the disease. Barnes et al have shown that the use of celecoxib, which is a selective inhibitor of COX-2, reduces tumour growth and lymph angiogenesis in a mice model of breast cancer [246]

1.6. Pharmacological modulation of tumour cell-induced platelet aggregation

Various agents that play an important role in platelet function have been tested as potential inhibitors of TCIPA (figure 1-6):

Prostacyclin inhibits platelet aggregation by increasing cyclic AMP levels. It has been shown to inhibit TCIPA induced by a variety of tumour cells from different origins [176, 215, 247-251] and to delay the disruption of the aggregate form by tumour cells surrounded by platelets under flow condition using an ultrasound standing wave trap [252]. The administration of prostacyclin has also shown to decrease *in vivo* metastasis induced in rodents by B16a melanoma cells [215].

Acetyl salicylic acid (aspirin) inhibits platelet aggregation by inhibition of the cyclooxygenases (COXs) and the subsequent TXA₂ generation by platelets [253]. The epidemiological data available in the literature supports the idea that the regular use of aspirin could potentially reduce cancer incidence, metastasis and mortality, especially in colorectal cancer [254, 255]. The inhibition of COX-2 in cancer cells requires a high dose of aspirin (~1,000 mg daily) but low doses (< 100 mg) have been shown to be effective as prophylaxis decreasing the incidence of colorectal adenomas, thus the risk of colorectal cancer [224, 256]. However, the use of high doses of aspirin (0.6-1 g /day) did not protect patients from metastasis due to colorectal or small-cell lung cancer [257, 258]. [215]Consistent with its limited therapeutic efficacy *in vivo*, aspirin has failed to inhibit TCIPA by Caco-2 cells [242] and it is in fact a weak inhibitor of TCIPA *in vitro* [210, 240, 259-261]. The main effect of aspirin on TCIPA and cancer growth and metastasis take place by inhibition of thromboxane generation, however, because of the short half-life of aspirin ($t_{1/2}$ = 20 minutes in blood) and the rapid regeneration of COX-1 and COX-2 in nucleated cells, aspirin affects platelet's but not cancer cells' TXA₂ generation [213]. It has been demonstrated that platelet

aggregation induced by MDA-MB-231, MCF7 or Caco-2 cells was not affected by a pre-treatment of platelets with aspirin, but it was completely abolished by the ADP scavenger apyrase[262]. Isosorbide-based aspirin and ST0702, a nicotinate aspirin pro-drug, showed a consistent inhibition of TCIPA by HT1080, 59-M and Caco2 cell lines under both static and flow conditions whereas aspirin did not [263]. The effect of pharmacological agents that selectively inhibit thromboxane synthase and TXA₂ receptor antagonist on TCIPA have been also investigated. The use of OKY-046, a selective inhibitor of the thromboxane synthase, failed to reduce the ability of osteogenic sarcoma cells to induce TCIPA [264]. However, the use of thromboxane synthase inhibitors and TXA₂ receptor antagonist have been found to reduce TCIPA and metastasis by B16a melanoma and MG-63 osteosarcoma cells [215]. [264]. Furthermore, the TXA₂ receptor antagonist, SQ-29,548 and BM-567, a combined thromboxane synthase inhibitor and receptor antagonist, both effectively reduced TCIPA [224, 264]

NO is mostly generated by endothelial cells, platelets and leukocytes [265]. NO inhibits platelet aggregation by increasing cyclic GMP levels. Cancer cells can generate NO and this ability of cancer cells may determine their potency for aggregating platelets. Human colon carcinoma cells (SW-480 and SW-620) have shown different abilities to induce platelet aggregation due to the production of different levels of NO [209, 251, 266] and the inhibitory effect of NO on TCIPA by those cell lines was also potentiated by prostacyclin [251]. Interestingly, NO-releasing prodrugs (ortho and metanitate) had no effect on TCIPA under flow conditions [267]. NO can also participate in cancer growth, invasion, and metastasis most likely due to its regulatory role in vasodilation [268], cell adhesion [269], cellular growth, proliferation and cell migration [270-272]

The local release of ADP, by platelets or other cells like red blood cells or tumour cells, is associated with platelet aggregation.

ADP scavengers such as apyrase, P2Y receptor antagonists as 2-methylthio-AMP (2-MeSAMP) and ticlopidine have been shown to inhibit TCIPA [180, 200, 207, 209, 210, 273]. Clopidogrel mitigated tumour growth rate and significantly reduced the number of metastatic foci in a mouse model of orthotopic pancreatic tumour [274]. Furthermore, ticagrelor and clopidogrel have demonstrated to

reduce tumour growth and metastasis in B16-F10 melanoma mouse models [275]. Targeting ADP-receptors on platelets with P2Y₁₂ antagonists such as clopidogrel or ticagrelor have been demonstrated to inhibit platelet activation in cancer patients.[210, 274, 275]

As discussed previously, the translocation and subsequent release of MMP-2 by platelets is associated with platelet aggregation [41]. Therefore, the use of **MMPs inhibitors or MMP-2 antibodies** is expected to prevent platelet aggregation and therefore modulate TCIPA. In fact, co-incubation of platelets with apyrase and phenanthroline (a MMP inhibitor) have also proved to inhibit TCIPA by MCF7 breast cancer cells [210]. MMP-2 antibodies and the tissue inhibitor of metalloproteinase-4 (TIMP-4) have also decreased TCIPA induced by MCF7 and HT-1080 cells *in vitro* [180, 210, 276]. However, clinical trials using pharmacological inhibitors of MMPs to delay the progression of advanced malignancies have not shown significant benefits on those cohorts of patients [277].

GPIIb/IIIa receptor antagonists have been shown to be extremely effective as inhibitors of TCIPA [278]. Intravenous (Abciximab) [279] and oral (XV454) [183] GPIIb/IIIa receptor antagonists have been found to act as potent inhibitors of TCIPA *in vitro*. GPIIb/IIIa receptor antagonists demonstrated also to reduce the adhesion of tumour cells to the vascular endothelium and angiogenesis [280-283].

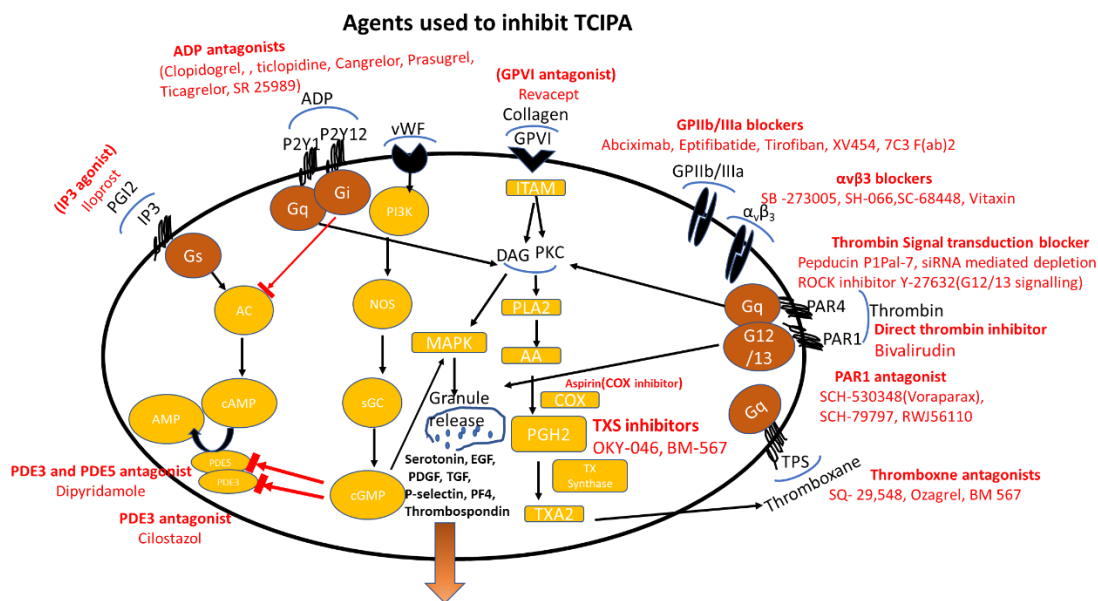


Figure 1-6: Common agents used to control TCIPA in experimental models. Cox2: cyclooxygenase enzyme; IX: coagulation factor IX; X coagulation factor X; MMP-2: Matrix metalloproteinase-2; GPVI: collagen receptor; GPIb: von Willebrand receptor; ADP: adenosine diphosphate; IP3: prostacyclin receptor; Gs, Gq and Gi: G-protein coupled receptors; PI3K: phosphatidyl Inositol-3 kinase; NOS: nitric oxide synthase; sGC: soluble guanylyl cyclase; cGMP: Cyclic guanosine monophosphate; BTK: tyrosine kinase; DAG: diacyl glycerol; PDE: phosphodiesterase enzyme; MAPK: mitogen activated protein kinase; AA: arachidonic acid; PLA2: phospholipase A2; PGH2: prostaglandin H2; EGF: endothelial growth factor; TGF: transforming growth factor; PDGF: Platelet-derived growth factor; PF4: platelet factor-4; AC: adenylyl cyclase; TXA2: thromboxane A2.

1.7. Involvement of kynurenine in cancer biology

Tumour cells are known to be able to evade and suppress the activity of the host immune system by different mechanisms. Tryptophan is an essential amino acid for the proliferation and survival of CD8+ and CD4+ T-lymphocytes and it is metabolised to kynurenine by the action of the indoleamine 2,3-di-oxygenase (IDO) enzyme. Kynurenine is considered one of the strongest mediators of the tumour-induced immunosuppression by activating the AhR receptor and inhibition of T- lymphocytes differentiation and activation [284, 285].

Tumour expression of IDO and high serum kynurenine/tryptophan ratio has been associated with cancer development, progression and with poor clinical prognosis. IDO-1 induction is considered as an independent variable for the reduced survival of patients suffering from acute myeloid leukaemia (AML),

melanoma, small-cell lung, ovarian, colorectal, pancreatic, and endometrial cancers [286-291].

Targeting IDO with specific inhibitors and regulation of tryptophan catabolism may be considered as effective strategies for the treatment of certain types of human malignancies [292]. Clinical trials that involved the use of IDO inhibitors together with chemotherapy or immunotherapy are currently underway. However, and despite the encouraging results obtained in early-phase clinical trials in a range of tumour types, the phase III study of the IDO1-selective inhibitor epacadostat in combination with pembrolizumab, which is immunotherapy against programmed cell death (PD-1) receptor on T-lymphocyte for treatment of melanoma, head and neck cancer, non-small lung cancer and Hodgkin's lymphoma, has not demonstrated the desirable effect in patients with metastatic melanoma [293].

In the first part of this research it has been demonstrated that kynurenine was able to inhibit platelet aggregation induced by collagen, ADP, thrombin, a thromboxane analogue and arachidonic acid by a mechanism involving cGMP and cAMP regulation. As discussed in the previous sections, both platelet agonists and platelet receptors play a major role in the pathophysiology of TCIPA and numerous agents have been tested to modulate their effect in TCIPA.

Taking together the recognised involvement of kynurenine in cancer and the discovery of the inhibitory effect of kynurenine on platelet function, this research also aimed to investigate the potential effect of kynurenine on TCIPA.

2. Aims of the project

1. Investigating the effect of kynurenine on platelet function using different agonists having different mechanism of action by light transmission aggregometer (LTA).
2. Investigating the expression of AhR receptor in platelets
3. Comparing the effect of kynurenine as AhR receptor agonist to various AhR receptor agonists and antagonists.
4. Exploring the potential mechanism by which kynurenine affect platelet function.
5. To investigate the ability of wide range of cancer cell lines to induce tumour cells induced platelet aggregation
5. To explore the effect of kynurenine on tumour cells induced platelet aggregation and the potential role of kynurenine in this interaction
6. To investigate the different tendencies of different cancer cells to induce tumour cells induced platelet aggregation and the role of kynurenine in this tendency.

3. Materials and Methods

3.1. Reagents

All reagents were purchased from Sigma (Ireland) unless otherwise stated (Appendix 1)

3.2. Blood Collection

Blood was collected from fully consented healthy volunteers who had not taken any drugs known to affect platelet function for at least 14 days before blood collection. The study was approved by The School of Pharmacy and Pharmaceutical Sciences Research Ethics Committee, Trinity College Dublin (2015-06-01 MS).

Blood was gently taken from a forearm vein using a butterfly needle (21-gauge) attached to a syringe and slowly released, in order to ensure that platelets were not activated, through the wall of a falcon tube containing 3.15% solution of sodium citrate (9:1 v/v ratio). For accurate and reproducible results blood samples were drawn with minimal or no venostasis [294].

Platelet rich plasma (PRP) was obtained by blood centrifugation at 250 xg for 20 minutes at room temperature and identified as the upper yellow layer. PRP was transferred carefully, to avoid potential contamination with white and red blood cells, using a 1 mL pipette to another falcon tube.

Washed platelets (WP) were prepared by centrifugation of prostacyclin treated PRP (0.3 µg/mL) at 900 xg for 10 minutes at room temperature. After centrifugation, the top layer of platelet poor plasma (PPP) was removed and the platelet pellet gently re-suspended in Tyrode's solution.

Platelet count was adjusted to 250,000 platelets/µL before experiments for all the donors using a Beckman Coulter Z1 series Coulter Counter (Labplan, Ireland). The instrument works according to the "Coulter Principle" where particles suspended in an electrolyte solution are counted using the electrical sensing zone method. This method is based on the detection of changes in electrical impedance as particles pass through an aperture tube immersed in the electrolyte solution [295]. Platelets were counted using a 50 µm aperture and sizing inclusion threshold was set to count particles between 1.789-3.856 µm. Three consistent and consecutive measurements of the samples were taken, an average of the readings were used as the sample concentration and

PRP and/or WP were then diluted to 250,000 platelets/ μL using Tyrode's salt solution.

3.3. Cell culture

A number of human cancer cell lines from different origins: lung carcinoma (A549 cells); cervix adenocarcinoma (HeLa cells); colorectal adenocarcinoma (HT-29 and SW-480 cells) and breast ductal carcinoma (HCC-1954 cells), were obtained from the European Collection of Authenticated Cell Cultures (ECACC) or the American Type Culture Collection (ATCC). Cells were cultured, following their recommendations as monolayers in T-75 culture flasks at 37 °C and in a humidified atmosphere of 5% of CO_2 . A549 cells were cultured in advanced DMEM / F12 medium (Gibco, USA); SW-480 and HCC-1954 in RPMI (Gibco, USA); HT-29 in McCoy's medium (Sigma, UK) supplemented with (7.5 % w/v) sodium bicarbonate (Sigma, UK) and HeLa cells in DMEM (Sigma, UK). Media were supplemented in all cases with 10% foetal bovine serum (FBS) and 1% of L-glutamine (both from Sigma, UK) and replaced 2-3 times a week with fresh media. Sub-culturing was performed when cells in the flask were approximately 80% confluent.

For TCIPA experiments, cells were first detached from the flasks using 7mM EDTA in Ca^{+2} and Mg^{+2} free Dulbecco's Phosphate Buffer saline (DPBS) (Sigma, Ireland) and centrifuged at 300 xg for 5 minutes. Afterwards, cells were washed with Tyrode's salt solution (Sigma, Ireland), centrifuged once again and resuspended in 500 μL -1mL of Tyrode's salt solution, Cells were kept on ice until performing TCIPA experiments. Cell concentrations were determined using a Beckman Coulter Z1 series Coulter Counter (Labplan, Ireland) and diluted, using Tyrode's solution, to obtain a final concentration of 1,000; 2,000; 4,000 or 10,000 cells in 500 μL (final volume required to run aggregation experiments by light transmission aggregometry).

3.4. Light Transmission Aggregometry (LTA)

Platelet aggregation was studied using an eight-channel PAP-8E Platelet Aggregometer (Biodata Corporation, USA). This methods for looking at platelet function is based on the principles and technique first described by Born in 1962 [296]. Platelet aggregation is determined by the amount of light passing through a stirring (900 rpm) suspension of platelets, while they are stimulated by a platelet agonist, and detected by a photocell on the other side of the cuvette (figure 3-1), PPP and Tyrode's salt solution are used as blanks and therefore considered as 100% of aggregation for PRP and WP; respectively.

To examine the potential effect of different compounds tested during the course of this project on platelet aggregation, the compounds of interest were first incubated with platelets at 37 °C for at least 2 minutes under stirring and then their effects recorded for at least eight minutes by the software provided with the device following the addition of a platelet agonist.

The platelet agonists used in this study included: collagen (Labmedics, UK), ADP, thromboxane analogue U1333961 (Biosciences, UK), arachidonic acid (Bio data corporation, USA) and serotonin (Sigma, UK). For tumour cells induced platelet aggregation, TCIPA was initiated by adding cancer cells at various concentrations to the WP suspension and monitored by the software until a plateau was reached.

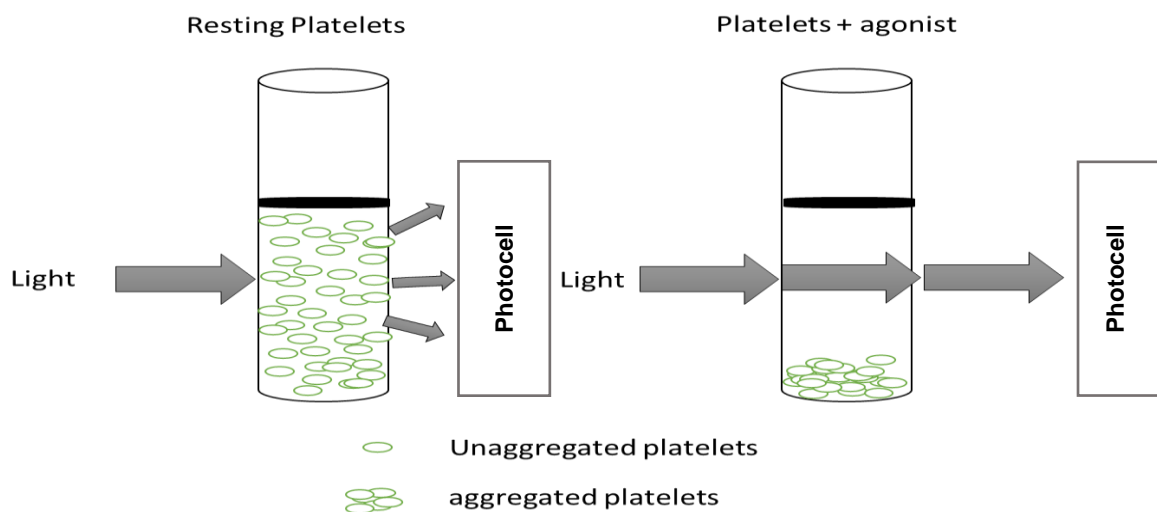


Figure 3-1: Schematic illustration of light transmission aggregometry. When an agonist is added to a platelet suspension and platelets aggregate, the amount of light that passes through the cuvette and that is detected by the photocell increases. This is reflected by the aggregometer's software as a drop in the trace that it is correlated with the percentage of aggregation.

3.5. Cytotoxicity assay

When the compounds tested inhibited platelet aggregation and to verify that the changes observed during LTA were indeed due to their effect of platelet function and not to a potential lytic effect, a CytoTox-ONE™ Homogeneous Membrane Integrity Assay (Promega, USA) was performed. This is a fluorometric based assay that indirectly measures the amount of lactate dehydrogenase (LDH) released from damaged cells and that could therefore be used to measure 'potential platelet lysis' induced by the compounds if toxic to platelets. The percentage of cytotoxicity (related, in this particular case, with platelet lysis) was determined following the manufacturer's instructions and calculated using the following equation:

$$\% \text{ of cytotoxicity} = \frac{\text{Experimental} - \text{culture medium background}}{\text{maximal LDH release} - \text{culture medium background}}$$

Equation 1: Percentage of cytotoxicity. Experimental: WP incubated in the presence of the compounds to be tested. Culture medium background: Tyrode's salt solution. Maximal LDH release (normalised as 100%): WP in the presence of lysis solution supplied with the assay.

The assay was performed for each compound in triplicate for each donor and with at least three independent blood donors.

3.6. Optical microscopy

To corroborate the effect of the compounds tested on platelet function, platelet aggregates and tumour cell-platelet aggregates formed during LTA were further visualised using a BX51M Olympus Microscope (Olympus corporation, Japan). Platelet samples were fixed following the experiments with 2% paraformaldehyde under stirring conditions for 30 minutes at 37 C° and afterwards, samples mounted on slides using a Cytospin™ 4 Cytocentrifuge (Thermo Shandon, UK) at 1500 rpm for 10 minutes. Slides were visualized under the microscope using 5x, 10x and 50x objectives and photomicrographs captured with a digital camera.

3.7. Immunoblotting

3.7.1. *Sample preparation*

Platelet samples for immunoblotting were prepared following the incubation of platelet suspensions with the compounds of interest for the required incubation time. Afterwards, samples were pelleted by centrifugation (13,000 rpm for 15 minutes) at 4°C. The pellet re-suspended in extraction buffer (Life technologies, USA) containing 1X protease inhibitor cocktail (Thermo scientific, USA), and sonicated on ice for three seconds twice. Samples were centrifuged once again, and the resultant supernatants kept at -20°C until further used.

Cancer cells samples were prepared by growing HCC-1954, SW-480 and A549 cells in 6 wells plates (seeding density 0.4×10^6 cells/well) and incubated with IFN- γ (Sigma, UK) and/or Epcadostat (Bioscience, UK) in FBS free medium for 48 hours. After incubation, cells monolayers were washed twice with phosphate buffer saline (PBS) (Thermo fisher, UK) and scrapped in the presence of 200-300 μ L extraction buffer (Life technologies, USA) containing 1X protease inhibitor cocktail (Thermo scientific, USA) per well and transferred into sterile Eppendorf tubes. Samples were then sonicated twice on ice (for 10 seconds each) with 20 seconds interval and centrifuged at 13,000 rpm for 20 minutes at 4 °C. Supernatant was collected and stored at -20 °C until performing the electrophoresis.

3.7.2. *Protein quantification*

Total protein concentration in each sample was determined using bradford assay (Biorad, Ireland) following the manufacturer instructions. Briefly, serial dilutions of bovine serum albumin (BSA) from 25 μ g/mL to 400 μ g/mL were prepared for the standard curve and absorbance at 595 nm measured using a Fluorstar Optima microplate reader (BMG Labtech, Germany). The total protein concentration for each sample was calculated then from the standard curve by linear regression.

3.7.3. Electrophoresis

After protein quantification, 18 μL of each sample containing an equal amount of protein (25-50 μg) were mixed with 6 μL of 4X loading buffer, vortexed and heated at 72 $^{\circ}\text{C}$ for 10 minutes using a thermomixer (Fisher, USA). The denatured protein samples were then loaded into sodium dodecyl sulphate-polyacrylamide electrophoresis gels (SDS-PAGE) (Appendix 2) and subjected to 150 V for 60-90 minutes. A molecular weight protein ladder (Biorad, Ireland) was loaded in every gel to monitor the progression of the samples during electrophoresis. After protein separation by electrophoresis, gels were washed in ice-cold towbing transfer buffer at room temperature for 30 minutes and proteins transferred to polyvinylidene fluoride (PVDF) membranes using a semi-dry transfer system (Bio-Rad, Ireland) at 22 V for 40 minutes. Afterwards, membranes were blocked with 5% bovine serum albumin (BSA) in tris-buffered saline (TBS) with 0.05% Tween 20 (TBST) for 60 minutes under continuous agitation to prevent antibody unspecific binding. Membranes were then washed three times (5 minutes each) with TBST and incubated with the relevant primary antibody overnight at 4 $^{\circ}\text{C}$. PVDF membranes were washed once again to remove unbound antibody and incubated with the relevant secondary antibody for 60 minutes at room temperature. Finally, membranes were washed, and peroxidase activity detected using Immobilon Western Chemiluminescent Horseradish Peroxidase (HRP) substrate (Millipore, USA). The expression of the protein of interest was quantified later on by densitometry analysis using a ChemiDoc Documentation System (Bio-Rad, Ireland). To confirm equal amount of protein loaded for each sample, β -actin was always used as internal control.

3.7.4. Protein expression detection

For AhR receptor detection whole platelets lysate was prepared and subjected to electrophoresis in 8% acrylamide ge Anti AhR antibody (Santacruz, USA) used to detect AhR receptor.

Non-phosphorylated and phosphorylated VASP at serine 238 and serine 157 was investigated using 10% acrylamide gel. 50 μg of platelet protein were loaded in each lane and phosphorylated VASP was determined at 49 KD using

anti-phosphorylated VASP 238 and anti-phosphorylated VASP 157 (LSBio, USA). Non phosphorylated VASP was investigated at 46 KDa using VASP antibody (Santacruz, USA). SNAP 250 μ M used as positive control for VASP phosphorylation at serine 238 [297] while forskolin 4 μ M as positive control for VASP phosphorylation at serine 157 [56]. The percentage of phosphorylated VASP was calculated by dividing the intensity of the bands of phosphorylated VASP measured by densitometry by its corresponding total VASP (phosphorylated plus the non-phosphorylated VASP).

Primary antibody against indoleamine dioxygenase (IDO) (Abcam, UK), which detects the induced IDO protein expression at 50KDa was used to investigate IDO induction in A549, SW-480 and HCC-1954 cell samples using 8% acrylamide gel.

3.8. Flow cytometry

The abundance of activated GPIIb/IIIa and P-selectin receptors on the surface of platelets in the presence and absence of kynurenine (250 μ M -1 mM) was investigated to corroborate the inhibitory of kynurenine on platelet aggregation induced by collagen 4 μ g/ml and TCIPA induced by 2000 cell/mL. Kynurenine was incubated with PRP (250,000 platelets/ μ L) for at least 2 minutes under stirring at 37 °C in the aggregometer prior to platelet activation with collagen or in the presence and absence of ODQ 10 μ M. For TCIPA, kynurenine (100-500 μ M) was incubated with WP for at least 2 minutes prior to induction of TCIPA by 2000 cell/mL of A549 or HCC-1954. Percentage of platelet aggregation was continuously monitored and once the traces reached 50% of the maximal light transmission, 10 μ L of PRP for every sample was taken from the cuvette and placed in an Eppendorf tube with 0.25 μ g of the correspondent antibody : monoclonal FITC conjugated mouse anti-human PAC-1 antibody and PE conjugated mouse anti human CD62P antibody (Biosciences, UK) for measuring both, GPIIb/IIIa and P-selectin expression respectively. Samples were then diluted with physiological saline (five-fold dilution) and incubated in the dark for 5 minutes. Finally, samples were diluted once again with physiological saline (five-fold dilution) and analysed by a BD ACCURI C6

(Biosciences, UK). Resting platelets and platelets activated with collagen in the absence of kynurenine were used as controls.

The instrument was set up to measure size (forward scatter), granularity (side scatter) and fluorescence (FITC: excitation 480nm and emission 530 and PE: excitation 488 and emission 590). Antibody binding was measured by analysing individual platelets for fluorescence (10,000 events). A two-dimensional analysis gate of forward and side scatter was drawn so as to include single platelets and exclude platelet aggregates and microparticles. The mean fluorescence intensity was determined after correction for cell autofluorescence. For each sample, the fluorescence was analysed using a logarithmic scale using the BD-Accuri software and expressed as a percentage of control fluorescence in arbitrary units.

3.9. Intraplatelet cGMP and cAMP measurement

Intraplatelet cGMP and cAMP were determined using enzyme-linked immunosorbent assay (ELISA) kits (Genie, Ireland) following manufacturer instructions. Briefly, 1 mL of PRP was incubated with 3-isobutyl-1-methylxanthine (IBMX) (1 mM) for 10 minutes prior to incubation with kynurenine (500 μ M and 1 mM) for 2 minutes in the presence or absence of collagen and ODQ (Sigma, Germany). SNAP (Sigma, Germany) is a nitric oxide donor and was used as a positive control for activation of sGC enzyme by NO. Afterwards, platelets were pelleted by centrifugation at 3,000 rpm for 10 minutes at 4 °C, hydrolysed in 300 μ L of 0.1 M HCl, centrifuged at 1000 xg for 10 minutes at 4 °C. and cGMP and cAMP concentration measured in the supernatants.

Standards and samples from three independent blood donors were tested in duplicate.

3.10. HPLC

High Performance Liquid Chromatography (HPLC) was used to quantify the concentration of tryptophan and kynurenine in culture media samples by reverse-phase HPLC method using an Alliance HPLC System from Waters equipped with vacuum degasser; UV and fluorescence wavelength detectors. Luna C18 column (250 mm×4.6 mm, 5 µm) was used for the analysis at 40°C. Separation was carried out using mobile phase consists of 15 mM acetate buffer (pH 4) and acetonitrile (95:5, v/v) at a flow rate of 1 mL/min and 100 µL injection volume.

Kynurenine was detected by the UV detector at 360 nm whereas tryptophan was detected by the fluorescence detector at excitation wavelength of 254 nm and emission wavelength at 404 nm. Retention time of kynurenine was 6.4 minutes, and 11.9 minutes for tryptophan.

3.10.1. Kynurenine measurements

A standard curve was constructed using seven standard concentrations from 1,000 nM to 3.9 nM of kynurenine by serial dilution. The mean peak area of at least 3 independent experiments was calculated by linear regression (table 3-1 and figure 3-2). The regression slope and standard deviation were used to obtain the limit of detection (LOD) and the limit of quantification (LOQ) resulting in 4.5 nM and 13.7 nM respectively:

Limit of Detection (LOD)= $(3.3 \times \text{SD}) / \text{Slope} = (3.3 \times 22.67) / 16.46 = 4.5 \text{ nM}$

Limit of Quantification (LOQ)= $(10 \times \text{SD}) / \text{Slope} = 13.7 \text{ nM}$

Kynurenine Concentration (nM)	Mean peak area
1,000	16493.66667
500	8249.166667
250	4159.833333
125	2085.5
62.5	1090.166667
31.25	517.3333333
15.7	225.27537
Standard deviation (SD)	22.67
Slope	16.46
Correlation Coefficient	1

Table 3-1: Mean peak area of Kynurenine standard (1,000-15.7nM). Data represent the mean of at least three experiments carried out on different days.

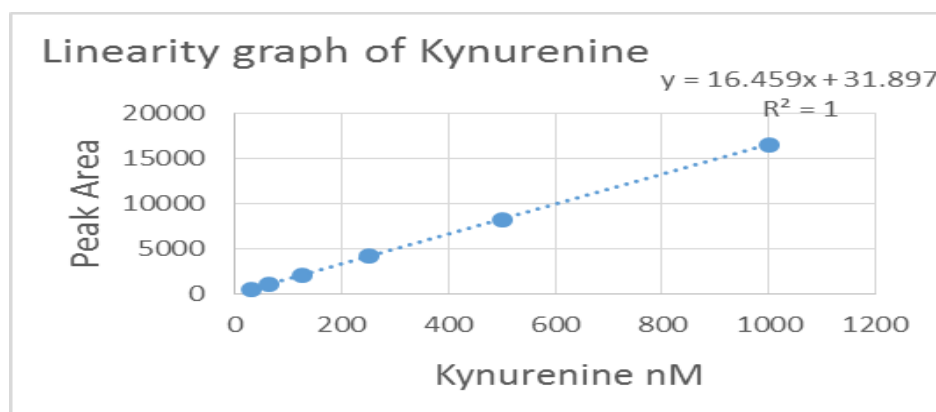


Figure 3-2: Standard curve for measuring kynurenine concentrations by HPLC. Representative graph showing the linear regression relationship between kynurenine concentration (nM) (1000-31.25nM) and the peak area obtained for each concentration.

To determine the accuracy of the method, six replicate standard solutions of kynurenine (at 1 μM) were prepared and analysed using the proposed method. The relative standard deviation (% RSD) for peak responses was calculated and found to be less than 2.0% (table 3-2)

INJECTION	INTRA DAY	INTER DAY
1	16504.5	16504.5
2	16576	16400.5
3	16400.5	16576
4	16504.5	16795
5	16564	16391
6	16445	16580
RSD %	0.40957543	0.900090078

Table 3-2: Relative standard deviation (RSD) of six kynurenine (1 μM) replicates on interday and intraday intervals.

3.10.2. Tryptophan measurements

Standard curves were constructed using standard concentrations of tryptophan from 1,000 nM to 3.9 nM of by serial dilution. The mean peak area was plotted versus concentrations for calculating tryptophan concentration by linear regression (table 3-3 and figure 3-3). Slope and standard deviation were used to quantify the limit of detection (LOD) and the limit of quantification (LOQ).

Tryptophan Concentration (nM)	Mean Peak area
1000	2161122
500	1118247.5
250	578235.5
125	294172
62.5	154902.5
31.25	80450
15.625	40050
7.8	24760
3.9	11330
Standard deviation	12620
Slope	2196
Correlation coefficient	0.9997

Table 3-3: Mean peak area of Tryptophan standards (1,000-3.9nM) of at least three experiments on different days.

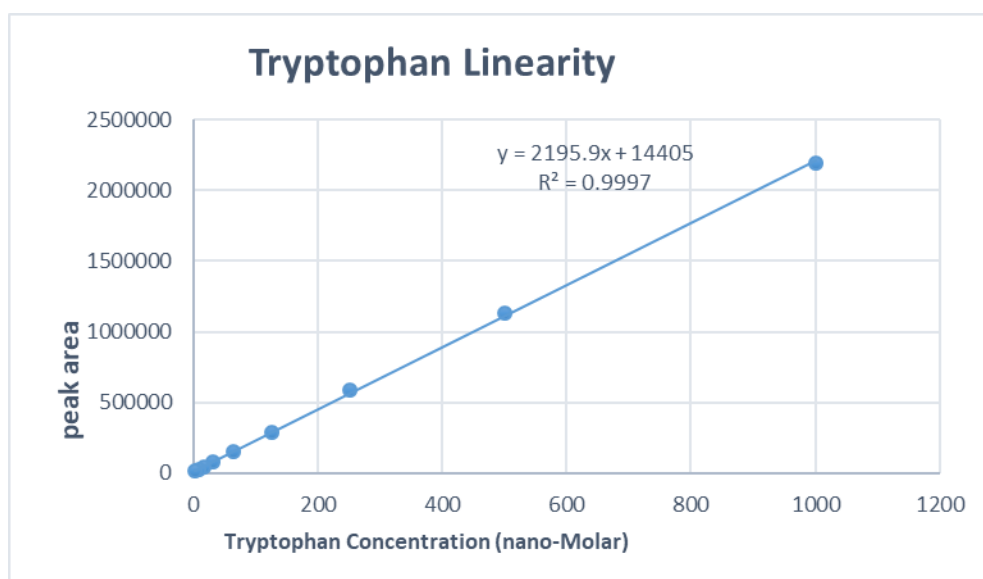


Figure 3-3: Linear regression relationship of Tryptophan concentrations (nM) (1000-3.9nM) and the mean peak area

To determine the accuracy of the method, six replicate standard solutions of tryptophan (1 μM) were prepared and analysed using the proposed method. The relative standard deviation (% RSD) for peak responses was calculated and it was found to be less than 2.0% (table 3-4)

INJECTION	INTRA DAY	INTER DAY
1	2178673	2161122
2	2170148	2167312
3	2165063	2174410.5
4	2169561	2261022.5
5	2162139	2262459
6	2160105	2259586
RSD %	0.309736407	2.11

Table 3-4: The relative standard deviation (RSD) of six Tryptophan (1 μM) replicates on interday and intraday intervals

Limit of detection (LOD)= $(3.3 \times \text{SD}) / \text{Slope} = (3.3 \times 12620) / 2196 = 18.96 \text{ nM}$

Limit of Quantification (LOQ)= $(10 \times \text{SD}) / \text{Slope} = (10 \times 12620) / 2196 = 57.46 \text{ nM}$

3.11. Statistical analysis

Data from at least three independent experiments were analysed using GraphPad Prism 5 software (GraphPad Software, La Jolla, CA, USA). All means are reported with standard deviation. Paired Student's t-tests, one-way analysis of variance (ANOVA) followed by Dunnett's or Tukey multiple comparisons post-test were performed as appropriate. Statistical significance was considered at $P < 0.05$.

4. Results and discussion

4.1. Effect of kynurenine on platelet function

The main and first aim of this research was to investigate the potential role of kynurenine on platelet function. For this purpose, platelets first incubated with various kynurenine concentrations (25 μ M-1mM) for two minutes and response to platelet agonists measured by LTA. Different agonists that have different potencies and act through different pathways were used to induce platelet aggregation on PRP and/or WP. The physiological adults' plasma concentration of kynurenine is about (1.5-2.5 μ M) while the induced plasma concentration during sepsis approximately (2.4-5.2 μ M)[298]. However, supraphysiological concentrations of kynurenine and platelet 's agonists were used during the course of this study to confirm the potency of kynurenine in modulation of platelet function.

4.1.1. *Thromboxane analogue (U46619)*

Thromboxane analogue act through the G protein–coupled thromboxane receptor(TP) on the platelet surface activating Gq and G12/G13 pathways [27]. The thromboxane analogue U46619 (1 μ M), which is the same concentration used by other researchers to induce platelet aggregation [299],was used to induce platelet aggregation in PRP and WP preincubated for 2 minutes with increasing concentrations of kynurenine (from 25 μ M up to 1 mM) using LTA. Kynurenine inhibited platelet aggregation induced by U46619 in a concentration dependent manner in both PRP and WP, as shown in figures 4-1 and 4-2.

Note: dimethyl sulfoxide (DMSO) was used as vehicle for kynurenine, therefore the effect of this solvent was also tested in all experiments at the relevant or maximum volume used due to its potential effect on platelet function [300].

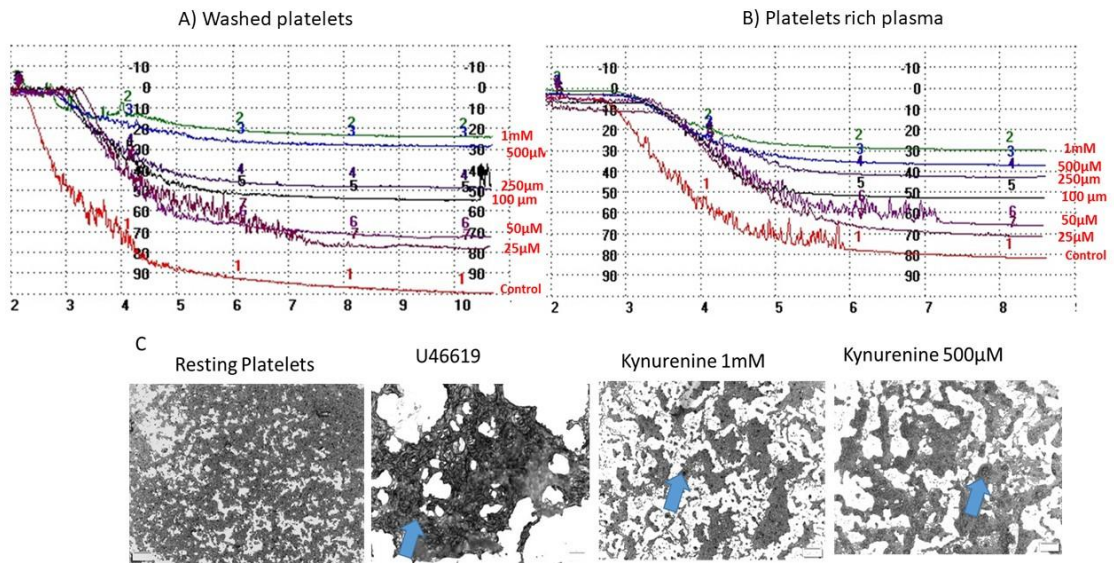


Figure 4-1: Effect of kynurenine on thromboxane analogue (U46619) induced platelet aggregation.

Representative traces from light transmission aggregometer showing that kynurenine inhibits platelet aggregation induced by U46619 in a concentration dependent manner in (A) Washed platelets and (B) Platelet Rich Plasma. Representative micrographs from optical microscopy (C) showing Resting platelets , Platelet aggregation induced by U46619 and the effect of kynurenine at 1 mM and 500 µM on platelet aggregation induced by U46619 (5X objective). The light grey areas represent resting platelets and the darker areas (blue arrows) platelet aggregates.

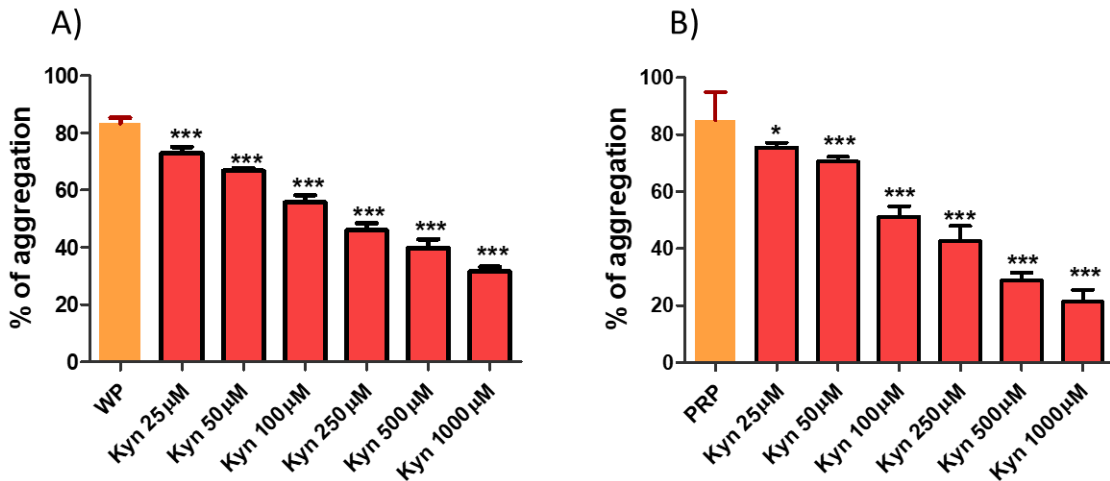


Figure 4-2: Effect of kynurenine on thromboxane analogue (U46619) induced platelet aggregation.

Statistical analysis showing that kynurenine (Kyn) inhibited platelet aggregation induced by the thromboxane analogue (U46619) in washed platelets (WP) (A) and platelet rich plasma (PRP) (B). Data is represented as mean \pm SD; n=4; One-way ANOVA & Dunnett's Multiple Comparison Test. *** P < 0.001; ** P < 0.01 vs Control (WP or PRP).

4.1.2. Arachidonic acid

Arachidonic acid (AA) is the precursor of TXA₂ by the action of the cyclooxygenase (COX-1) and thromboxane synthase enzymes [27, 222]. Incubation of WP and PRP with kynurenine also resulted in inhibition of AA-induced platelet aggregation (figures 4-3 and 4-4). Aspirin 1 mM was used as a positive control for COX-1 inhibition in this set of experiments [301].

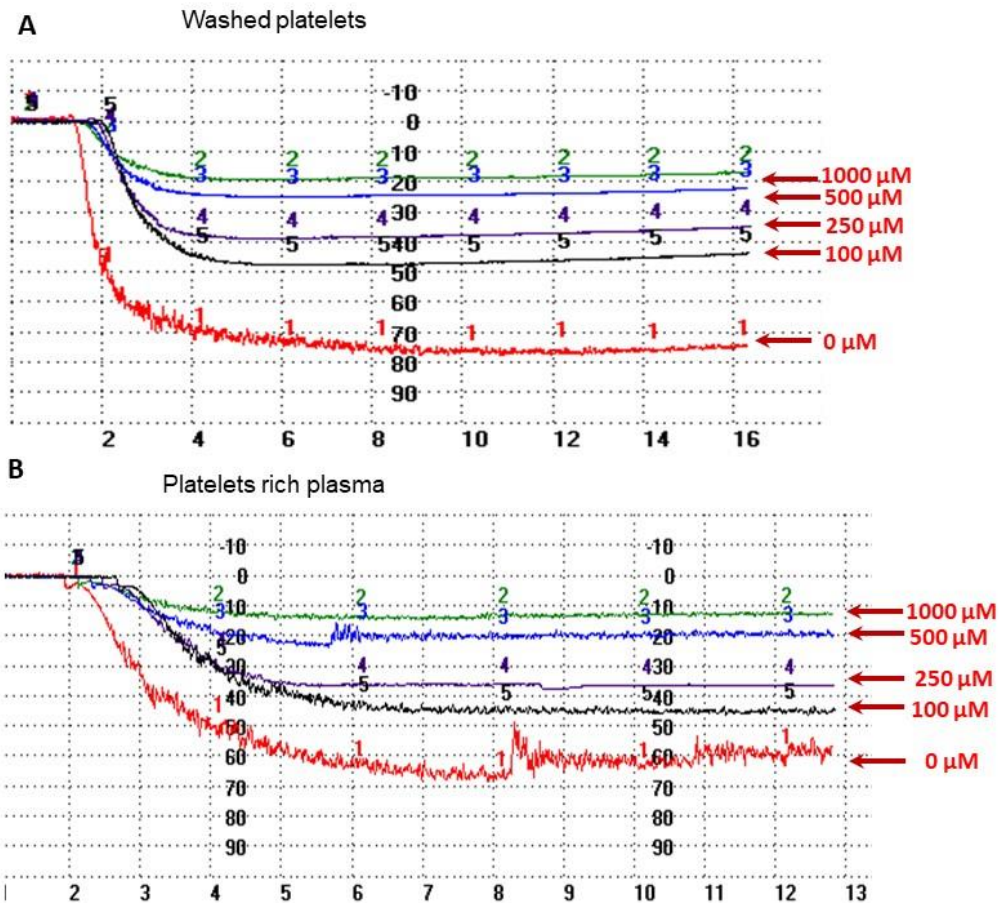


Figure 4-3: Effect of kynurenine on arachidonic acid- induced platelet aggregation.

Representative traces from light transmission aggregometry showing that kynurenine inhibits platelet aggregation induced by arachidonic acid in a concentration dependent manner in washed platelets (A) and platelet rich plasma (B)

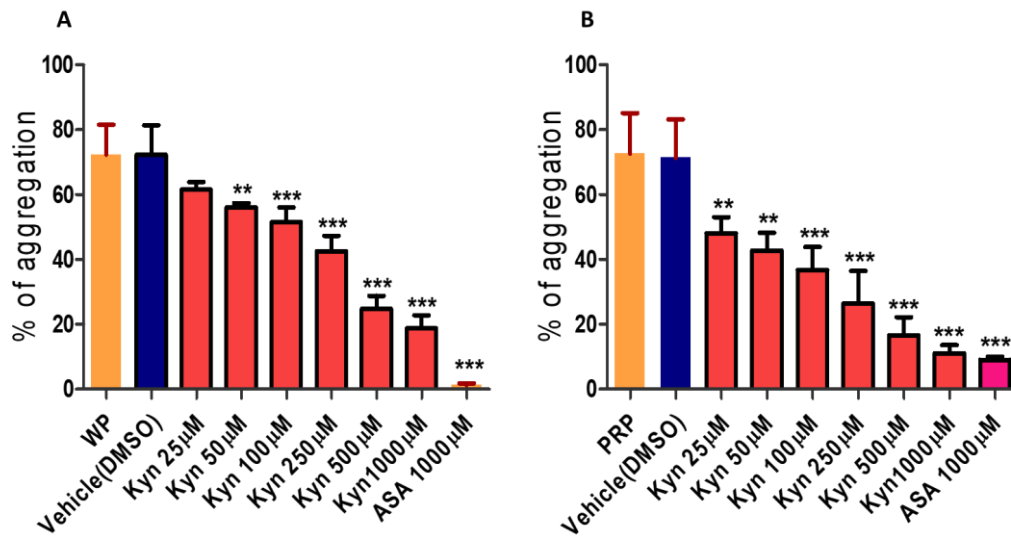


Figure 4-4: Effect of Kynurenine on arachidonic acid induced platelet aggregation.

Statistical analysis. Kynurenine inhibited arachidonic acid- (7.65 μM) induced platelet aggregation in washed platelets (WP) (A) and arachidonic acid- (1.53 mM) induced platelet aggregation in platelet rich plasma (PRP) (B). Aspirin 1mM was used as a positive control as inhibitor of arachidonic acid- induced platelet aggregation. Data is presented as mean ± SD, One-way ANOVA & Dunnett's Multiple Comparison Test; n=4; *** P<0.001, **P<0.01 VS Control (PRP and/or WP).

4.1.3. Adenosine diphosphate (ADP)

ADP induces platelet aggregation acting on P2Y1 and P2Y12 G-protein coupled receptors on platelets surface and activating Gq and Gi proteins [15, 16].

Kynurenine significantly inhibited ADP(10 μ M)- induced platelet aggregation in PRP (figures 4.5 and 4.6).

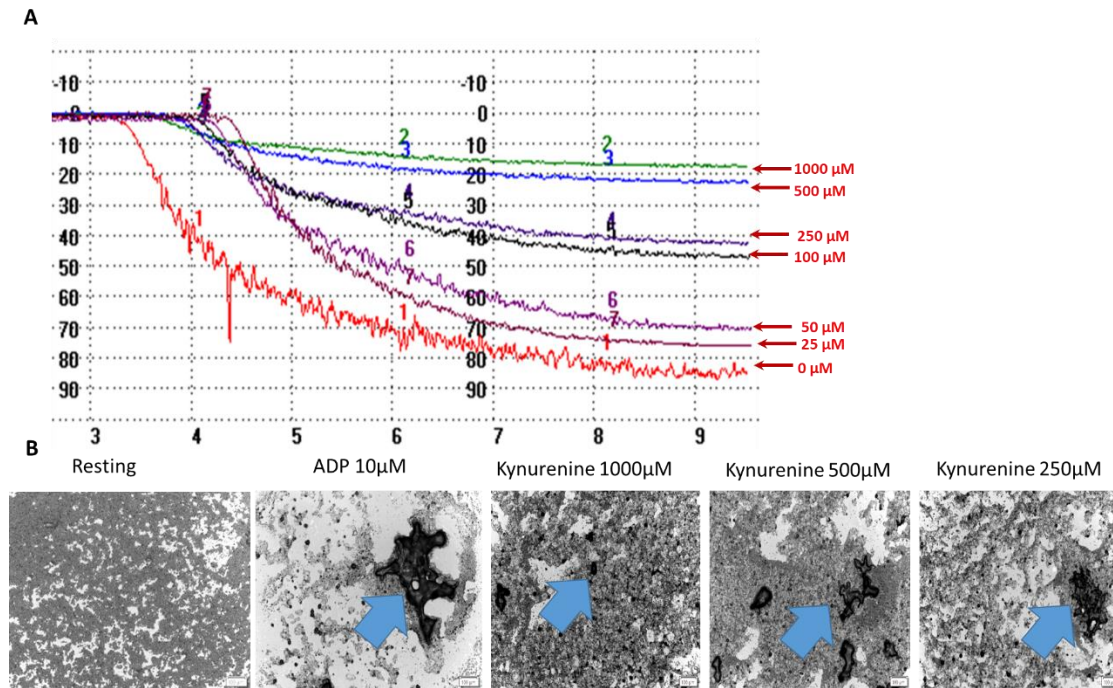


Figure 4-5: Effect of kynurenine on ADP- induced platelet aggregation. (A) Representative traces from light transmission aggregometer in platelet rich plasma (PRP). Kynurenine inhibited platelet aggregation induced by ADP 10 μ M in a concentration dependent manner. (B) Micrographs from optical microscopy showing the effect of Kynurenine on ADP- induced platelet aggregation in PRP (10X objective). The light grey areas correspond to non-aggregated (resting) platelets and the darker areas to platelet aggregates (blue arrows).

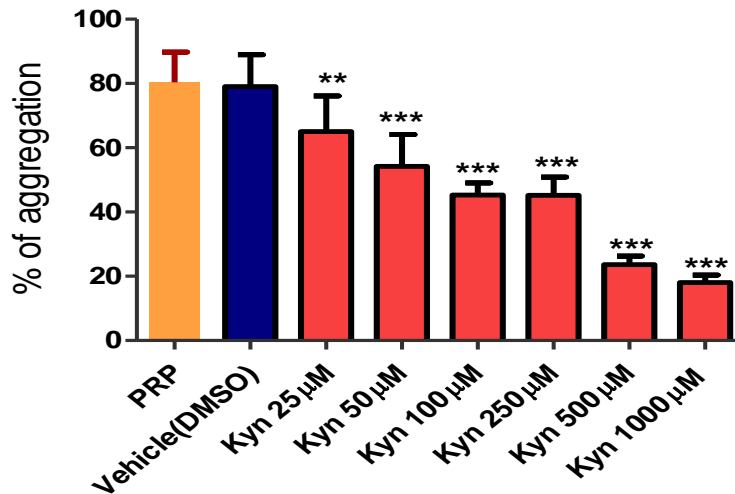


Figure 4-6: Effect of Kynurenine on ADP- induced platelet aggregation. Statistical analysis. Kynurenine (from 25µM to1mM) inhibited ADP-10µM induced platelet aggregation in platelet rich plasma. Data is presented as mean ± SD; One-way ANOVA & Dunnett's Multiple Comparison Test; n=6; *** P<0.001, **P<0.01 VS control (PRP).

4.1.4. Serotonin

Both, kynurenine and serotonin, derived from tryptophan [81] and an increased tryptophan metabolism into kynurenine limits the synthesis of other tryptophan metabolites including serotonin [302] [96]. It is known that serotonin (5-HT) has the ability to enhance the aggregating response of platelets to platelet agonists such as ADP [303]. In this set of experiments serotonin, at 10 µM in PRP and 50 µM in WP was used, as previously described in the literature, to induce platelet aggregation [304, 305]. However, the percentage of platelet aggregation obtained using those concentrations was very limited (as shown in figure 4.7) and therefore, higher concentrations (up to 200 µM) were also tested. Unfortunately, platelet aggregation induced by serotonin at higher concentrations was not consistent and not reproducible. Similar results have been also obtained by other researchers in the past [303]. Therefore, those experiments were not pursued further as it was considered not appropriated to evaluate the potential effect of kynurenine under these circumstances.

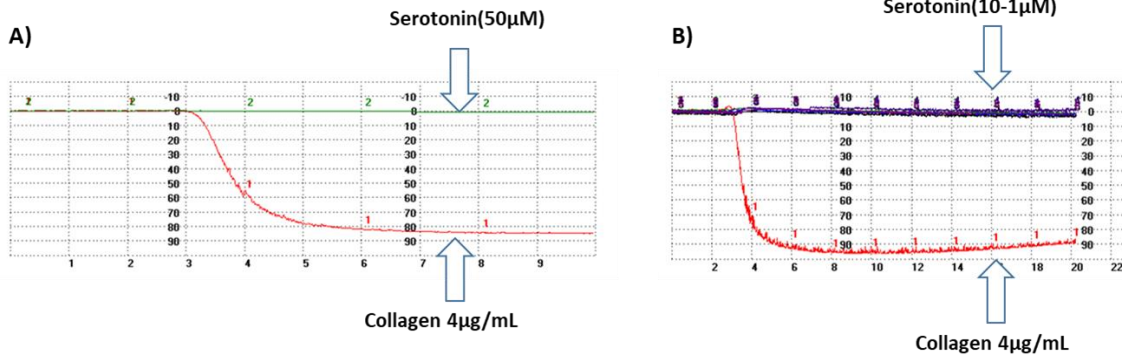


Figure 4-7: Effect of serotonin on platelet aggregation. Representative traces from light transmission aggregometry showing no effect of serotonin (50µM) on washed platelets (A) and serotonin (1-10µM) on platelet rich plasma. Collagen 4 µg/mL used as positive control for testing platelets reactivity.

4.1.5. Collagen

Collagen is a potent activator of platelet aggregation. It works by binding to the platelet glycoprotein receptor GPVI and integrin receptor GPIa/IIa and activates different signalling pathways that result in platelet aggregation [13, 14].

Collagen 4 $\mu\text{g}/\text{mL}$ was used to induce platelet aggregation in both WP and PRP. Kynurenine (25 μM -1 mM) pre-incubated for 2 minutes with WP and PRP significantly inhibited collagen-induced platelet aggregation in a concentration-dependent manner (figures 4.8, 4.9 and 4.10).

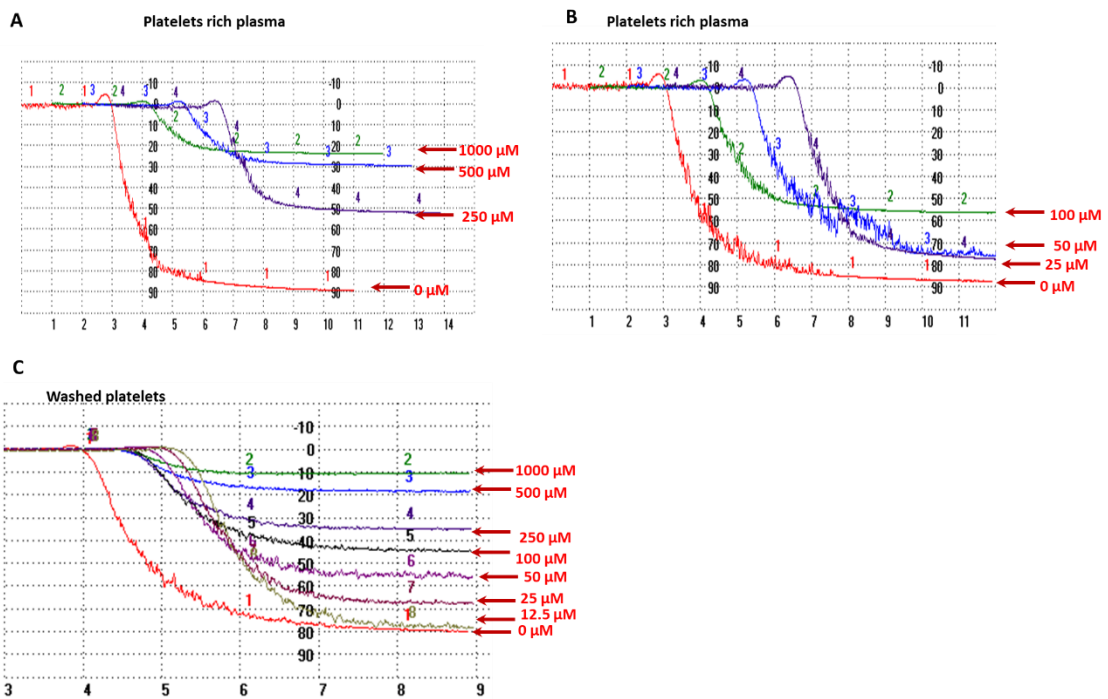


Figure 4-8: Effect of kynurenine on collagen- induced platelet aggregation. Representative traces from light transmission aggregometry showing that Kynurenine inhibits platelets aggregation induced by collagen 4 $\mu\text{g}/\text{mL}$ in a concentration- dependent manner in platelet rich plasma (A and B) and washed platelets (C).

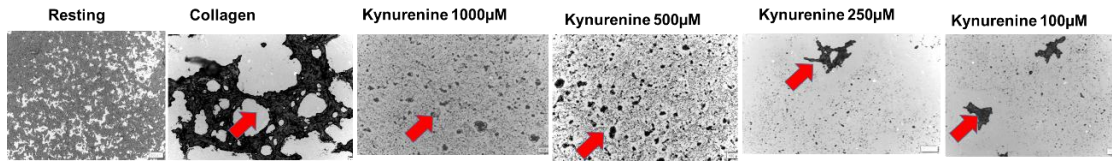


Figure 4-9: Micrographs from optical microscopy (5X objective) showing the effect of kynurenine on platelet aggregation induced by collagen. The light grey areas correspond to non-aggregated (resting) platelets and the darker areas to platelet aggregates (red arrows)

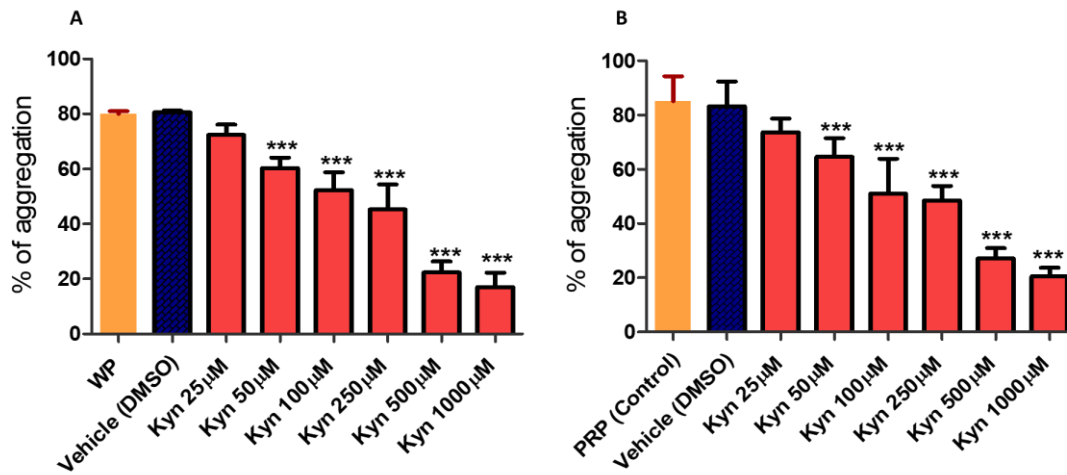


Figure 4-10: Effect of kynurenine on collagen- induced platelet aggregation Statistical analysis. Kynurenine (25-1000µM) inhibited collagen- induced platelet aggregation in washed platelets (WP) (A) and platelet rich plasma (PRP) (B). Data is presented as mean \pm SD of n=6 experiments. One-way ANOVA & Dunnett's Multiple Comparison Test. *** P<0.001 VS Control (WP, PRP).

4.1.6. Effect of kynurenine on the expression of platelet receptors

To confirm further the inhibitory effect of kynurenine on platelet's function, the expression of activated GPIIb/IIIa and P-selectin on platelets surface was measured by flow cytometry. The expression of the activated integrin GPIIb/IIIa, which is responsible for the cross bridging of activated platelets by fibrinogen[36, 37], was significantly decreased in platelets incubated with kynurenine when compared to platelets incubated with the vehicle and stimulated with collagen. In fact, kynurenine downregulated the expression of activated GPIIb/IIIa in a concentration dependent manner as shown in figures 4-11 and 4-12A. Kynurenine also downregulated the surface expression of P-selectin as shown in figures 4-11 and 4-12B, thus kynurenine seems to stabilise platelet granules and prevent the release and translocation of P-selectin receptors to the platelet surface following platelet activation by collagen.

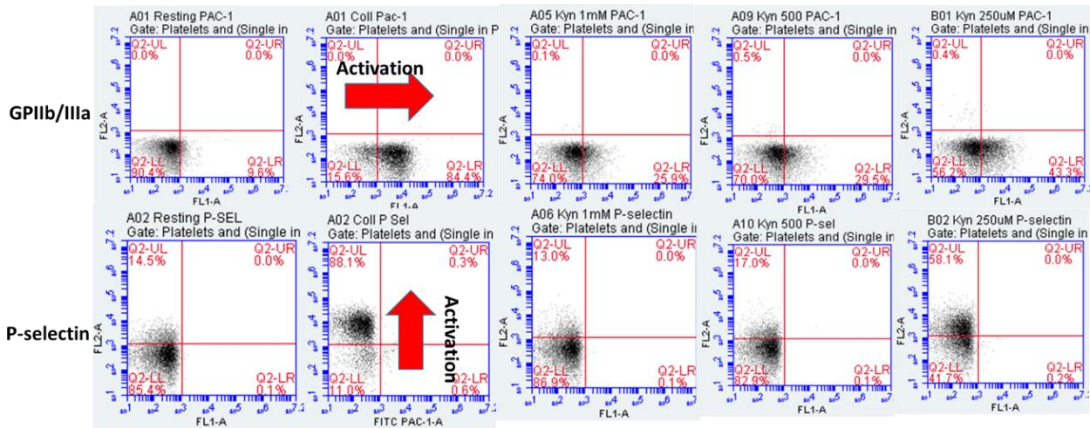


Figure 4-11: Representative gates from flow cytometry showing the effect of kynurenine on platelet expression of GPIIb/IIIa and P-selectin. Shifting of platelets population from left lower (LL)quadrant to right lower (RL) quadrant, indicates increased GPIIb/IIIa expression while shifting from in left lower(LL) quadrant to left upper (LU) quadrant indicates higher P-selectin expression.

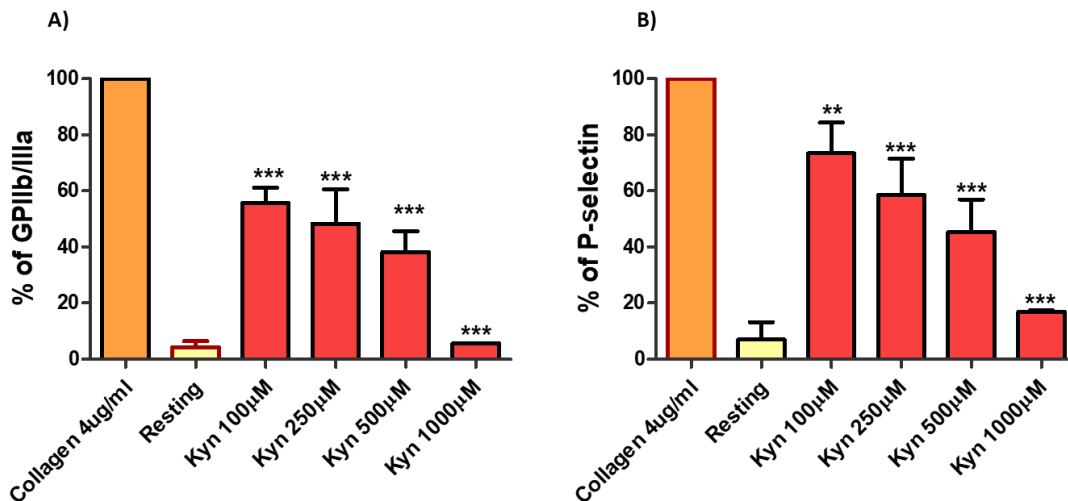


Figure 4-12: Effect of kynurenine on platelet expression of GPIIb/IIIa and P-selectin by flow cytometry. Statistical analysis showing a significant decrease of activated GP IIb/IIIa (A) and P-selectin (B) receptors expression by kynurenine (100 µM- 1 mM-) in response to collagen 4 µg/mL. Results were compared to the number of receptors present of platelets stimulated with collagen that were considered as 100% of expression. Data is presented as the mean ± SD; n=4; One-way ANOVA and post Tukey's test. *** P < 0.001; ** P < 0.01 vs collagen.

It was demonstrated for the first time that kynurenine was able to inhibit platelet aggregation induced by a wide range of platelet agonists, the next steps in this research were focused on investigating further this phenomenon to elucidate the potential mechanism of action of kynurenine on human platelets

4.2. Potential mechanisms of action of kynurenine on human platelets

4.2.1. *Kynurenine and the aryl hydrocarbon receptor.*

Having found that kynurenine can inhibit collagen, ADP, AA- and thromboxane analogue (U46619)- induced platelet aggregation in a concentration dependent manner, and because kynurenine is an AhR receptor agonist, the following step was to find out if kynurenine could exert its effect through the AhR receptor.

However, platelets are unnucleated and AhR genomic pathway may not be the proper pathway through which kynurenine exerted its effect. Also, AhR non genomic pathway involve elevation in AA and COX activity in platelets causing platelet aggregation [306].

First, immunoblotting was performed using an anti AhR antibody (Santacruz, USA) to demonstrate the presence of AhR in platelets. As shown in figure 4-13 AhR was expressed in human whole platelet lysate of four independent blood donors which is in agreement with the results previously obtained by Pombo et al [306] and Lindsey et al [307]

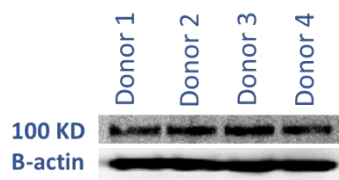


Figure 4-13: Immunoblotting showing the expression of AhR receptor (100KD) in platelets. Washed platelets from four donors analysed in 8% acrylamide gel using semidry transfer to PVDF membrane. 50µg of protein was loaded per lane. B-actin was used as protein-loading control.

It was proposed that if kynurenine was able to modify platelet function through AhR receptor, other AhR agonists might exert the same effect as kynurenine and inhibit platelet function and AhR receptor antagonists may attenuate inhibitory effect of kynurenine. Based on these assumptions, three different compounds were tested for their potential ability to modulate platelet function: (a) 2,3,7,8-tetrachlorodibenzo-p-dioxin (TCDD), a potent AhR ligand, and (b) 6-formylindolo [3, 2-b] carbazole (FICZ), a highly selective AhR ligand, [1, 4] were first used to examine if they would exert any inhibitory effect on platelet function and (3) 6,2',4'-trimethoxyflavone (TMF), a selective AhR antagonist [5] was used to investigate if the inhibitory effect of kynurenine on platelets could be affected.

4.2.2. Effect of FICZ on collagen-induced platelet aggregation

FICZ is a photoproduct of tryptophan and a highly selective AhR receptor agonist [308]. Preincubation of WP and PRP with FICZ (100 nM) for 2 minutes had no effect on platelet response to platelet aggregation induced by collagen at 4 µg/mL (Figure 4-14).

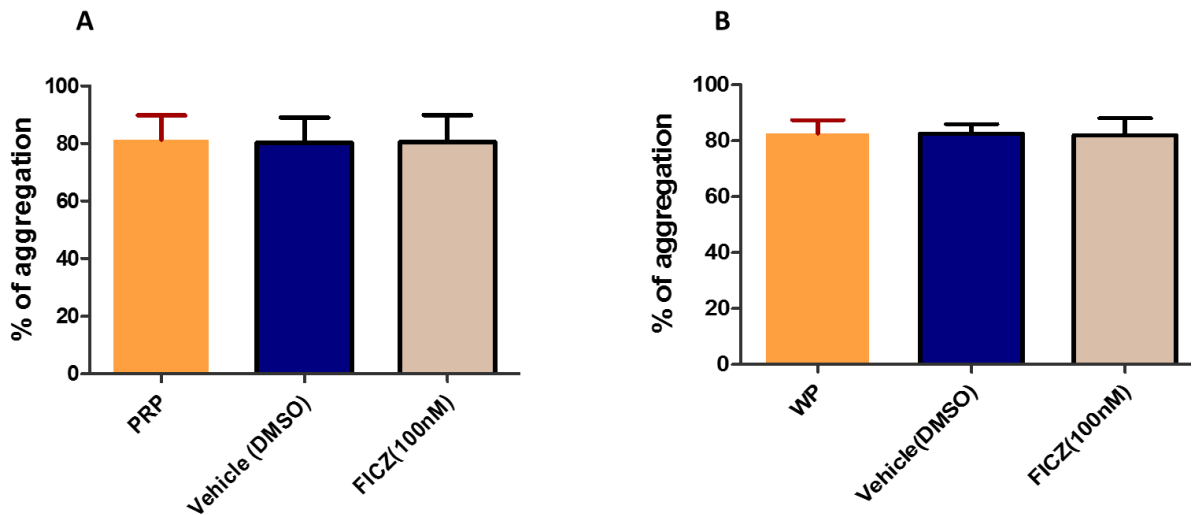


Figure 4-14: Effect of FICZ on collagen-induced platelet aggregation. Statistical analysis. FICZ did not modify platelets response to collagen after 2 minutes of incubation with washed platelets (WP) (A) and platelet rich plasma (PRP) (B). Data is presented as the mean \pm SD of four independent experiments. One-way ANOVA ($P > 0.05$)

4.2.3. Effect of TCDD on collagen-induced platelet aggregation

The halogenated aromatic hydrocarbon TCDD is a potent AhR ligand [134]. TCDD was used at 10, 20, 40 and 62 nM to examine its effect on platelets in the presence of collagen at 4 $\mu\text{g}/\text{mL}$. Incubation of WP and PRP for 2 minutes with TCDD at the concentrations tested did not modify the effect of collagen on platelet aggregation (figure 4-15)

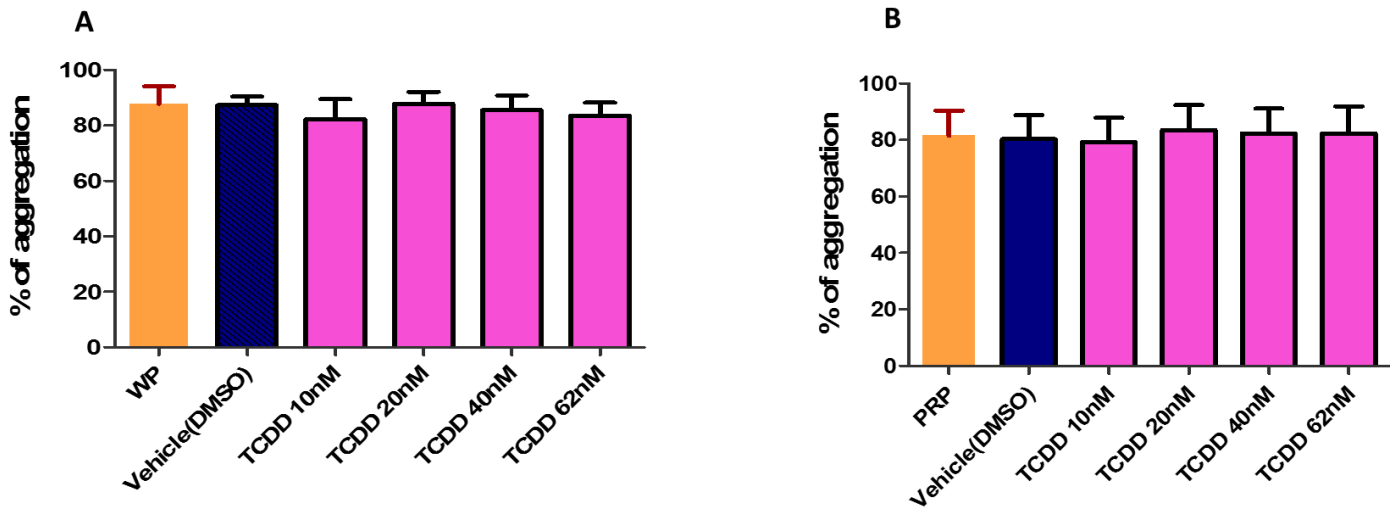


Figure 4-15: Statistical analysis of the effect of TCDD on collagen-induced platelet aggregation. TCDD did not affect platelets response to collagen 4 $\mu\text{g}/\text{mL}$ after 2minutes incubation with washed platelets (WP) (A) and platelet rich plasma (PRP) (B). Data is presented as mean \pm SD; n=4; One-way ANOVA ($P > 0.05$)

4.2.4. Effect of TMF on collagen-induced platelet aggregation

TMF is classified as a pure AhR receptor antagonist [136]. TMF at 10 μM incubated for 2 minutes with WP and PRP did not induce platelet aggregation and did not modify the effect of collagen on platelet aggregation as shown in figure 4-16.

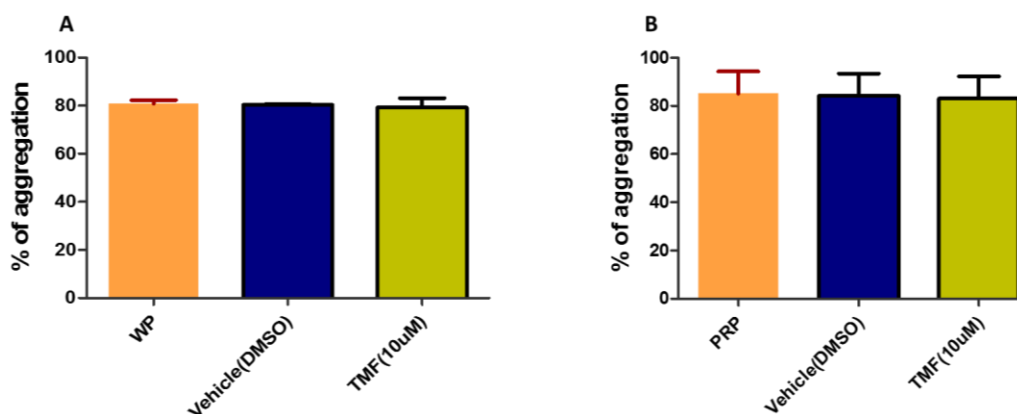


Figure 4-16: Effect of TMF on collagen-induced platelet aggregation. TMF showed no effect on collagen-induced platelet aggregation after 2 minutes of incubation with washed platelets (WP) (A) and platelet rich plasma (PRP) (B). Data is presented as the mean \pm SD; n=4 (WP); n=6 (PRP). One-way ANOVA ($P > 0.05$)

At the concentrations tested, neither AhR agonists nor AhR antagonist significantly induced or inhibited collagen-induced platelet aggregation when human platelets were preincubated for a period of time up to 2 minutes. However, Lidsey et al, have recently shown that platelets from AhR null mice had impaired aggregation in response to collagen, but not to thrombin and ADP when compared to wild type. The group proposed a role of the AhR in collagen signalling pathway as platelets from the AhR null mice showed a drastic downregulation of Vav1 and Vav3, which interfere with PLC- γ 2 activation; reducing Rac1 activation and consequently, platelet activation [307]. Although, TMF pre-incubated with human platelets did not show any abnormal response to collagen, one would argue that it is not expected that TMF would block the AhR receptor completely or would interfere with Vav1 or Vav 3 expression within such a short period of time.

ADP acts through P2Y1 and P2Y12 surface receptor activating Gq and Gi proteins leading to activation of PLC- β (Gq), inhibition of adenylyl cyclase [31, 32] and activation of PI3K through activation of β/γ -complex [309]. Kim et al found that, in zebrafish thrombocytes, TCDD 10nM activated cytosolic src-family kinase (c-src) and signalled the activation of Akt and ERK1/2 involved in generation of TXA₂. Furthermore, they also observed that ADP was able to activate AhR in the absence of TCDD and that ADP potentiated TCDD effect [310].

Therefore, we next sought to examine the effect of AhR agonists and antagonist in ADP-induced platelet aggregation.

4.2.5. Effect of FICZ and TCDD on ADP-induced platelet aggregation

In this set of experiments, FICZ (100 nM) and TCDD (10, 20, 40 and 62 nM) preincubated for 2 minutes in PRP did not cause any significant change in platelets response to 10 μ M of ADP as shown in figure 4-17.

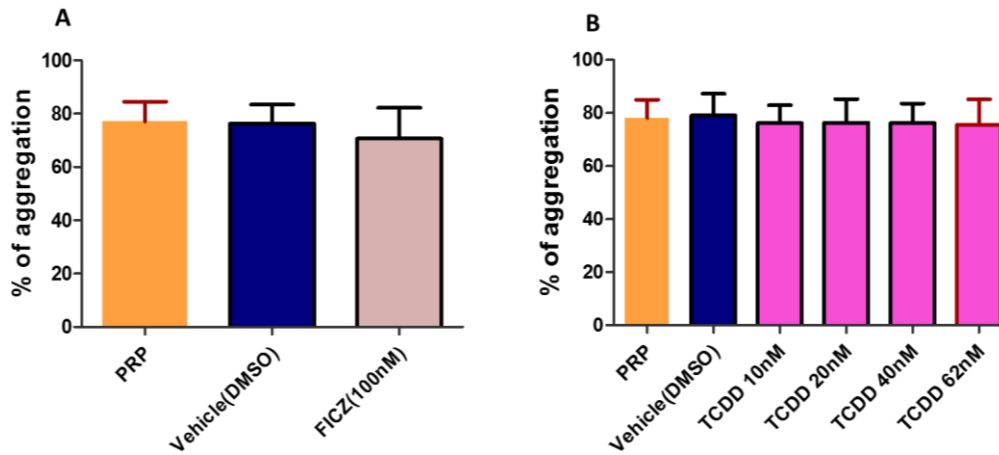


Figure 4-17: Statistical analysis of the effect of FICZ and TCDD on ADP-induced platelet aggregation. (A) Effect of FICZ 100 nM.(B) Effect of TCDD. Data is presented as the mean \pm SD, One-way ANOVA ($P > 0.05$)

Pumbo et al have previously found that the preincubation of AhR agonists (TCDD up to 1 nM and Omeprazole up to 100 nM) for 1 hour with human PRP primed platelets to SFLLRN 10 μ M (thrombin analogue) and induced phosphorylation of P38 MAPK and its downstream effector PLA2 which mediates the movement of AA from the plasma membrane to the cytosol in platelets through the AhR non-genomic pathway [306].

Therefore, and to exclude the possibility that the AhR agonists used in our study might need longer incubation times to exert their effect, PRP was incubated in the presence and absence of TCDD and FICZ at the same concentrations that previously tested but for up to 60 minutes, and platelet aggregation induced by ADP 10 μ M and monitored by LTA.

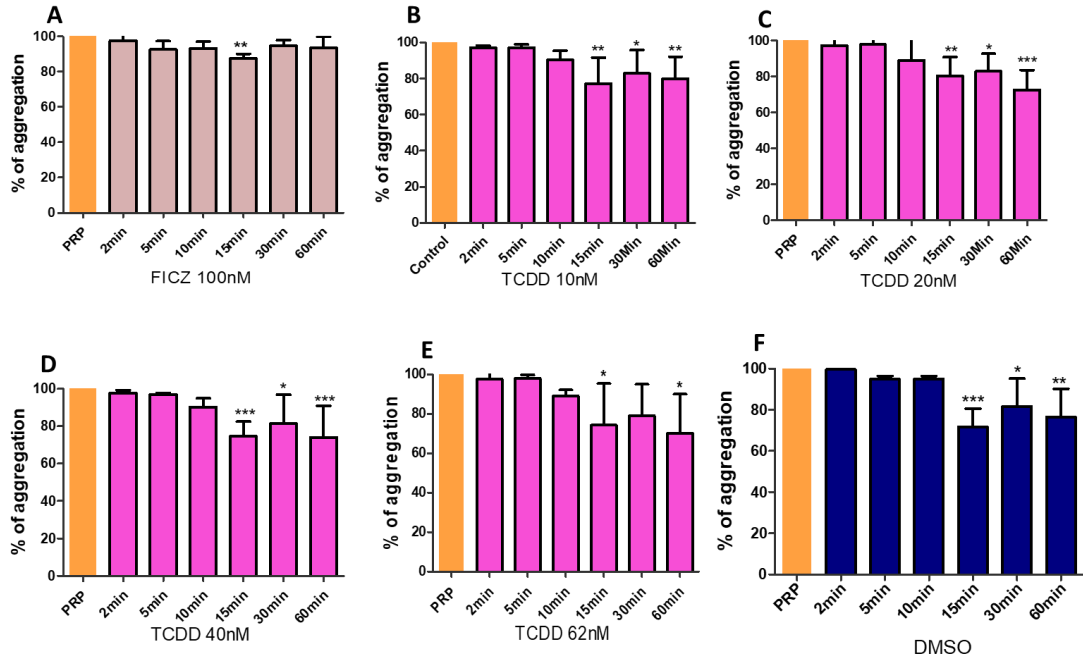


Figure 4-18: Statistical analysis of the effect of incubation over-time of FICZ and TCDD on ADP-induced platelet aggregation. FICZ 100 nM (A); TCDD 10 nM (B); TCDD 20 nM (C); TCDD 40 nM (D); TCDD 62nM (E) and DMSO (F). Data is presented as mean \pm SD; n=5; One-way ANOVA & Dunnet post-test; *** P < 0.001, ** P < 0.005, * P < 0.05 vs platelet rich plasma (PRP).

As shown in figure 4-18, preincubation of platelets for longer periods of time with FICZ, TCDD and DMSO (vehicle) resulted, most of the times, in a significant inhibition of ADP-induced platelet aggregation when they were incubated with the platelet suspension for 15 minutes or longer. However, when the inhibitory effect of the AhR agonists was compared to the effect of the vehicle (DMSO), incubated for the same periods of time, no significant differences were found (figure 4-19). It has been previously reported in the literature that the use of 0.5% of DMSO strongly inhibits shear stress-induced adhesion of human platelets. Additionally, DMSO seems to enlarge the lag phase and decrease the maximal aggregation response of human platelets in response to AA but not to ADP, collagen, epinephrine and ristocetin [311]. Ju-Ye et al have found that 0.5% of DMSO inhibited collagen-induced rat platelet aggregation after 30 minutes of incubation [300]. However, in our hands and under our experimental conditions, lower concentrations of DMSO (0.2%) inhibited ADP-induced platelet aggregation after 15 minutes of incubation. In fact, although it is widely recognized that the use of more than 0.5% of DMSO

can affect platelet aggregation, to our knowledge, nobody has previously reported that lower concentrations of DMSO could affect human platelet function after incubations time of 15 minutes or longer. Therefore, the use of alternative solvents needs to be considered and tested if long periods of incubation are required.

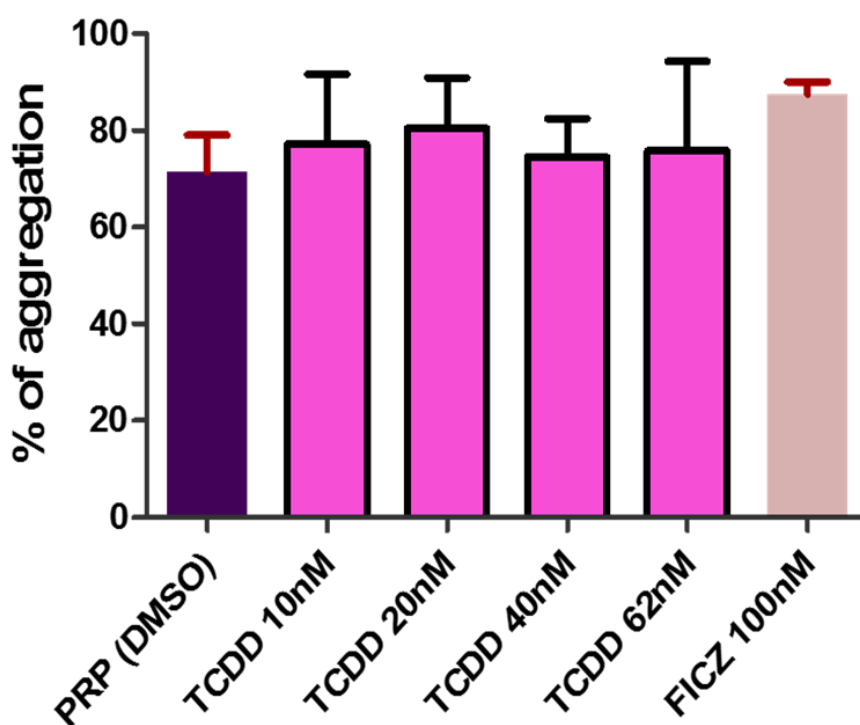


Figure 4-19: Statistical analysis of the effect of DMSO on ADP- induced platelet aggregation. The effect of TCDD (10, 20, 40 and 62 nM) and FICZ 100 nM preincubated for 15 minutes on ADP-induced platelet aggregation compared to vehicle (DMSO). Data is presented as mean \pm SD; n=5; One-way ANOVA ($P > 0.05$)

4.2.6. The effect of TMF on ADP-induced platelet aggregation

TMF at 10 μ M exhibited significant inhibition of ADP- (10 μ M) induced platelet aggregation when PRP was incubated with the compound from 2 to 30 minutes independently to the effect that DMSO could exert during the incubation time as shown in figures 4-20, 4-21 and 4-22. In this case, it can be suggested that the inhibitory effect of TMF might be due to an effect on P2Y1 and/or P2Y12 activation pathways but not on GPVI or GPIa/IIa pathway as TMF inhibited ADP- but not collagen- induced platelet aggregation.

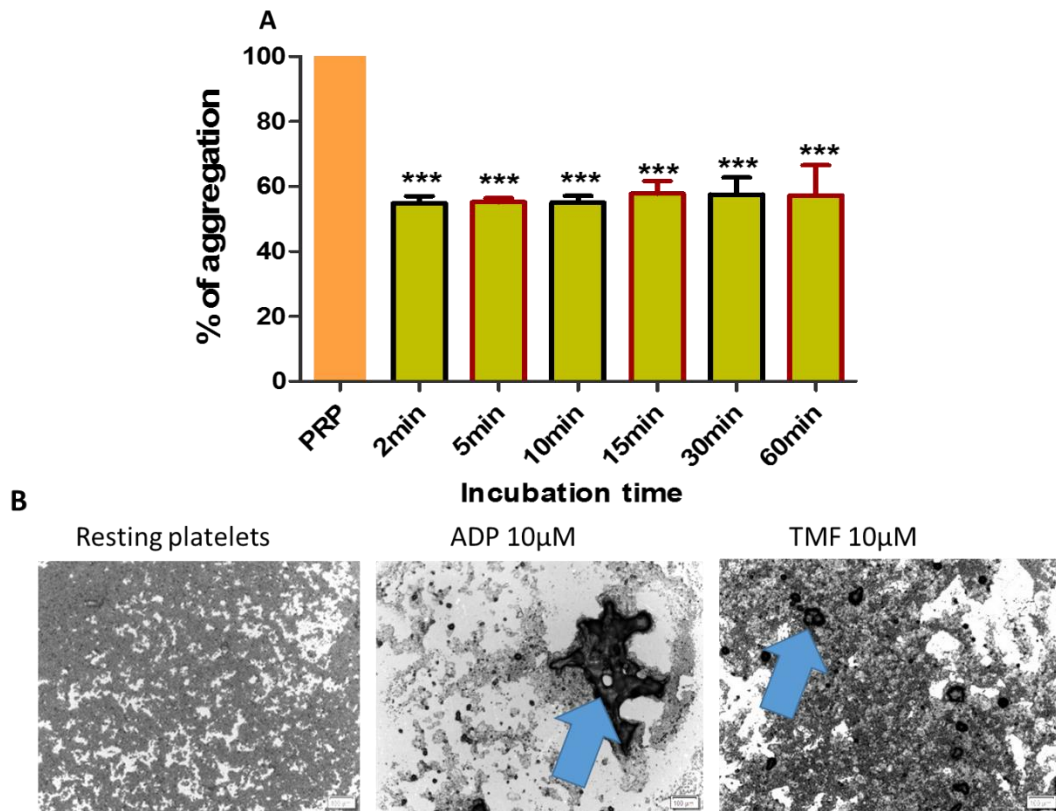


Figure 4-20: Effect of TMF on ADP-induced platelet aggregation. (A) TMF significantly inhibited platelet aggregation induced by ADP when TMF (10 µM) was preincubated from 2 minutes with platelet rich plasma (PRP) prior to addition of ADP (10 µM). Data is presented as mean ± SD; n=5; One-way ANOVA & Dunnett post-test; *** P <0.001 vs PRP. (B) Representative micrographs (10X objective) showing the effect of TMF 10µM incubated for 2 minutes on ADP induced platelet aggregation. The light grey areas represent non activated platelets and the darker areas (blue arrow) correspond with platelet aggregates.

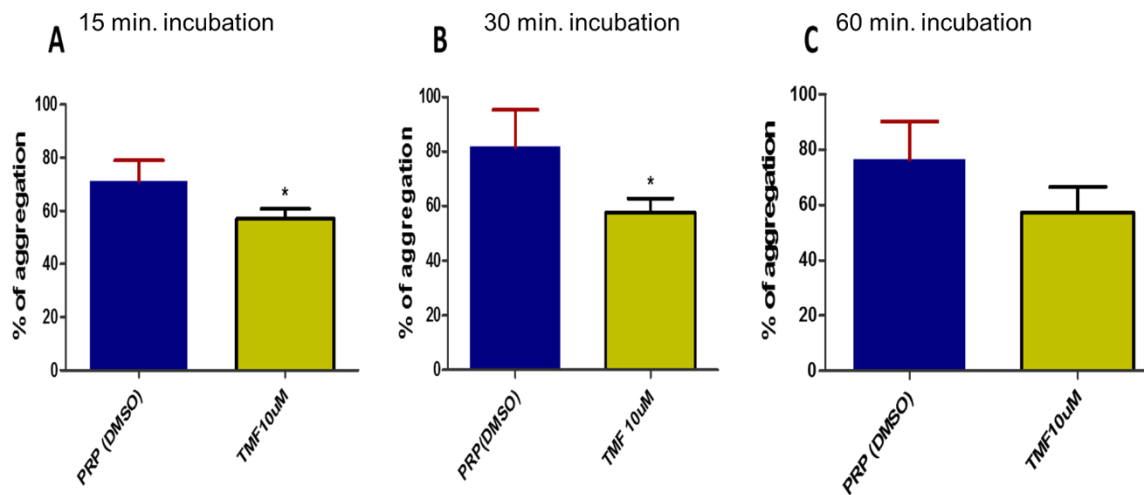


Figure 4-21: Statistical analysis of the effect of incubation overtime of DMSO (vehicle) and TMF with platelet rich plasma in ADP-induced platelet aggregation. TMF significantly inhibited ADP-induced platelet aggregation compared to the vehicle (DMSO) when incubated for 15 and 30 minutes (A and B; respectively) with $P= 0.0288$ and 0.0484 ; respectively. No significant inhibition was observed with TMF $10\ \mu\text{M}$ after 60 minutes of incubation ($P=0.0589$). DMSO was normalised as the percentage of platelet aggregation to 100% PRP aggregation induced by ADP. Data is presented as mean \pm SD; $n=5$. Student paired t-test. * $P < 0.05$ vs PRP (DMSO).

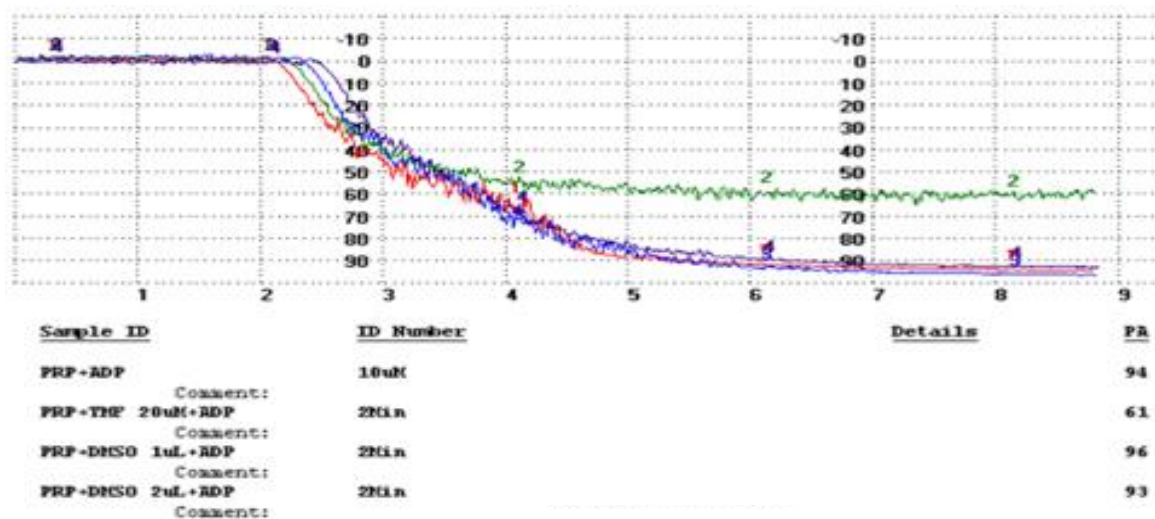


Figure 4-22: Light transmission aggregometry traces showing the effect of 2 minutes incubation time of TMF ($10\ \mu\text{M}$) and DMSO on ADP- ($10\ \mu\text{M}$) induced platelet aggregation. TMF $10\ \mu\text{M}$ inhibited platelet aggregation in the presence of ADP when compared to DMSO

In summary, AhR receptor does not seem to be involved in the inhibitory effect of kynurenine on platelet function since AhR agonists tested had no effect on ADP- nor on collagen- induced platelet aggregation when the compounds were incubated with platelets up to 60 minutes. However, the AhR receptor antagonist (TMF) significantly inhibited ADP- induced but not collagen- induced platelet aggregation after two minutes incubation time.

Next, the platelet response to both agonists (ADP and collagen) after the incubation of platelets with AhR agonists (FICZ and TCDD) and the AhR receptor antagonist (TMF) prior to the addition of kynurenine was also evaluated using LTA to confirm any synergism or antagonism at AhR receptor

4.2.7. Effect of kynurenine in PRP pre-incubated with TMF in the presence of collagen or ADP

Taking into account that kynurenine could exert its action through the AhR receptor in platelets, the AhR receptor antagonist TMF, was foreseen to antagonise to some extent the effect of kynurenine in platelet function. Platelets stimulation with ADP (10 μ M) resulted in a significant increase of the inhibitory effect of kynurenine (25 μ M to 250 μ M) when TMF 10 μ M was preincubated with platelets for 2 minutes. However, no significant differences in platelet response to kynurenine were observed in the presence or absence of TMF when collagen (4 μ g/mL) was used to induce platelet aggregation as shown in figure 4-23.

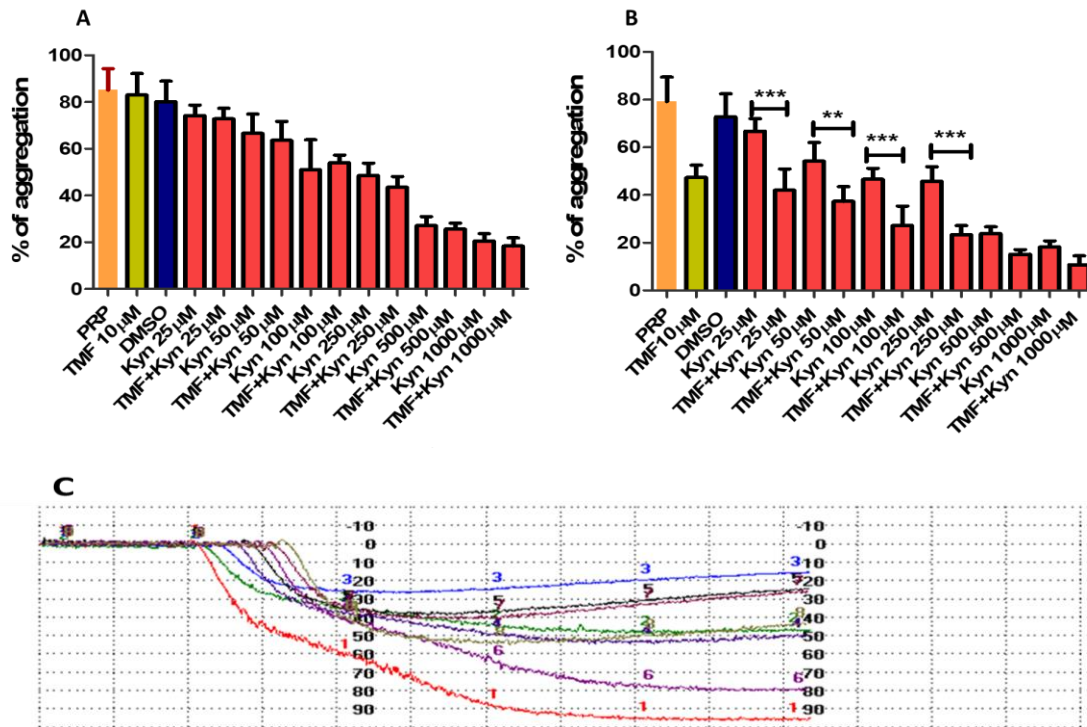


Figure 4-23: Effect of collagen and ADP on platelets preincubated with TMF 10µM and Kynurenine. (A) Statistical analysis on platelet rich plasma (PRP) stimulated with collagen 4 µg/ml. Data is presented as the mean ± SD; n=6; One-way ANOVA & Tukey's post-test. (B) Statistical analysis showing the synergistic effect of TMF 10 µM in PRP stimulated with ADP 10 µM. Data is presented as the mean ± SD; n=6; One-way ANOVA & Tukey's post-test. *** P < 0.001; ** P < 0.01 vs PRP (C) Representative aggregometer traces showing the effect of 10 µM TMF and Kynurenine (25, 50 and 100 µM) in PRP in the presence of ADP 10 µM.

4.2.8. Effect of FICZ and TCDD preincubated with kynurenine in PRP stimulated with collagen or ADP.

To evaluate the potential effect of the co-incubation of AhR agonists with kynurenine of platelet function, platelets were incubated with FICZ 100nM and TCDD 62nM and kynurenine (from 25 μ M to 1mM) and stimulated with collagen or ADP. AhR agonists did not modify the inhibitory effect of kynurenine on platelet aggregation as shown in figure 4-24.

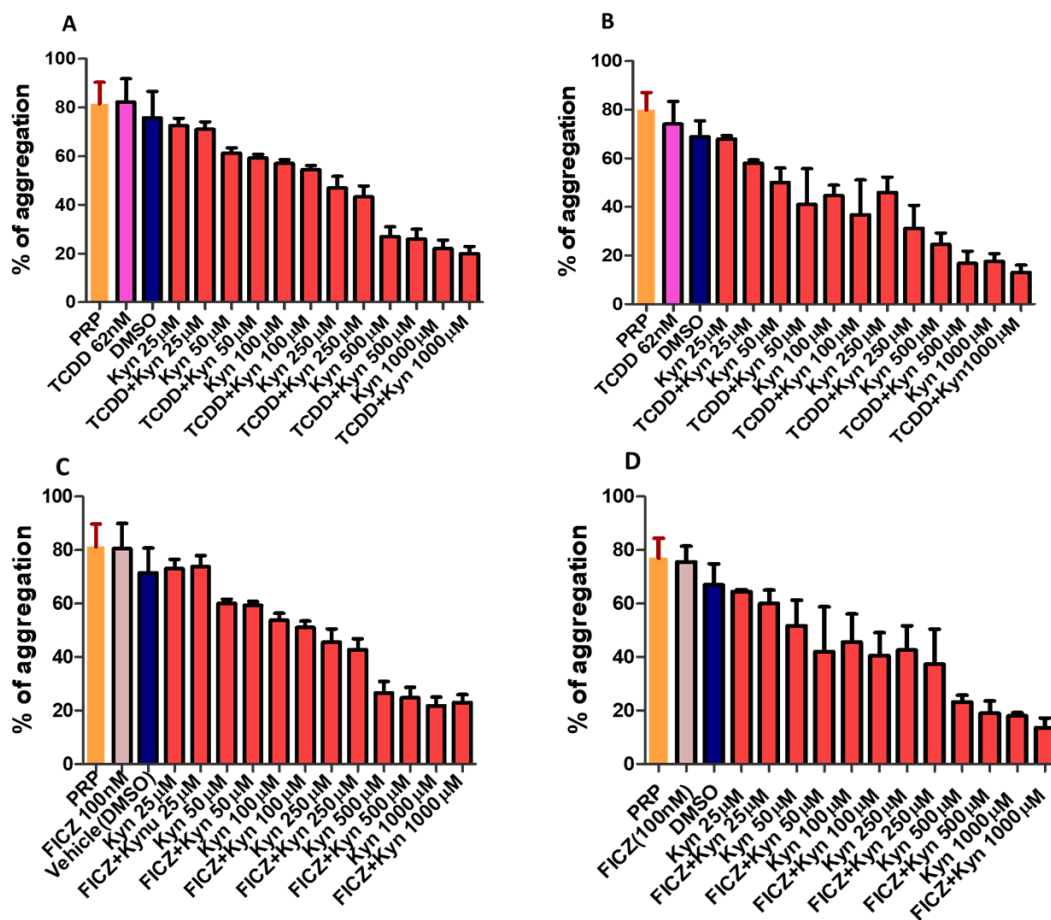


Figure 4-24: Effect of TCDD and FICZ on the inhibitory effect of Kynurenine in collagen and ADP induced- platelet aggregation. (A) Statistical analysis showing no significant effect of TCDD 62 nM on the inhibitory effect of kynurenine on platelet rich plasma (PRP) stimulated with collagen 4 μ g/mL. (B) Statistical analysis showing no significant effect of TCDD 62 nM on the inhibitory effect of Kynurenine on PRP stimulated with ADP. (C) Statistical analysis showing no significant effect of FICZ 100 nM on the inhibitory effect of Kynurenine on PRP stimulated with collagen (D) Statistical analysis showing no significant effect of FICZ 100 nM on the inhibitory effect of Kynurenine on PRP stimulated with ADP 10 μ M. Data is presented as the mean \pm SD; n=5; One-way ANOVA (P > 0.05).

To confirm that Kynurenine, FICZ, TCDD, TMF and DMSO at the concentrations used were not toxic to platelets, and to corroborate their effect on platelets a cytotoxicity assay based on LDH detection was carried out. Washed platelets were incubated with the highest concentration of the compounds for at least 15 minutes and the amount of LDH measured and compared with the amount of LDH obtained in resting platelets. None of the compounds exhibited significant platelets toxicity as shown in figure 4-25.

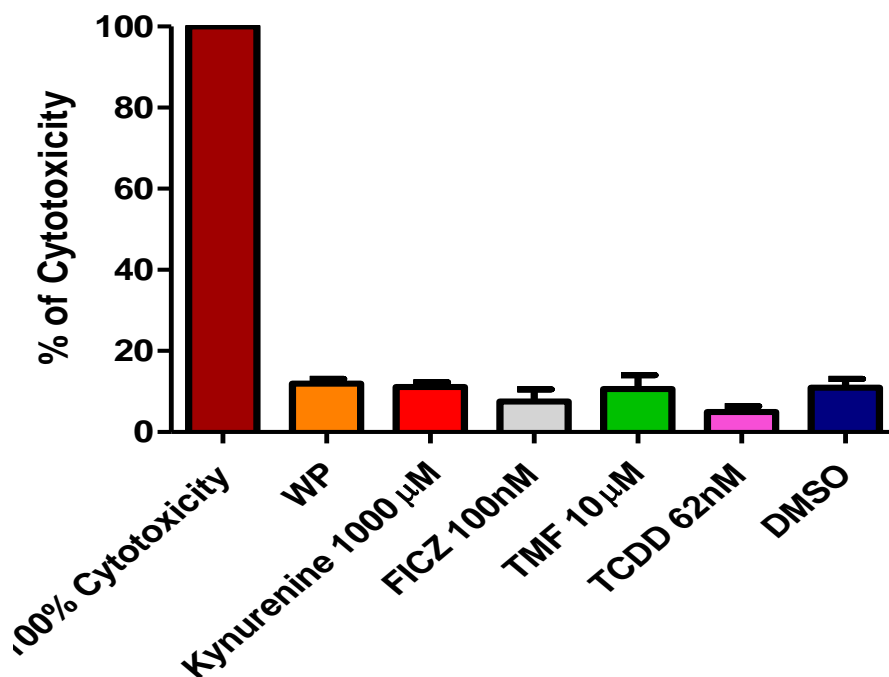


Figure 4-25: Cytotoxicity assay.Effect of Kynurenine, FICZ, TMF, TCDD and DMSO on platelets.

Statistical analysis showing that Kynurenine, FICZ, TMF, TCDD and DMSO have no cytotoxic effect on washed platelets (WP) when incubated for 15 minutes. Results were compared to 100% cytotoxicity. Data is presented as the mean \pm SD; n=4; One-way ANOVA ($p > 0.05$).

From those results and despite kynurenine is considered as an AhR receptor agonist, it doesn't appear that kynurenine could inhibit platelet aggregation through AhR receptor since:

1. Preincubation of platelets with the AhR receptor antagonist (TMF) did not attenuate the inhibitory effect of kynurenine on platelet aggregation induced by collagen but induced, instead, a synergistic effect when ADP was used.
2. Incubation of platelets with highly selective and potent AhR receptor agonists (FICZ and TCDD) did not show any inhibitory effect similar to Kynurenine on platelets when they were stimulated with collagen or ADP.

4.3. Does Kynurenine act through a platelet surface receptor or intraplatelet compartment?

Kynurenine might exert its effect through other platelet's membrane or cytosolic receptor but not AhR as shown by the previous experiments. To investigate this hypothesis further, PRP was incubated with kynurenine for 15 minutes and tested for collagen 4 μ g/mL induced platelet aggregation. Afterwards, WP was prepared from the kynurenine incubated PRP and tested for collagen induced platelet aggregation to investigate the effect of washing step on the inhibitory effect of kynurenine compared to the effect of kynurenine incubated with PRP. Although kynurenine inhibited collagen-induced platelet aggregation in PRP washing of platelets resulted in abolishing the inhibitory effect of kynurenine on collagen induced platelet aggregation as shown in figure 4-26.

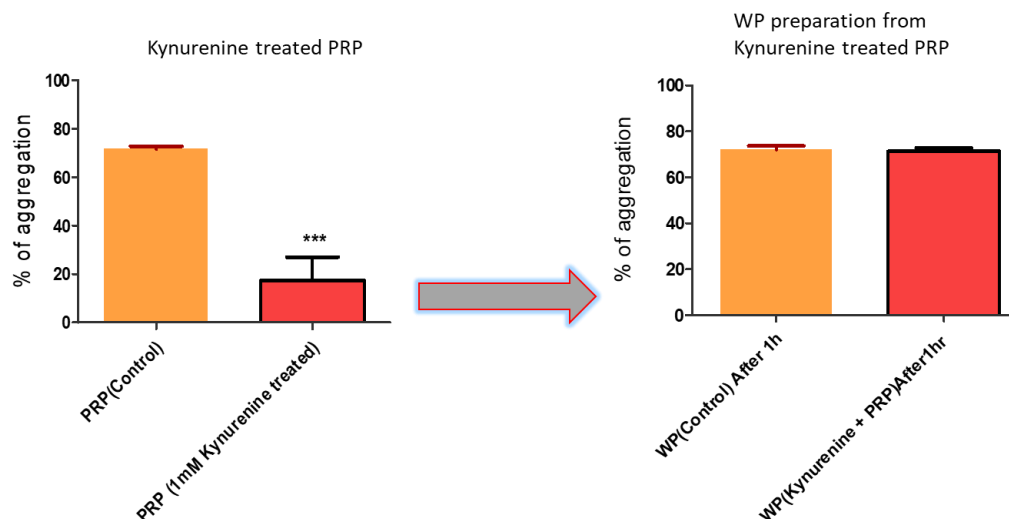


Figure 4-26: Statistical analysis of the effect of collagen on washed platelets (WP) prepared from kynurenine treated platelet rich plasma (PRP) after 45 minutes of incubation. The inhibitory effect of kynurenine preincubated with platelet rich plasma on collagen-induced platelet aggregation reverted after the preparation of WP from Kynurenine treated PRP. Data is presented as mean \pm SD; n=4; student t-test. *** P < 0.001 vs control,

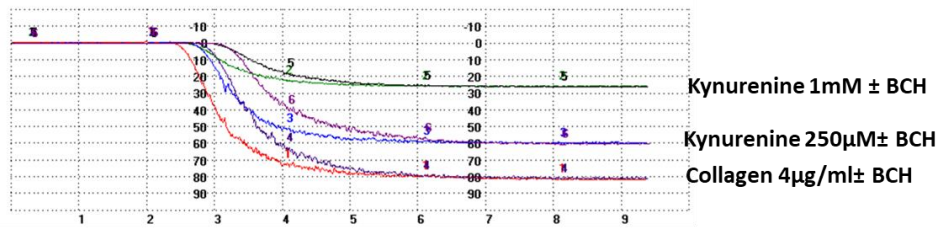
Based on this finding, it could be deduced that kynurenine may be acting through a platelet surface receptor as its effect decreased dramatically after the “washing process”. However, this observation deserved further investigation as kynurenine may be transported inside platelets to exert its action or it may be a short acting molecule working at platelet surface or at intraplatelet level. To the best of our knowledge no information is available in the literature about how kynurenine transport takes place in platelets. However, it is known that platelets exhibit uptake mechanisms for several amino acid neurotransmitters such as serotonin, tryptophan, γ -aminobutyric acid (GABA), glutamate, aspartate and glycine resemble those of the central nervous system [312, 313]. Kynurenine has been shown to be transported by large neutral amino acid transporters (LAT) which are subdivided into four subfamilies, LAT1 (SLC7A5), LAT2 (SLC7A8), LAT3 (SLC43A1) and LAT4 (SLC43A2) associated with Na⁺-independents L-system in rat astrocytes [314]. Kynurenine is also transported across the T-cell membrane by the SLC7A5. Solute carriers’ protein (SLCs) which comprises different types of carriers for a huge spectrum of substrates including nutrients such as inorganic ions, sugars, amino acids, nucleotides and vitamins, as well as drugs has been also identified in platelets [315]. The 2-aminobicyclo-(2,2,1)-heptane-2-carboxylic acid (BCH) compound has been

shown to inhibit almost completely all members of LAT family at concentrations higher than 10 mM [316] and it has shown to completely inhibit kynurenine uptake in astrocytes [317].

4.4. Kynurenine platelet uptake study

For kynurenine uptake studies, Tyrode's solution containing BCH (25 mM) was used to prepare WP and the effect of Kynurenine (250 μ M and 1 mM) on collagen- induced platelet aggregation investigated by LTA. BCH had no effect on platelet aggregation induced by collagen. However, the inhibitory effect of 1mM Kynurenine was not affected by the presence of BCH, BCH significantly reduced the inhibitory effect of 250 μ M Kynurenine after 120 minutes of incubation(figure 4-27 and 4-28).

A)



B)

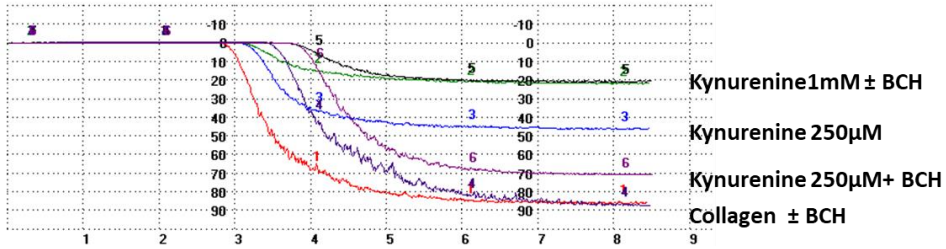


Figure 4-27: Representative traces from light transmission aggregometry showing the effect of BCH 25mM on the inhibition of collagen induced platelet aggregation by kynurenine when incubated for 60 minutes (A) and 120 minutes(B).

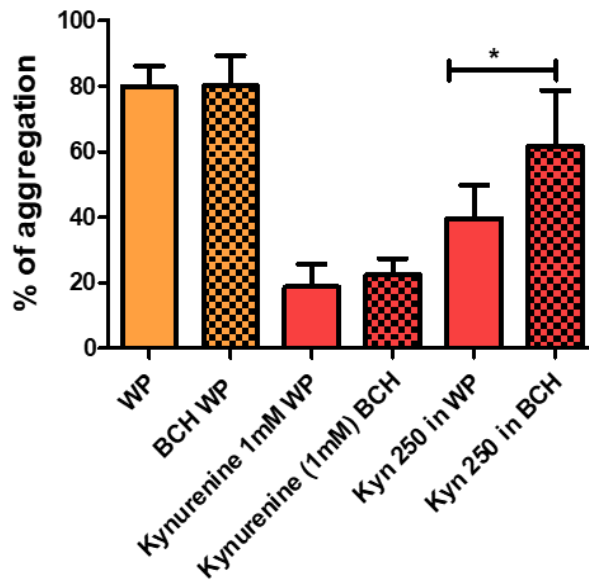


Figure 4-28: Effect of BCH on kynurenine inhibitory effect.. BCH incubated for 2 hours with washed platelets (WP) reverted the inhibitory effect of Kynurenine 250µM on collagen-induced platelet aggregation. Data is presented as mean ± SD; n=4; student paired t-test * P < 0.05.

As BCH suppressed the inhibitory effect of kynurenine 250 μ M but not kynurenine 1mM, it seemed reasonable to suggest that kynurenine needs to be transported by LTAs to exert its inhibitory effect and that it may not work through a platelet surface receptor. The variability in response to BCH could be due to involvement of more than one mechanism of transport by SLC, as many of the SLC proteins function by facilitating passive diffusion along the concentration gradient of the substrate or by co- and counter-transport following the concentration gradient of another solute [313]. In astrocytes, concentrative transport of kynurenine may occur by counter- transport of endogenous free amino acids [317] such as intracellular glutamine or other endogenous L system substrates [318].

More transport studies need to be done to confirm the uptake of kynurenine by platelets, such as identification of intraplatelet concentration of kynurenine after incubation, transporters that could be involved in kynurenine uptake; and the use of potential inhibitors of such transporters.

4.5. Potential relationship between nitric oxide and kynurenine.

4.5.1. Our first hypothesis.

Oxidative arginine and tryptophan metabolism in IFN γ -primed mononuclear phagocytes are functionally related as both exogenous and endogenous NO inhibits IDO activity and decrease kynurenine production, whereas inducible nitric oxide synthase activity and NO production can be induced by picolinic acid and inhibited by 3-Hydroxy anthranilic acid, which enhance haem oxygenase enzyme, both of them are kynurenine metabolites [139, 319, 320]. The L-arginine /NO pathway is reported to be present in platelet and include both, the constitutive and the inducible forms of the nitric oxide synthase (NOS) enzyme [61].

Therefore, a relationship between NO and kynurenine, through which Kynurenine could exert its inhibitory effect on platelets, was hypothesised here (figure 4-29).

It was proposed that kynurenine or its metabolites could activate NOS and increase NO production which a well-known and potent physiological inhibitor of

platelet function [61]. The proposed relationship between kynurenine and NO may involve a mechanism by which NO inactivates IDO and prevents the conversion of tryptophan to kynurenine as a negative feedback mechanism. Kynurenine might directly activate NOS or might support NOS activity by increasing the bioavailability of the NADPH co-enzyme (through the nicotinamide adenine dinucleotide (NAD) formed along the kynurenine metabolic pathway) as shown in figure 4-29, although it is worth to note that platelets have limited ability for de-novo protein synthesis [321]

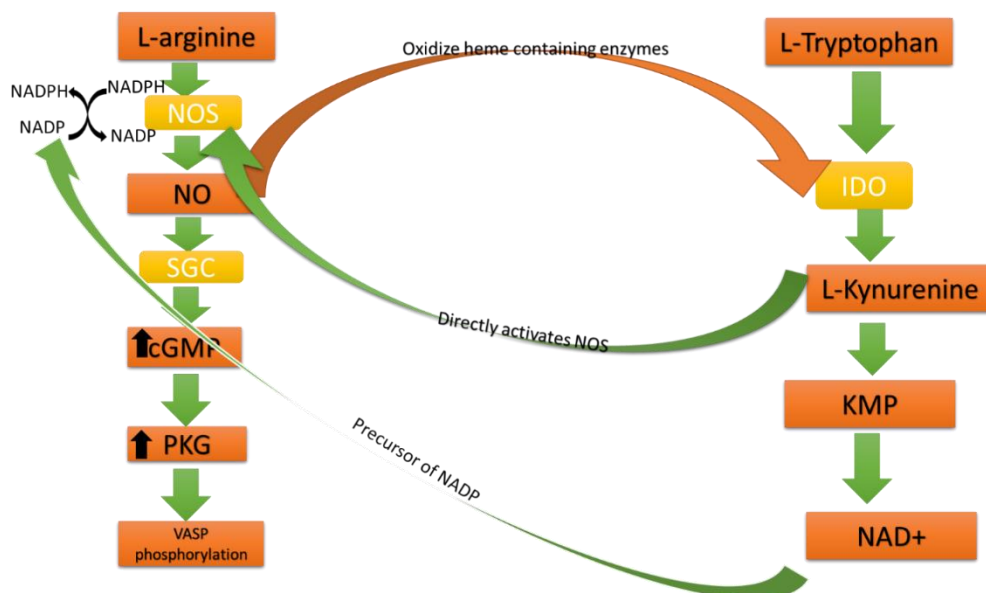


Figure 4-29: Proposed relationship between nitric oxide and kynurenine. Kynurenine may activate nitric oxide synthase (NOS) enzyme or nicotinamide dinucleotide (NAD⁺) may increase nitric oxide synthase activity by increasing the availability of NADPH. As a negative feedback mechanism, nitric oxide (NO) would oxidise heme in the indoleamine dioxygenase (IDO) enzyme leading to its inactivation and, therefore, to a decreased kynurenine production. NOS: nitric oxide synthase; NO: nitric oxide; sGC: soluble guanylyl cyclase; cGMP: cyclic Guanosine monophosphate; PKG: cGMP dependent protein kinase, IDO: indoleamine dioxygenase; KMP: kynurenine metabolic pathway, NAD: nicotine adenine dinucleotide. Red arrows: Inhibition. Green arrows: activation.

A series of experiments were designed to investigate the potential effect of kynurenine on NOS. Platelets were preincubated with inhibitors of NOS or the downstream soluble guanylyl cyclase enzyme (sGC) through which NO exerts its inhibitory effect on platelet aggregation:

1. L-NG-Nitroarginine methyl ester (L-NAME) was used to inhibit NOS in platelet prior to platelets incubation with kynurenine to find out if Kynurenine could act as a NOS activator.
2. 1H-[1,2,4] oxadiazolo [4,3-a]quinoxalin-1-one (ODQ) was used to inactivate platelet's soluble guanylyl cyclase (sGC) which is downstream of NO and responsible for the conversion of guanosine 5'-triphosphate (GTP) into cyclic guanosine 3',5'-monophosphate (cGMP), activating cGMP dependent protein kinase (PKG) [322] .

4.5.2. Effect of kynurenine on L-NAME treated platelets

WP were preincubated with L-NAME (100 μ M) for 10 minutes and then stimulated with collagen (4 μ g/mL) after 2 minutes of incubation with kynurenine (100 μ M-1 mM).

Incubation of platelets with L-NAME did not modify the inhibitory effect of kynurenine on platelet aggregation (figure 4-30) suggesting that kynurenine does not exert any effect on the basal activity of NOS in platelets (as exogenous L-arginine and NADPH that are required for maximal activity of NOS were not added to the platelet suspension) [61]

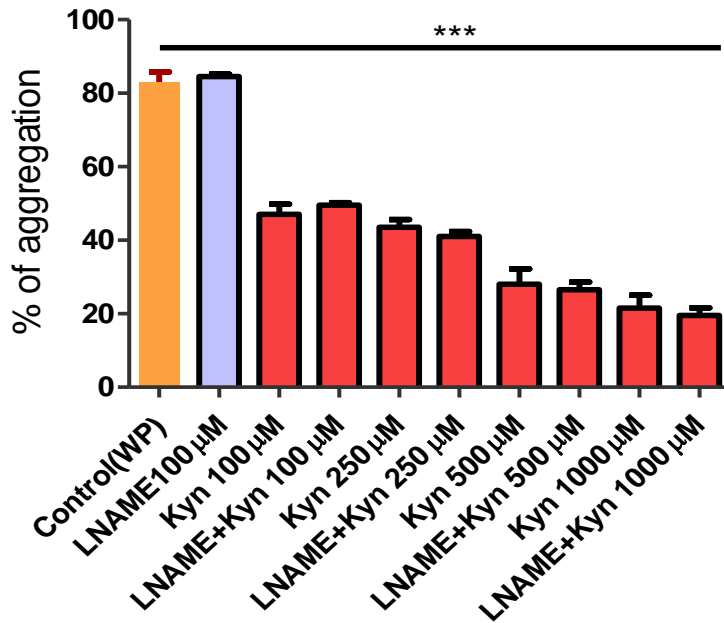


Figure 4-30 : Effect of kynurenine on L-NAME treated platelets. L-NAME showed no significant effect on washed platelets preincubated with kynurenine and activated by collagen. L-NAME was incubated for 10 minutes and Kynurenine for 2 minutes. Data is presented as mean \pm SD; n=4; One-way ANOVA & Tukey's post-test. ***P<0.001 vs control (WP).

4.5.3. Effect of Kynurenine on platelet's soluble guanylyl cyclase

Although, the possibility of basal NOS activation by kynurenine could be rule out, the downstream effect of NO needed to be investigated next. As ODQ counteracts the effect of NO and NO donors in platelets by inhibition of sGC enzyme activity [323], WP were preincubated for 10 minutes with ODQ (10 μ M) prior to the addition of increasing concentrations of Kynurenine (100 μ M to 1mM). Platelet aggregation was then induced with collagen (4 μ g/mL) after at least 2 minutes of incubation with the tryptophan metabolite. Surprisingly, ODQ failed to suppress the inhibitory effect of kynurenine at any of the concentrations tested but significantly enhanced kynurenine 100 μ M inhibitory effect (figure 4-31)

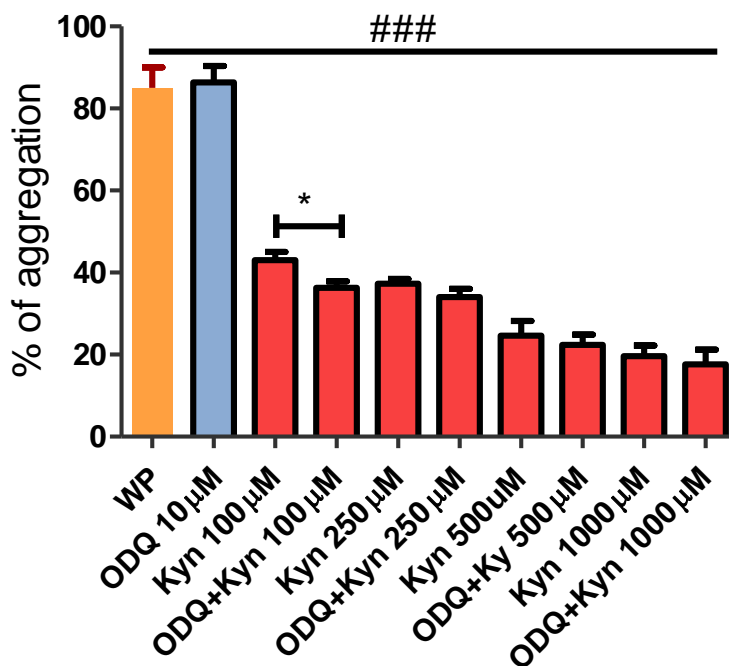


Figure 4-31: Effect of Kynurenine on ODQ treated platelets. ODQ 10µM resulted in significant enhancement of Kynurenine 100 µM inhibitory effect on platelet aggregation induced by collagen. ODQ was incubated for 10 minutes and Kynurenine for 2 further minutes with washed platelets (WP) prior to addition of collagen. Data is presented as mean ± SD; n=4; One-way ANOVA; Tukey's post-test. ###P < 0.001 vs control (WP); and student paired t-test * P < 0.05.

4.5.4. Effect of ODQ on platelet expression of GPIIb/IIIa and P-selectin

Flow cytometry was performed to corroborate the effect of ODQ (10 µM) on platelet function. ODQ was preincubated for 10 minutes with platelets prior to incubation of kynurenine for 2 minutes and induction of platelet aggregation by collagen. Kynurenine (250-1mM) caused a significant downregulation of activated GPIIb/IIIa and P-selectin expression in the presence and absence of ODQ. In addition, downregulation of the activated GPIIb/IIIa by Kynurenine 250 µM was enhanced in the presence of ODQ but had no significant effect on P-selectin expression as shown in figure 4-32 and figure 4-33. More experiments may be needed to decrease the high standard deviation accompanied the effect of kynurenine on platelet expression of GPIIb/IIIa and P-selectin.

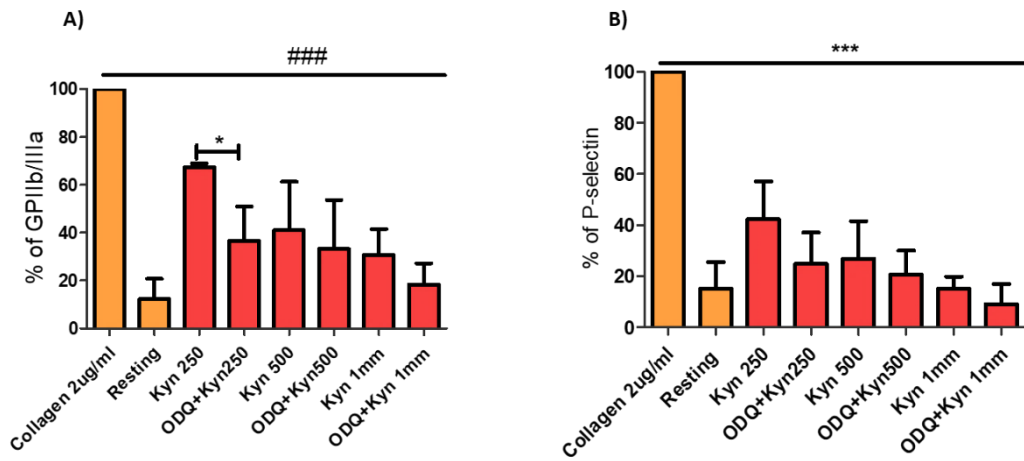


Figure 4-32: Effect of ODQ on platelet's expression of activated GPIIb/IIIa and P-Selectin. Statistical analyses showing the effect of ODQ 10 μ M and kynurenine on platelet expression of GPIIb/IIIa (A) and P-selectin (B) in platelets stimulated with collagen 4 μ g/mL. Data is presented as mean \pm SD; n=4; One-way ANOVA; Tukey's post-test and paired t-test; * P < 0.05, ###P < 0.001 vs collagen, ***P < 0.001 vs collagen.

GPIIb/IIIa

P-selectin

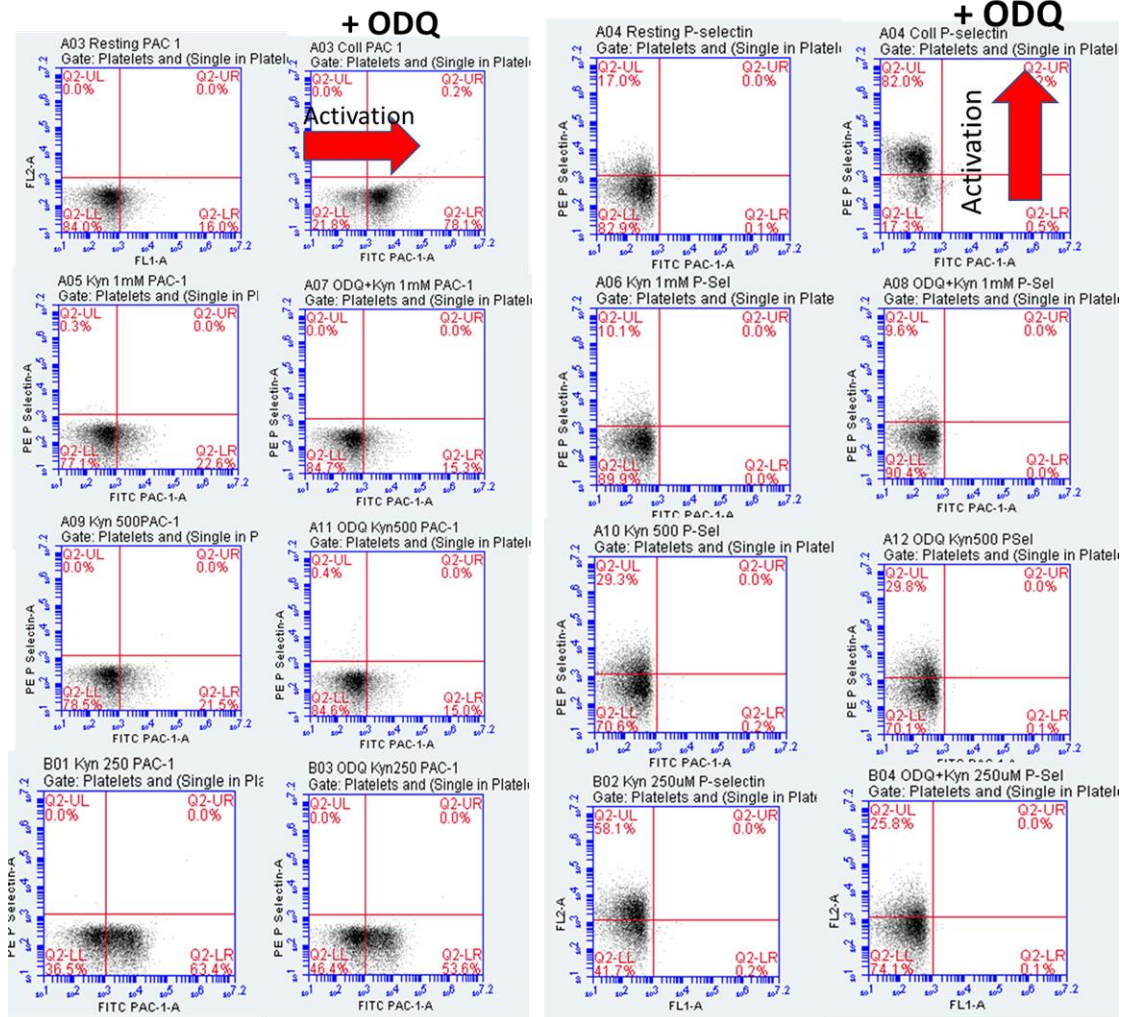


Figure 4-33: Representative gates from flow cytometry showing the effect of ODQ on collagen induced platelet aggregation in the presence of kynurenine. Shifting of platelets population from left lower quadrant (LL) to right lower quadrant (LR) indicates increased GPIIb/IIIa expression while shifting from left lower quadrant (LL) to left upper quadrant (UL) indicates higher P-selectin expression.

Guanylyl cyclase enzymes catalyse the conversion of GTP to cGMP and exists in two forms: the membrane-bound and the cytosolic soluble form [324, 325]. The membrane-bound guanylyl cyclase consist of homodimers or highly ordered structures that can be stimulated by a variety of peptide, while the soluble guanylyl cyclase (sGC) consists of two different subunits, designated α and β , with a prosthetic heme moiety attached to the β subunit (figure 4-34) [326].

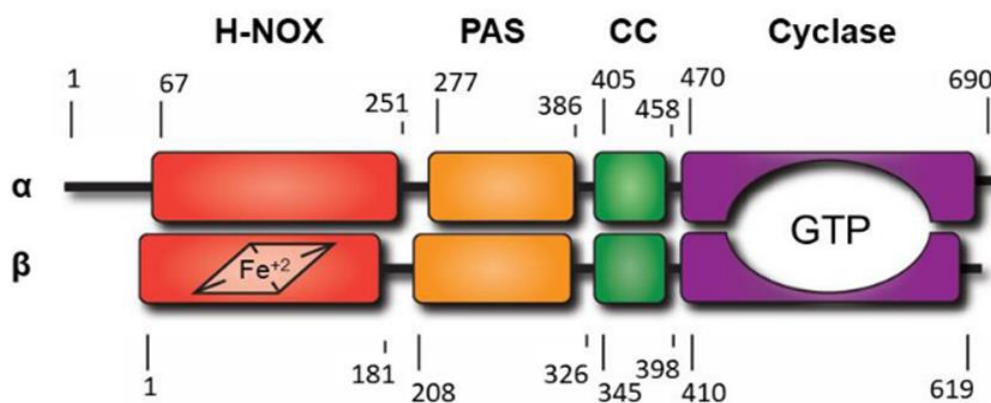


Figure 4-34: Soluble guanylyl/guanylate cyclase (sGC) domain structure. sGC proteins are dimeric since the active site forms at the interface of two catalytic domains, one from each subunit. Each sGC subunit is composed of four recognizable domains—a heme-domain (H-NOX), a Per-ARNT-Sim (PAS) domain, a coiled-coil signaling helix (CC), and a cyclase domain—that are fused together into a single polypeptide chain of 600–700 amino acids [326]

The sGC enzyme is stimulated by NO by binding to the enzyme's prosthetic heme group containing the reduced (Fe^{2+}) heme-moiety, and inducing conformational changes that lead to up 200-fold increase the catalytic activity of the enzyme [327, 328].

In the presence of an intact heme-moiety, sGC is a constitutively active enzyme that induces the formation of cGMP from GTP in basal conditions. NO and NO donors cannot activate the enzyme when it is heme-free [329] or when the heme-moiety is oxidized (Fe^{3+}) [330]. The latter occurs following oxidative stress, caused by reactive oxygen and nitrogen species, or by the effect of the ODC used in this project that oxidises the heme-moiety of the enzyme [331-334]. However, Cinaciguat (BAY 58-2667), a compound developed by Bayer, is known to activate both, the oxidized heme and the heme-free sGC but not the

reduced haem for by binding to the sGC heme pocket on the β -subunit mimicking the heme group (figure 4-35) [335, 336].

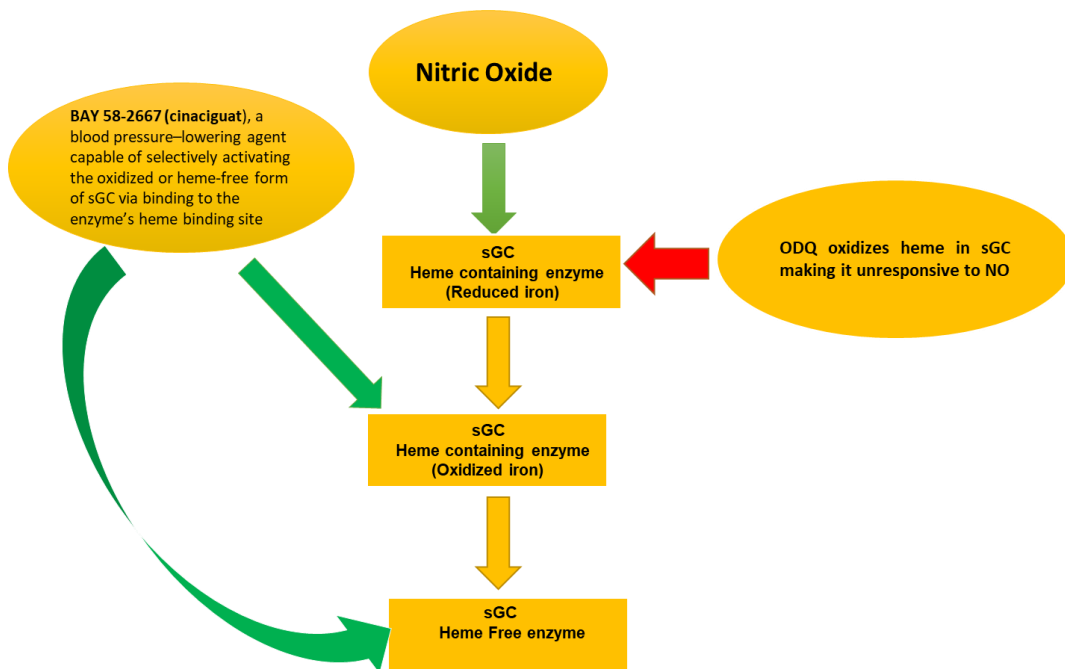


Figure 4-35: Activation of soluble guanylyl cyclase by nitric oxide and BAY58-2667. ODQ inhibits NO induced activation of sGC by oxidizing the heme moiety in the enzyme so it becomes refractory to NO. BAY 58-2667 activates the heme free and the oxidized heme forms of the enzyme. Red arrow: inhibition. Green arrows: activation

Wang et al described in their work that kynurenine activated the heme-containing and heme-free purified rat sGC with equal efficacy and also activated the oxidised-heme sGC in porcine coronary arteries, while NO only activated the reduced heme-containing enzyme [102].

4.5.5. updated hypothesis.

Taking together the literature findings described above and the results obtained during the course of this research (enhancement of the inhibitory effect of kynurenine on platelet aggregation by ODQ), it seems reasonable to suggest that kynurenine may have the ability to activate, not only the reduced heme form but also the oxidised-heme and heme free forms of sGC enzyme in platelets to exert its inhibitory action as shown in figure 4-36.

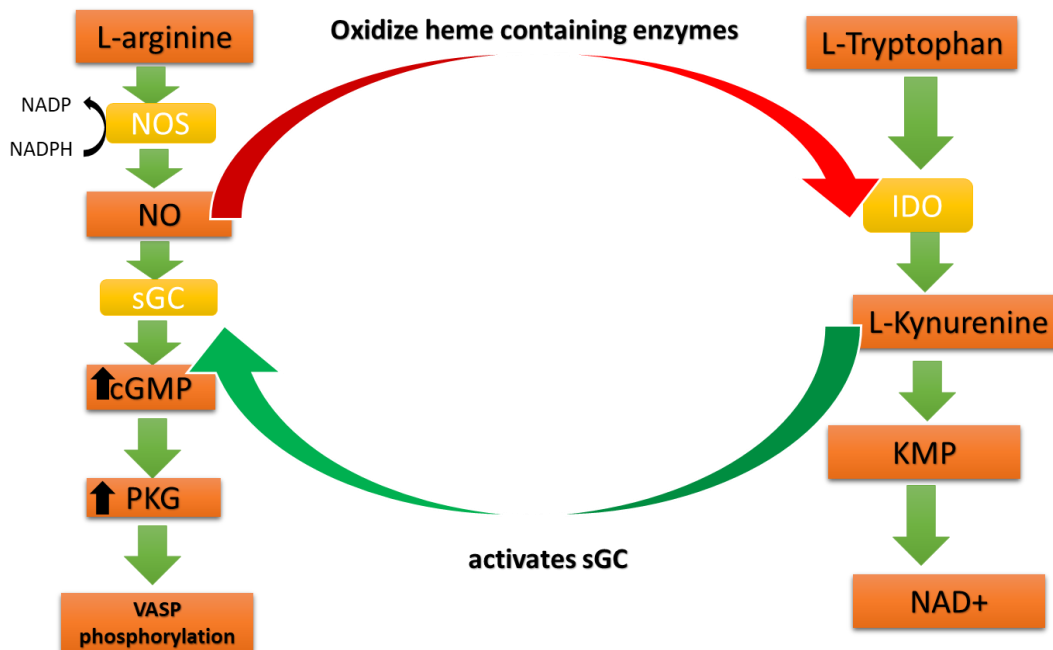


Figure 4-36: Updated proposed relationship between nitric oxide and Kynurenine. Kynurenine may activate soluble guanylyl cyclase and increase cGMP level. Nitric oxide (NO) can oxidize heme in indoleamine dioxygenase (IDO) enzyme leading to its inactivation and, therefore, decreased Kynurenine production as negative feedback. NOS: nitric oxide synthase; NO: nitric oxide; sGC: soluble guanylyl cyclase; cGMP: cyclic Guanosine monophosphate; PKG: cGMP dependent protein kinase, IDO: indolamine dioxygenase; KMP: kynurenine metabolic pathway, NAD: nicotine adenine dinucleotide. Red arrows: Inhibition. Green arrows: activation.

To investigate the ability of kynurenine to activate both the reduced and the oxidised form of sGC in platelets, downstream of sGC activation (shown in figure 4-37) were investigated by measuring intraplatelet cGMP levels and phosphorylation of the VASP protein in the presence of kynurenine [51]

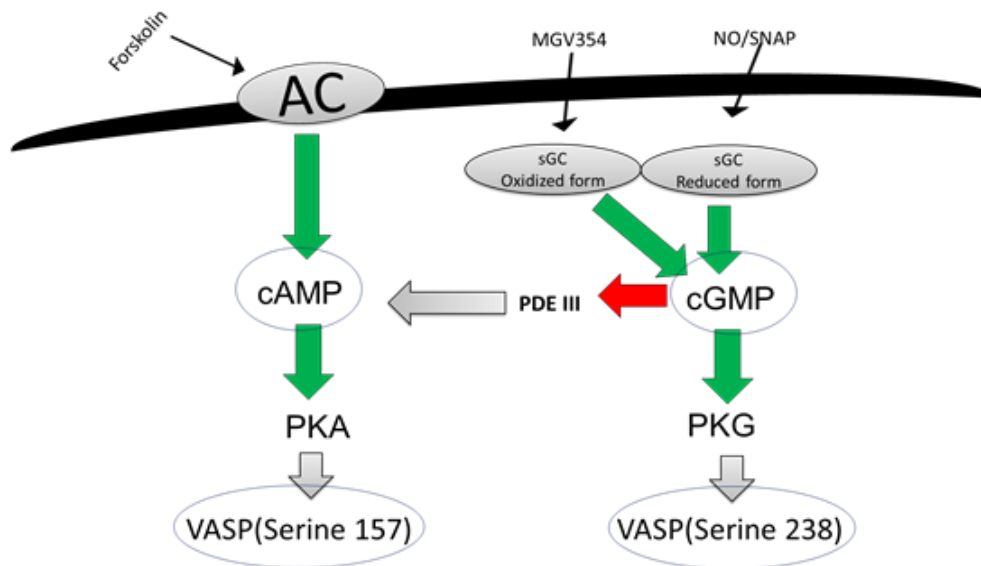


Figure 4-37: Downstream of soluble guanylyl cyclase (sGC). Activation of reduced form sGC by NO or NO- donor (SNAP) or oxidised form sGC by MGV354 results in elevation of cGMP level, activation of cGMP-dependent protein kinase (PKG) and subsequent VASP phosphorylation at serine 238. cAMP can be elevated by activation of adenylyl cyclase (AC) by forskolin or by inhibition of phosphodiesterase enzyme III (PDE III) by cGMP leading to activation of cAMP- dependent protein kinase which phosphorylate VASP protein at serine 157. AC: Adenylyl cyclase; cAMP: cyclic adenosine monophosphate; PKA: cAMP-dependent protein kinase; sGC: soluble guanylyl cyclase; cGMP: cyclic guanosine monophosphate; PKG: cGMP-dependent protein kinase; VASP: vasodilator stimulated vasoprotein.

4.5.6. Activation of platelet sGC

Effect on intraplatelet cGMP

Kynurenine (500 μ M and 1 mM) incubated at least for 2 minutes with PRP caused a significant increase in intraplatelet cGMP in the absence and presence of collagen (4 μ g/mL) with no significant differences were observed among the concentrations tested (figure 4-38). S-nitroso-N-acetylpenicillamine (SNAP 250 μ M) was used as positive control for activation of the reduced heme form sGC and caused a significant increase in cGMP level.

To examine the ability of kynurenine to activate the oxidised heme form of the enzyme which is refractory to NO, ODQ (10 μ M) was preincubated for 10 minutes to oxidise haem moiety the enzyme in platelets prior to the addition of Kynurenine (500 μ M and 1 mM) and cGMP levels measured in the presence and absence of collagen (4 μ g/mL). As expected, ODQ inhibited sGC activation

induced by SNAP and significantly reduced intraplatelet cGMP concentration induced by SNAP (figure 4-39). However, kynurenine activated the oxidized sGC enzyme and significantly increased cGMP levels with significant difference between kynurenine concentrations tested.

Kynurenine showed greater activation of sGC when the enzyme in the oxidised form than in the reduced form as supported by the significant increase of cGMP levels when the iron status changed from the reduced (Fe^{+2}) to the oxidised form (Fe^{+3}) by the action of ODQ as shown in figure 4-40. Those results are in concordance with those obtained by Wang et al when investigating the vascular relaxation effect of kynurenine on porcine coronary arteries [102].

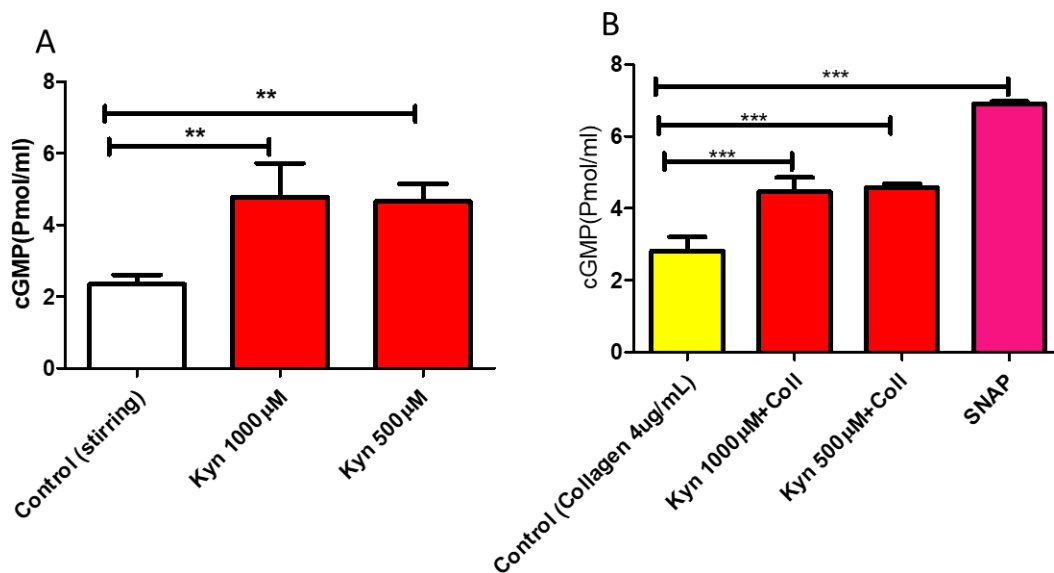


Figure 4-38: Effect of kynurenine on intraplatelet cGMP when sGC in the reduced heme form.

Statistical analysis showing the effect of kynurenine (1 mM and 500µM) on intraplatelet cGMP in the absence and presence of collagen, A and B; respectively. Data presented as mean ± SD; n=3; One- way ANOVA; Tukey's post-test ***P< 0.001 VS control ** P<0.01, *** P<0.001

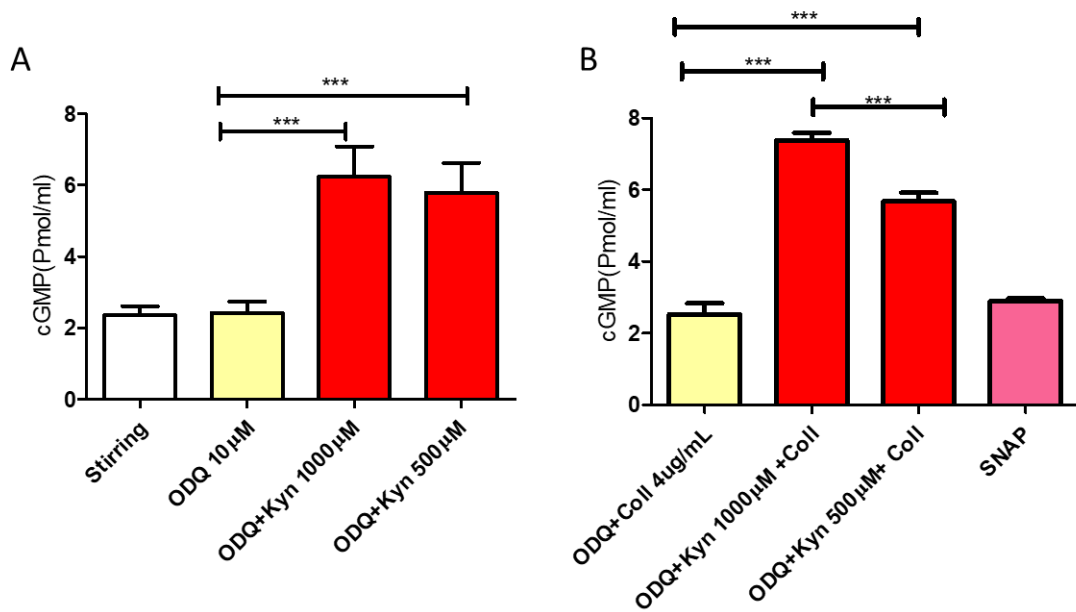


Figure 4-39: Effect of kynurenine on intraplatelet cGMP when sGC in the oxidised heme form. Statistical analysis showing that kynurenine significantly increasing intraplatelet cGMP in non-activated (A) and collagen 4µg/mL activated(B) platelets in the presence of ODQ 10µM while SNAP has no significant effect. Data presented as mean ± SD; n=3; One- way ANOVA; Tukey's post-test ***P < 0.001 VS control

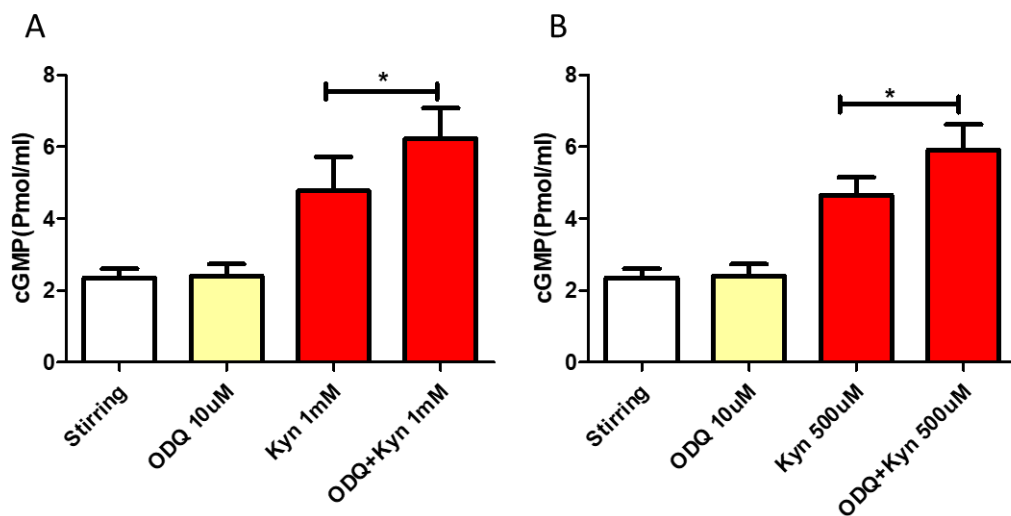


Figure 4-40: Activation of reduced and oxidised heme moiety of sGC by kynurenine. Statistical analysis showing that kynurenine causes higher activation of oxidised heme form of sGC compared to the reduced form. Data presented as mean ± SD; n=3; One-way ANOVA; Tukey's post-test *P < 0.05

4.5.7. Activation of platelet adenylyl cyclase Effect on intraplatelet cAMP

Kynurenine (250 μ M to 1 mM) incubated at least for 2 minutes with PRP caused a significant increase in intraplatelet cAMP in non-activated (figure4-41A) and collagen (4 μ g/mL) activated (figure 4-41B) platelets with significant differences between kynurenine 250 μ M and kynurenine 1mM. However, this effect on cAMP could result from activation of AC enzyme by kynurenine or due to inhibition of PDE3 by cGMP.

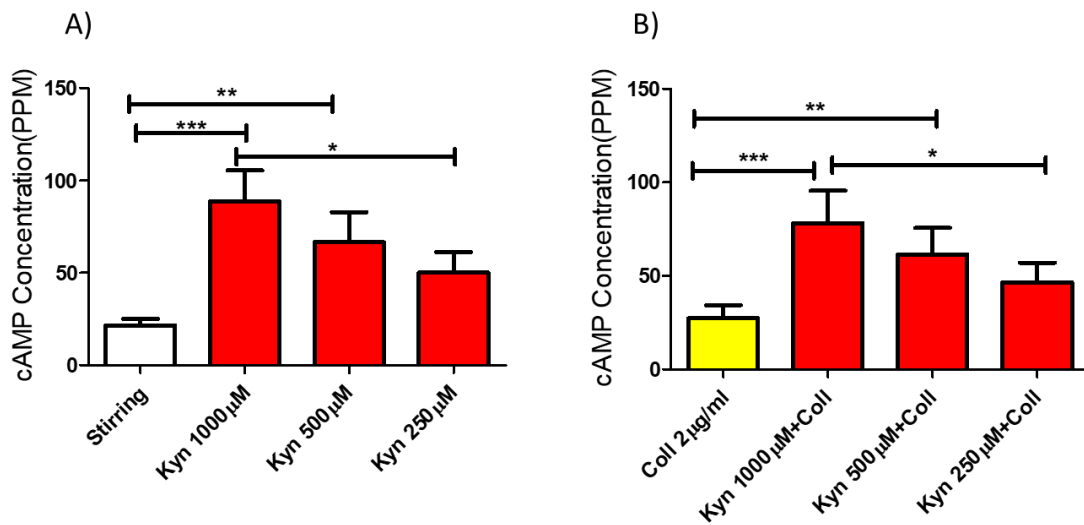


Figure 4-41: Effect of kynurenine on intraplatelet cAMP. Statistical analysis showing that kynurenine increased platelet cAMP concentration. Data presented as mean \pm SD; n=3; One-way ANOVA; Tukey's post-test *P < 0.05 ** P < 0.01 ***P < 0.001.

4.5.8. Phosphorylation of VASP by kynurenine

Immunoblotting was used to investigate whether activation of sGC enzyme and elevation of intraplatelet cGMP by kynurenine results in activation of cGMP dependent protein kinase (PKG) and VASP phosphorylation at serine 238 as downstream of the enzyme activation. Since cGMP has the ability to inhibit phosphodiesterase 3 and therefore, to increase cAMP with the subsequent activation of cAMP-dependent protein kinase (PKA) which phosphorylates VASP at serine 157 [337], VASP phosphorylation at serine 157 was also investigated.

Incubation of platelets with kynurenine induced VASP phosphorylation at both serine 238 (figure 4-42) and serine 157 (figure 4-43) in concentration dependent manner. The effect of DMSO was also tested for its ability to induce VASP phosphorylation (at the concentration used as kynurenine vehicle). DMSO did not phosphorylate VASP at any of those sites as shown in figure 4-44.

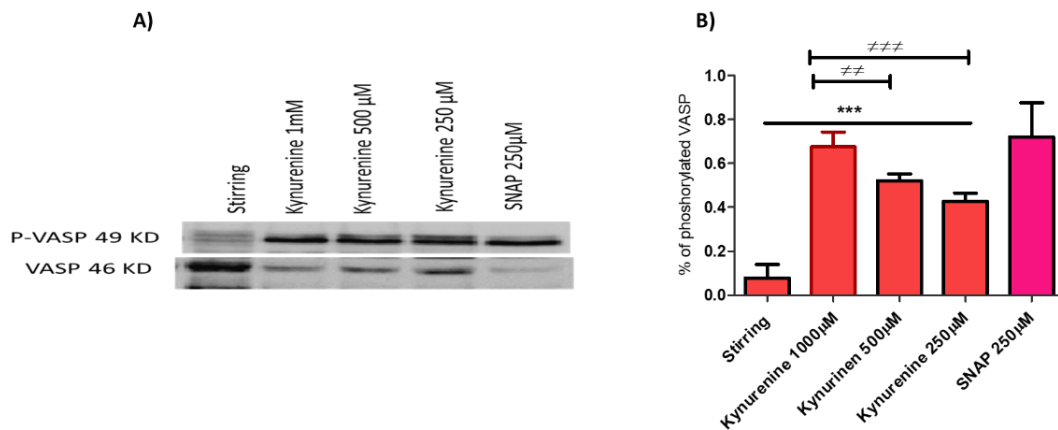


Figure 4-42: VASP phosphorylation (at serine 238) by Kynurenine. (A) Representative immunoblotting showing VASP phosphorylation at serine 238 (49 KD) by kynurenine (1 mM-250 μM). (B) Statistical analysis of the densitometry analysis showing VASP phosphorylation at serine 238 by Kynurenine 1mM, 500μM and 250μM. SNAP 250μM was used as positive control. Data is presented as mean ± SD; n=3; One-way ANOVA & Tukey's post-test. *** P < 0.001 VS control (stirling), ### P < 0.001, ** P < 0.01.

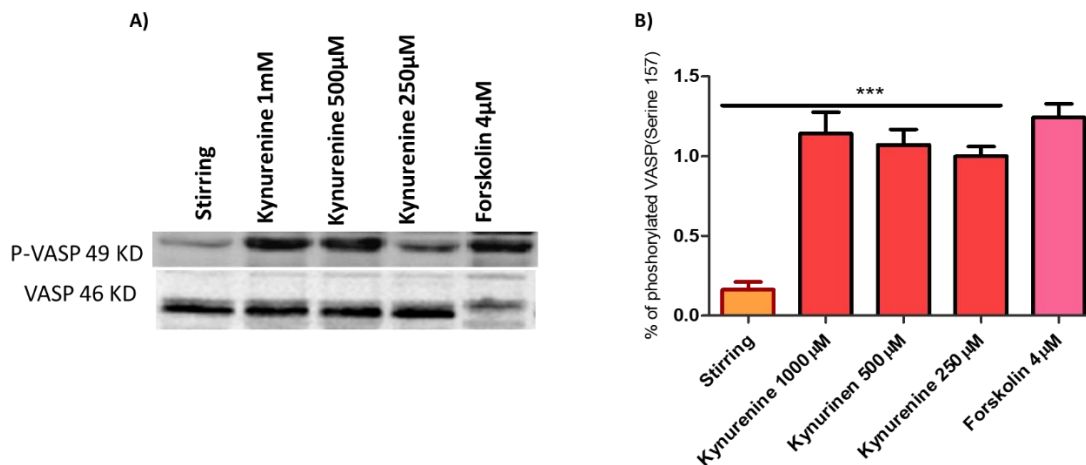


Figure 4-43: Effect of Kynurenine on platelet VASP (at serine 157) phosphorylation. (A) Immunoblotting showing VASP phosphorylation by kynurenine (1mM-250μM) at serine 157 at (49 KD) (B) Statistical analysis from the densitometry analysis showing a significant VASP phosphorylation at serine 157 by Kynurenine 1mM, 500μM and 250μM. The percentage of phosphorylated VASP was calculated to the correspondent total VASP. Forskolin 4μM was used as positive control. Data is presented as mean ± SD; n=3; One-way ANOVA & Tukey's post-test. *** P<0.001 VS control (stirling).

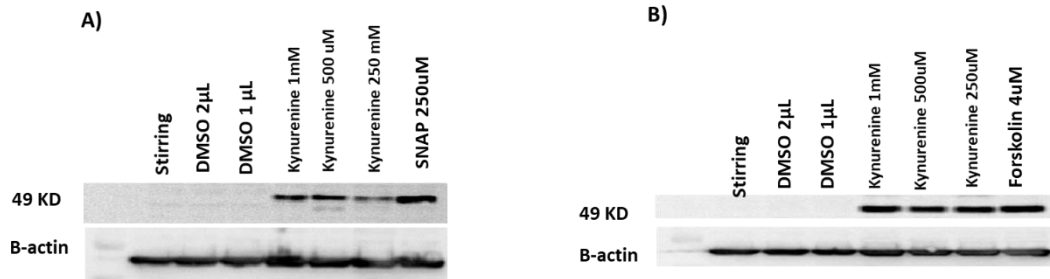


Figure 4-44: Effect of Kynurenine vehicle (DMSO) on VASP phosphorylation. Immunoblotting showing that DMSO has no effect on platelet VASP phosphorylation at serine 238 (A) and at serine 157 (B) compared to Kynurenine (1mM-250µM) and the positive controls (SNAP and Forskolin). 50µg of platelet protein loaded in each lane. (n=3).

The phosphorylation of VASP at serine 238 indicates that Kynurenine can activate the reduced form sGC, in a concentration dependent manner, as the NO donor (SNAP) can only activate the reduced form of the enzyme. Kynurenine also phosphorylated VASP at serine 157 which might happen as a result of PDE3 inhibition by cGMP leading to cAMP elevation or by activating the platelet adenylyl cyclase enzyme as both result in PKA activation and VASP phosphorylation at serine 157.

To investigate if Kynurenine activation of the oxidised form sGC induces VASP phosphorylation at serine 238 and whether VASP 238 phosphorylation by Kynurenine is PKG dependent and not by other mechanisms such as by protein kinase C [338], ODQ (10µM) was used to oxidise the heme moiety of the platelet enzyme prior to platelet incubation with Kynurenine. Rp-8-CPT-cGMP (500µM) is a potent cGMP-dependent PKG inhibitor with no effect on cAMP-dependent protein kinase or the cGMP-regulated phosphodiesterase (PDE) activity. Rp-8-CPT-cGMP has the ability to antagonise SNAP- induced activation of PKG and subsequent VASP phosphorylation [339, 340] [297, 337]. To examine if VASP phosphorylation at serine 157 induced by kynurenine was secondary to PDE3 enzyme inhibition by cGMP or due to the direct activation of the adenylyl cyclase (AC) enzyme, the adenylyl cyclase enzyme inhibitor SQ-22,536 (100µM) was also used. Since VASP phosphorylation at serine 157 can occur in PKA dependent mechanism [337] or by other mechanisms [338], the PKA-inhibitor (Rp-cAMP 100µM) [341] was also incubated with platelets prior to platelet incubation with Kynurenine (figure 4-45). All enzymes and protein

kinases inhibitors were incubated for at least 10 minutes with WP prior to Kynurenine (1 mM) incubation for 2 minutes and were examined separately in each pathway for VASP phosphorylation by immunoblotting.

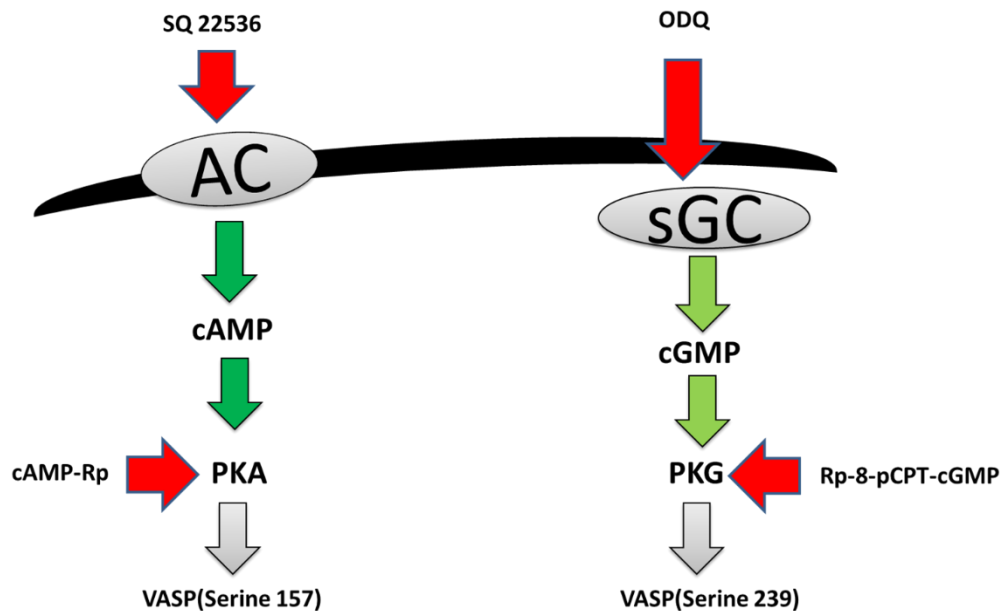


Figure 4-45: Diagram showing soluble guanylyl cyclase(sGC) inhibitor (ODQ) and adenylyl cyclase(AC) inhibitor (SQ 22536) enzymes ; and the correspondent protein kinases inhibitors (RP-8-Pcpt-cGMP) and (Rp-cAMP) ; respectively. AC: adenylyl cyclase; cAMP: cyclic adenosin monophosphate; PKA: cAMP-dependent protein kinase; VASP: vasoactive stimulating protein; sGC: soluble guanylyl cyclase; cGMP: cyclic guanosine monophosphate; PKG: cGMP- dependent protein kinase

4.5.9. Effect of sGC inhibitor and PKG inhibitor on Kynurenine VASP 238 phosphorylation

ODQ 10 μ M incubated for 10 minutes caused a significant reduction of SNAP induced VASP phosphorylation by oxidizing heme moiety in sGC which become insensitive to the effect of NO and NO-donors [330, 331]. However, ODQ enhanced VASP phosphorylation by Kynurenine indicating that Kynurenine could activate the oxidized heme form of sGC with more affinity toward the oxidised haem form than to the reduced heme form of the enzyme as demonstrated by the significant differences in VASP phosphorylation when the enzyme haem moiety was oxidized by ODQ and shown in figure (4-46).

The PKG inhibitor, Rp-8-CPT-cGMP 500 μ M, caused a significant reduction of both, SNAP and Kynurenine VASP phosphorylation at serine 238 (figure 4-46) indicating that VASP 238 phosphorylation by Kynurenine is PKG dependent.

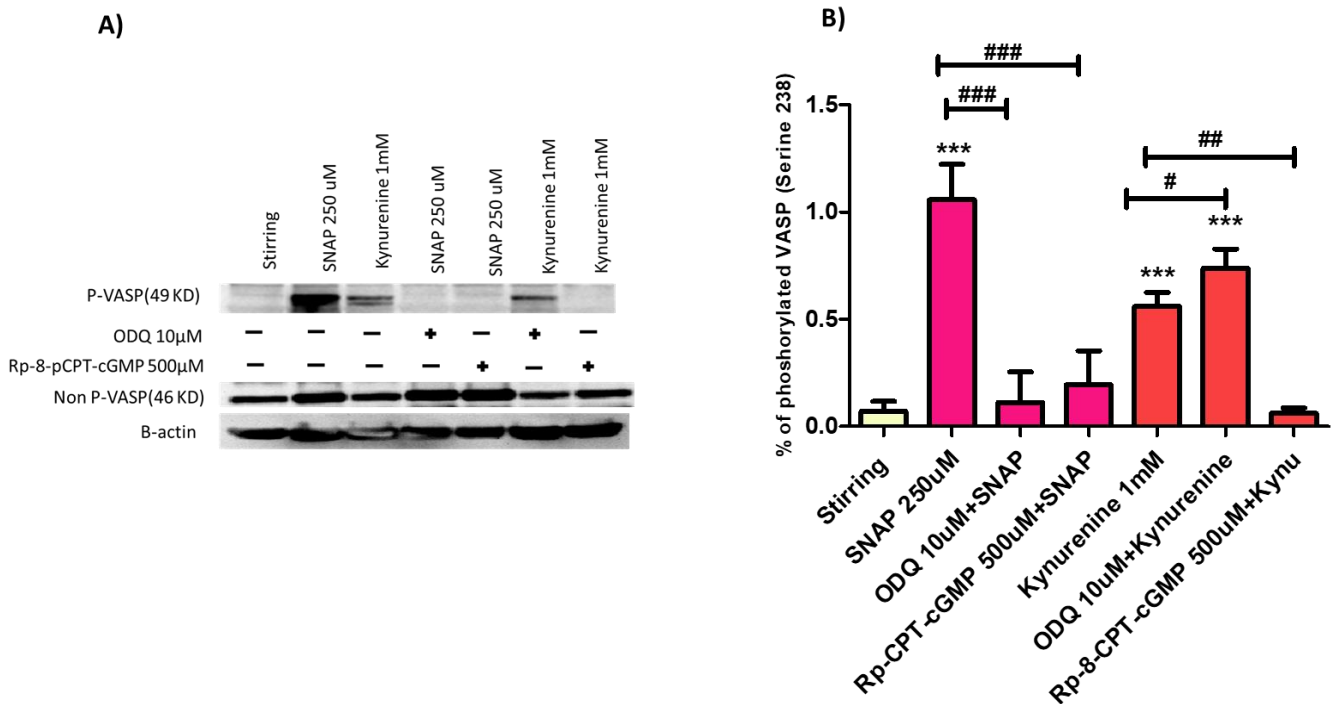


Figure 4-46: Effect of ODQ and cGMP inhibitor on SNAP and Kynurenine induced VASP phosphorylation at serine 238. (A) Representative Immunoblotting showing that ODQ 10 μ M inhibited SNAP 250 μ M VASP phosphorylation but enhanced Kynurenine VASP phosphorylation. Rp-8-pCPT-cGMP 500 μ M inhibited both SNAP and Kynurenine induced VASP phosphorylation. B-actin was used as loading control. (B) Statistical analysis of the densitometry analysis of the effect of ODQ and cGMP inhibitor on SNAP and Kynurenine induced VASP phosphorylation at serine 238. ODQ 10 μ M and Rp-8-pCPT-cGMP 500 μ M significantly reduced SNAP 250 μ M induced VASP phosphorylation at serine 238. Rp-8-pCPT-cGMP 500 μ M significantly reduced Kynurenine induced VASP phosphorylation. Data is presented as mean \pm SD; n=3; One way ANOVA & Tukey's post-test ***P<0.001 VS control (stirring), # P<0.05, ## P<0.01, ### P<0.001. The percentage of phosphorylated VASP was calculated to the correspondent total VASP.

4.5.10. Effect of AC and PKA inhibitors on Kynurenine induced VASP phosphorylation at serine 157.

SQ- 22,536 (100 μ M) was used to examine if kynurenine was able to phosphorylate VASP at serine 157 by acting as AC activator or by another mechanism that could lead to increasing cAMP level by cGMP; for example, by PDE-3 inhibition. Rp-cAMP (100 μ M) was used to examine whether Kynurenine induced VASP phosphorylation at serine 157 was PKA dependent. Forskolin phosphorylates VASP at serine 157 in cAMP dependent mechanism, therefore, it was used as control at 4 μ M. As expected, both SQ-22,536 and Rp-cAMP, significantly inhibited forskolin induced VASP phosphorylation at serine 157 as shown by Rukoyatkina et al [342]. When kynurenine 1 mM was incubated with platelets in the presence of SQ-22,536 and Rp-cAMP, VASP phosphorylation at serine 157 was also significantly decreased as shown in figure 4-47 indicating that Kynurenine increases intraplatelet cAMP by activation of the AC enzyme and phosphorylates VASP at serine 157 in a PKA dependent mechanism

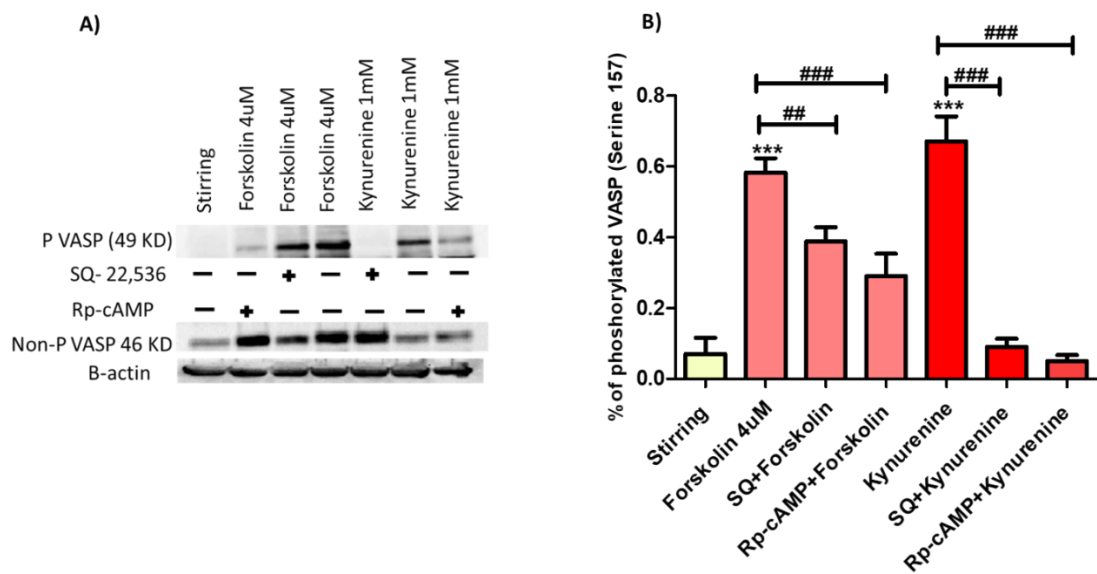


Figure 4-47: Effect of adenylyl cyclase inhibitor and cAMP inhibitor on Forskolin and Kynurenine induced VASP phosphorylation at serine 157. (A) Representative Immunoblotting showing that SQ-22,536 100μM inhibited Forskolin and Kynurenine VASP phosphorylation. Rp-cAMP 100μM inhibited both Forskolin and Kynurenine induced VASP phosphorylation. B-actin used as loading control; n=3 (B) Statistical analysis of the densitometry analysis of phosphorylated VASP at serine 157 showing that SQ-22,536 and Rp-cAMP significantly reduced Forskolin 4μM and Kynurenine 1mM VASP phosphorylation at serine 157. Data is presented as the mean ± SD; n=3; One-way ANOVA & Tukey's post-test. *** P<0.001 vs control (stirring). ## P <0.01 ### P < 0.001.

Although platelet agonists have specific mechanisms of action and follow different signalling pathways to induce platelet aggregation, collagen, ADP, thromboxane analogue and arachidonic acid all share a final common signalling pathway that results in GPIIb/IIIa activation and P-selectin translocation to the platelet membrane. Briefly, collagen acts through GPVI and GPIa/IIa leading to the activation of PLCγ which increases intraplatelet Ca⁺² level, PKC and Rab activity leading to platelet shape change, degranulation and integrin activation. ADP activates G-protein-coupled receptors, Gq and Gi, leading to activation of PLCβ and inhibition of adenylyl cyclase activity culminating in a decrease of cAMP, increase of intracellular Ca⁺² and Rab activity leading also to integrin activation. Thromboxane analogue and AA act mainly through Gq and G12/G13 leading to an increase in intraplatelet Ca⁺² level and integrin activation. Under the experimental conditions used in this project, kynurenine inhibited platelet aggregation induced by all agonist tested, meaning that its mechanism of action could be linked to any of the molecular pathways involved in platelet activation/aggregation. There is no doubt that cAMP and cGMP are important

players within the different pathways that regulate platelet function. Their role in NO and prostacyclin mode of action, the most potent physiological inhibitors of platelet aggregation, is well documented [73, 74]. They act by blocking platelet activation mediated by , thrombin, ADP, thromboxane, collagen, von Willebrand factor (VWF) and fibrinogen [51] controlling the release of Ca^{+2} from intracellular stores, G-protein activation and granule release [343, 344]. Several proteins are phosphorylated by PKG and PKA including VASP [51]. Inositol triphosphate receptor (IP3-R), expressed in platelets, can also be phosphorylated by PKA and PKG [345] leading to inhibition of Ca^{2+} release in platelets [346, 347].

During the course of this research it has been shown, for the first time, that Kynurenine inhibits platelet aggregation and that its mechanism of action is mediated by the activation of sGC and AC enzymes, leading to an increase in cGMP and cAMP levels and the subsequent activation of cGMP dependent-protein kinase (PKG) and cAMP-dependent protein kinase (PKA) (figure 4.48).

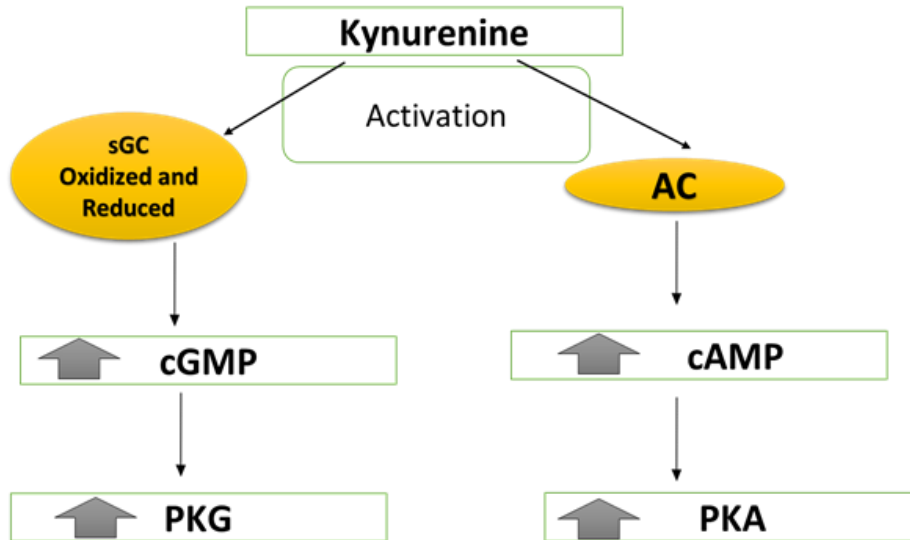


Figure 4-48: Mechanism of action of Kynurenine on platelet aggregation. Kynurenine activates soluble guanylyl cyclase (sGC) leading to conversion of guanosine 5'-triphosphate into guanosine 3',5'-monophosphate (cGMP) which in turn activates cGMP dependent protein kinase (PKG). Kynurenine also activates adenylyl cyclase (AC) increasing cAMP level which in turn activates cAMP-dependent protein kinase (PKA).

4.6. Pharmacological modulation of kynurenine on collagen-induced platelet aggregation-by PKG and PKA inhibitors.

To examine if adenylyl cyclase and guanylyl cyclase activation pathways are the predominant pathways through which Kynurenine exerts its inhibitory effect on platelets, enzymes and protein kinases inhibitors of each pathway were used next in functional studies using LTA.

4.6.1. Pharmacological modulation of adenylyl cyclase- cAMP-protein kinase A pathway.

To investigate if the pharmacological inhibition of adenylyl cyclase enzyme and protein kinase A, individually or in combination, could attenuate the inhibitory effect of kynurenine on collagen induced platelet aggregation. PRP pre-incubated with adenylyl cyclase inhibitor (SQ-22,536 at 100 μ M) and/or a PKA inhibitor (Rp-cAMP at 100 μ M) for at least 10 minutes in the presence and absence of 1mM Kynurenine. Kynurenine was incubated for further 2 minutes and platelet aggregation induced by 4 μ g/mL of collagen. The results obtained from the LTA studies showed that SQ-22,536 had no effect on the inhibitory effect of kynurenine on collagen induced platelet aggregation. However, Rp-cAMP and the combination of adenylyl cyclase inhibitor and PKA inhibitor (Rp-cAMP) significantly reduced the inhibitory effect of kynurenine on platelet aggregation induced by collagen (figure 4-49). It has been previously reported that inhibition of a PKA pathway partially reversed the inhibitory effect of a NO donor on collagen-induced platelet activation [68]. Dual effect of Kynurenine on AC and sGC may verify the ability of PKA inhibitor to attenuate the inhibitory effect of kynurenine as activation of PKA can be performed by cGMP by inhibition of PDE3[69] .

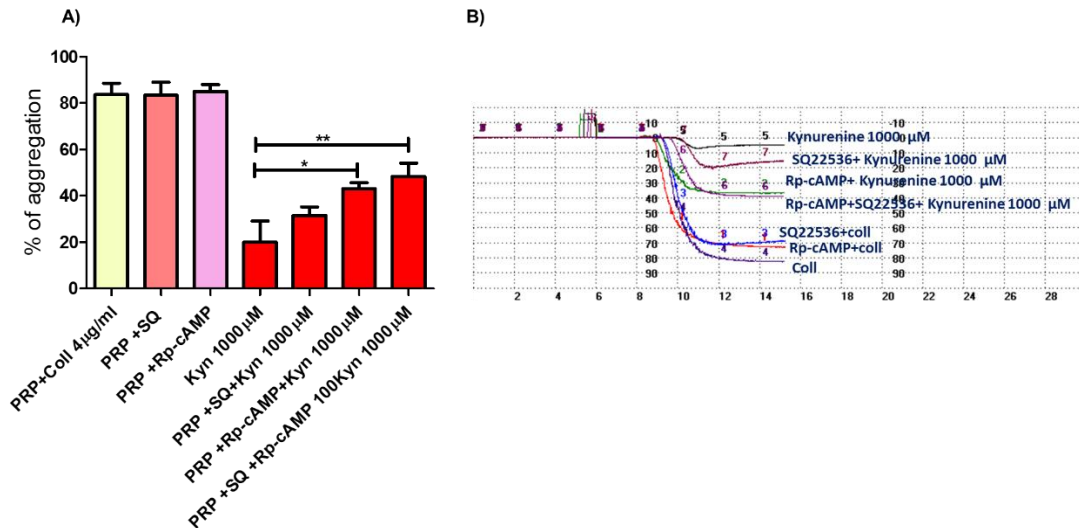


Figure 4-49: Pharmacological modulation of Kynurenine activation of platelet's adenylyl cyclase and protein kinase A in collagen induced platelet aggregation. (A) Statistical analysis showing that Rp-cAMP and combination of SQ-22,536 and Rp-cAMP significantly reduced the inhibitory effect of kynurenine on collagen induced platelet aggregation. Data is presented as the mean \pm SD; n=3; One-way ANOVA & Tukey's post-test. **P<0.01, * P<0.05. (B). Representative traces from light transmission aggregometry showing kynurenine effect in the presence of SQ-22,536 and Rp-cAMP in collagen induced platelet aggregation in PRP.

4.6.2. Pharmacological modulation of guanylyl cyclase- cGMP- protein Kinase G pathway.

Previous results (figure 4-32) shown that the sGC inhibitor, ODQ 10µM, failed to reverse the inhibitory effect of kynurenine at various concentration on collagen-induced platelet aggregation but significantly enhanced Kynurenine inhibitory effect due to the ability of Kynurenine to activate both the reduced and the oxidised form of sGC. Incubation of the PKG inhibitor (Rp-8-CPT-cGMP 500µM) with PRP for 10 minutes did not modify the inhibitory effect of kynurenine 1mM incubated for 2 minutes on collagen induced platelet aggregation as shown in figure 4-50. It was reported by other researchers that PKG inhibitor were not able to inhibit collagen-induced platelet aggregation [18]. The ability of kynurenine to act through more than one pathway could limit the potential of the PKG inhibitor to attenuate the inhibitory effect of kynurenine on collagen induced platelet aggregation due to its interaction with PKA pathway by phosphodiesterase's inhibition which is upstream of PKA.

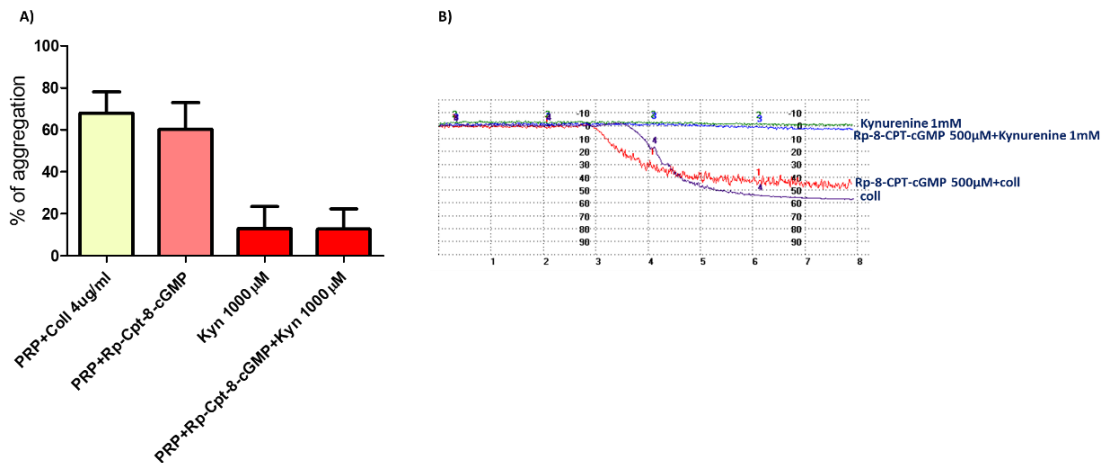


Figure 4-50: Effect of PKG inhibitor on Kynurenine in collagen- induced platelet aggregation. (A) Statistical analysis showing that cGMP- dependent protein kinase (PKG) inhibitor (Rp-8-CPT-cGMP 500 μ M) has no effect on the inhibitory effect of Kynurenine on collagen induced platelet aggregation. Data is presented as the mean \pm SD; n=3; One-way ANOVA. (B) Representative traces from light transmission aggregometry showing the effect of Kynurenine 1mM in the presence of PKG inhibitor

The major endothelium-derived inhibitors of platelet activation are nitric oxide (NO) and prostacyclin (PGI₂). PGI₂ acts by stimulation of adenylyl cyclase whereas NO activates guanylyl cyclase [5]. It has been found that vascular endothelial cells represent a major source of IDO activity *in vivo* and IDO induction was associated with an increased conversion of tryptophan to kynurenine and vascular tone regulation [102]. Hence, it cannot be excluded that kynurenine may represent a natural endothelial derived factor able to modulate platelet aggregation through activation of both, adenylyl cyclase and guanylyl cyclase. It may be that, under pathological situations such as inflammatory and cardiovascular diseases where oxidative stress is responsible for oxidizing the heme form of sGC making the enzyme refractory to the effect of nitric oxide [26], kynurenine may play a key role as an alternative activator of the enzyme. This is undoubtedly an important discovery that will certainly have significant clinical implications and that can open the door for future novel therapeutic approaches.

4.7. Soluble guanylyl cyclase enzyme activators and stimulators

4.7.1. *Kynurenine pharmacophores and their potential effect on soluble guanylyl cyclase*

Two main types of compounds that modulate sGC have been identified: sGC stimulators and sGC activators (figure 4-51). sGC stimulators are NO-independent but heme-dependent compounds that bind to the reduced heme-moiety to activate the enzyme. Riociguant (Ademps™) is the only sGC stimulator currently in the market and it is approved for the treatment of pulmonary hypertension [348]. sGC activators are NO- and heme-independent compounds as they can activate the oxidized heme-moiety or the heme-free sGC by binding and restoring the catalytic activity of the enzyme thus having, an additive effect in the presence of NO [348]. Since the discovery of cinaciguat (Bay 58-2667) in 2006, only the sGC activator MGV354 is in the latter stage of drug development to treat glaucoma [349].

Those compounds bind to two distinct sites in the sGC and, to our knowledge no compound has been shown so far to activate both, the reduced and the oxidized heme-groups of the enzyme[350] except kynurenine.

However, the binding site of kynurenine on the enzyme or the molecular mechanism through which kynurenine can increase the catalytic activity of the enzyme is still unknown.

NO-independent Haem-dependent sGC stimulators

NO-independent Haem-independent sGC activators

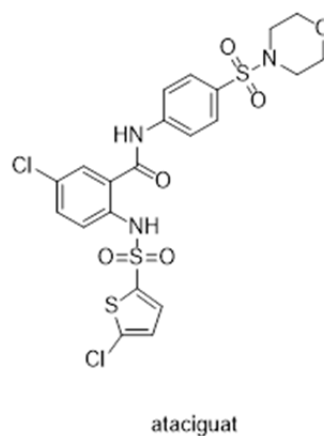
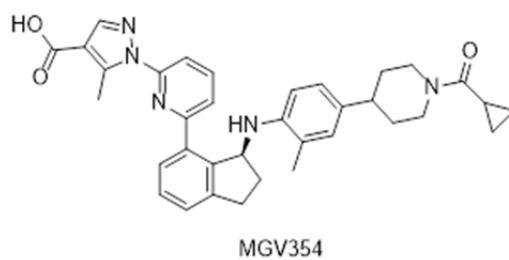
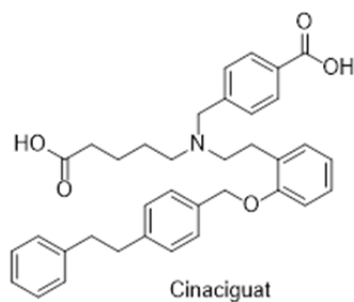
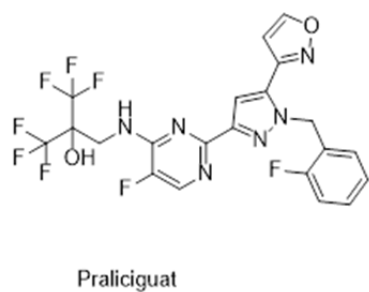
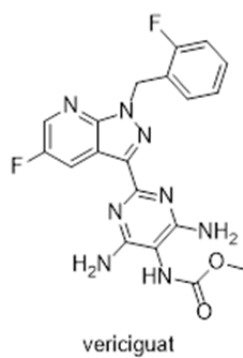
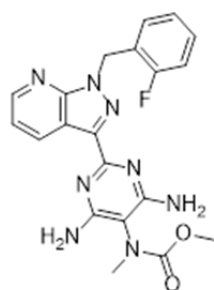
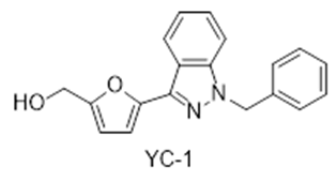


Figure 4-51: Structures of common soluble guanylyl enzyme activators and stimulators.

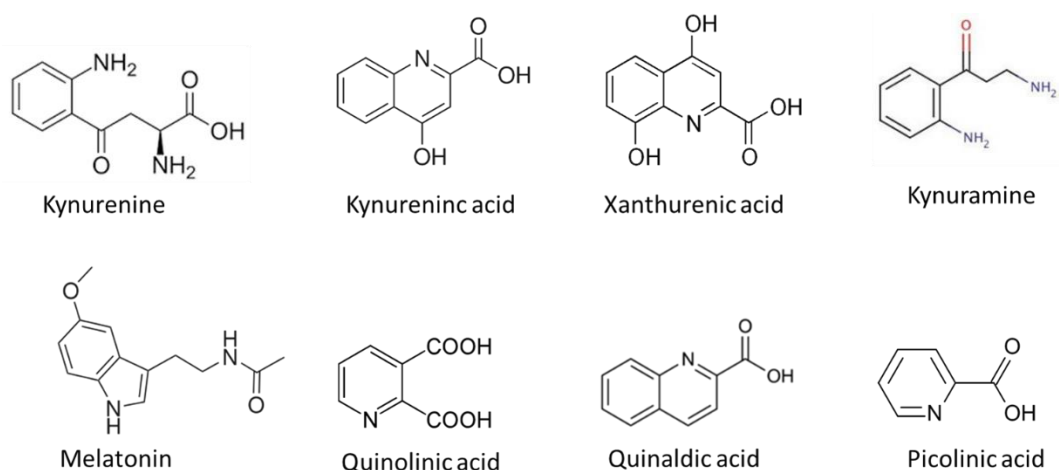


Figure 4-52: Chemical structure of compounds that have structural and metabolic relationship with kynurenine. The compounds structure is composed of hydrophilic aminobenzene and a hydrophobic butyl carboxylate.

modification in kynurenine structure to increase its affinity to the reduced sGC form and to activate the enzyme at nanomolar concentrations sought to be made according to the structure activity relationship (SAR) of Kynurenine and its similarity with sGC stimulators and activators. Furthermore, there is still possibility that the observed effect of kynurenine on platelet function could be due to any of its metabolites and need to be excluded (figure 4-52)

Therefore, the next step in this research was focused on investigating the ability of a number of compounds to activate platelet's sGC by measuring the levels of intraplatelet cGMP using ELISA.

4.7.2. Effect on platelet cGMP concentration

Kynurenine, kynurenic acid, quinolinic acid, xanthurenic acid, quinaldic acid and picolinic acid and the tryptophan metabolite melatonin, were all examined for their potential effect on both, the reduced and the oxidised forms of sGC by measuring the intraplatelet cGMP. 250 μ M of each compound was incubated for 5 minutes with PRP in the presence and absence of OQD10 μ M and SNAP was used as a positive control. The results obtained are shown in figure 4-53 and as expected, kynurenine and SNAP significantly increased the levels of cGMP by activating the intact (reduced heme-) form of the sGC. However, when the sGC enzyme was oxidized following platelets incubation with ODQ, kynurenine but not SNAP retained its ability to activate the enzyme.

Picolinic acid, was also able to activate both forms of the enzyme and significantly increase cGMP. Picolinic acid is an end catabolite of L-tryptophan that act as iron chelating agent and a co-inducer of NO production [351] and its potential effect as sGC activator or stimulator has not been previously investigated.

Quinaldic acid and melatonin increased reduced-heme sGC activity but failed to activate the oxidized form of the enzyme.

It has been reported that melatonin, at physiological concentrations (less than 1 μ M) facilitated platelet aggregation [352], whereas at concentrations higher than 10 μ M, it attenuated platelet aggregation induced by collagen, ADP and epinephrine [353, 354] by a mechanism that involves the cyclooxygenase pathway [355].

Quinolinic acid significantly increased intraplatelet cGMP levels when the enzyme in the oxidized but not the reduced form. Quinolinic acid is a N-methyl-D-aspartate (NMDA) receptor agonist (neurotoxic) and its effect on platelet sGC has not been investigated.

kynurenic acid, kynuramine and xanthurenic acid showed no effect on platelet cGMP.

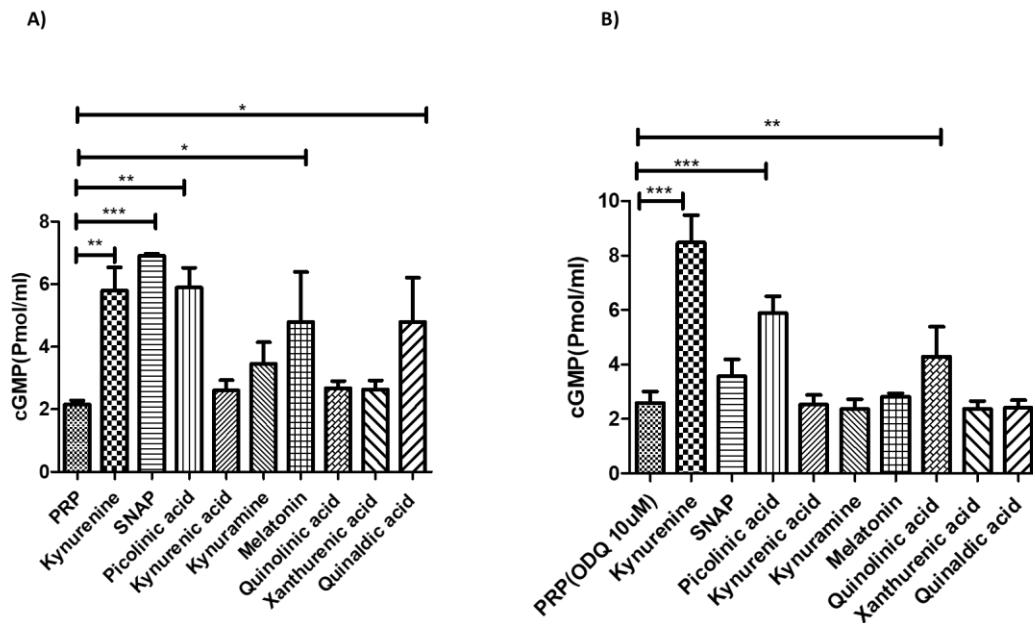


Figure 4-53: Effect of compounds structurally or metabolically related to kynurenine on intraplatelet cGMP. Statistical analysis showing the effect of the compounds when sGC is reduced form (A) and oxidised form (B). Data are presented as the mean \pm SD; n=3; One-way ANOVA & Tukey's post-test. ***P < 0.001, **P < 0.01, * P <0.05.

pharmacological effect of the compounds that caused significant increase in cGMP level, on collagen 4µg/ml induced platelet aggregation was investigated using LTA to investigate their effect on platelet function.

4.7.3. Pharmacological effect

To assess the effect of the compounds that caused a significant increase in cGMP, 250µM of picolinic acid, quinaldic acid and melatonin as well as kynuramine (despite not causing a significant increase in cGMP level but has structural similarity with kynurenine) were incubated with PRP for 10 minutes prior to induction of platelet aggregation by collagen 4µg/mL in LTA (figure 4-54 and 4-55).

Results shown that melatonin and kynuramine significantly inhibited collagen induced platelet aggregation and these results were corroborated by micrographs from optical microscopy showing that the size of platelet aggregate induced by collagen was considerably smaller in the presence of melatonin and kynuramine. Melatonin concentrations higher than 10 μM , was reported to attenuates aggregation induced by agonists like collagen, ADP and epinephrine [352, 354, 356] by affecting cyclooxygenase enzyme. However, this effect was not examined if it is cGMP dependent.

Despite not affecting intraplatelet cGMP, kynuramine counteracted the effect of collagen on platelet. Kynuramine has not been tested for its effect on platelets aggregation and such effect deserves a lot of attention and further investigation due to the small size of kynuramine molecule.

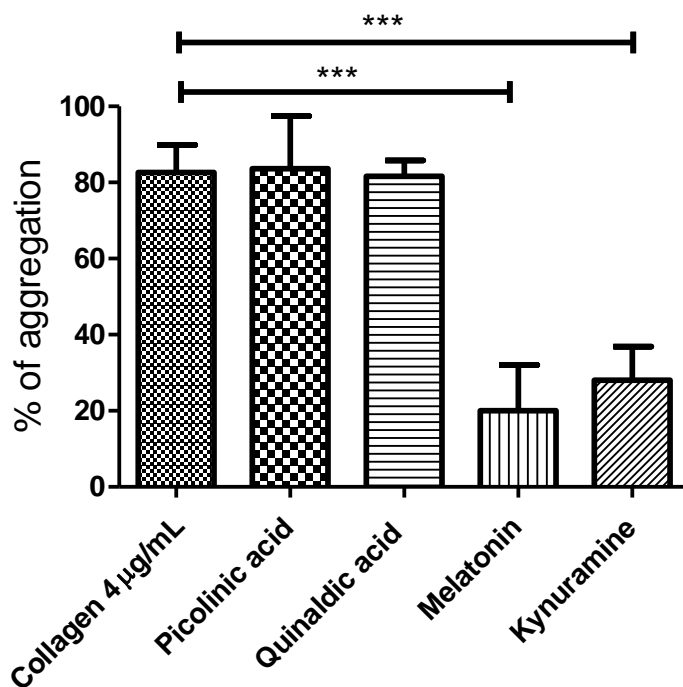


Figure 4-54: Effect of picolinic acid, quinaldic acid, melatonin and kynuramine on collagen induced platelet aggregation. Statistical analysis showing the effect 250 μM of picolinic acid, quinaldic acid, melatonin and kynuramine on collagen 4 $\mu\text{g/mL}$ induced platelet aggregation in PRP. *Data are presented as the mean \pm SD; n=3; One-way ANOVA & Tukey's post-test. ***P < 0.001*

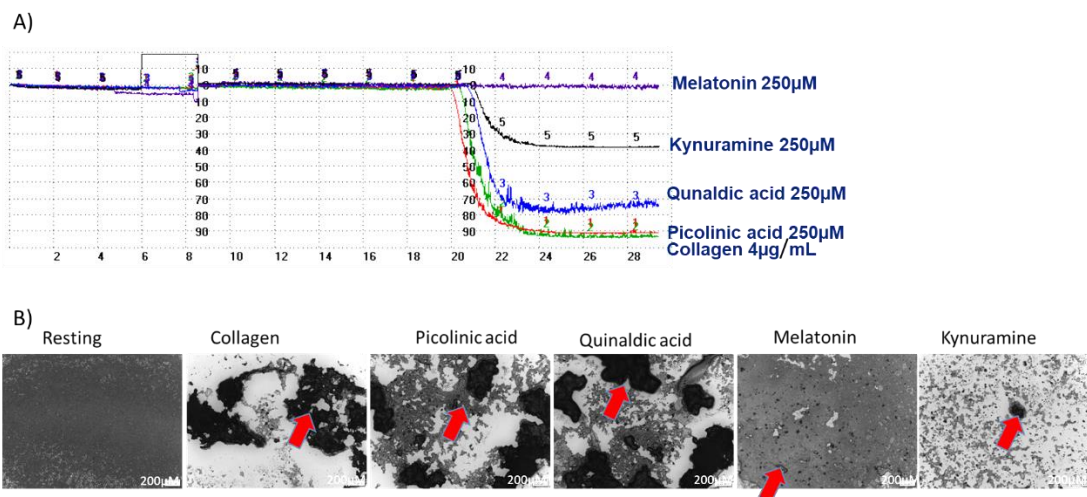


Figure 4-55: A) Representative traces from LTA showing the effect of picolinic acid, quinaldic acid, melatonin and kynuramine on collagen induced platelet aggregation in PRP. B) Micrographs (5x) from optical microscopy showing platelet aggregate induced by collagen in the presence of picolinic acid, quinaldic acid, melatonin and kynuramine. Red arrows indicate platelet aggregates.

Our results indicate that the significant increase in platelet's cGMP was not enough to modulate platelet function by picolinic acid and quinaldic acid. However, melatonin which also inhibits cyclooxygenase enzyme and arachidonic acid synthesis; and kynurenine which activates sGC and AC could modulate platelet function.

AC-cAMP-PKA seems to be the predominant pathway for kynurenine to modulate platelet function since PKG inhibitor could not affect the inhibitory effect of kynurenine on collagen induced platelet aggregation while PKA inhibitor significantly reduced the inhibitory effect of kynurenine. Furthermore, phosphorylation of VASP at serine 157 by PKA is higher than the phosphorylation of VASP at serine 238 by PKG. Additionally, agents that significantly increased cGMP were not able to inhibit collagen induced platelet aggregation.

More experiments are needed to explore the binding site of kynurenine and its ability to activate sGC in both forms. Kynurenine analogue which retains kynurenine effect, evades decarboxylation and in turn has longer half-life may represent an excellent opportunity to examine kynurenine effect on platelets and blood vessels in preclinical studies.

4.8. Role of kynurenine in TCIPA

Kynurenine has a potent inhibitory effect when a wide range of platelets agonists, which act via different pathways, were used to induce platelet aggregation. The mechanism of action of kynurenine involves increasing intraplatelet cGMP and cAMP, leading to inhibition of platelet aggregation mediated by collagen and ligands of G-protein-coupled receptors like ADP, thrombin, thromboxane and AA. Kynurenine is produced by cancer cells and it plays an important role in tumour-induced immunosuppression. However, the role of kynurenine in tumour cells induced platelet aggregation has not been investigated.

4.8.1. *Tumour cell-induced platelet aggregation (TCIPA) study*

A wide range of tumour cell lines from different origins (A549, HeLa, HT-29, SW-480 and HCC-1954) were tested, at 1000, 2000, 4000 and 10000 cells final concentration, for their ability to induce platelet aggregation using LTA. Addition of tumour cells to platelets suspensions resulted in platelet aggregation for all the cell lines tested as shown in figure 4-56. Note, that it is expected that the extent of platelet aggregation obtained does not correlate with the different concentrations of tumour cells used since, once TCIPA is initiated, platelet aggregation is always maximal and irreversible [251]. The lag phase instead (time elapsing from the addition of the tumour cells to the occurrence of aggregation) can be used as an inverse index of the aggregatory potency of the tumour cell line tested inferring that, the shorter the lag phase, the more potent the cell line can be considered.

A549, Hela, HT-29 and SW-480 cells caused TCIPA in a concentration dependent manner as when the duration of the lag phase was compared to the number of cells used to induce platelet aggregation for every cell line (figure 4-57). Figures 4-58, 4-59, 4-60 and 4-61 are representative traces from LTA where this difference can be observed. On the other hand, the induction of TCIPA by HCC-1954 cells showed the same duration of the lag phase independently of the concentration of cells used (figure 4-62). It has been previously reported that cancer is associated with a pro-thrombogenic state that leads to platelet activation and induction of platelet secretion which is crucial for TCIPA [357]. The

ability of tumour cells to induce platelet secretion; called TCIPS, occurs before TCIPA [358] and the rapid dense-granule secretion is the primary platelet response to cancer cells that determines their lag phase and consequently their potency [358].

When the duration of the lag phase of the different cell lines for TCIPA by 1000 cells were compared between the cell lines tested, A549 appeared to be the least potent cell line inducing TCIPA with a lag phase of about 14 minutes (13.63 ± 0.63) whereas HCC-1954 was the most aggressive cell line, inducing TCIPA after less than 3 minutes of incubation (2.17 ± 0.29 minutes) as shown in figure 4-63.

The reduced potency of A549 to induce platelet aggregation has been also demonstrated by other researchers [208, 359] and the lag phase duration obtained for the other cell lines comparable to the results obtained in previous reports available in the literature: HeLa (10 ± 0.55 minutes) [360], HT-29 (7.83 ± 0.29 minutes) [361] and SW-480 (6.000 ± 0.82 minutes) [362]. It is not surprising that the tumour cells tested in this research were different in their potency to induce platelet aggregation as they may have different ability to produce different pro-aggregatory mediators[240] or anti-aggregatory agents like NO [118]. Cancer cells also vary in their ability to induce platelet granule release and to interact with platelet surface receptors[251, 358]

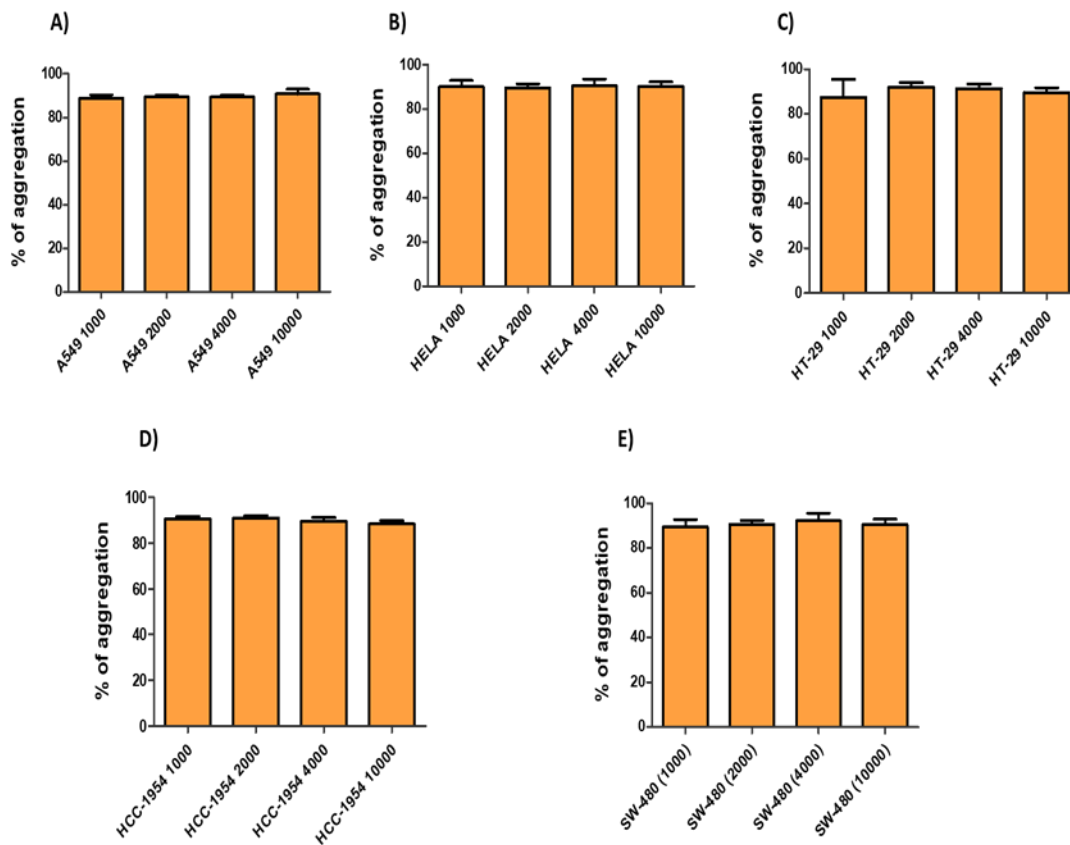


Figure 4-56: Effect of cell number on tumour cell-induced platelet aggregation (TCIPA) by different cell lines. Statistical analysis showing maximal aggregation induced by A549 (A), HeLa (B), HT-29 (C), HCC-1954 (D) and SW-480 (E). Data is presented as mean \pm SD; n=4; One-way ANOVA ($P > 0.05$)

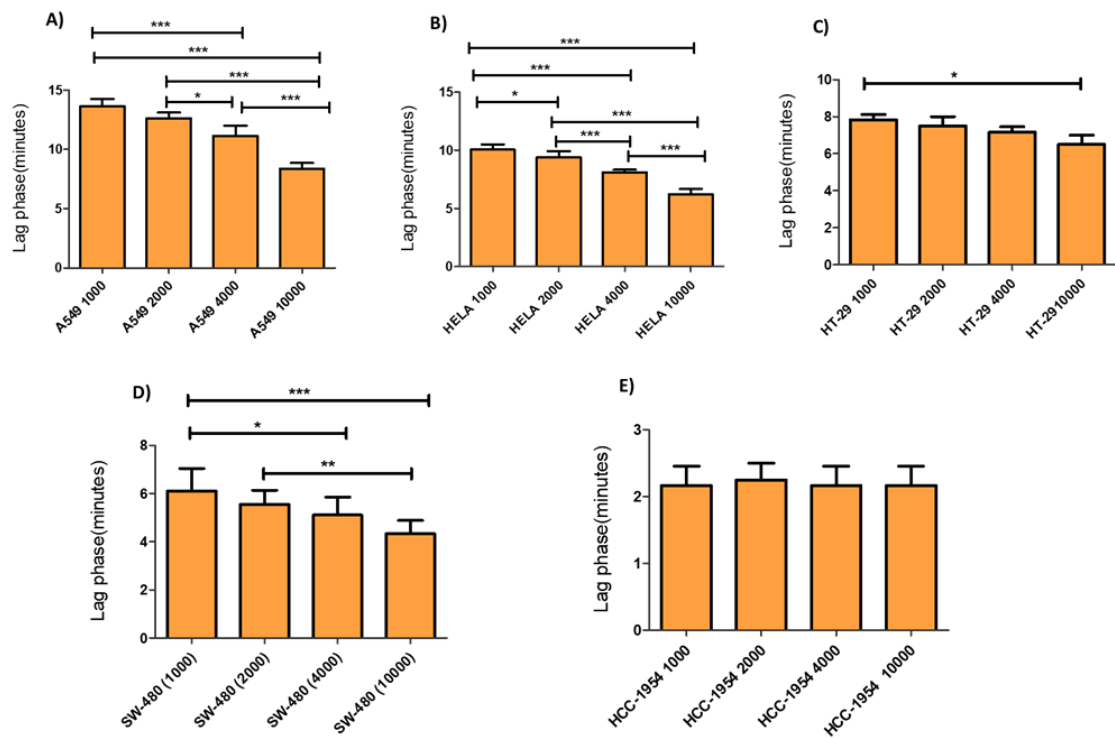
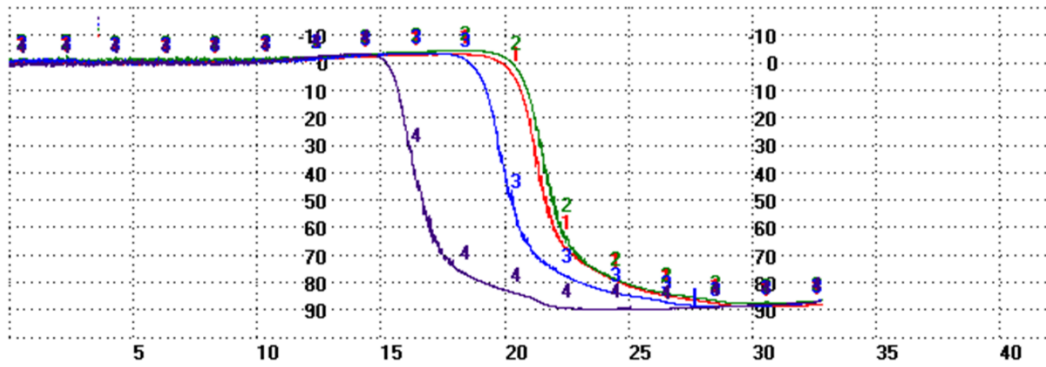
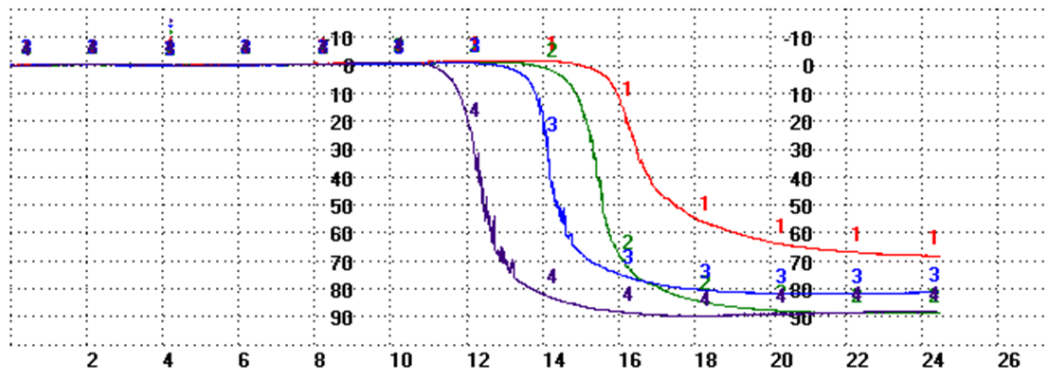


Figure 4-57: Effect of cell number on lag phase of tumour cell-induced platelet aggregation (TCIPA) by different cell lines. Statistical analysis of TCIPA lag phase induced by (1000-10000 cells/500 μ L) of A549 (A), HeLa (B), HT-29 (C), SW-480 (D) and HCC-1954 (E). Data is presented as mean \pm SD; n=4; One-way ANOVA & Tukey's post-test. *** P < 0.001 ** P < 0.01 *P < 0.05



Ch	Sample ID	ID Number	PA
1	WP+A549	1000	89
2	WP+A549	2000	88
3	WP+A549	4000	89
4	WP+A549	10000	90

Figure 4-58: Representative traces from light transmission aggregometer showing the differences in the lag phase of A549-induced platelet aggregation, No difference in maximal platelet aggregation independently of the number of cells used. Note that the time in minutes is represented at the bottom of the graph.



Ch	Sample ID	ID Number	PA
1	WP+HELA	1000	68
2	WP+HELA	2000	89
3	WP+HELA	4000	82
4	WP+HELA	10000	90

Figure 4-59: Representative traces from light transmission aggregometer showing the variation in lag phase of TCIPA induced by HT-29 cells when various number of cells were used. Note that the time in minutes is represented at the bottom of the graph. In this case 10000 cells induced platelet aggregation after 11 minutes of incubation vs 15 minutes when 1000 cells were used.

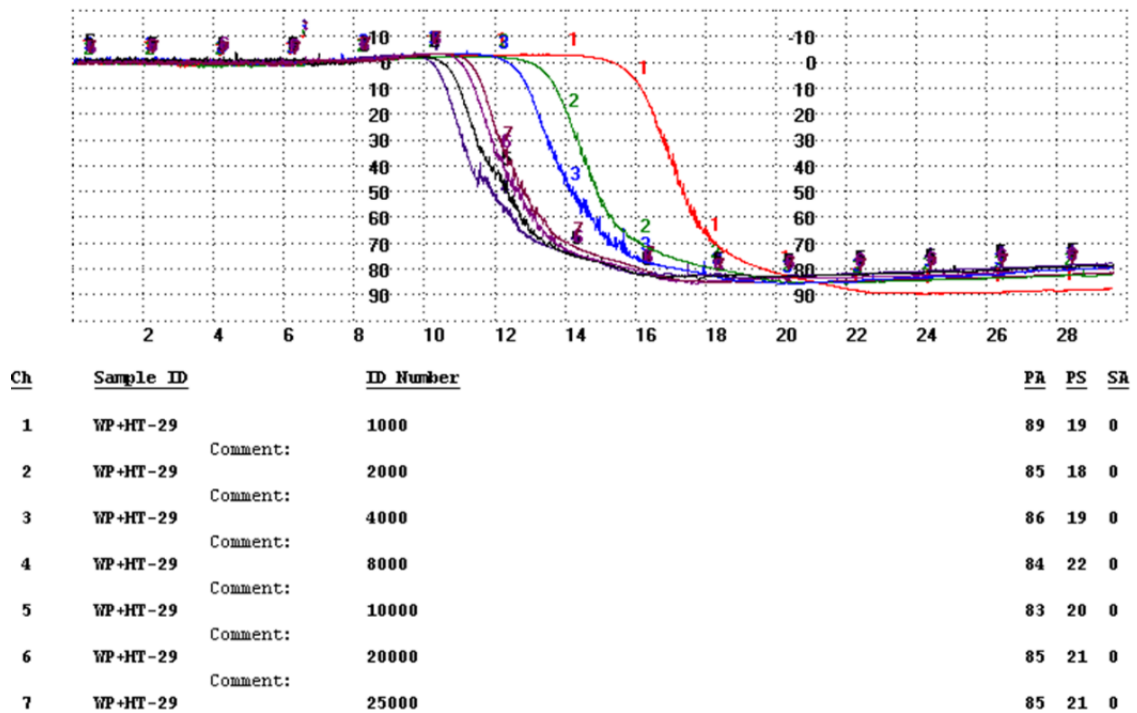
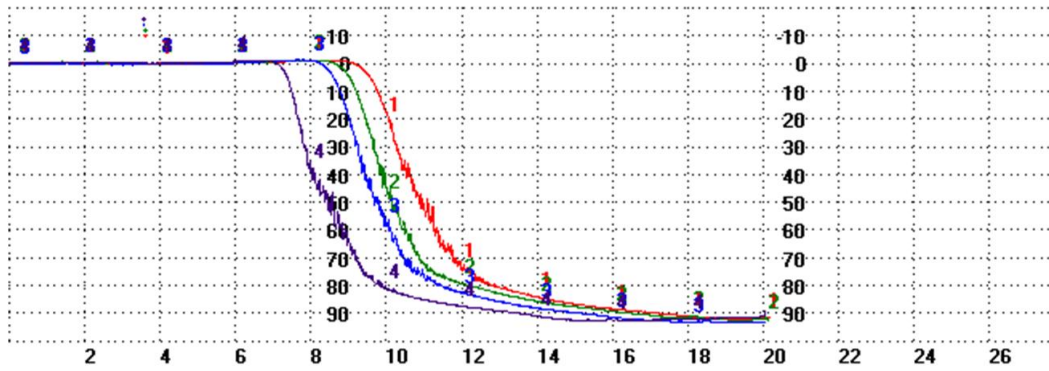
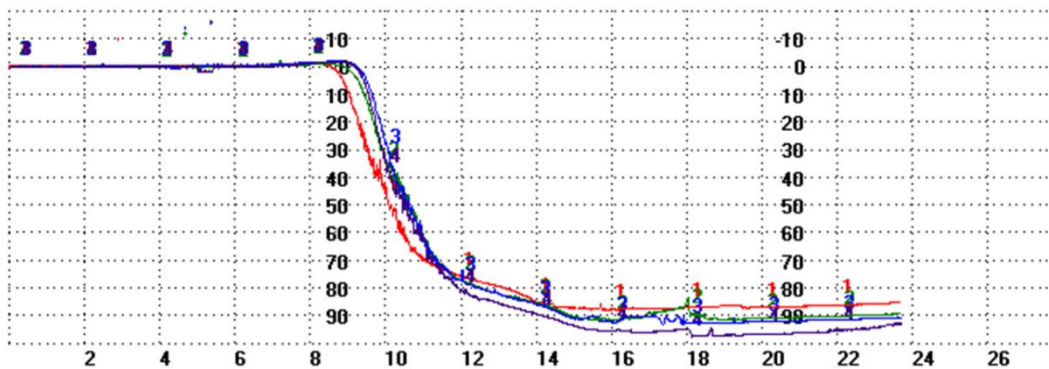


Figure 4-60: Representative traces from light transmission aggregometer showing the difference in lag phase but not in maximal platelet aggregation induced by HT-29 cells when various number of cells were tested. The time in minutes is represented at the bottom of the graph. In this particular case 10000 cells induced platelet aggregation after 10 minutes of incubation vs 15 minutes when 1000 cells were used.



Ch	Sample ID	ID Number	PA
1	WP+SW480	1000	92
2	WP+SW480	2000	93
3	WP+SW480	4000	93
4	WP+SW480	10000	93

Figure 4-61: Representative traces from light transmission aggregometer showing the short lag phase of TCIPA induced by various cell number of SW-480 colon cancer cells. The lag phase time, in minutes, is represented at the bottom of the graph. In this particular case 10000 cells induced platelet aggregation after 7 minutes of incubation vs 9 minutes when 1000 cells were used.



Ch	Sample ID	ID Number	PA
1	HCC+WP	1000	88
2	HCC+WP	2000	91
3	HCC+WP	4000	93
4	HCC+WP	10000	97

Figure 4-62: Representative traces from light transmission aggregometer showing the potency of HCC-1954 inducing platelet aggregation regardless of cell number used. The time in minutes is represented at the bottom of the graph. In this particular case all number of cells induced platelet aggregation after less than 10 minutes of incubation.

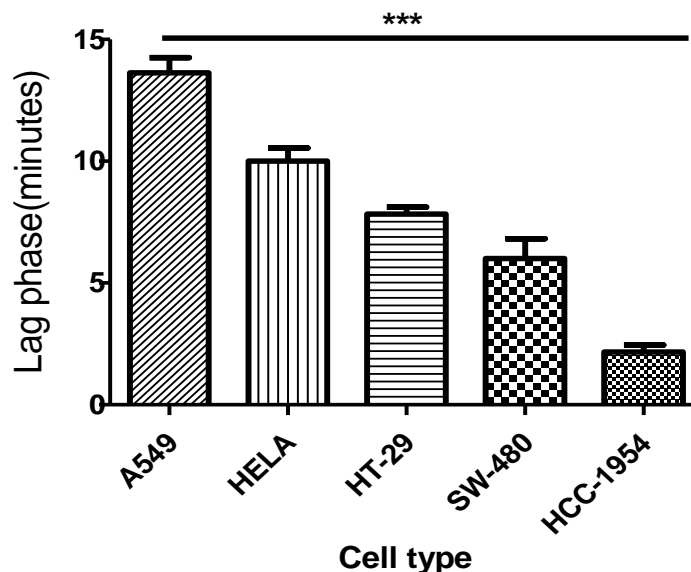


Figure 4-63: Statistical analysis showing the differences in the duration of the lag phase induced by 1000 cells for the different cell lines. Data is expressed as mean \pm SD; n=4; One-way ANOVA & Tukey's post-test. *** P < 0.001 vs each other.

4.8.2. Effect of kynurenine on TCIPA

To investigate the potential effect of kynurenine on TCIPA, kynurenine (100-500 μ M) was incubated for at least 2 minutes with WP prior to induction of TCIPA by A549, HeLa, HT-29, SW-480 and HCC-1954 cells (1000, 2000, 4000 and 10000 cells) and platelet aggregation monitored by LTA.

4.8.2.1. Effect of Kynurenine on A549-induced platelet aggregation

Kynurenine significantly inhibited A549-induced platelet aggregation in a concentration dependent manner (figure 4-64) but had no effect on the duration of the lag phase as shown in figure 4-65 and figure 4-66. DMSO, used as kynurenine vehicle, did not exert any effect neither on platelet aggregation nor in the duration of the lag phase induced by A549 (figure 4-67)

According to the data published in the literature, the mechanisms by which A549 cells induce platelet aggregation (figure 4-68) can involve the release of MMP-2

[240]. In fact, the inhibition of MMP-2 by phenanthroline, a broad-spectrum MMP inhibitor, or by anti-MMP-2 antibodies has been demonstrated to reduce TCIPA in different cell lines [145, 363]. MMP-2 has been shown to up-regulate platelet GPIb receptor expression and to interact with the GPIIb/IIIa receptor [364, 365]. In addition, adhesion of fibrinogen to GPIIb/IIIa receptors, that plays a pivotal role in TCIPA, can be regulated by MMP-2 [364].

Interactions of A549 cells with platelets have also resulted in the activation of Bruton tyrosine kinase (Btk) signalling pathway in platelets, leading to platelet activation as demonstrated by a significant upregulation of Btk tyrosine phosphorylation, PLC γ 2 activation and release of platelet granules content (serotonin, EGF, VEGF, PDGF, and TGF β) mediated by Galectin 3 which is highly expressed on A549 cells [366]. Btk plays an essential role in the modulation of platelet activation and aggregation downstream of GPVI in human platelets leading to the activation of GPIIb/IIIa and P-selectin translocation [367]. Since both, the platelet integrin receptor GPIIb/IIIa and P-selectin play a major role in TCIPA and our previous experiments demonstrated that kynurenine had a dramatic effect on platelet expression of GPIIb/IIIa activated and P-selectin induced by collagen, the effect of kynurenine on those receptors in platelets stimulated with A549 cells was next investigated by flow cytometry..

4.8.2.2. Effect of Kynurenine on platelet expression of GPIIb/IIIa and P-selectin induced by A549 cells

Kynurenine (100-500 μ M) was incubated for at least 2 minutes with platelets and then TCIPA initiated by the addition of A549 (1000 cells). Flow cytometry results confirmed the inhibitory effect of kynurenine on TCIPA as shown by the significant differences observed on the expression of GPIIb/IIIa activated and P-selectin translocation, from alpha granules to platelet surface (figure 4-69) and represented by the flow cytometry gates in figure 4-70. Downregulation of GPIIb/IIIa expression by kynurenine in TCIPA induced by A549 cells confirms the inhibitory effect of this tryptophan metabolite during this interaction. Kynurenine also inhibited α -granules content release, as it reduces the translocation and expression of P-selectin which play a significant role in TCIPA and mediates platelet adhesion to tumour cells [368]. Inhibition of P-selectin expression when

kynurenine is incubated with platelets during TCIPA implies that kynurenine may inhibit the release of pro-aggregatory mediators like PF4 and thrombospondin, known to play a pivotal role in TCIPA induced by A549 [369, 370]. Furthermore, in our previous study it was also demonstrated that kynurenine antagonises the effect of thromboxane and arachidonic acid on platelet function and hence, it may mitigate the effect of PGE2 and thromboxane induced by Galectin-3 in TCIPA by A549 [244].

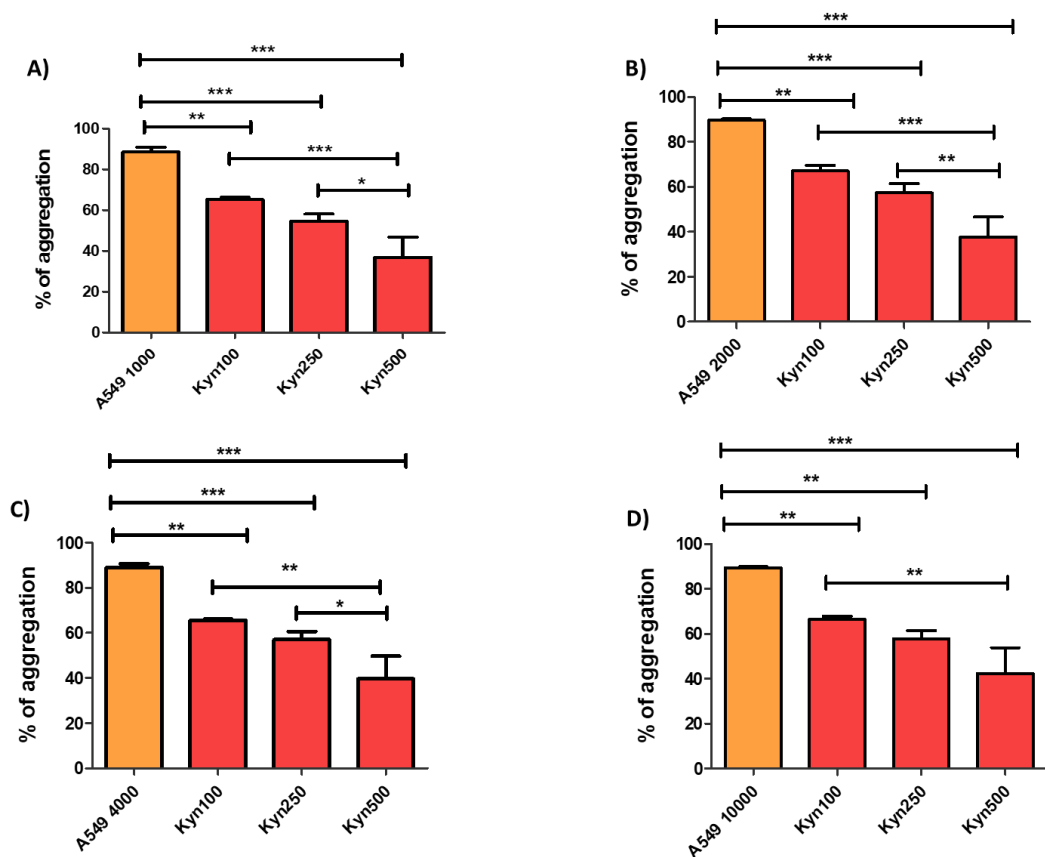


Figure 4-64: Effect of Kynurenine on tumour cell-induced platelet aggregation (TCIPA) by A549 lung carcinoma cells. Statistical analysis showing that kynurenine (100-500 μM) significantly inhibited platelet aggregation induced by A549: 1000 cells (A), 2000 cells (B), 4000 cells (C) and 10000 cells (D). Data is expressed as mean ± SD; n=4; One-way ANOVA & Tukey's post-test. *** P < 0.001, ** P < 0.01 and *P < 0.05.

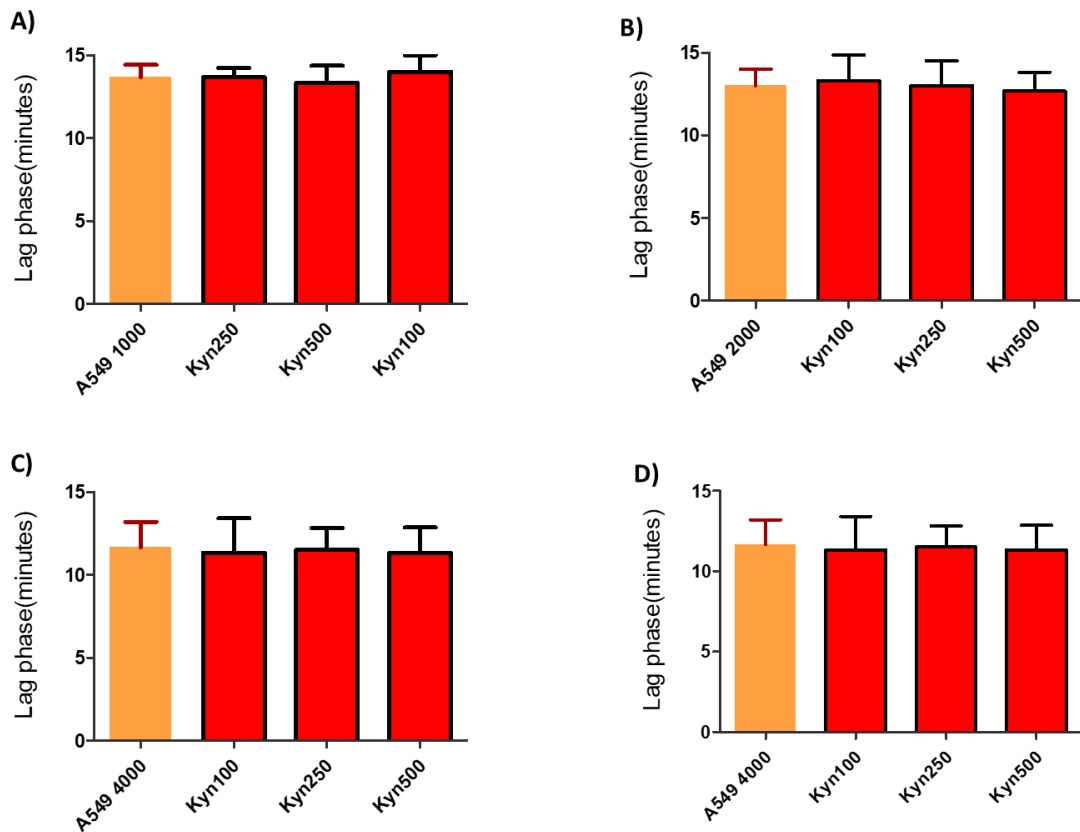


Figure 4-65: Effect of Kynurenine on lag phase duration induced by A549. Statistical analysis showing that kynurenine (100-500 μ M) has no effect on lag phase induced by A549: 1000 cells (A), 2000 cells (B), 4000 cells (C) and 10000 cells (D). Data is expressed as mean \pm SD; n=4; One-way ANOVA & Tukey's post-test.

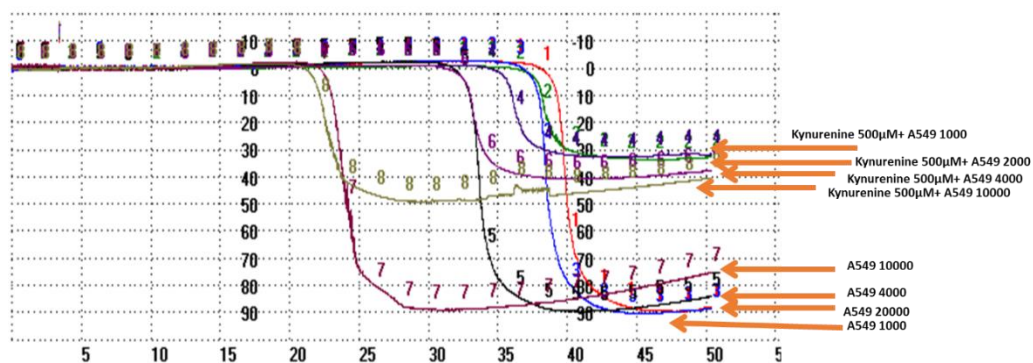


Figure 4-66: Representative traces from light transmission aggregometer showing the effect of kynurenine 500 μ M on maximal aggregation and lag phase of A549-induced platelet aggregation. The time in minutes is represented at the bottom of the graph.

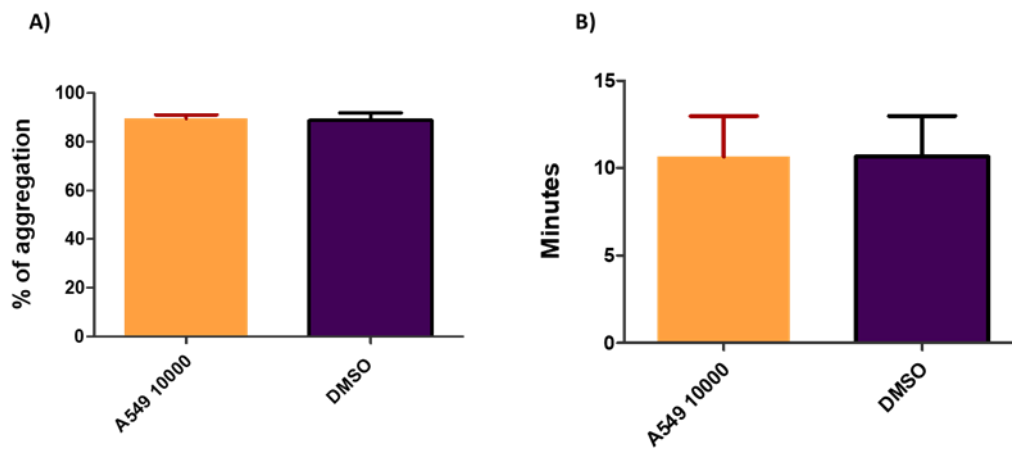


Figure 4-67: Effect of Vehicle (DMSO) on A549 induced platelet aggregation. Statistical analysis showing that DMSO 0.4% (equivalent to kynurenine vehicle) has no effect on maximal aggregation (A) and lag phase (B) during A549-induced platelet aggregation. Data is expressed as mean \pm SD; n=4; Paired-t test.

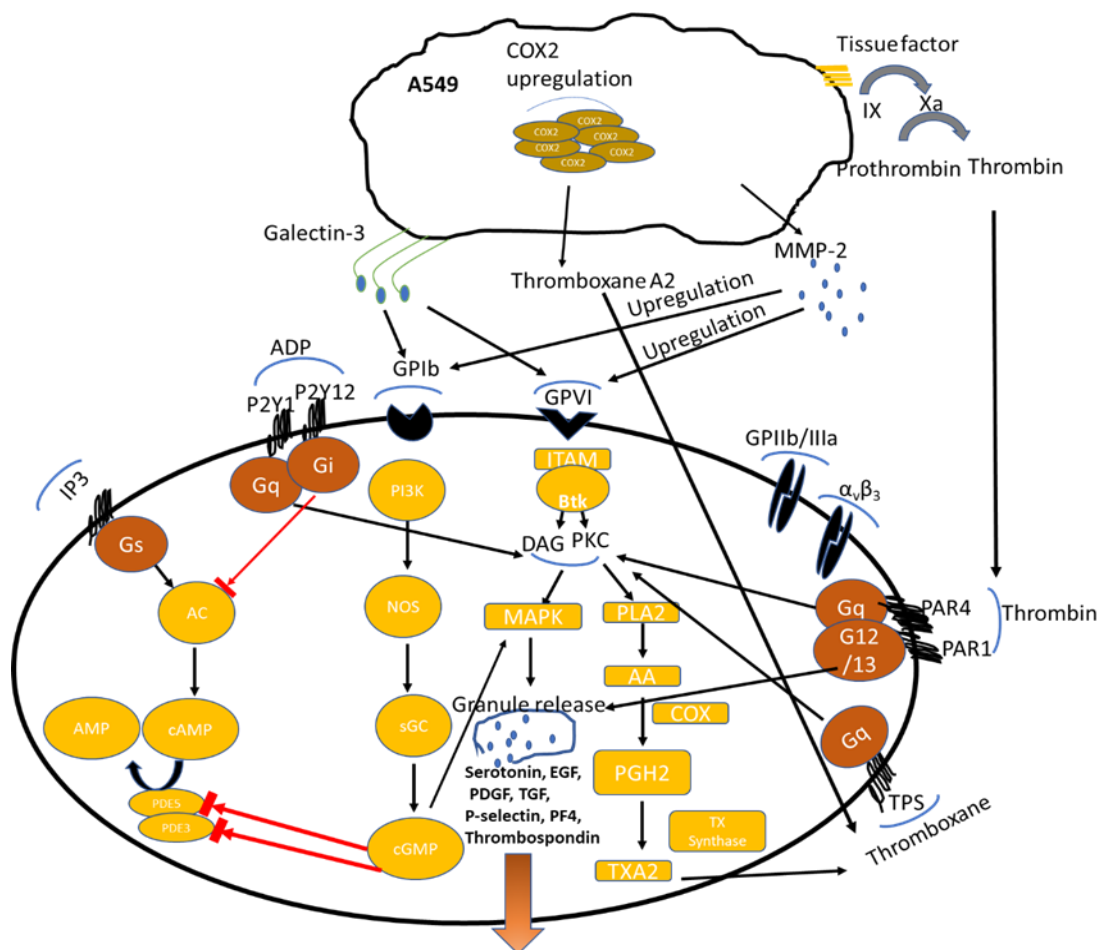


Figure 4-68: Potential mechanism of TCIPA by A549. A549 induces TCIPA by mechanisms involve the release of MMP-2 which activates platelets von Willebrand factor (GPIb) and collagen receptor (GPVI) initiating a cascade of events leading to platelet aggregation. Tissue factor (TF) and Galectin-3 which are associated with thrombin generation and von Willebrand factor receptor activation; respectively, participate in A549 induced TCIPA. Cox2: cyclooxygenase enzyme IX: coagulation factor IX, X coagulation factor X, MMP-2: Matrix metalloproteinase-2, GPVI: collagen receptor; GPIb: von Willebrand receptor; ADP: adenosine diphosphate; IP3: prostacyclin receptor; Gs, Gq and Gi: G-protein coupled receptors; PI3K: phosphatidyl Insositol-3 kinase; NOS: :nitric oxide synthase; sGC: soluble guanylyl cyclase; cGMP: Cyclic guanosine monophosphate; BTK: bruton tyrosine kinase; DAG: diacyl glycerol; ITAM: immunoreceptor tyrosine activation motif; PDE: phosphodiesterase enzyme; MAPK: mitogen activated protein kinase; AA: arachidonic acid; PLA2: phospholipase A2; PGH2: prostaglandin H2; EGF: endothelial growth factor; TGF: transforming growth factor; PDGF: Platelet-derived growth factor; PF4: platelet factor-4; AC: adenylyl cyclase; TXA2: thromboxane A2. Red arrow: inhibit; black arrow: activate

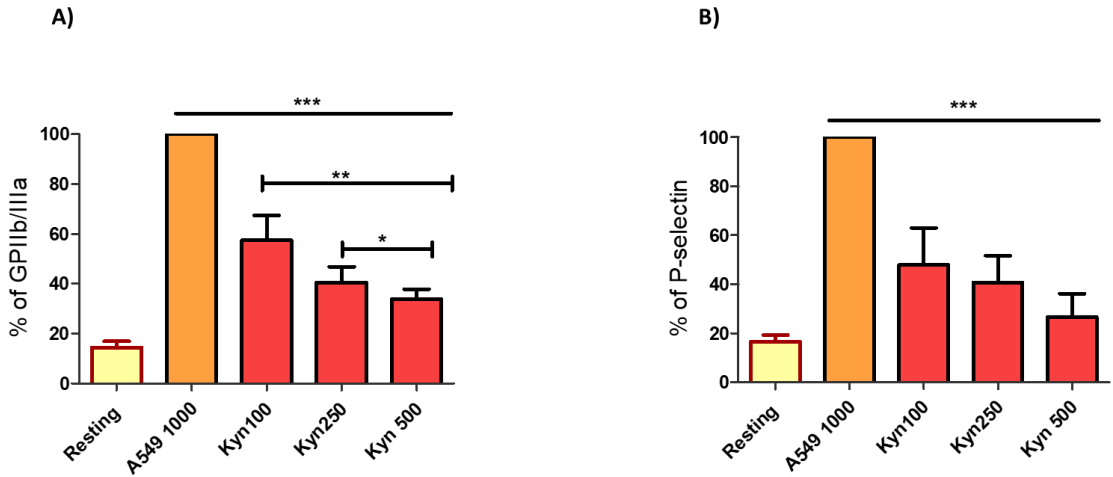


Figure 4-69: Effect of kynurenine on A549-induced platelet expression of activated GPIIb/IIIa and P-selectin. Statistical analysis showing that kynurenine (100-500 μ M) significantly reduced platelet expression of GPIIb/IIIa activated (A) and P-selectin (B) induced by A549. Data is represented as mean \pm SD; n=4; One-way ANOVA & Tukey's post-test. *** P < 0.001 ** P < 0.01 *P < 0.05.

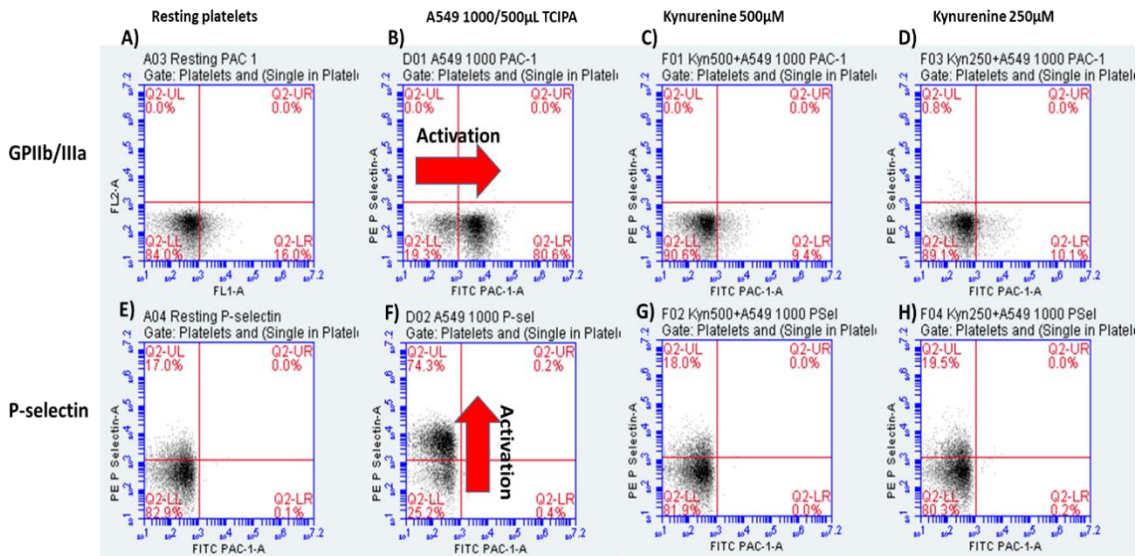


Figure 4-70: Representative gates from flow cytometry showing the effect of kynurenine (500 and 250 μ M) on A549-induced platelet expression of GPIIb/IIIa activated (PAC 1) and P-selectin. The lack of rightward shifting of platelet population from lower left quarter (Q2-LL) to the lower right quarter (Q2-LR) indicates inhibition of GPIIb/IIIa expression and the lack of upward shifting of platelet population from lower left quarter (Q2-LL) to the upper left quarter(Q2-UL) indicates inhibition of platelet P-selectin expression induced by A549 cells in the presence of kynurenine at the concentrations tested..

4.8.2.3. Effect of Kynurenine on HeLa-induced platelet aggregation

Kynurenine, when incubated with platelets, significantly reduced HeLa-induced platelet aggregation in a concentration dependent manner as demonstrated by decreasing the percentage of aggregation induced by HeLa cells at various concentrations (figure 4-71). However, kynurenine had no effect on the lag phase induced by HeLa cells (figure 4-72) which indicate that kynurenine has no effect on platelets' dense granules contents release in this cell line either. Kynurenine vehicle (DMSO), incubated at the same volume and time as kynurenine, did not modify the ability of HeLa cells to induced platelet aggregation (figure 4-73). A representative trace from LTA showing the effect of kynurenine on HeLa cells is displayed in figure 4-74.

HeLa cells have been previously found to induce platelet aggregation (figure 4-74) via thrombin generation associated with tissue factor (TF) like activity expressed on tumour cell surface and via interaction with platelet GPIb and GPIIb/IIIa receptors which was inhibited by antibodies against the integrins [230]. TF is responsible for local thrombin generation and fibrin deposition in the tumour microenvironment and thereby influences multiple cellular interactions of tumour and host cells [371]. Thrombin induces platelet aggregation through activation of platelet's PAR1, PAR4 and GPIb receptors [372-374] leading to activation of phospholipase C β (PLC β) in human platelets. Upon activation, PLC β hydrolyses phosphatidylinositol 4,5-bisphosphate to inositol-3-phosphate, leading to calcium release from internal stores, and diacylglycerol (DAG) activation, which in turn activates the protein kinase C (PKC). PAR1 and PAR4 also couple to G12/13 to activate Rho/Rho kinase [375]. The Gq/PLC β pathway is essential for GPIIb/IIIa activation and platelet aggregation, while the G12/13/Rho pathway is mainly involved in platelet shape change [5]. Also, PAR4 couples to Gi leading to AC enzyme inhibition. Kynurenine may antagonise the effect of thrombin on AC enzyme as, demonstrated in the first part of this work, it activates the enzyme elevating intraplatelet cAMP. Furthermore, activation of sGC by kynurenine increases intraplatelet cGMP which affects intraplatelet Ca⁺² level by the interaction with type I IP3 (IRAG) and type II IP3 receptors (activating transient receptor potential protein-C6-TRPC6) [376, 377] and can block thrombin-induced Rap1-GTP formation [378, 379]. cGMP can also inhibit platelet shape change which is

a crucial step in platelet aggregation by preventing Rho-mediated inhibition of myosin light chain phosphatase (MLP) [380].

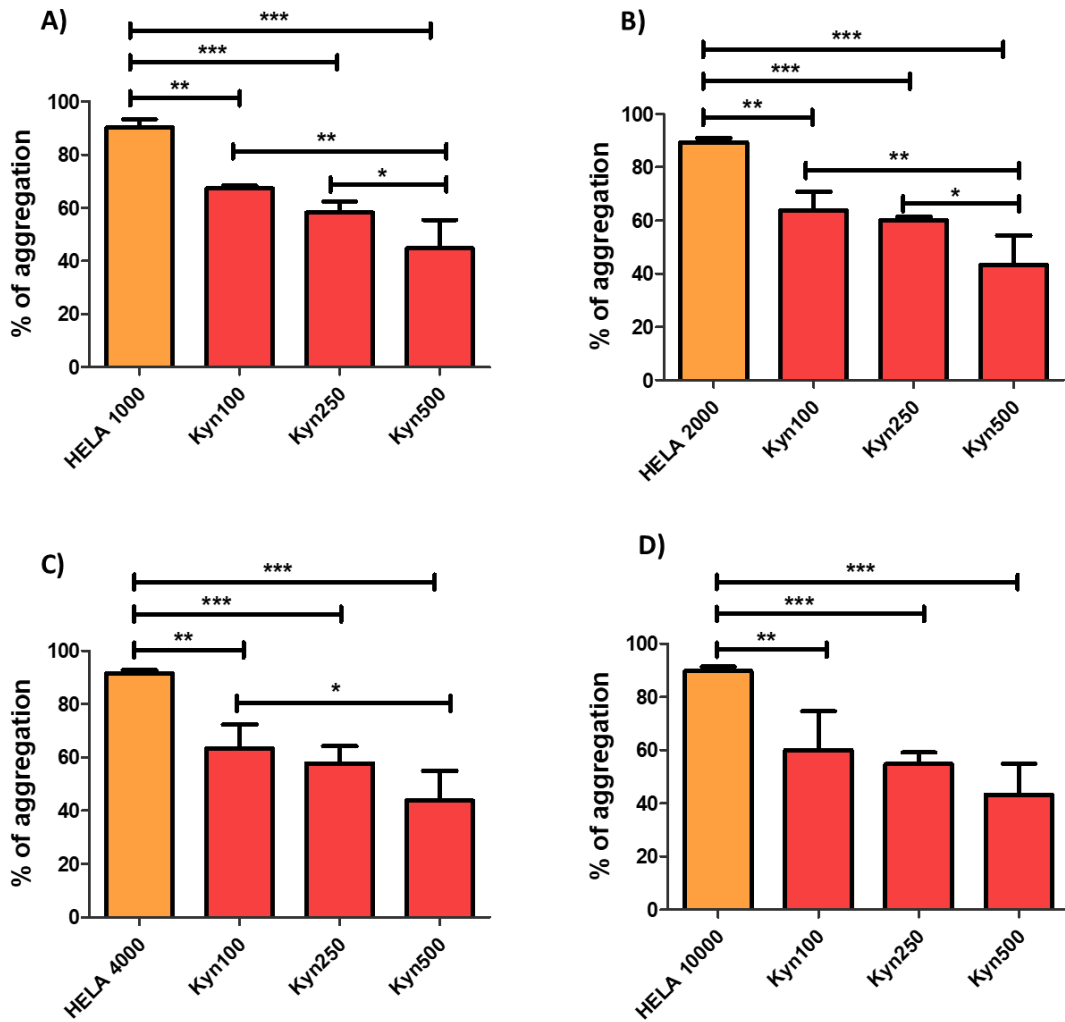


Figure 4-71: Effect of Kynurenine on HeLa cells-induced platelet aggregation. Statistical analysis showing that kynurenine (100-500 μM) significantly reduced maximal platelet aggregation induced by HeLa cells: 1000 (A), 2000 (B), 4000 (C) and 10000 (D). Data is represented as mean ± SD; n=4; One-way ANOVA & Tukey's post-test. *** P < 0.001 ** P < 0.01 and *P < 0.05.

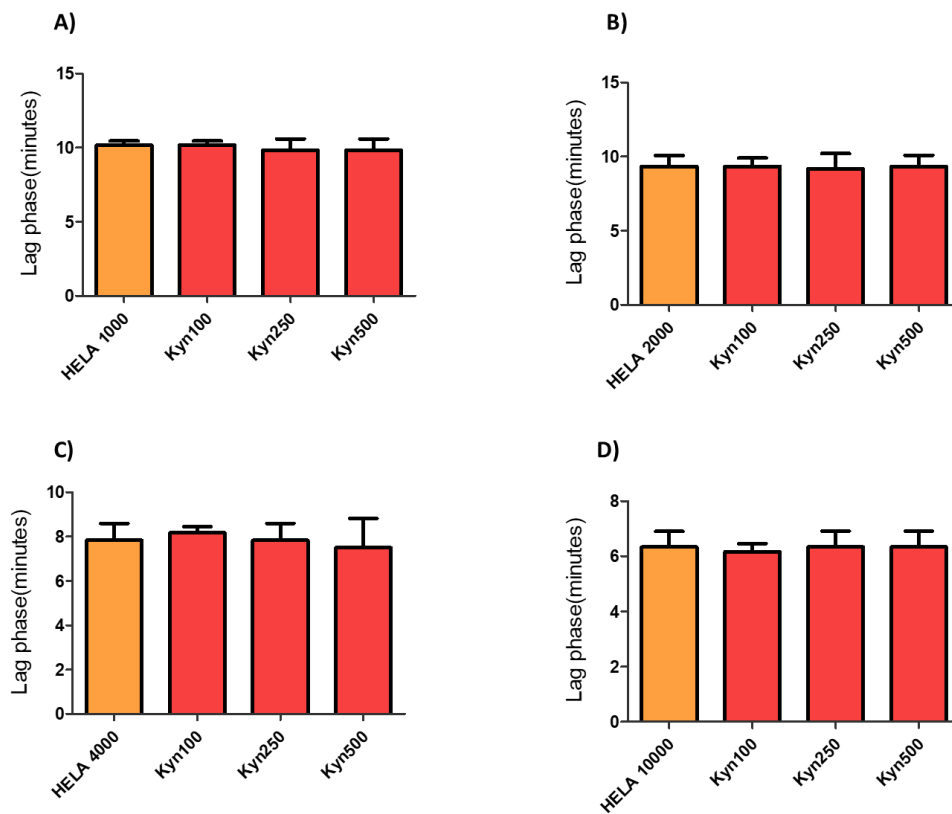


Figure 4-72: Effect of kynurenine on lag phase of HeLa -induced platelet aggregation. Statistical analysis showing that kynurenine (100-500 μ M) has no effect on the lag phase induced by HeLa: 1000 (A), 2000(B), 4000 (C) and 10000 (D) cells. Data is expressed as mean \pm SD; n=4; One-way ANOVA ($P > 0.05$)

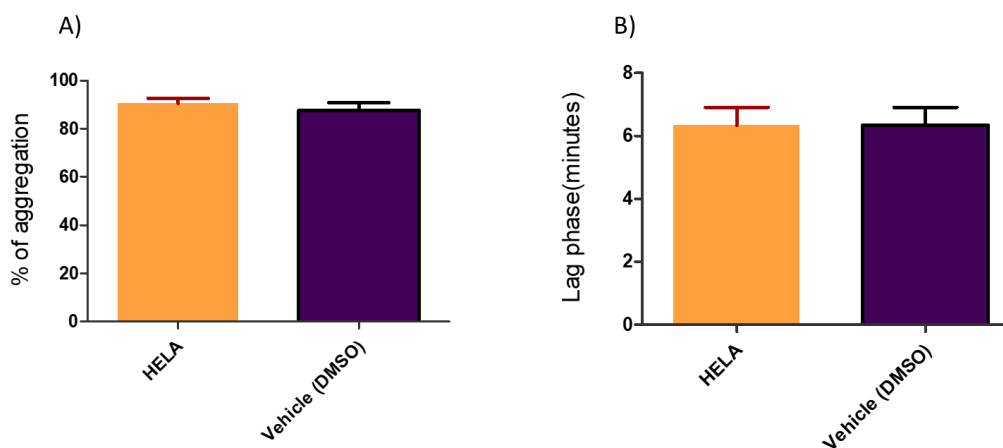


Figure 4-73: Effect of vehicle (DMSO) on TCIPA induced by HeLa cells. Statistical analysis showing that kynurenine vehicle, DMSO 0.4% (equivalent to kynurenine vehicle) has no effect on maximal aggregation (A) and lag phase (B) of HeLa cells-induced platelet aggregation. Data is expressed as mean \pm SD; n=4, Student t-test

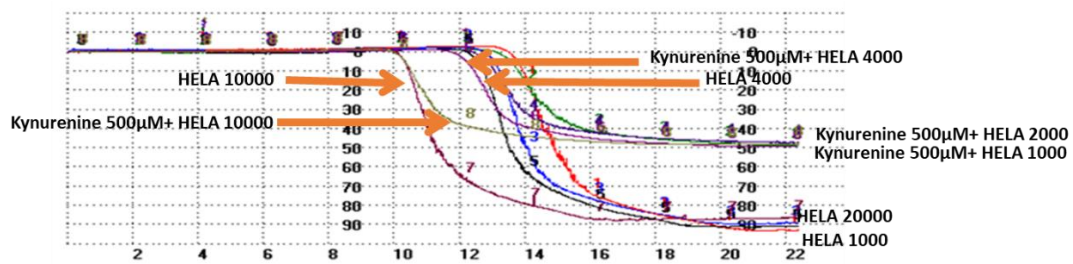


Figure 4-74: Representative traces from light transmission aggregometer showing the effect of kynurenine at 500 μ M on maximal aggregation and lag phase induced by HeLa cells . The time in minutes is represented at the bottom of the graph.

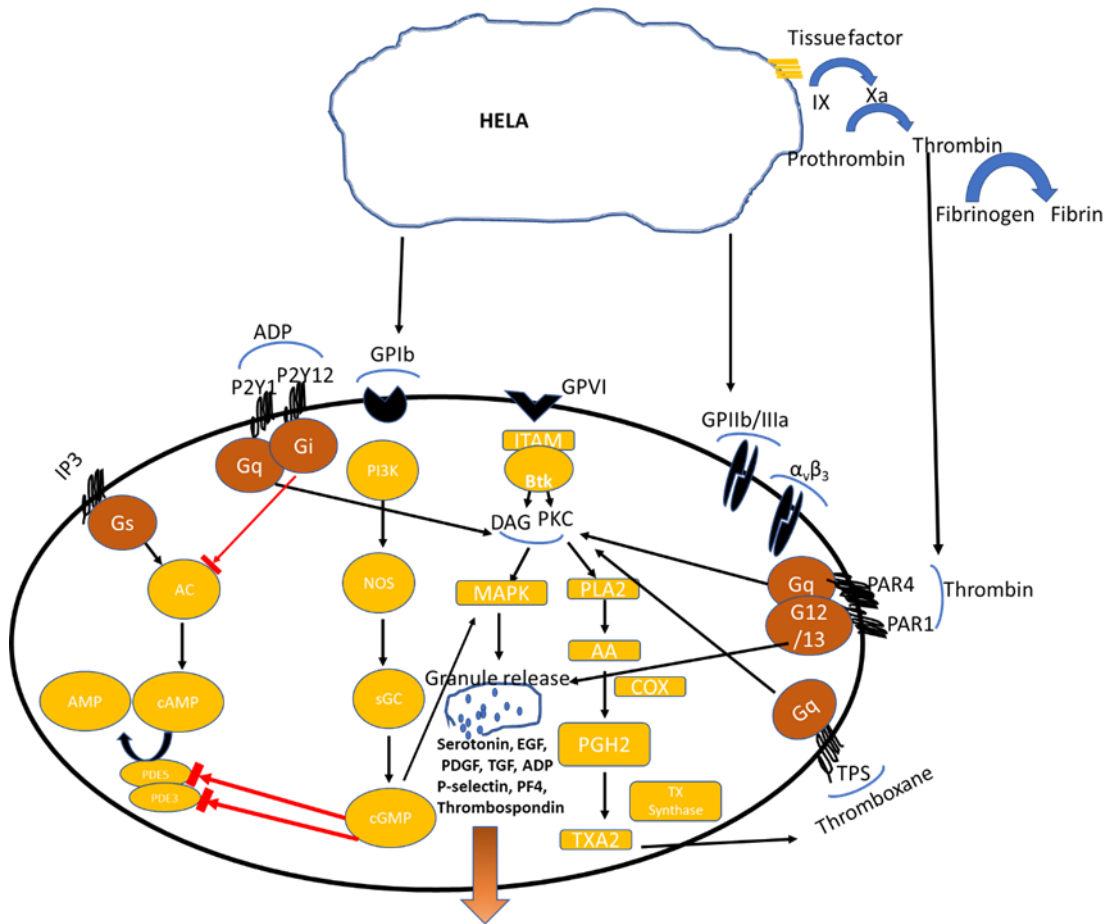


Figure 4-75: HeLa cells induced TCIPA. HeLa cells induces TCIPA by via thrombin generation associated with tissue factor (TF) like activity expressed on tumour cell surface and via interaction with platelet GPIb and GPIIb/IIIa receptors. Cox2: cyclooxygenase enzyme IX: coagulation factor IX, X coagulation factor X, MMP-2: Matrix metalloproteinase-2, GPVI: collagen receptor; GPIb: von Willebrand receptor; ADP: adenosine diphosphate; IP3: prostacyclin receptor; Gs, Gq and Gi: G-protein coupled receptors; PI3K: phosphatidyl Inositol-3 kinase; NOS: :nitric oxide synthase; sGC: soluble guanylyl cyclase; cGMP: Cyclic guanosine monophosphate; BTK: tyrosine kinase; DAG: diacyl glycerol; ITAM: immunoreceptor tyrosine activation motif; PDE: phosphodiesterase enzyme; MAPK: mitogen activated protein kinase; AA: arachidonic acid; PLA2: phospholipase A2; PGH2: prostaglandin H2; EGF: endothelial growth factor; TGF: transforming growth factor; PDGF: Platelet-derived growth factor; PF4: platelet factor-4; AC: adenylyl cyclase; TXA2: thromboxane A2

4.8.2.4. Effect of Kynurenine on HT-29-induced platelet aggregation

Kynurenine also induced a concentration dependent inhibition of HT-29-induced platelet aggregation regardless of cell number used as observed by the significant reduction of platelet aggregation percentage studied by LTA (figure 4-76). This effect was corroborated further by optical microscopy where, the large reduction of aggregate sizes induced by HT-29 cells when platelets were previously incubated with kynurenine can be clearly seen in figure 4-77. Once again, the duration of the lag phase when HT-29 were tested for their ability to induce TCIPA in the presence of kynurenine was not affected (figure 4-78). Representative traces from LTA shown in figure 4-79 confirm that although kynurenine could inhibit TCIPA by HT-29, had no effect on the lag phase. No significant changes in maximal platelet aggregation or lag phase of TCIPA induced by HT-29 was observed when DMSO was tested (figure 4-80).

The mechanism by which HT-29 cells induce platelet aggregation has been previously investigated and reported in the literature (figure 4-81). HT-29 seems to mediate TCIPA on one hand by direct contact with platelets through the collagen receptor (GPVI) and on the other hand by PGE₂ and TXA₂ generation. HT-29 highly expresses Galectin-3 that, as discussed before, is unique among galectins since it contains a collagen-like domain, HT-29 cells also overexpress COX-2, that can lead to synthesis of PGE₂ and platelet activation. Dovicio et al demonstrated that inhibition of galectin 3 action reduced significantly COX-2 expression in colon cancer cells. On the other hand, Revacept, a dimeric platelet collagen receptor (GPVI-Fc) inhibitor also prevented COX-2 expression and inhibited HT-29 -platelets interactions [381, 382]. Furthermore, HT-29 cells have been reported to induce platelet TXA₂ generation through the COX-1-pathway, which was almost completely inhibited by pre-treatment of platelets with aspirin, and to generate MMP-2 which also contributes to TCIPA by HT-29 [383, 384]. All the above mentioned mechanisms are Ca⁺² dependent, therefore the inhibition of TCIPA induced by HT-29 by kynurenine could be mediated through the modulation of intraplatelet Ca⁺² level through cGMP and cAMP and their associated protein kinases leading to inhibition of RAP 1 and integrin GPIIb/IIIa activation induced by collagen receptors [14]. PGE₂ promotes platelet activation via the EP3 receptor. The EP3 receptor expressed on platelets is believed to be coupled to Gi-type G proteins and thus linked to the AC enzyme which can be

antagonised by kynurenine through its direct activation that would results in an increase of cAMP and PKA activation. Thromboxane receptors on platelet surface can be phosphorylated by PKG and PKA [385] thus preventing platelet activation by HT-29.

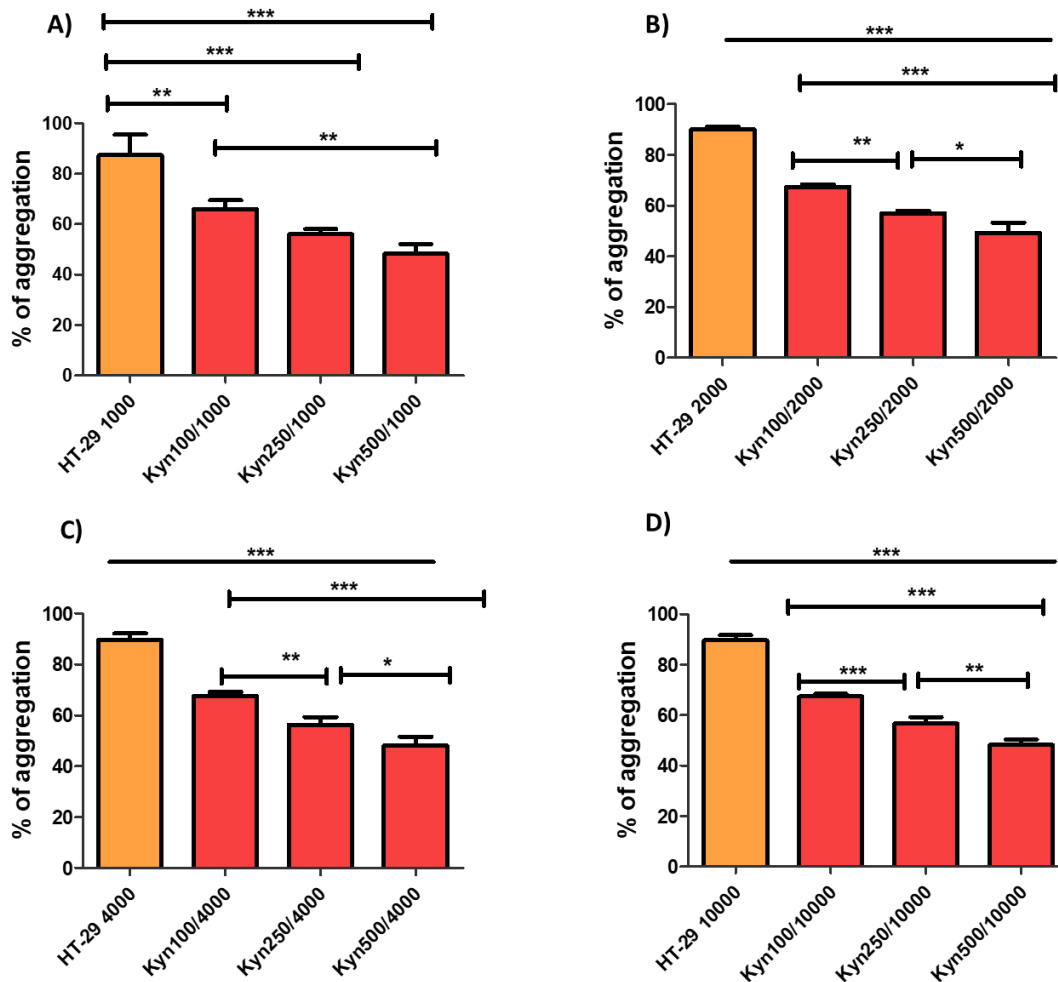


Figure 4-76: Effect of kynurenine on HT-29 cells-induced platelet aggregation. Statistical analysis showing that kynurenine (100-500 μ M) significantly reduced maximal platelet aggregation induced by HT-29: 1000 (A), 2000 (B), 4000 (C) and 10000 (D) cells. Data is represented as mean \pm SD; n=4; One-way ANOVA & Tukey's post-test. *** P <0.001 ** P <0.01 and *P <0.05.

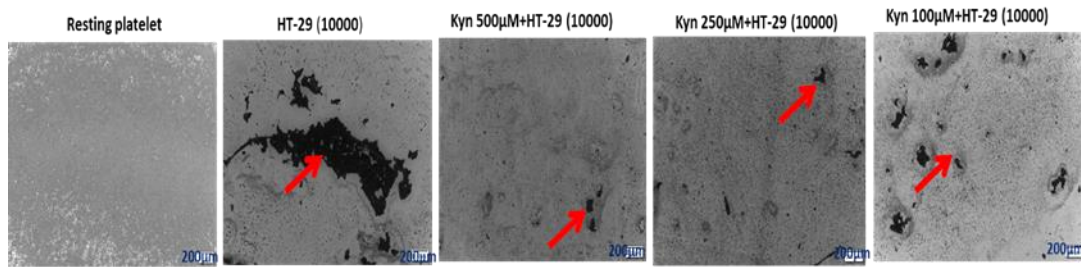


Figure 4-77: Representative micrographs (5X objective) showing the effect of kynurenine (500, 250 and 100 µM) on TCIPA by 10000 HT-29 cells. The light grey areas represent non activated platelets and the darker areas (red arrows) correspond with platelet aggregates.

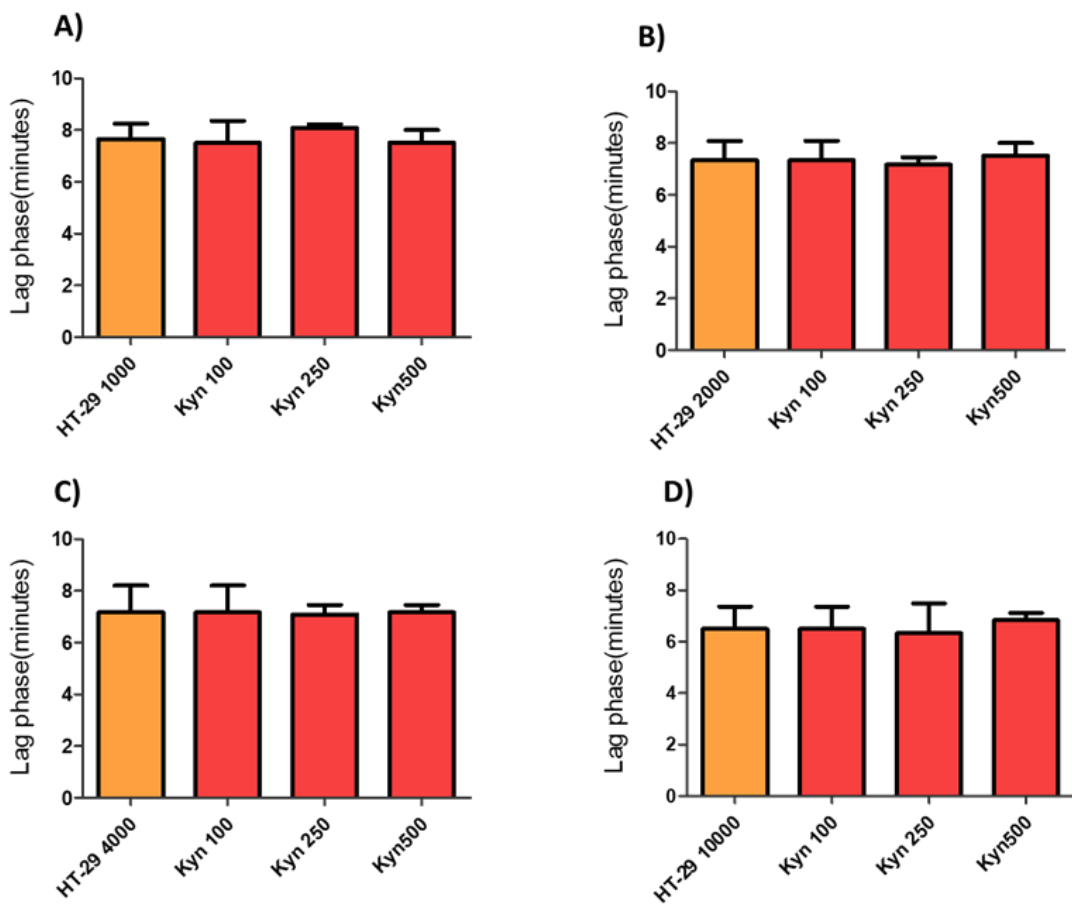


Figure 4-78: Effect of kynurenine on the duration of the lag phase of HT-29 induced platelet aggregation. Statistical analysis showing that kynurenine (100-500 µM) had no effect on the lag phase induced by HT-29: 1000 cells (A), 2000 cells (B), 4000 cells (C) and 10000 cells (D) . Data is expressed as mean ± SD; n=4; One-way ANOVA (P > 0.05)

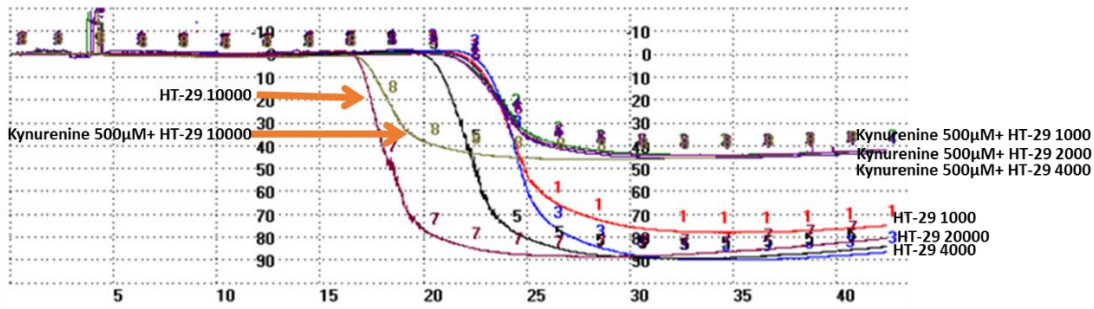


Figure 4-79: Representative traces from light transmission aggregometer showing the effect of kynurenine 500 μ M on maximal aggregation and lag phase when HeLa cells (1000-10000) were used for inducing platelet aggregation. The time in minutes is represented at the bottom of the graph. Kynurenine inhibited platelet aggregation induced by HT-29 cells but did not modified the duration of the lag phase.

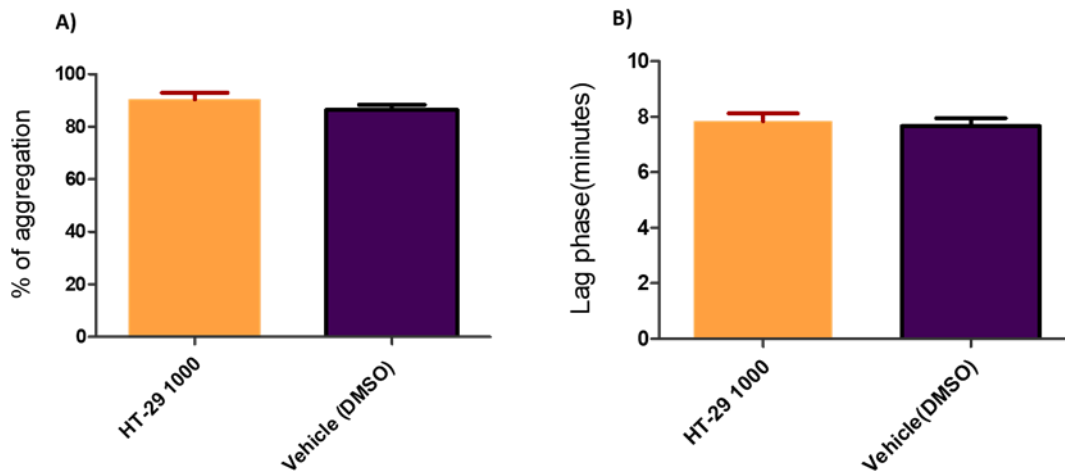


Figure 4-80: Effect of the vehicle (DMSO) on TCIPA by HT-29. Statistical analysis showing that DMSO 0.4% (equivalent to kynurenine vehicle) had no effect on maximal aggregation (A) and lag phase (B) of HT-29 cells-induced platelet aggregation. Data is expressed as mean \pm SD; n=4; Student t-test.

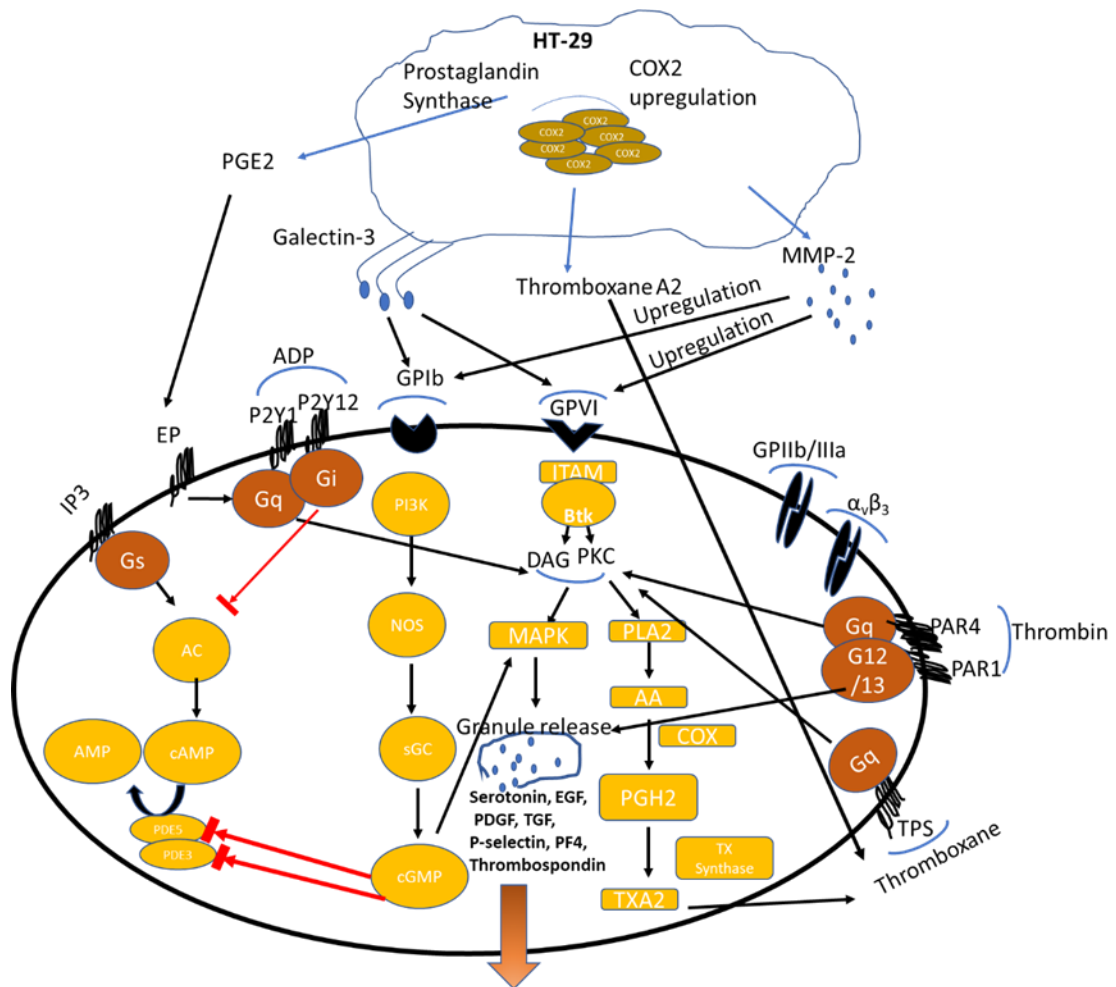


Figure 4-81: Mechanism of HT-29 cells induced platelet aggregation. HT-29 induces TCIPA by direct contact with platelets collagen receptor and PGE₂ and TXA₂ generation due to overexpression of cyclooxygenase enzyme. Galectin-3 is also involved in HT-29 induced TCIPA. Cox2: cyclooxygenase enzyme IX: coagulation factor IX, X coagulation factor X, MMP-2: Matrix metalloproteinase-2, GPVI: collagen receptor; GPIb: von Willebrand receptor; ADP: adenosine diphosphate; IP3: prostacyclin receptor; Gs, Gq and Gi: G-protein coupled receptors; PI3K: phosphatidyl Inositol-3 kinase; NOS: nitric oxide synthase; sGC: soluble guanylyl cyclase; cGMP: Cyclic guanosine monophosphate; BTK: tyrosine kinase; DAG: diacyl glycerol; ITAM: immunoreceptor tyrosine activation motif; PDE: phosphodiesterase enzyme; MAPK: mitogen activated protein kinase; AA: arachidonic acid; PLA2: phospholipase A2; PGH2: prostaglandin H2; EGF: endothelial growth factor; TGF: transforming growth factor; PDGF: Platelet-derived growth factor; PF4: platelet factor-4; AC: adenylyl cyclase; TXA2: thromboxane A2

4.8.2.5. Effect of Kynurenine on SW-480-induced platelet aggregation

When platelets were incubated with kynurenine (100-500 μ M) and platelet aggregation induced by SW-480, kynurenine was able, once again, to significantly inhibit SW-480-induced platelet aggregation in a concentration dependent manner for all the cell concentrations tested (figure 4-82). Although the percentage of aggregation induced by SW-480 at all cells number was significantly reduced, the tryptophan metabolite did not modify the time needed by the cancer cells to induce platelet aggregation (lag phase) as demonstrated in figure 4-83 and figure 4-84. DMSO did not exert any effect on SW-480 induced platelet aggregation (figure 4-85).

Like HeLa cells, SW-480 also express TF on the tumour surface and therefore, thrombin generation seems to play a pivotal role during SW-480 cells-platelets interactions (figure 4-86). TCIPA by SW-480 has been completely inhibited by the anticoagulant hirudin (5 U/mL), but unaffected by co-incubation of platelets with the ADP scavenger apyrase (10 U/mL) [386]. Additionally, it has been demonstrated that SW-480 cells express in their surface the integrin GPIIb/IIIa (fibrinogen receptor) and α V β 3 (vitronectin receptor), α V β 1 (required for fibronectin matrix assembly) and α 6 β 1 (laminin receptor) [387] that are required for cell-platelets binding and for induction of TCIPA. Trigramin and rhodostomin, RGD-containing snake venom peptides, which antagonise the binding of fibrinogen to platelet membrane through the GPIIb/IIIa have been reported to inhibit SW-480 induced platelet aggregation. Likewise, the synthetic peptide GRGDS as well as monoclonal antibodies against the platelet membrane GPIIb/IIIa and GPIb prevented TCIPA by SW-480 [386].

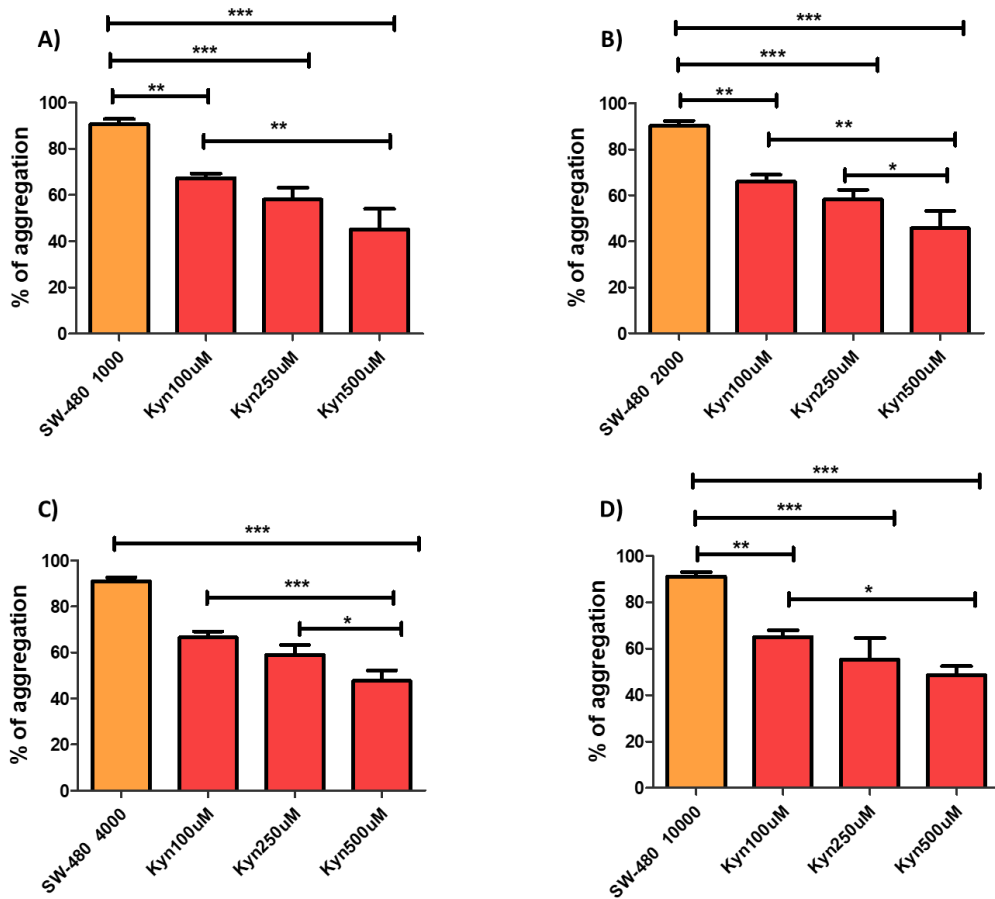


Figure 4-82: Effect of kynurenine on SW-480-induced platelet aggregation. Statistical analysis showing that kynurenine (100-500 μ M) significantly reduced maximal platelet aggregation induced by SW-480: 1000 cells (A), 2000 cells (B), 4000 cells (C) and 10000 cells/ 500 μ L (D). Data is represented as mean \pm SD; n=4; One-way ANOVA & Tukey's post-test. *** P < 0.001, ** P < 0.01 and *P < 0.05.

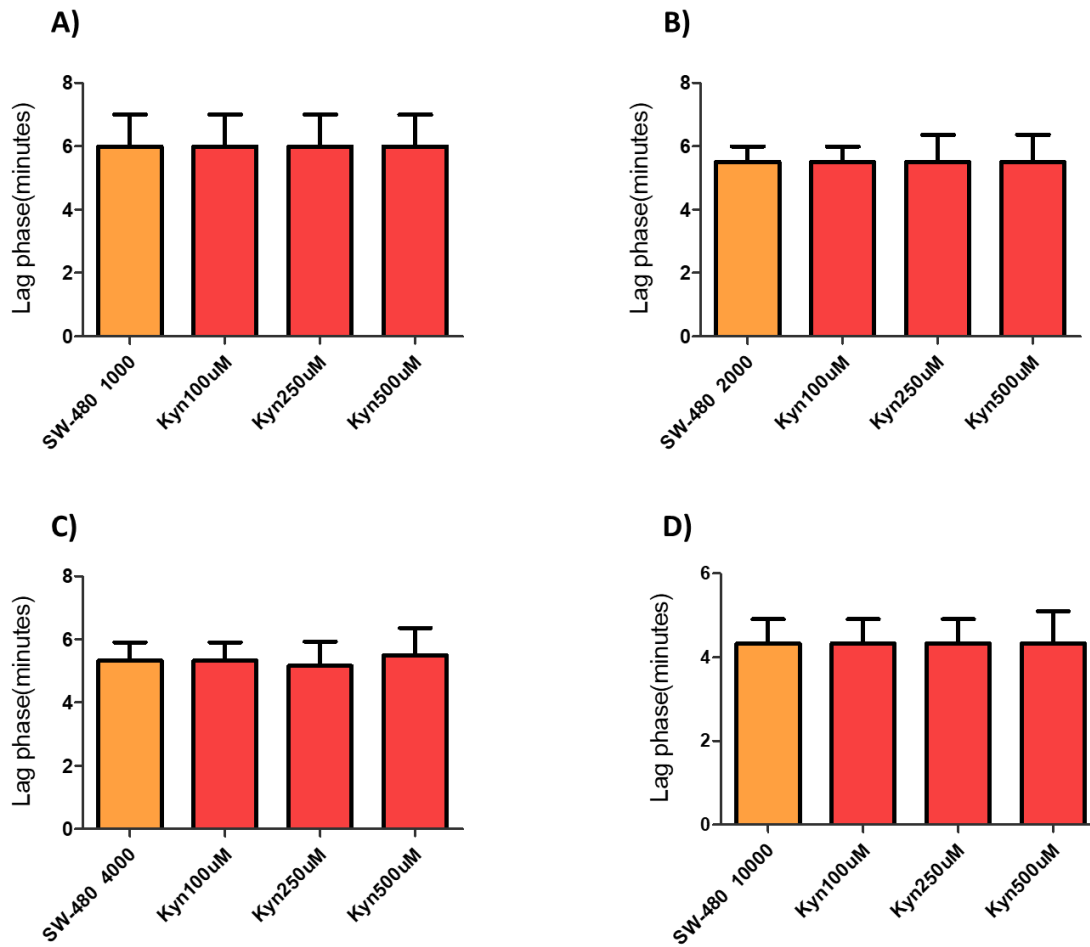


Figure 4-83 : Effect of kynurenine on lag phase during SW-480induced platelet aggregation. Statistical analysis showing that kynurenine (100-500 μM) had no effect on lag phase of TCIPA by SW-480 cells: 1000 (A), 2000 (B), 4000 (C) and 10000 (D) . Data is expressed as mean ± SD; n=4; One-way ANOVA (P > 0.05)

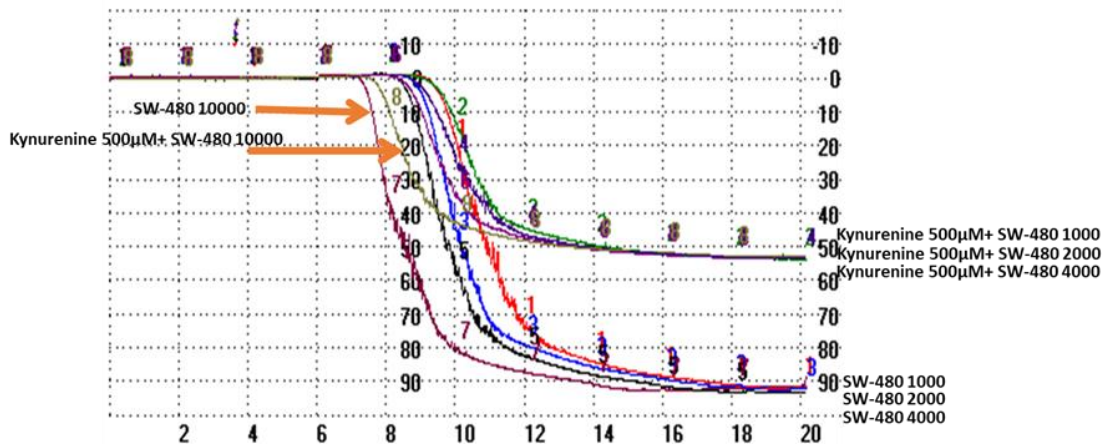


Figure 4-84: Representative traces from light transmission aggregometer showing the effect of kynurenine 500 µM on maximal aggregation and lag phase of SW-480 1000-10000 cells induced platelet aggregation. Kynurenine inhibited platelet aggregation induced by SW-480 cells but did not modified the duration of the lag phase. The time in minutes is represented at the bottom of the graph.

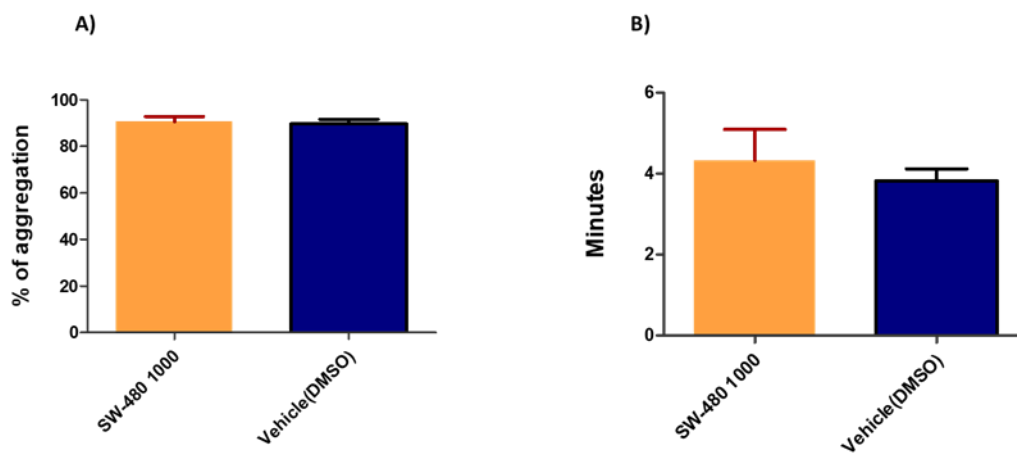


Figure 4-85: Effect of vehicle (DMSO) on TCIPA by SW-480. Statistical analysis showing that DMSO 0.4% (equivalent to kynurenine vehicle) had no effect on maximal aggregation (A) and lag phase (B) of platelet aggregation induced by SW-480 cells. Data is expressed as mean ± SD; n=4; Student's t-test.

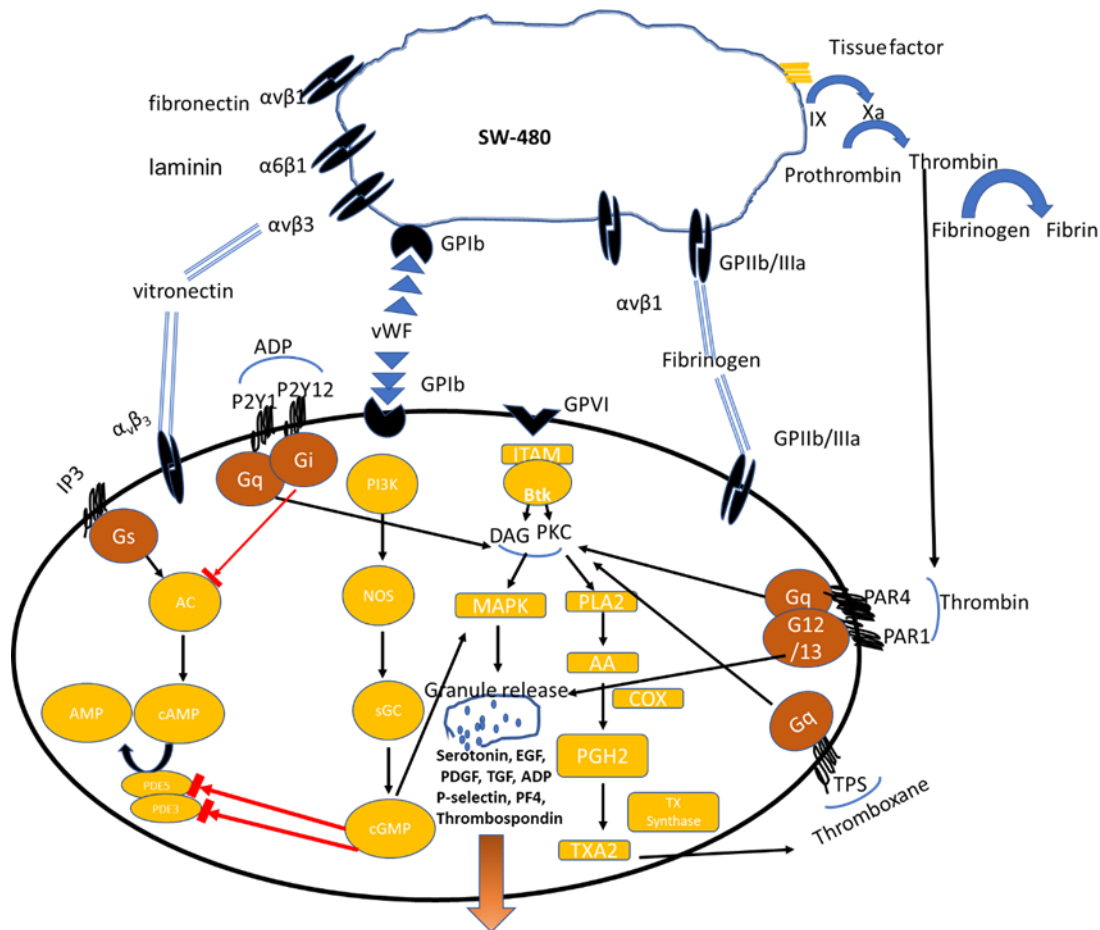


Figure 4-86: Mechanism of SW-480 induced TCIPA. SW-480 cells overexpressed integrin receptors and vonwillibrand receptors that interact directly with the platelet surface receptors. Tissue factor and thrombin generation also involved in SW-480 induced TCIPA. Cox2: cyclooxygenase enzyme IX: coagulation factor IX, X coagulation factor X, MMP-2: Matrix metalloproteinase-2, GPVI: collagen receptor; GPIb: von Willebrand receptor; ADP: adenosine diphosphate; IP3: prostacyclin receptor; Gs, Gq and Gi: G-protein coupled receptors; PI3K: phosphatidyl Insositol-3 kinase; NOS: :nitric oxide synthase; sGC: soluble guanylyl cyclase; cGMP: Cyclic guanosine monophosphate; BTK: tyrosine kinase; DAG: diacyl glycerol; ITAM: immunoreceptor tyrosine activation motif; PDE: phosphodiesterase enzyme; MAPK: mitogen activated protein kinase; AA: arachidonic acid; PLA2: phospholipase A2; PGH2: prostaglandin H2; EGF: endothelial growth factor; TGF: transforming growth factor; PDGF: Platelet-derived growth factor; PF4: platelet factor-4; AC: adenylyl cyclase; TXA2: thromboxane A2

4.8.2.6. Effect of Kynurenine on HCC-1954-induced platelet aggregation

Kynurenine (100-500 μ M) also significantly inhibited HCC-1954-induced platelet aggregation in a concentration dependent manner (figure 4-87 and figure 4-88). In fact, Kynurenine (100-500 μ M) reduced the aggregates size induced by HCC-1954 (1000-10000 cells) as shown in figure 4-89. However, as it happened with the previous cell lines, kynurenine did not modify the time that took HCC-1954 cells to induce platelet aggregation with any of the concentrations tested. (figure 4-90). DMSO did not modified the ability of HCC-1954 to induce TCIPA (figure 4-91)

Several mechanisms have been described as to be involved on HCC-1954 induced platelet aggregation (figure 4-92). HCC-1954 cells overexpress COX-2, and high levels of COX-2 seems to be associated with increased proliferation, higher histological grade, development of metastasis and reduced survival in breast cancer patients [388, 389]. Co-cultured HCC-1954 cells with macrophages led to increased expression of COX-2 and production of PGE₂ and reactive oxygen species (ROS) by cancer cells, triggering activation of Src and mitogen-activated protein kinases (MAPKs) [390]. Src family kinases (SFKs) play a pivotal role in mediating platelet activation. They not only contribute to G_q- and G_i-coupled receptor signalling but also transmit activation signals from other platelet surface receptors, such as GPIIb/IIIa, collagen receptor complex GPVI-FcR γ -chain, and vWf factor receptor complex GPIb-IX-V, contributing to platelet activation and aggregation [391]. Members of the MAPK family: p38, extracellular stimuli-responsive kinase (ERK) and c-Jun NH₂-terminal kinase (JNK) mediate platelet granule release in platelets, Rap 1 activation and GPIIb/IIIa expression leading to platelet aggregation [21, 392, 393]. Both, p38 MAPK and Rap1 activation are highly controlled and inactivated by cAMP and cGMP and their protein kinases [394, 395] although the PKA role in Rap1 inactivation has not been determined [396]. The diverse pathways of platelet activation by HCC-1954 may explain its potent TCIPA ability and its short lag phase. cGMP and cAMP activation pathways, thromboxane receptor phosphorylation and thromboxane pathway inhibition may significantly reduce HCC-1954 TCIPA [385, 394] and all can be performed by Kynurenine.

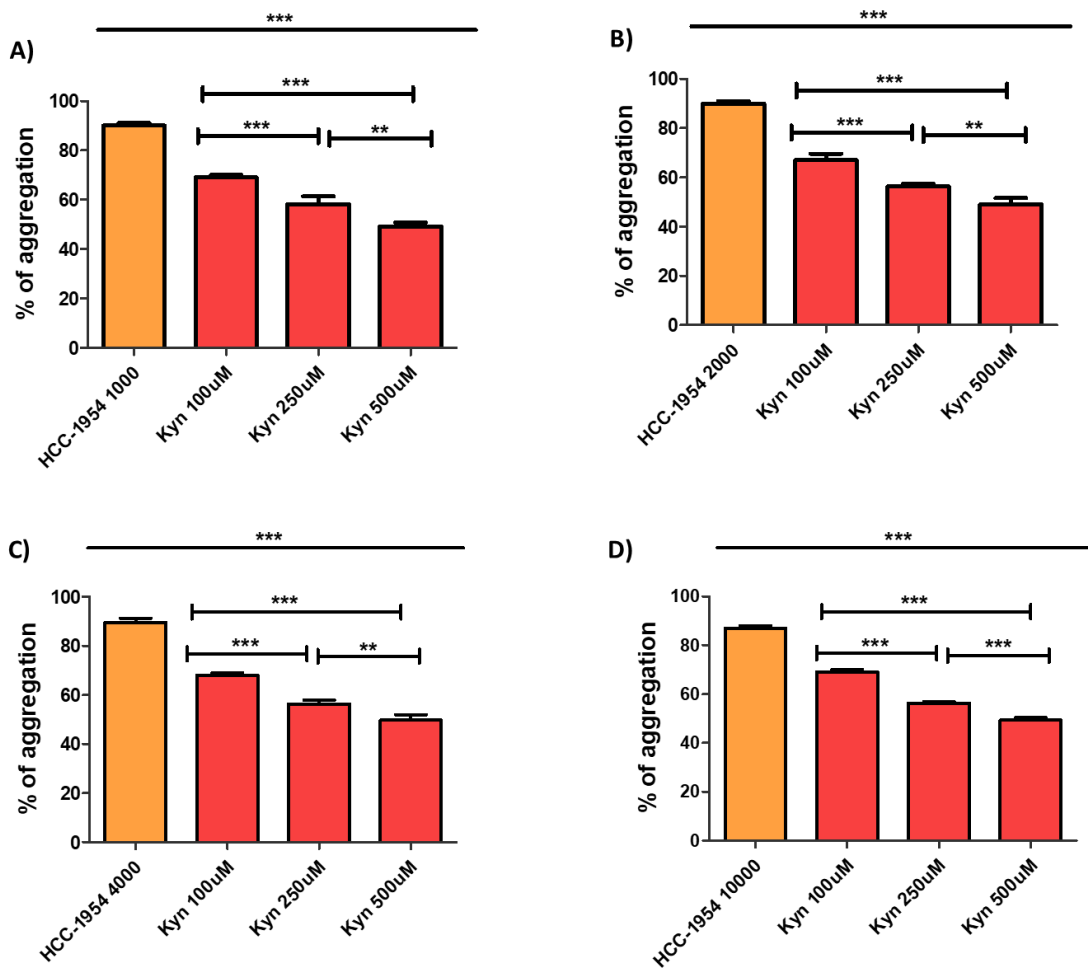


Figure 4-87: Effect of Kynurenine on HCC-1954 cells induced platelet aggregation. Statistical analysis showing that Kynurenine (100-500µM) significantly reduced maximal platelet aggregation induced by HCC-1954 1000 cells/500µL(A), HCC-1954 2000 cells/500µL(B), HCC-1954 4000 cells/500µL(C) and HCC-1954 10000 cells/500µL(D). Data is represented as mean ± SD; n=4; One-way ANOVA & Tukey's post-test. *** P<0.001 and ** P<0.01.

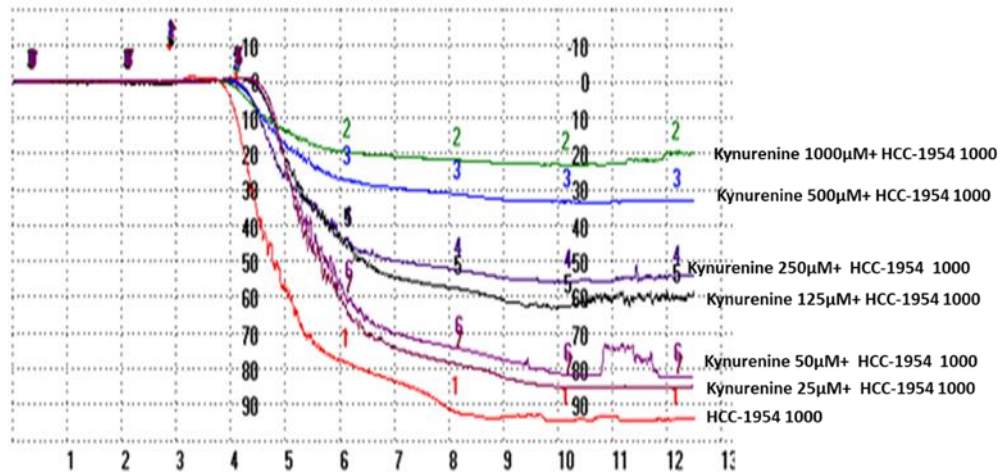


Figure 4-88: Representative traces from the light transmission aggregometer showing the concentration dependent inhibitory effect of kynurenine (25-1000 μM) on TCIPA induced by 1000 HCC-1954 cells. Kynurenine did not exert any effect on the lag phase. The time in minutes is represented at the bottom of the graph.

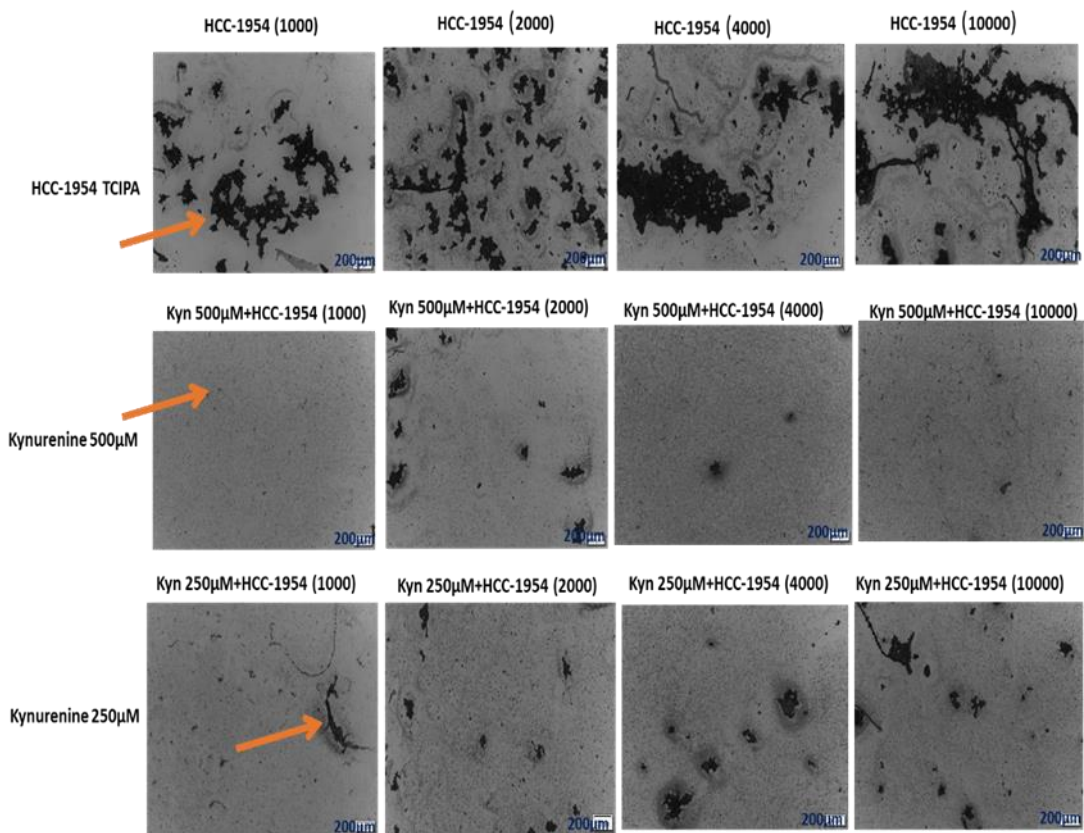


Figure 4-89: Representative micrographs (5X objective) showing the effect of Kynurenine (500 and 250 μM) on HCC-1954 1000, 2000, 4000 and 10000 cells/500 μL induced platelet aggregation. The light grey areas represent non activated platelets and the darker areas (red arrow) correspond with platelet aggregates.

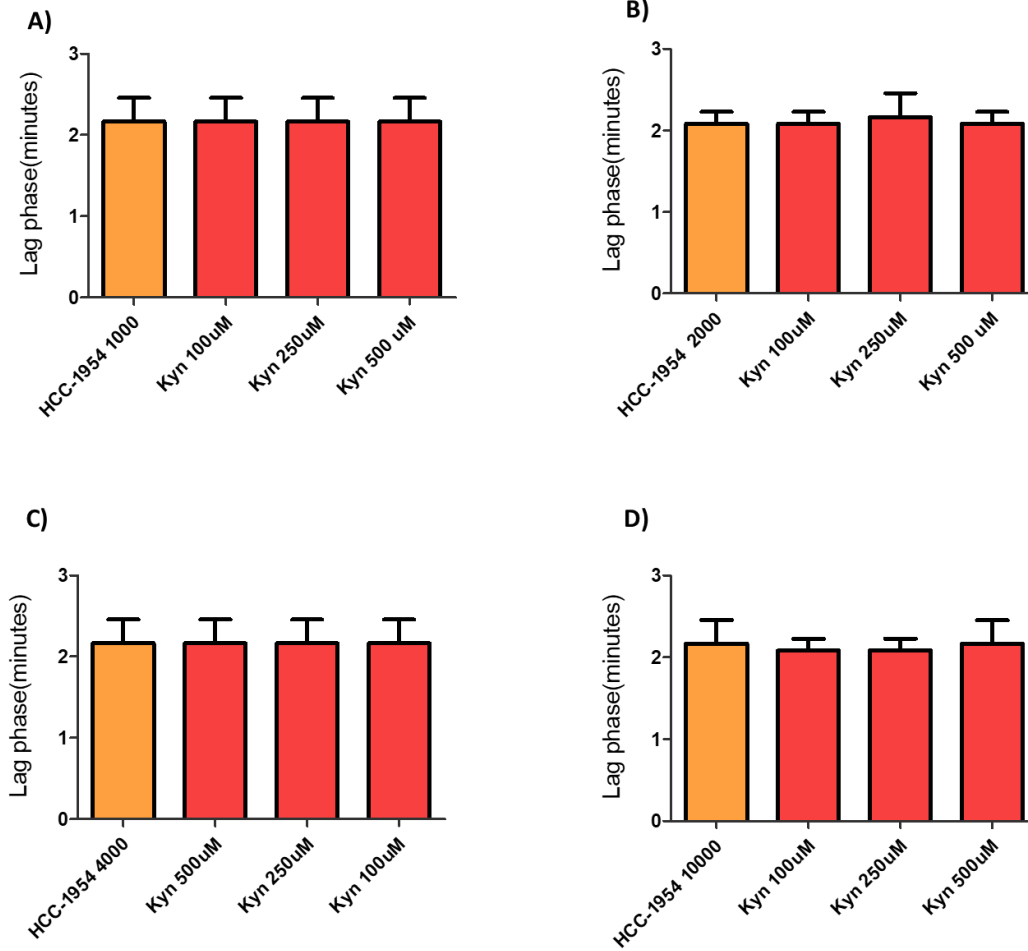


Figure 4-90: Effect of Kynurenine on Lag time of HCC-1954 induced platelet aggregation. Statistical analysis showing that Kynurenine (100-500 μ M) has no effect on lag phase of HCC-1954 1000 cells/500 μ L(A), HCC-1954 2000cells/500 μ L(B), HCC-1954 4000 cells/500 μ L(C) and HCC-1954 10000 cells/500 μ L(D) induced platelet aggregation. Data is expressed as mean \pm SD; n=4; One-way ANOVA & Tukey's post-test.

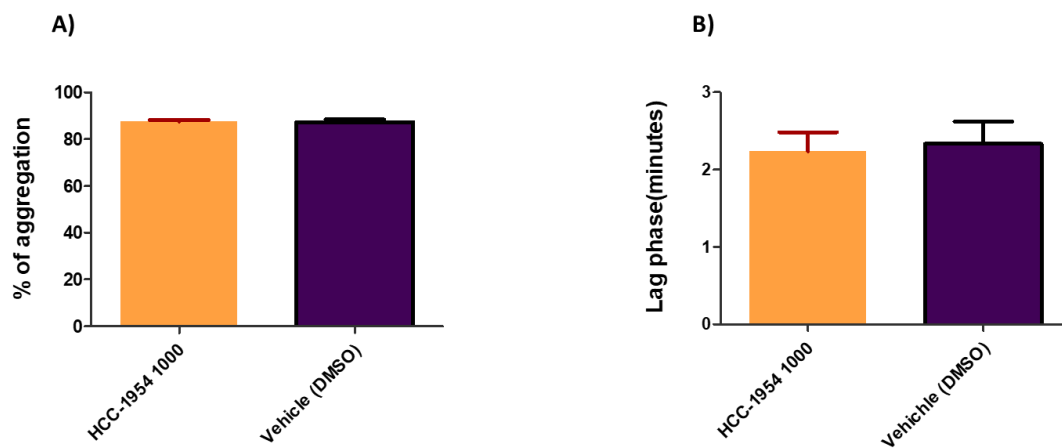


Figure 4-91: Effect of Vehicle (DMSO) on SW-480 TCIPA. Statistical analysis showing that Kynurenine vehicle DMSO 0.4% (equivalent to kynurenine vehicle) has no effect on maximal aggregation (A) and lag phase (B) of SW-480 cells induced platelet aggregation. Data is expressed as mean \pm SD; n=4. Student t-test.

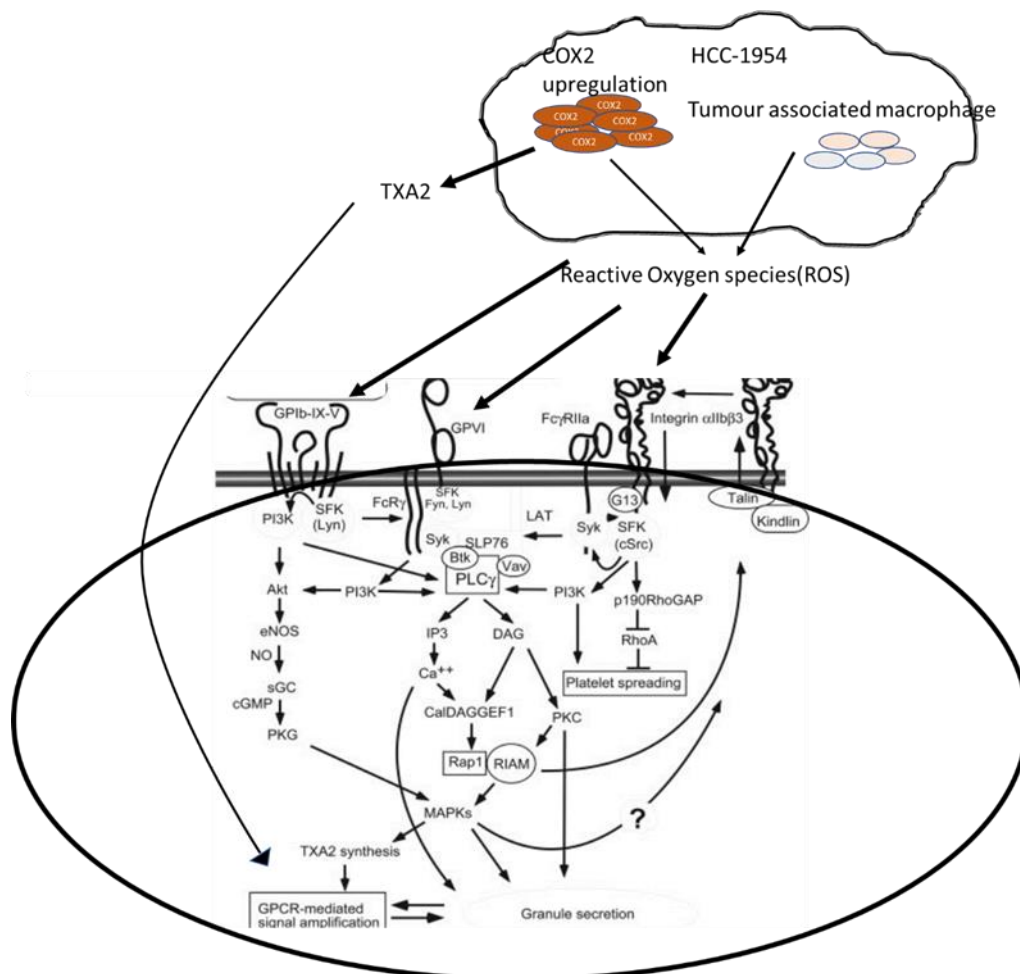


Figure 4-92: Mechanism of HCC-1954 induced TCIPA. HCC-1954 cells overexpress COX-2 and in the presence of tumour associated macrophages produces PGE2 and reactive oxygen species (ROS) triggering activation of platelet surface receptors, Src and mitogen-activated protein kinases (MAPKs). VWF: von Willebrand factor; GPIIb-IX-V: glycoprotein GPIIb-IX-V; PI3K: phosphatidylinositol-3 kinase; SFK: Src-family kinase (Lyn, Fyn); AKT: protein kinase B; eNOS: Endothelial nitric oxide synthase; NO: nitric oxide; sGC: soluble guanylyl cyclase; cGMP: Cyclic guanosine monophosphate; PKG: cGMP-dependent protein kinase; MAPKs: Mitogen activated protein kinases; TXA2: Thromboxane A2; SLP-76: Src homology (SH) 2 domain-containing leukocyte phosphoprotein of 76 kDa; BTK: tyrosine kinase; IP3: Inositol tri-phosphate; DAG: diacylglycerol; CalDAGGEF1: Calcium and DAG-regulated guanine nucleotide exchange factor 1; Rap (a small guanosine triphosphatase); RIAM: Rap1-GTP-interacting adaptor molecule; VAV (guanine nucleotide exchange factor); cSrc: cytosolic src-family kinase; RhoGAP: RhoA GTPase activating protein; PKC: protein kinase C; GPCR: G-protein coupled receptor; FcγRIIa: Fc receptor gamma

4.8.2.7. Effect of Kynurenine on platelet expression of GPIIb/IIIa and P-selectin induced by HCC-1954

Kynurenine (100-500 μM) was incubated at least for 2 minutes with platelets prior to the induction of TCIPA by 1000 HCC-1954 cells. The results obtained by flow cytometry confirmed the inhibitory effect of kynurenine on TCIPA induced by HCC-1954 as shown by the significant downregulation on the platelet surface of GPIIb/IIIa activated (figure 4-93 A) and P-selectin (figure 4-93 B) expression (represented in figure 4-94).

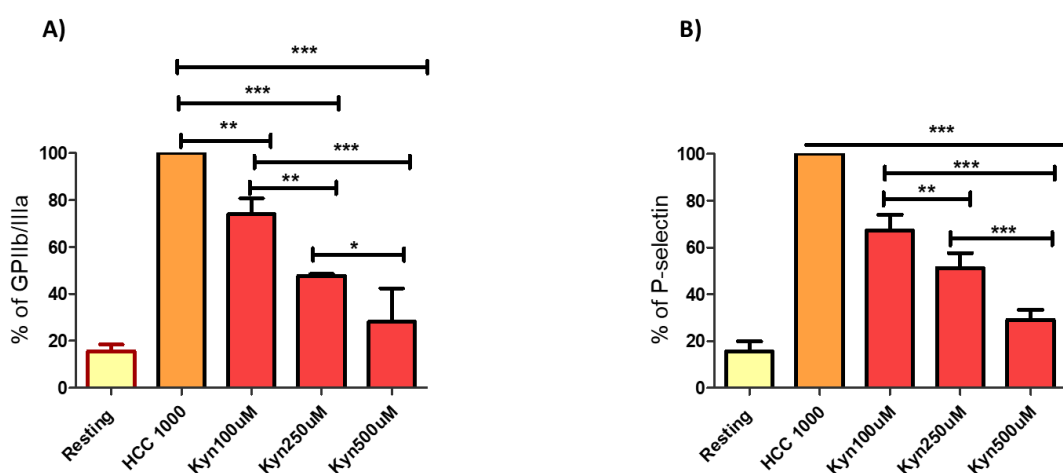


Figure 4-93: Effect of kynurenine on platelet expression of GPIIb/IIIa and P-selectin during TCIPA induced by HCC-1954. Statistical analysis showing that kynurenine (100-500 μM) significantly reduced platelet expression of GPIIb/IIIa (A) and P-selectin (B) induced by 1000 HCC-1954 cells. Data is represented as mean \pm SD; n=4; One-way ANOVA & Tukey's post-test. *** P < 0.001; ** P < 0.01 and * P < 0.05.

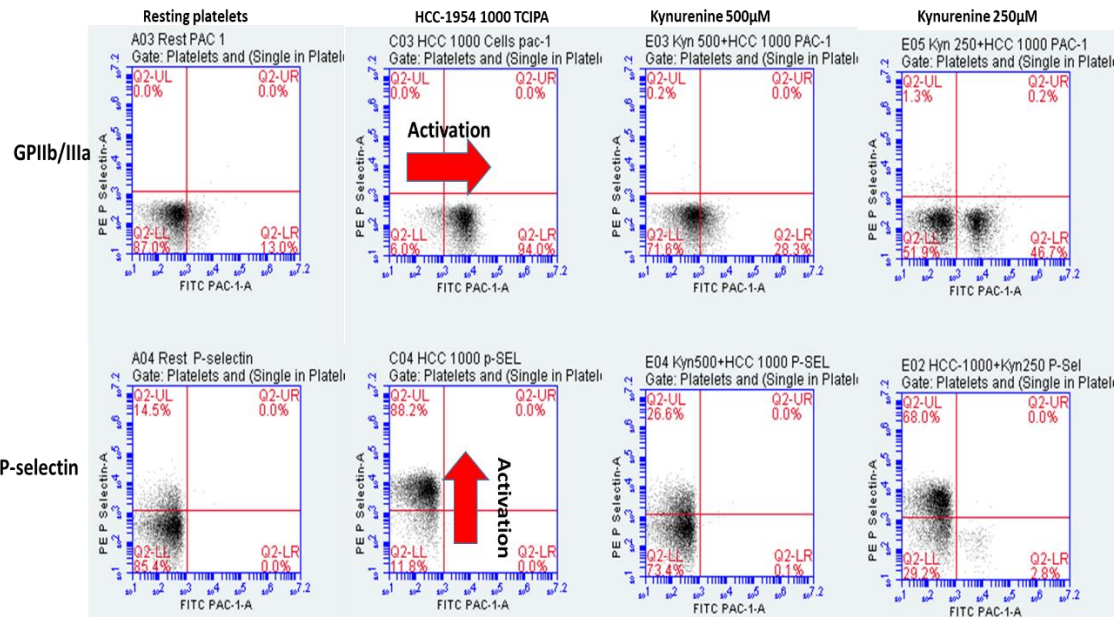


Figure 4-94: Representative gates from flow cytometry showing the effect of kynurenine (500 and 250 µM) on platelet expression of GPIIb/IIIa activated (PAC1) and P-selectin. Inhibition of GPIIb/IIIa expression is demonstrated by a reduced shifting of the platelet population from the lower left quarter (LL) to the lower right quarter (LR). Inhibition of platelet P-selectin expression is demonstrated by the reduced upward shifting of the platelet population from the lower left quarter (LL) to the upper left quarter (UL).

The ability of kynurenine to control most of the common pathways included in platelet aggregation by its dual effect on sGC and AC enzyme is making its effect resembling the combined effect of prostacyclin and NO as shown in figure 4-95. Therefore, kynurenine was able to inhibit TCIPA by A549, HELA, HT-29, SW-480 and HCC-1954.

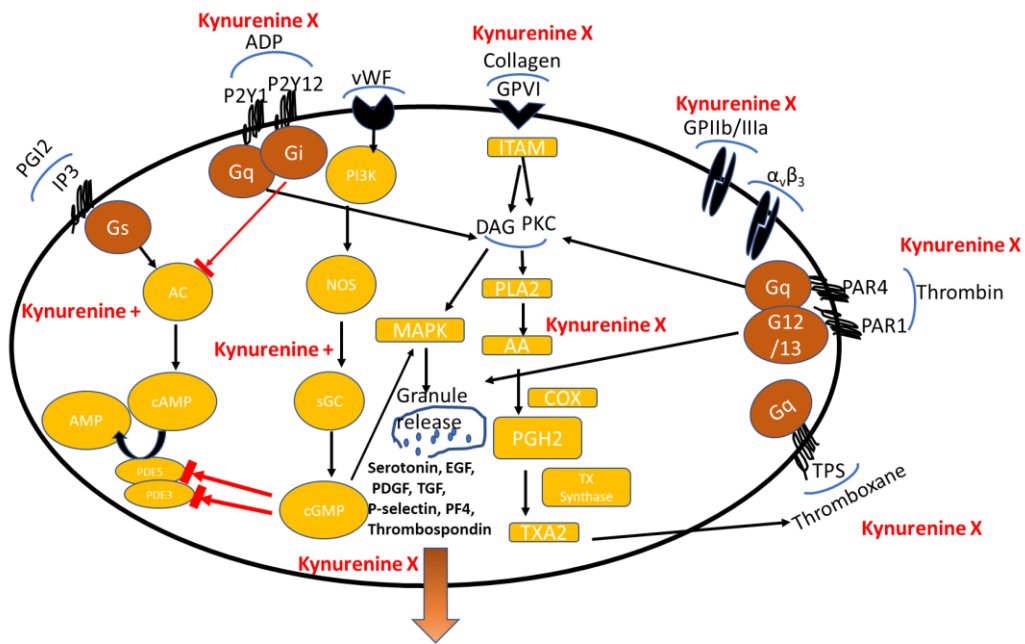


Figure 4-95: Platelet pathways controlled by kynurenine. Cox2: cyclooxygenase enzyme IX: coagulation factor IX, X coagulation factor X, MMP-2: Matrix metalloproteinase-2, GPVI: collagen receptor; GPIb: von Willebrand receptor; ADP: adenosine diphosphate; IP3: prostacyclin receptor; Gs, Gq and Gi: G-protein coupled receptors; PI3K: phosphatidyl Inositol-3 kinase; NOS: nitric oxide synthase; sGC: soluble guanylyl cyclase; cGMP: Cyclic guanosine monophosphate; BTK: tyrosine kinase; DAG: diacyl glycerol; ITAM: immunoreceptor tyrosine activation motif; PDE: phosphodiesterase enzyme; MAPK: mitogen activated protein kinase; AA: arachidonic acid; PLA2: phospholipase A2; PGH2: prostaglandin H2; EGF: endothelial growth factor; TGF: transforming growth factor; PDGF: Platelet-derived growth factor; PF4: platelet factor-4; AC: adenylyl cyclase; TXA2: thromboxane A2. X: inhibits, red arrow: inhibits, black arrow: activates.

Indolamine dioxygenase-1 (IDO-1) is constitutively expressed by many tumour cells and it is known to contribute to immunosuppression by both, depletion of the essential amino acid tryptophan and generation of immunosuppressive tryptophan metabolites such as kynurenine [397, 398]. In humans, the high expression of IDO in tumours has been associated with reduced effector T-lymphocyte infiltration [287, 399] and an increased number of regulatory T cells (Treg) [400]. However, to our knowledge, nobody has previously investigated the role and/or the potential effect that kynurenine could have on cancer cell-platelet interactions. The results obtained in this research so far, demonstrated that the cell lines tested have a different tendency to induce platelet aggregation (TCIPA) as revealed by the differences that they exerted on the duration of the lag phase in the traces from the LTA. Since kynurenine, at concentrations from 100 to 500 μ M, showed a significant reduction on the ability of all the tumours cell lines tested to induce platelet aggregation. It is worth to mention that kynurenine only affected the percentage of platelet aggregation induced TCIPA but not the lag phase. The

lag phase in TCIPA may be determined by the release of platelet agonists from platelet dense granules and the release of mediators from dense granules was not investigated. How kynurenine affected the α -granules but not the dense granules may be due to the effect of kynurenine on actin cytoskeleton by its effect on cGMP[401].

To investigate if the production of kynurenine by each cell line could be correlated with their potency to induce TCIPA, the concentration of kynurenine in their conditioned media was measured by HPLC in the presence and absence of platelets.

4.8.3. Kynurenine – Lag phase relationship

For this set of experiments, tumour cells were seeded in T-75 flasks (density 1×10^6). When cells reached about 70% of confluency, the complete media was changed by FBS free media. After 48 hours, the conditioned media was collected, filtered (0.2 μ M filters) and analysed using HPLC for measuring kynurenine and tryptophan concentrations. Cells were also detached from the flask and their ability to induce TCIPA tested and recorded by LTA.

The results obtained shown that the different cell lines produced different concentrations of kynurenine (figure 4-96 and figure 4-97) that were correlated with the amount of tryptophan consumed (figure 4-98). Consistently, those values were found to have an inverse relationship with the duration of the lag phase recorded for each cell line by LTA as demonstrated in figure 4-99.

High plasma kynurenine concentration has been associated with disease progression, invasiveness and poor prognosis in patients suffering from cancer [289-291], however, the concentrations of kynurenine used for in ex-vivo experiments to inhibit TCIPA are at least 50 times higher than the concentration of kynurenine in cell lines' conditioned media.

In this regard and among all the cell lines tested, A549 and HCC-1954 cell lines seemed to represent the two extremes in terms of aggressiveness based on their ability to induced platelet aggregation. However, although the A549 cell line was considered to be the least aggressive one, as it showed the longest lag phase as demonstrated by LTA, generated the lowest concentration of kynurenine. On the

other hand, the HCC-1954 cell line, that was considered to be the most aggressive cell line inducing the shortest lag phase, produced the highest concentration of kynurenine as detected by HPLC in the conditioned media.

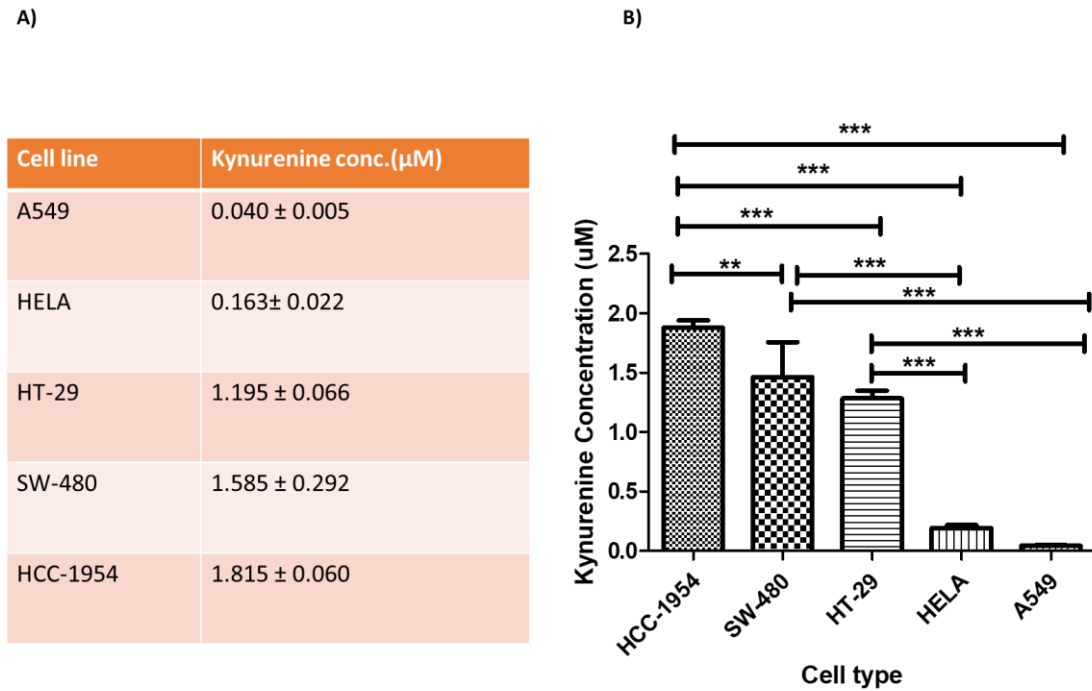


Figure 4-96: Basal concentration of kynurenine produced by the different cell lines as measured by HPLC. (A) Table showing the concentration of kynurenine generated by each cell line in T-75 flask: A549 cell line produced the lowest concentration and HCC-1954 the highest. (B) Statistical analysis showing the differences in the concentration of kynurenine generated by each cell lines. Data is represented as mean \pm SD; n=4; One-way ANOVA & Tukey's post-test. *** P <0.001 and ** P <0.01.

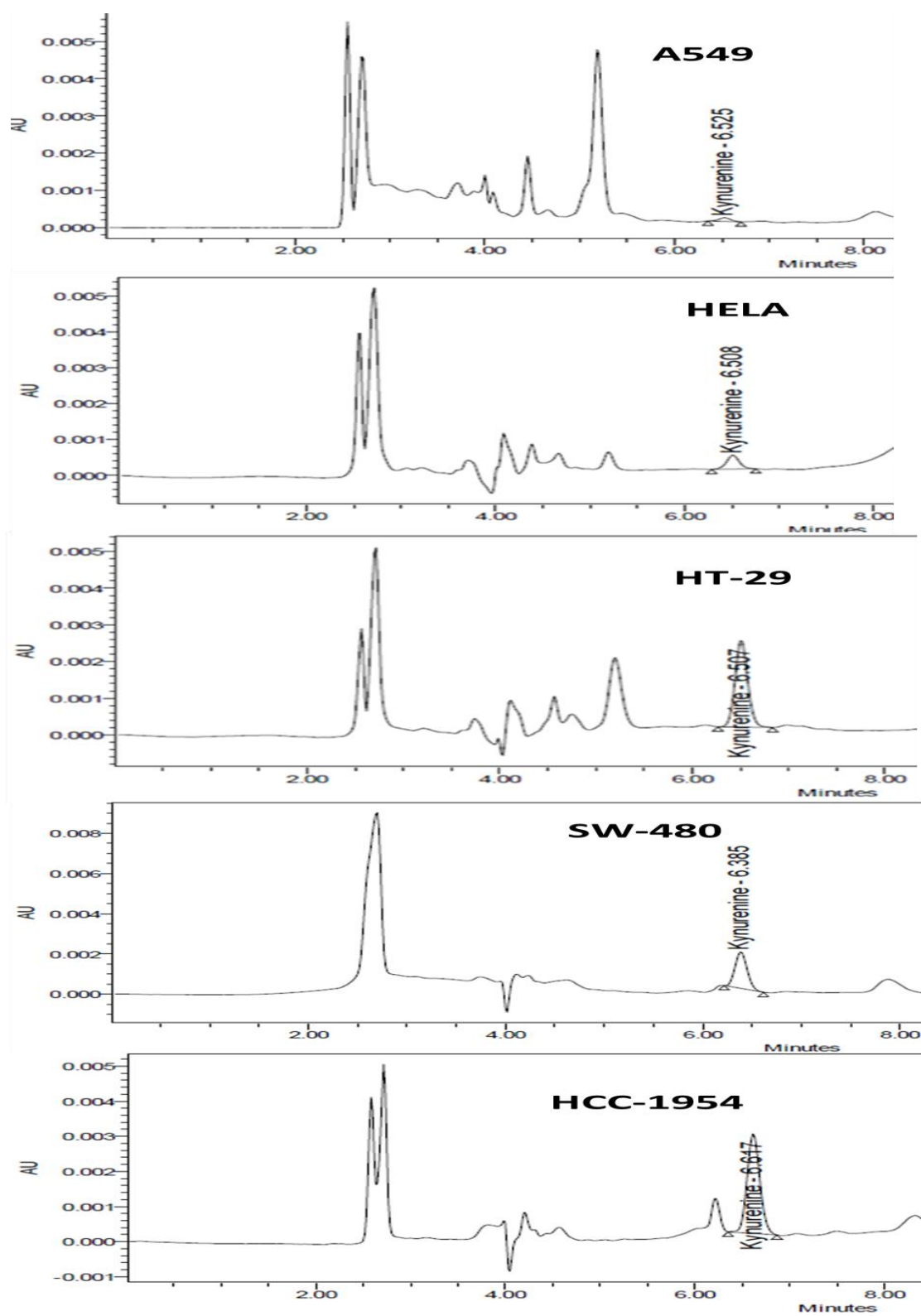


Figure 4-97: Traces from HPLC showing the area under the curve and peak height of kynurenine produced by each cell line in conditioned media after 48 hours of incubation.

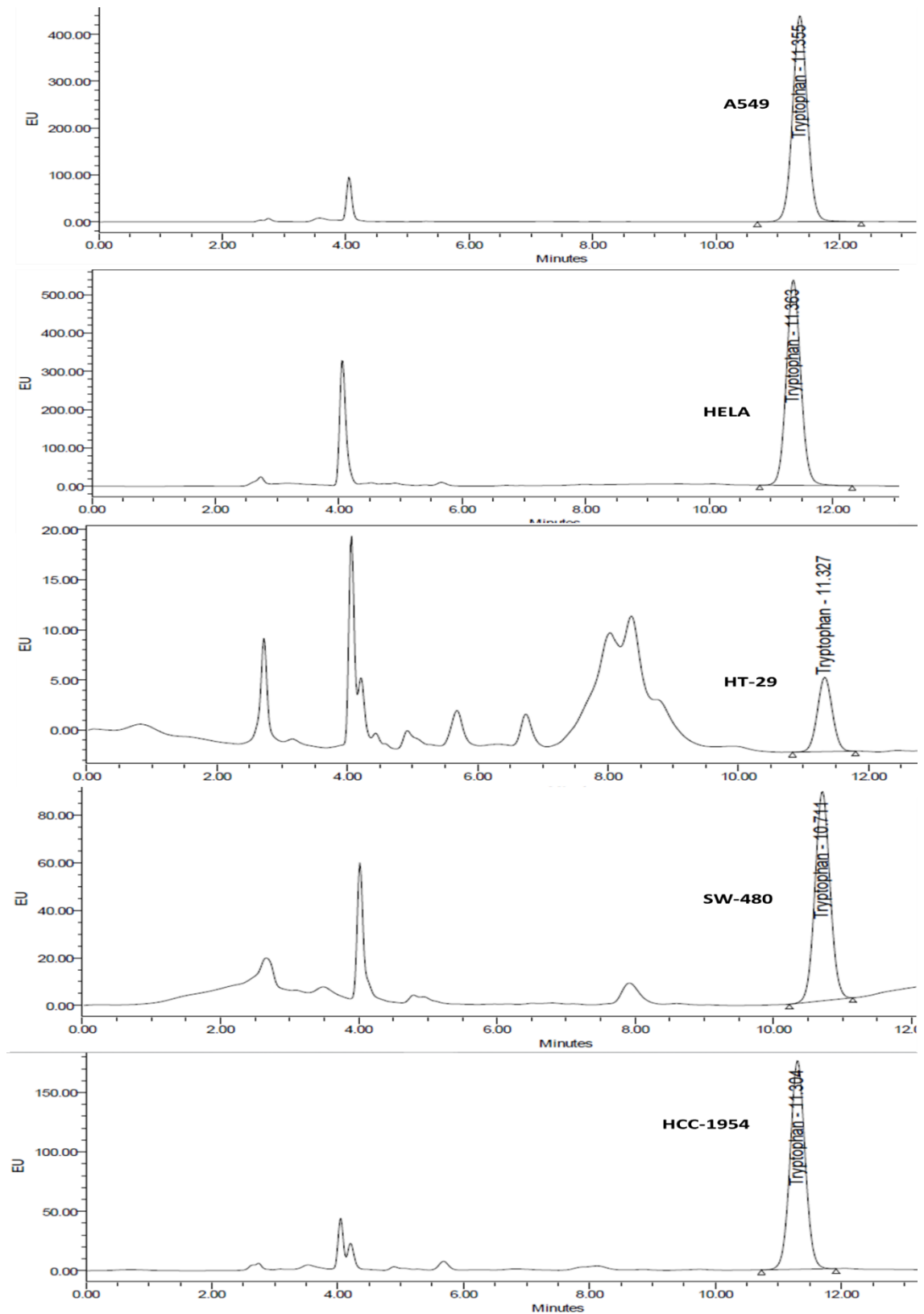


Figure 4-98: *Traces from HPLC showing the area under the curve and peak height of the remaining concentration of tryptophan in the in conditioned media of A549, HELA, HT-29, SW-480 and HCC-1954 after 48 hours of incubation with FBS free media.*

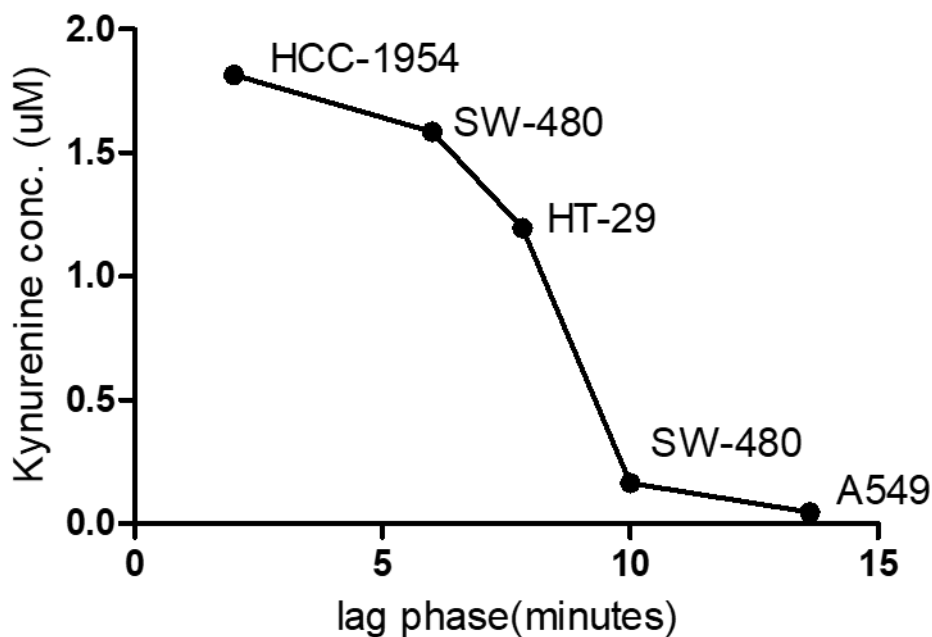


Figure 4-99: Relationship between kynurenine produced by each cell lines and their lag phase. Non-linear graph showing the inverse relationship between kynurenine concentration and duration of the lag time for every cell line.

It should be noted that the concentration of kynurenine produced by the cell lines under these circumstances and measured by HPLC were at least 50 times lower than the concentrations that demonstrated an inhibitory effect on TCIPA by LTA. Upon activation, platelets release their cargo from different types of granules as well as microparticles. During platelet aggregation and thrombus formation, platelet releasate, highly enriched in platelet granular and exosomal contents, contributes to the microenvironment of biologically active compounds and proteins that enhance the local response of platelets and surrounded cells in a positive feedback loop [402]. Platelets lysate contain a large quantity of growth factors needed for cell expansion like TGF- β 1, VEGF, EGF, PDGF-AB/BB, PF-4, and FGF-2 [403] [404-406]. Addition of VEGF to dendritic cells culture was found to enhance IDO expression and impact lymphocytes proliferation [407]. It could be that the basal concentration of kynurenine produced by the cell lines significantly differ from the concentration of kynurenine produced during tumour cells-platelets interactions; i.e. when cancer cells become in contact with platelets and platelets' products.

To investigate such hypothesis, A549 and HCC-1954 cells were seeded in T-25 culture flask (0.8×10^6). When reaching 70-80% of confluency cells were incubated with 3 mL of WP, WP lysate, WP releasate and/or 50 ng of IFN- γ , used as positive control for IDO induction for 24 hours [408]. Afterwards, conditioned media was collected, filtered using 0.2 μm pore filters and analysed by HPLC for kynurenine and tryptophan concentration.

For this set of experiments platelets were re-suspended in FBS free DMEM F12 and RPMI media. Platelets' lysate was prepared by freezing and thawing the platelet suspension in liquid nitrogen for at least 3 times followed by centrifugation at 3000 rpm for 10 minutes at 4 °C. Platelet releasate was obtained by induction of platelet aggregation induced by collagen (4 $\mu\text{g}/\text{mL}$) followed by centrifugation at 3000rpm for 10 minutes at 4 °C.

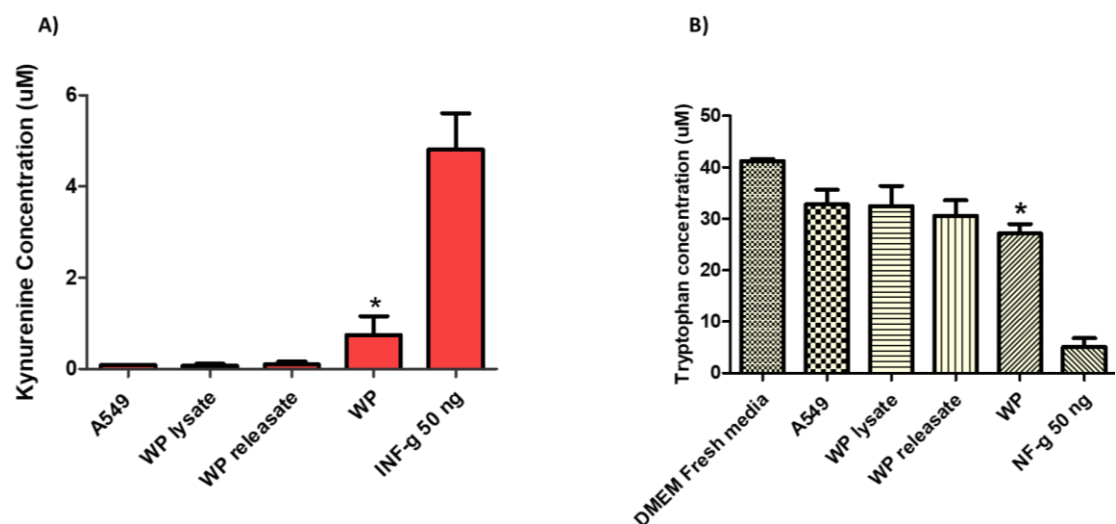


Figure 4-100: Effect of platelets on kynurenine production and tryptophan consumption in A549 cells. Statistical analysis showing kynurenine generation (A) and tryptophan consumption (B) in the presence of washed platelets, platelet lysate and release. IFN- γ was used as positive control. Data is represented as mean \pm SD; n=4; One-way ANOVA & Tukey's post-test. *P < 0.05 VS control (A549conditioned media).

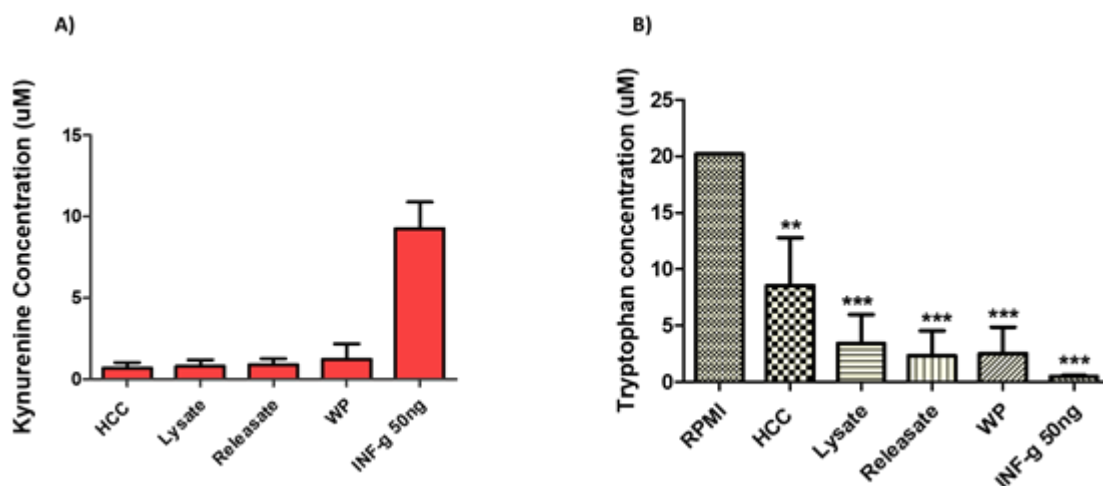


Figure 4-101: Effect of platelets on kynurenine production and tryptophan consumption in HCC-1954 cells. Statistical analysis showing kynurenine production (A) and tryptophan consumption (B) in the presence of platelets, (WP) and platelet lysate and release. IFN- γ was used as a positive control. Data is represented as mean \pm SD; n=4; One-way ANOVA & Tukey's post-test. *P <0.05 VS control (conditioned media)

When A549 cells were incubated with platelets, kynurenine generation significantly increased, from $0.08 \pm 0.01 \mu\text{M}$ to $0.74 \pm 0.41 \mu\text{M}$, and tryptophan concentration decreased, from $41.18 \pm 0.78 \mu\text{M}$ to $27.16 \pm 3.14 \mu\text{M}$, as shown in figure 4-100. Despite having a higher basal kynurenine level, incubation of HCC-1954 cells with WP did not result in significant increase in IDO induction and kynurenine generation (figure 4-101). Co-incubation of A549 and HCC-1954 cells with WP lysate and WP releasate had no significant effect on kynurenine level in both cell lines. However, a considerable consumption of tryptophan by HCC-1954 was observed. This effect may be due to the induction of the tryptophan hydroxylase enzyme responsible for the conversion of tryptophan to serotonin [409]. Tryptophan hydroxylase-1 enzyme has been found to be highly expressed on HCC-1954 along with high serotonin generation [410]. As expected IFN- γ at 50 ng caused a significant increase in kynurenine production with a significant reduction in tryptophan concentration.

The mechanism by which WP induced kynurenine production by A549 cells but not by HCC-1954 cells is not known as the mechanism of interaction between platelets and tumour cells and its relationship to IDO induction has not being

investigated. One of the limitations in this experimental setting may be related to the volume of WP, WP lysate and WP releasate used (3 mL each) and the incubation time might not be enough to show a distinct induction of IDO in A549 and HCC-1954 cells to WP, WP lysate and WP releasate.

4.8.4. Pharmacological modulation of Kynurenine production and its effect on TCIPA

To examine the potential involvement of kynurenine production during TCIPA, A549, HCC-1954 and SW-180 cells were treated with IFN- γ (inducer of IDO) and epacadostat (IDO inhibitor). Kynurenine and tryptophan concentrations were measured in conditioned media after 48 hours by HPLC and IDO expression by immunoblotting. Then, the ability of the treated cells to induce platelet aggregation was investigated by LTA.

4.8.4.1. Effects of incubation of cells with IFN- γ and epacadostat on tryptophan and kynurenine production and IDO expression

There is some controversy in relation to the type of IFN to induce IDO depending on the cell line. Some cell lines are responsive to and induce IDO by both IFN- α or by IFN- β ; however, IFN- γ seems to be the most effective inducer of IDO [408, 411]. IDO induction occurs for most cell lines after 12-18 hours of IFN- γ incubation with a plateau at 36-48 hours [412]. On the other hand, epacadostat is a potent and selective inhibitor of IDO enzyme that competitively binds and blocks tryptophan binding to IDO and its subsequent degradation to kynurenine, thus increasing tryptophan levels and decreasing the accumulation of its metabolites [413].

First, various concentrations of IFN- γ (from 50 to 400 ng/mL) were used to induce IDO in A549, SW-480 and HCC-1954 cell lines with the aim of determining the maximum concentration of kynurenine that could be achieved.

The results obtained for IDO expression, as measured by western blot and kynurenine and tryptophan concentrations, as measured by HPLC are shown below in figures 4-102, 4-103 and 4-104 for A549 cells; 4-105, 4-106 and 4-107 for HCC-1954 and 4-108, 4-109 and 4-110 for SW-480 cells.

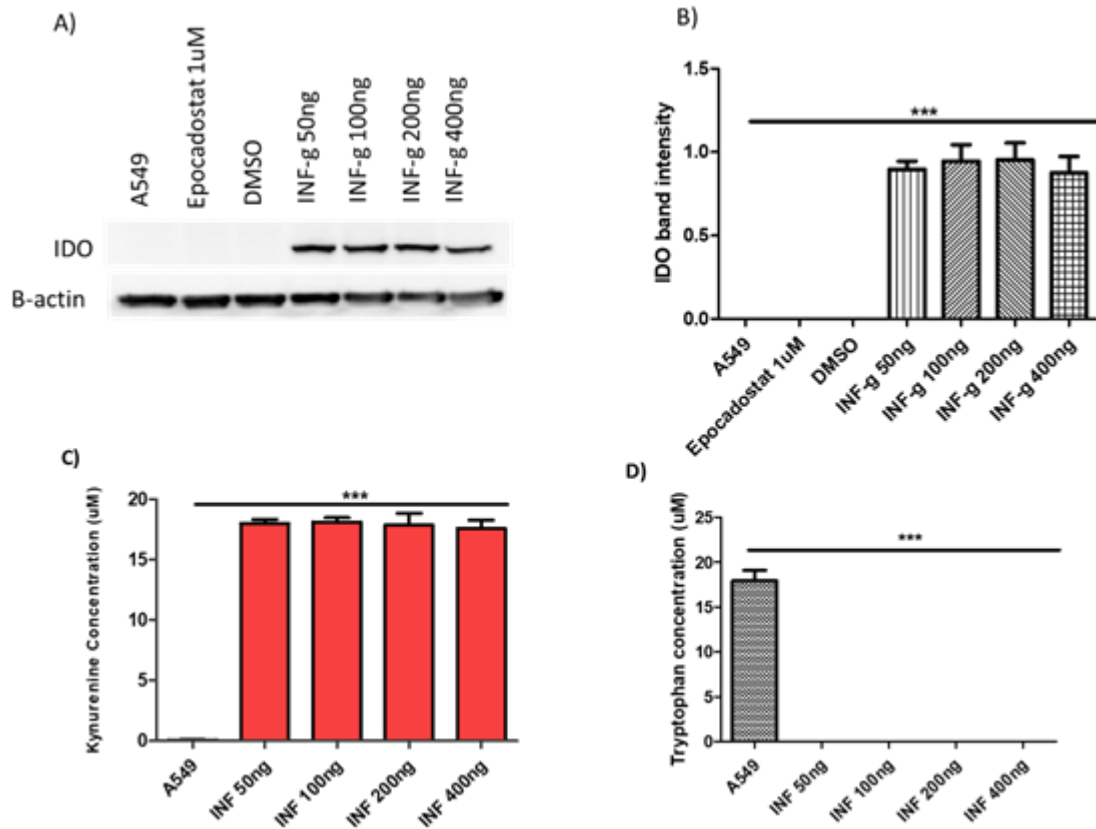


Figure 4-102: Induction of IDO and kynurenine production by A549 cells. (A) Representative immunoblotting showing the induction of IDO enzyme by IFN- γ in A549 cells 50 μ g of protein were loaded in each lane). (B) Statistical analysis showing no significant differences among various IFN- γ concentrations in IDO expression in A549 cells. (C) and (D) are statistical analyses showing the significant induction of kynurenine production and tryptophan consumption in A549 cells. Data is represented as mean \pm SD; n=3; One-way ANOVA & Tukey's post-test. *** P < 0.001.

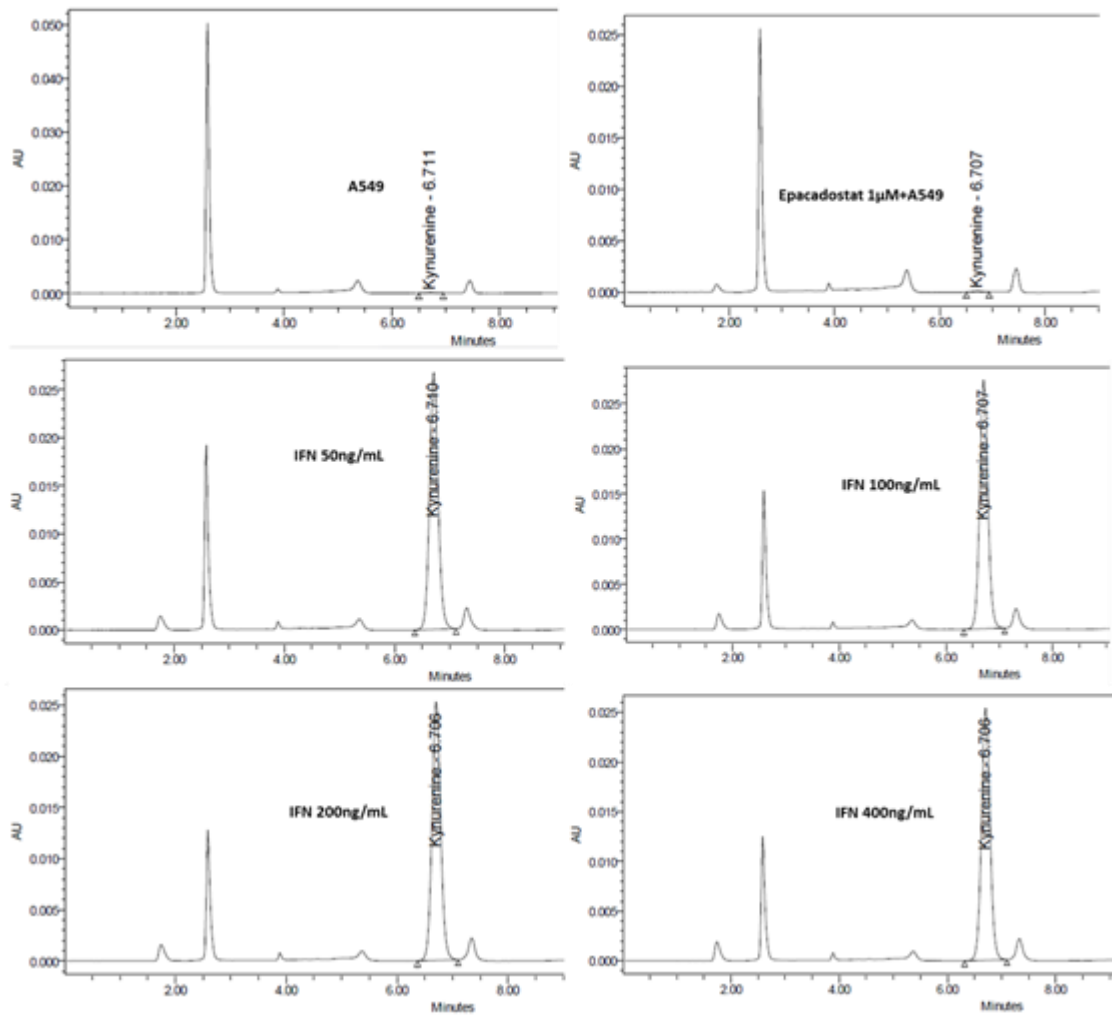


Figure 4-103: Representative HPLC traces showing the area under the curve and peak height of kynurenine measures in conditioned media from A549 cells incubated with epacadostat 1µM or IFN- γ (50-400 ng/mL) for 48 hours.

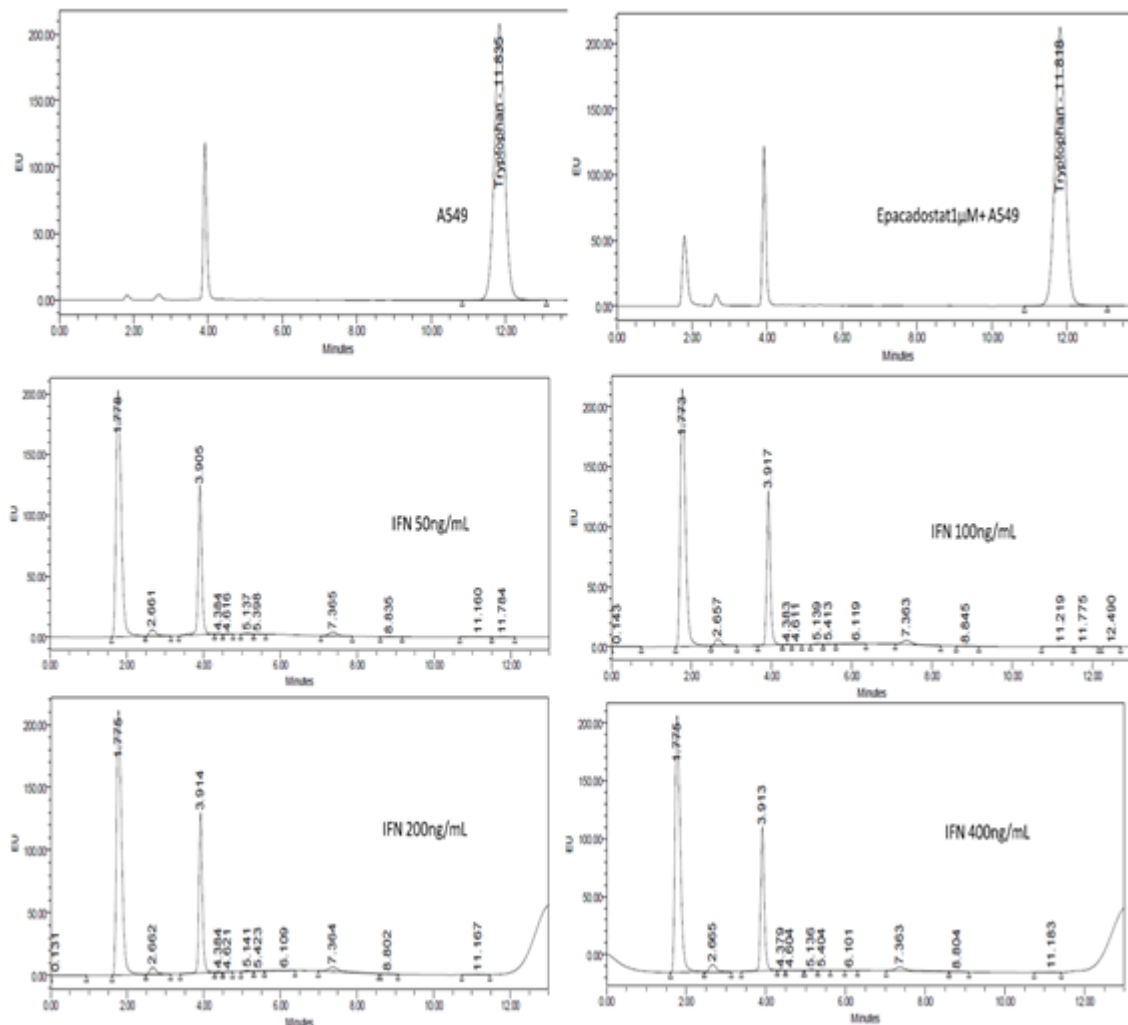


Figure 4-104: Representative HPLC traces showing the area under the curve and peak height of tryptophan measured in conditioned media from A549 cells after inhibition or induction of indoleamine dioxygenase-2 with epacadostat 1 μ M or IFN- γ (50-400 ng/mL) ;respectively.

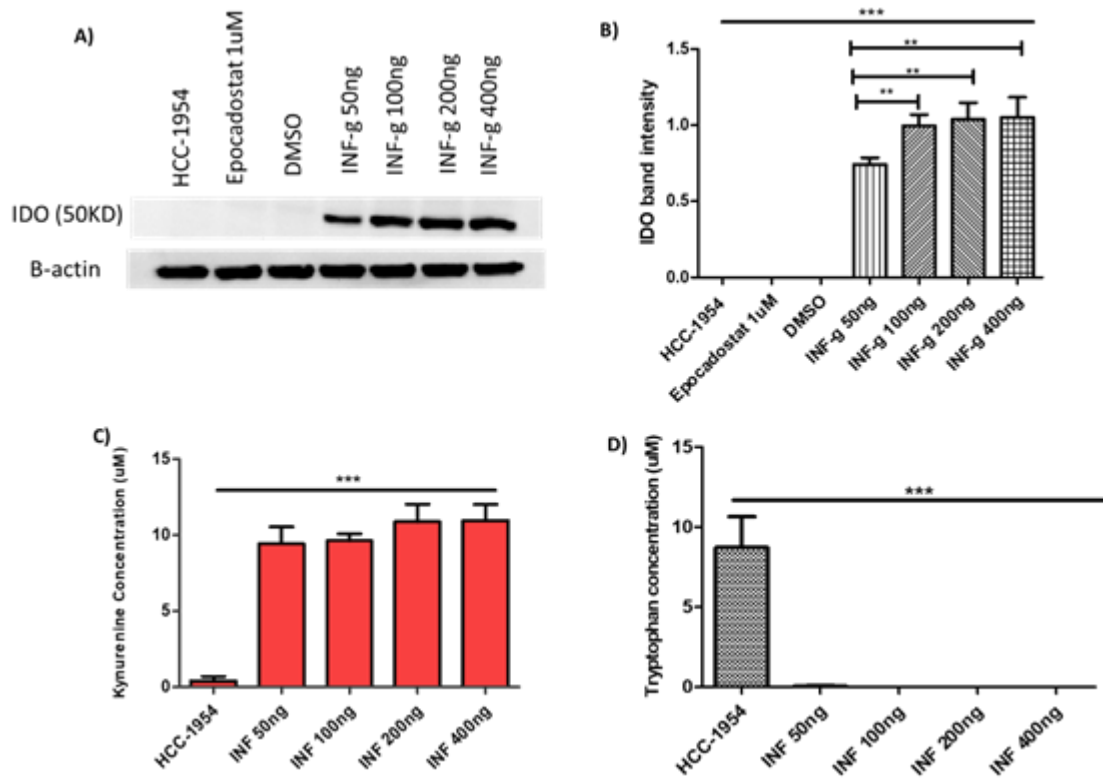


Figure 4-105: Induction of IDO and kynurenine production in HCC-1954 cells. (A) Representative western blot showing the dose-dependent induction of IDO enzyme by IFN- γ in HCC-1954 cells (50 μ g of protein were loaded in each lane). (B) Statistical analysis showing significant differences in IDO expression in HCC-1954 cells by various IFN- γ concentrations. (C) and (D) are statistical analyses showing kynurenine production and tryptophan consumption in conditioned media as measured by HPLC. Data is represented as mean \pm SD; n=4; One-way ANOVA & Tukey's post-test. *** P < 0.001.

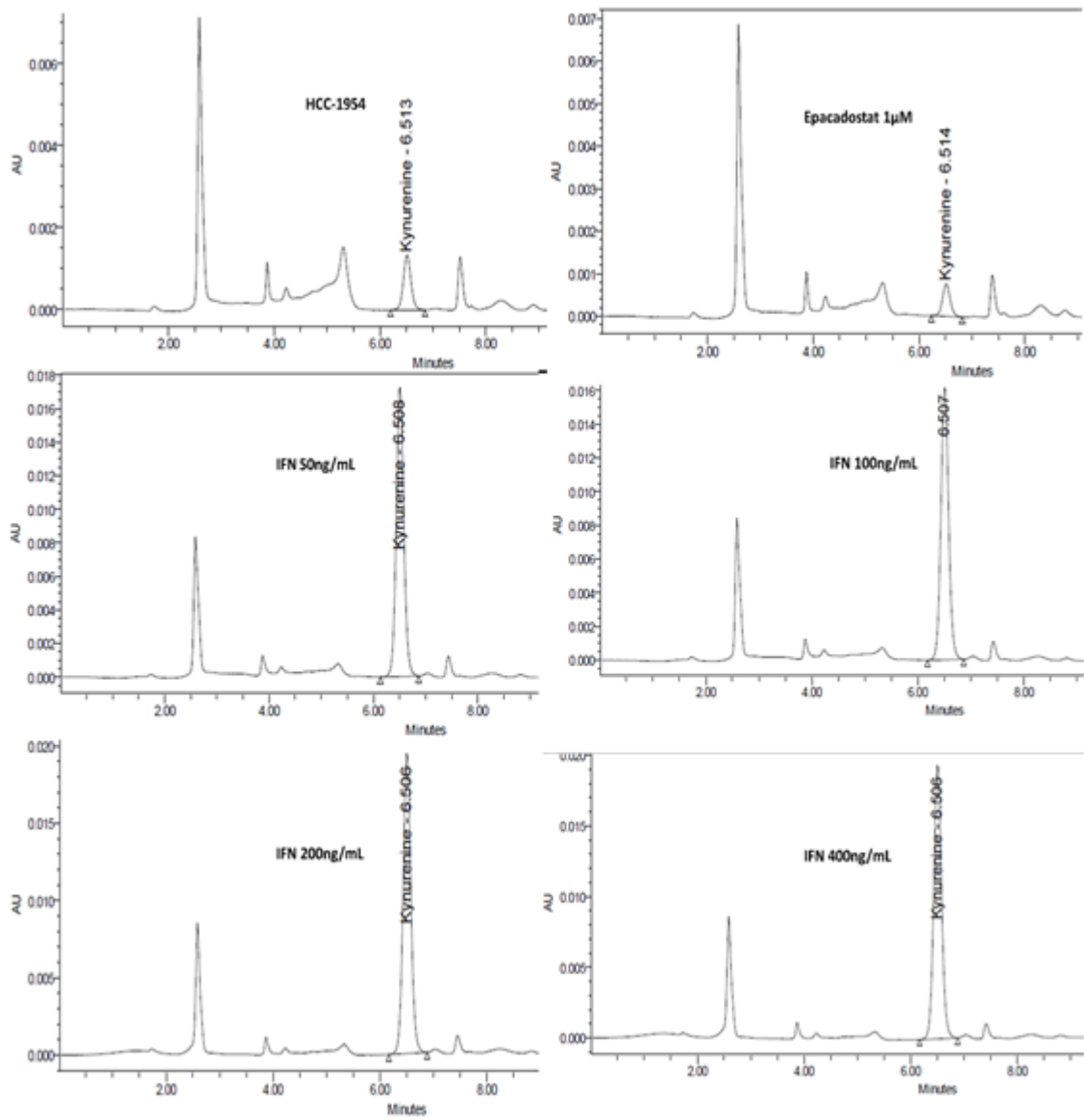


Figure 4-106: Representative HPLC traces showing the area under the curve and peak height of kynurenine produced in conditioned media by HCC-1954 cells incubated with epacadostat 1 µM or IFN-γ (50-400 ng/mL) for 48 hours.

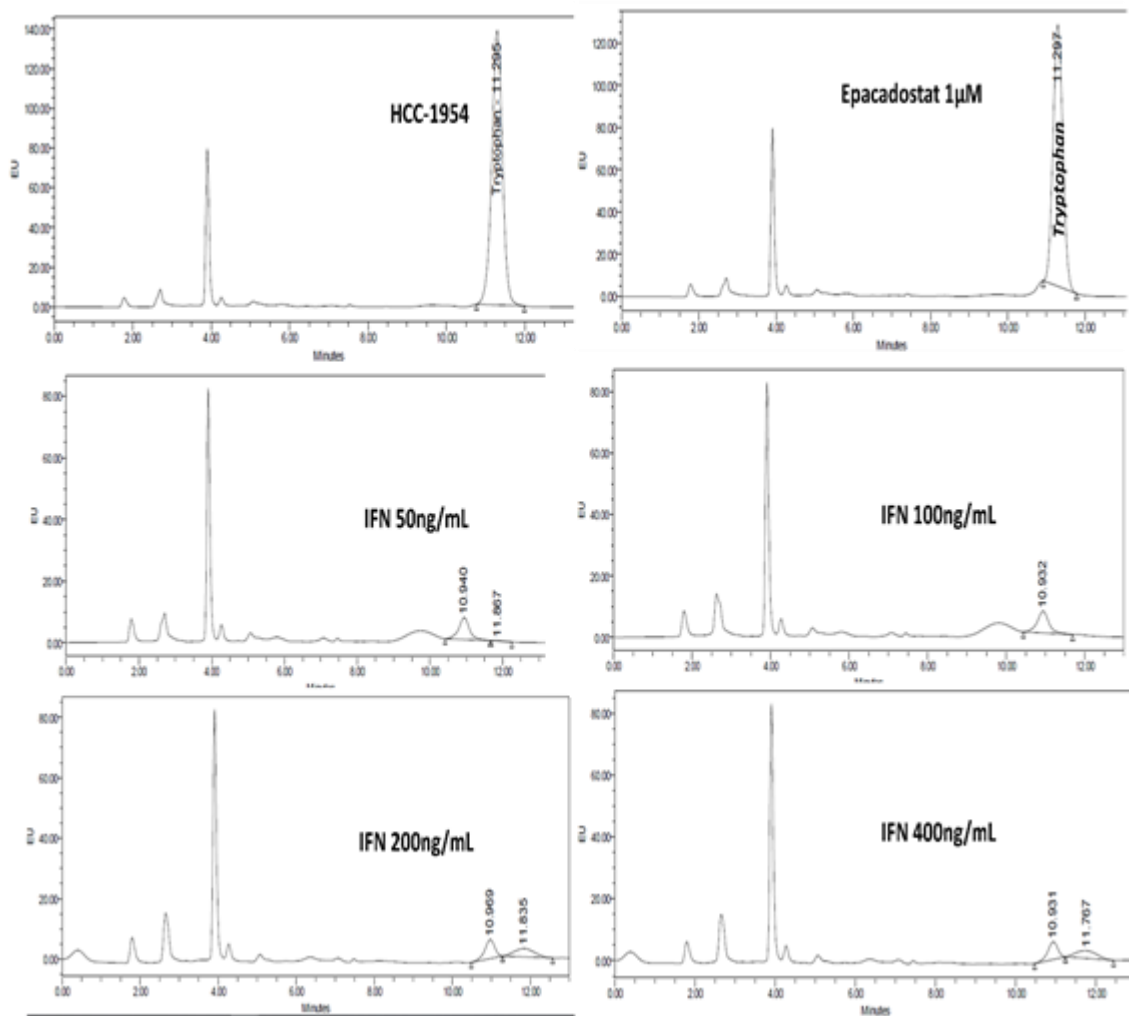


Figure 4-107: Representative HPLC traces showing the area under the curve and peak height of tryptophan in conditioned media following incubation of HCC-1954 cells with epacadostat 1 μM or IFN-γ (50-400 ng/mL) for 48 hours.

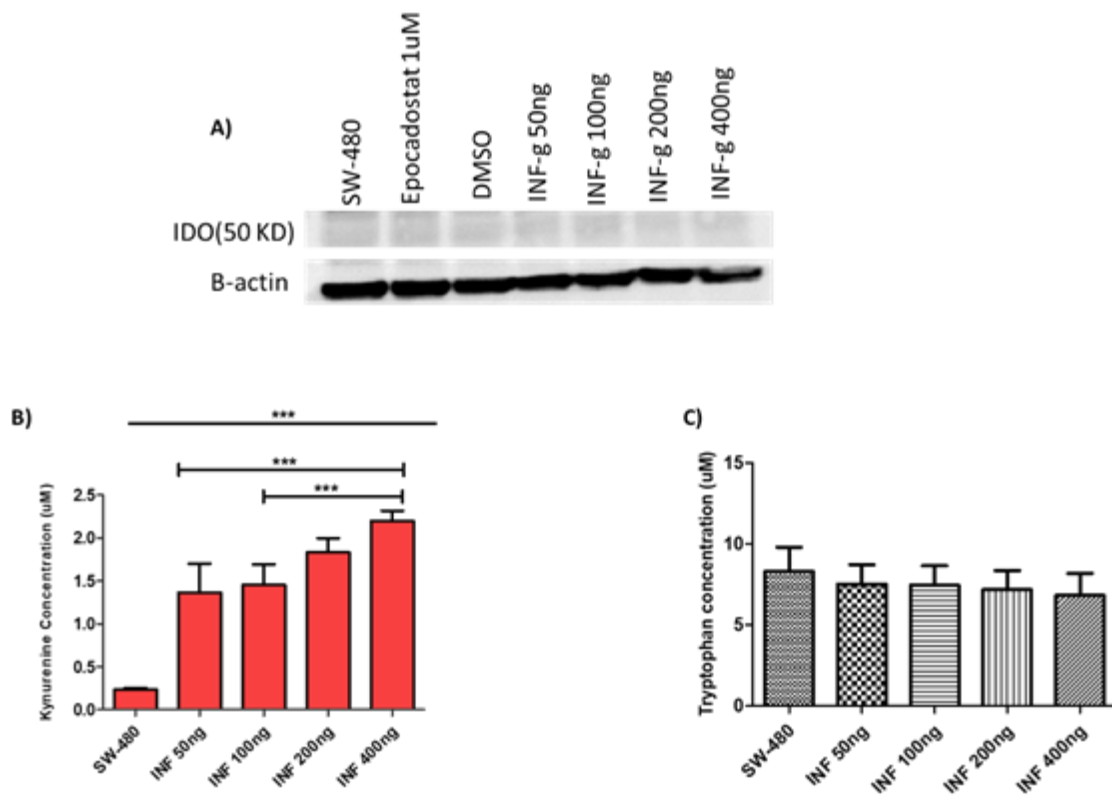


Figure 4-108: Induction of IDO and kynurenine production in SW-480 cells. (A) Representative immunoblotting that the lack of expression of IDO in SW-480 cells by IFN- γ (50 μ g of protein were loaded in each lane). Statistical analyses showing kynurenine production (B) and tryptophan consumption (C), in conditioned media from SW-480 incubated with IFN- γ . Data is represented as mean \pm SD; n=4; One-way ANOVA & Tukey's post-test. *** P < 0.001.

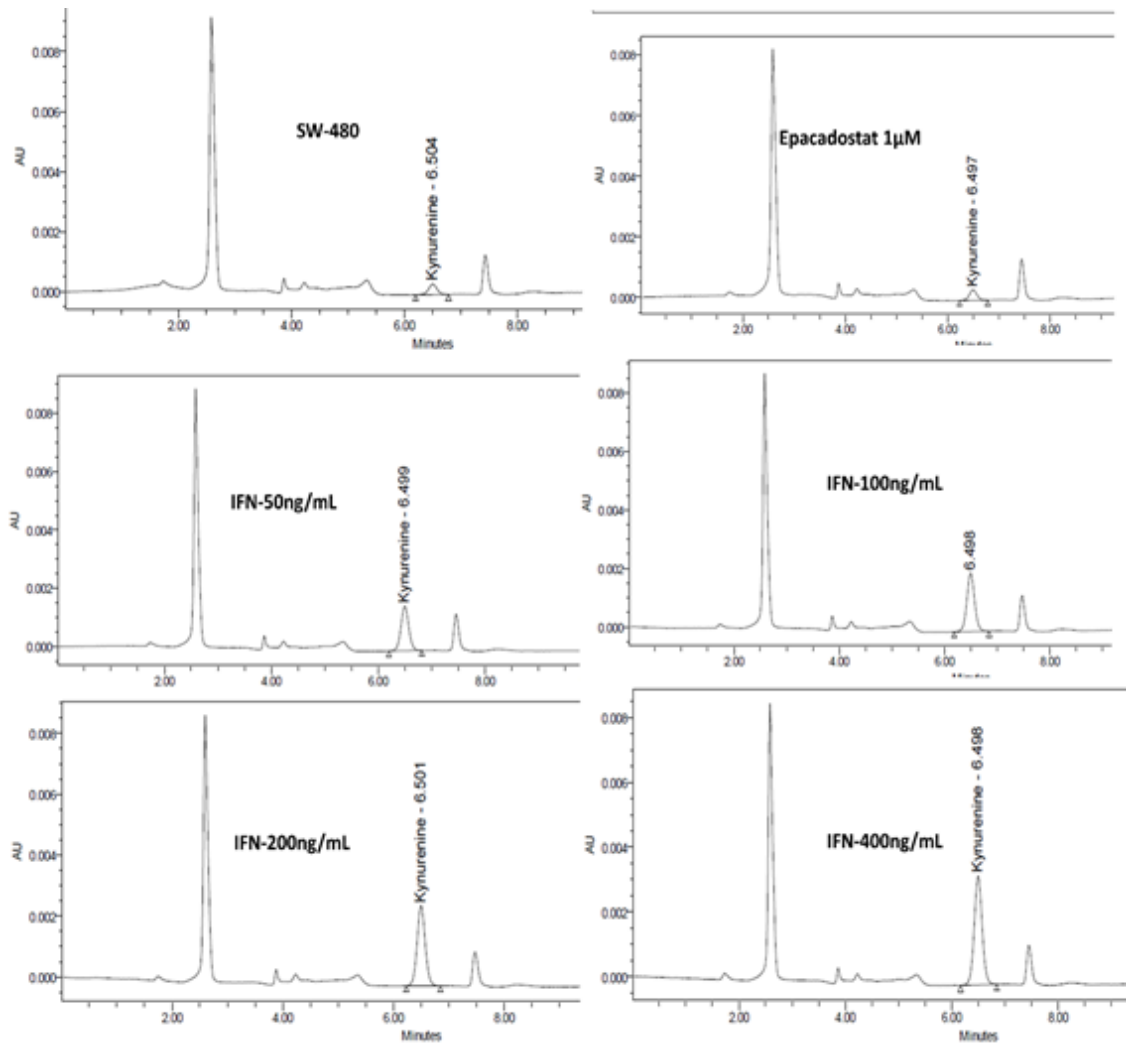


Figure 4-109: Representative HPLC traces showing the area under the curve and peak height of kynurenine produced by SW-480 cells in conditioned media after incubation with Epacadostat 1 μ M or IFN- γ (50-400 ng/mL) for 48 hours.

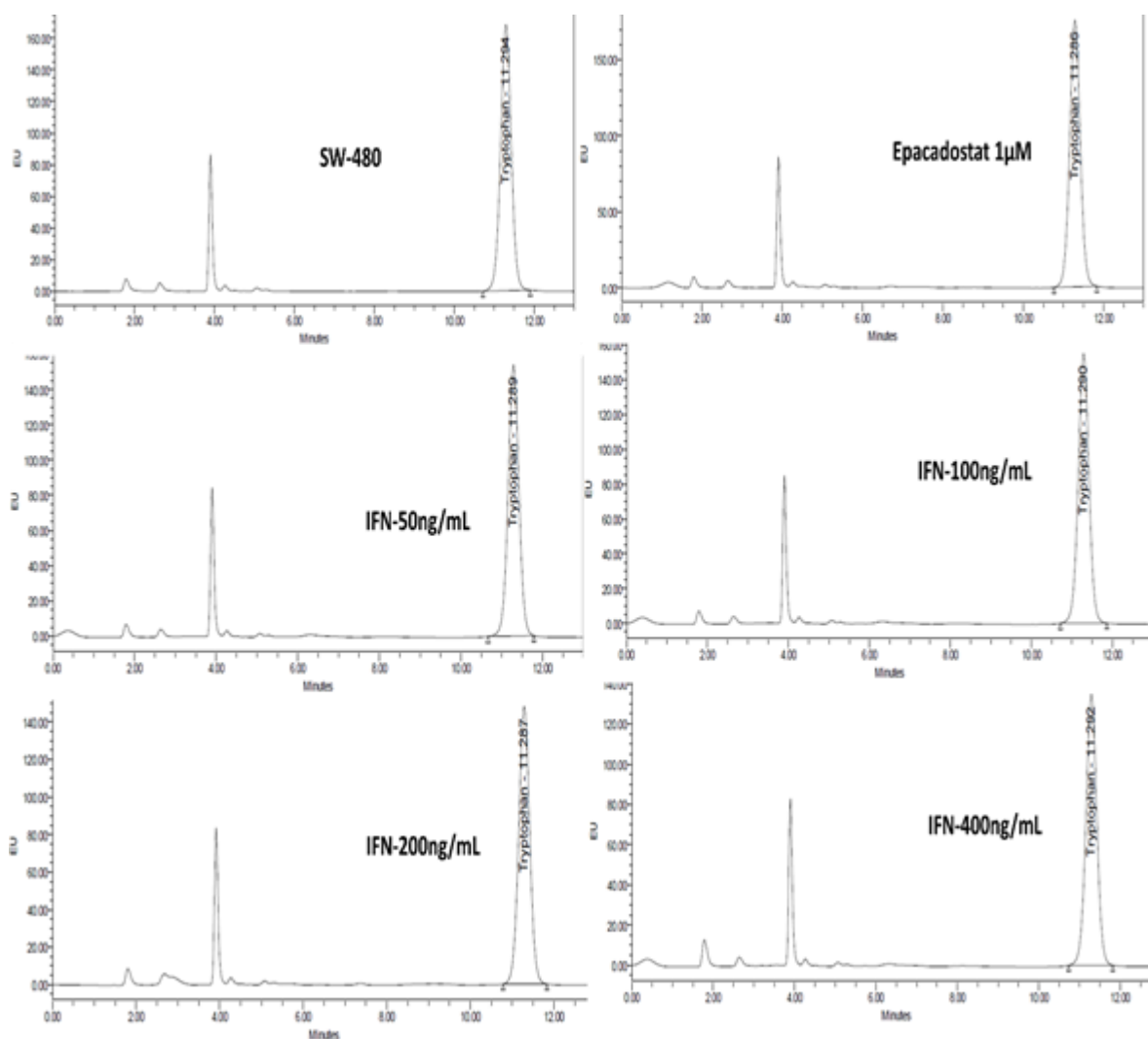


Figure 4-110: Representative HPLC traces showing the area under the curve and peak height of tryptophan in conditioned media from SW-480 cells incubated with epacadostat 1 μ M or IFN- γ (50-400 ng/mL).

The analysis of kynurenine and tryptophan concentrations in media and the expression of IDO in the homogenate from the cells treated with IFN- γ showed that IDO protein expression was significantly increased in both, A549 and HCC-1954 cells lines (figure 4-102 A and figure 4-105A). However, A549 cells seems to be more sensitive to IDO induction by IFN- γ than HCC-1954 cells as confirmed by the significant increase in kynurenine production and tryptophan consumption (figures 4-102 C and 4-102 D and figures 4-103 and 4-104) in the presence of IFN- γ . Similarly, IFN- γ caused a significant dose dependent

increase in kynurenine generation and decrease in tryptophan consumption by HCC-1954 cells as observed in figures 4-105 and HPLC traces (figures 4-106 and 4-107). It is worth to note that although a dose dependent response was achieved when HCC-1954 cells were treated with IFN- γ , A549 cells showed a similar response to all the concentrations of IFN- γ tested. These results are in agreement with previous reports available in the literature that have investigated effect of the induction of IDO in A549 cells and HCC-1954 cells by IFN- γ [414, 415].

SW-480 cell line did not show any changes in IDO protein expression when incubated with IFN- γ under the same conditions tested (figure 4-108 A). Despite the considerable concentration-dependent increase of kynurenine generation by this cell line as measured in conditioned media by HPLC (figure 4-108 B and figure 4-109), no significant consumption of tryptophan was observed (figure 4-108 C and figure 4-110). Although IDO induction has been demonstrated by Ogawa et al when SW-480 cells were incubated with IFN- γ (10 ng/mL) after 24 hours [292]. However, in a previous work IDO was not induced by IFN- γ (1000 units/mL) or IFN- α (5000 units/ml) in SW-480 cells when cells were incubated for 48 hours [292, 416]. IFN- γ induces IDO by promoting interferon-stimulated response element (ISRE) and IFN- γ activation sequence (GAS) elements through the activation of the Janus kinase (JAK) which activates protein-signal transducer and activator of transcription 1 (STAT1) signalling pathway [417]. The inability of IFN- γ to induce IDO expression in SW-480 cells suggests the presence of various mechanisms of action of IFN- γ to induce IDO expression [416]. It is worth to mention that the basal expression of IDO was not detected by immunoblotting in all the cell lines tested and more sensitive technique like PCR may be able to do so. However, basal kynurenine production reflects the basal activity of the enzyme.

Epacadostat exerted similar effects on A549 and HCC-1954 cell lines. The incubation of cell lines with epacadostat resulted in a significant reduction of the production of kynurenine induced by IFN- γ and in a significant restoration of tryptophan concentrations when compared to tryptophan concentrations in conditioned media of cells treated with IFN- γ . Those results are summarised in figure 4-111; figure 4-112 and figure 4-113 for A549 cells and figure 4-115; figure 4-116 and figure 4-117 for HCC-1954 cells. Despite the ability of epacadostat to inhibit IFN- γ induced kynurenine production in SW-480 cells, the drug didn't exert any effect on tryptophan consumption as shown in figures 4-118, figure 4-119 and figure 4-120. The co-incubation of IFN- γ and epacadostat has been reported to decrease kynurenine production and tryptophan consumption as it prevents the binding of tryptophan to IDO and its subsequent conversion to kynurenine [413, 418]. However, basal kynurenine generation was not affected by epacadostat, may be due to the absence of IDO induction in untreated cells as shown by the representative western blots in figures 4-102, figure 4-105 and figure 4-108.

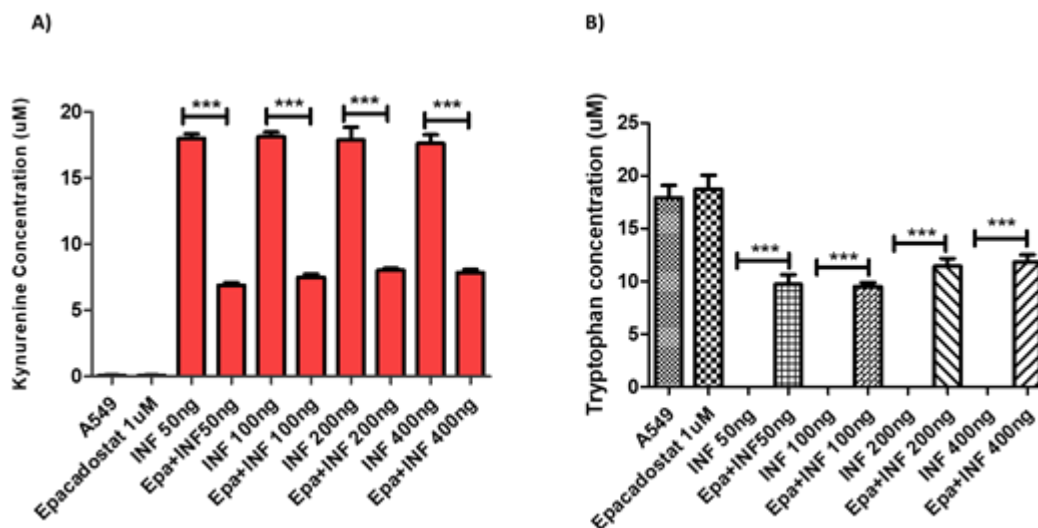


Figure 4-111: Effect of Epacadostat on kynurenine production and tryptophan consumption in IFN- γ treated A549 cells. (A) statistical analysis demonstrating the significant effect of Epacadostat on kynurenine generation induced by IFN- γ on A549 cells. (B) Statistical analysis exhibiting the significant effect of epacadostat on tryptophan consumption in conditioned media of A549 cells incubated with IFN- γ . Data is represented as mean \pm SD; n=4; One-way ANOVA & Tukey's post-test. *** P<0.001.

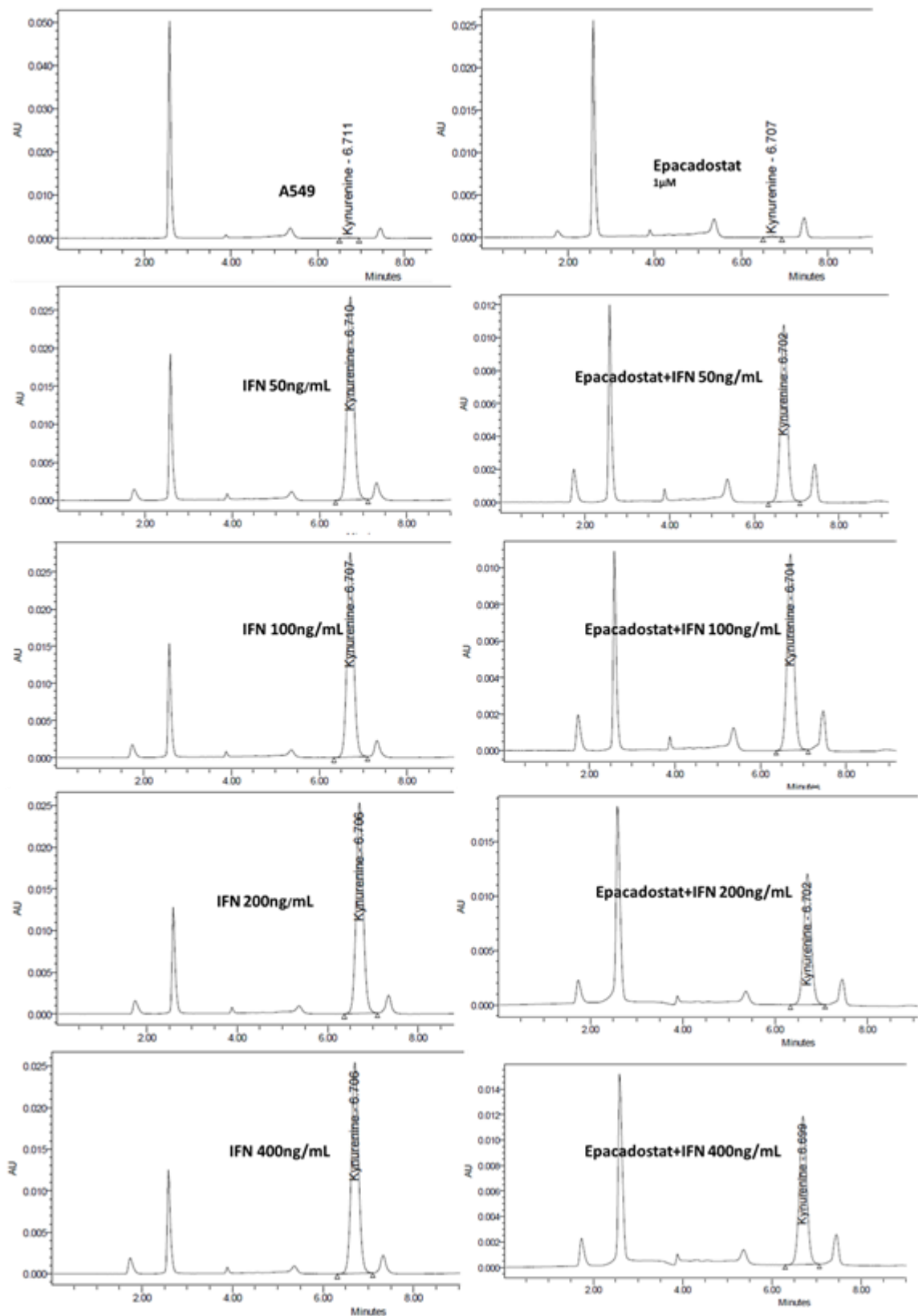


Figure 4-112: HPLC traces showing the effect of epacadostat 1 μ M on kynurenine production by A549 cells incubated with IFN- γ (50-400 ng/mL).

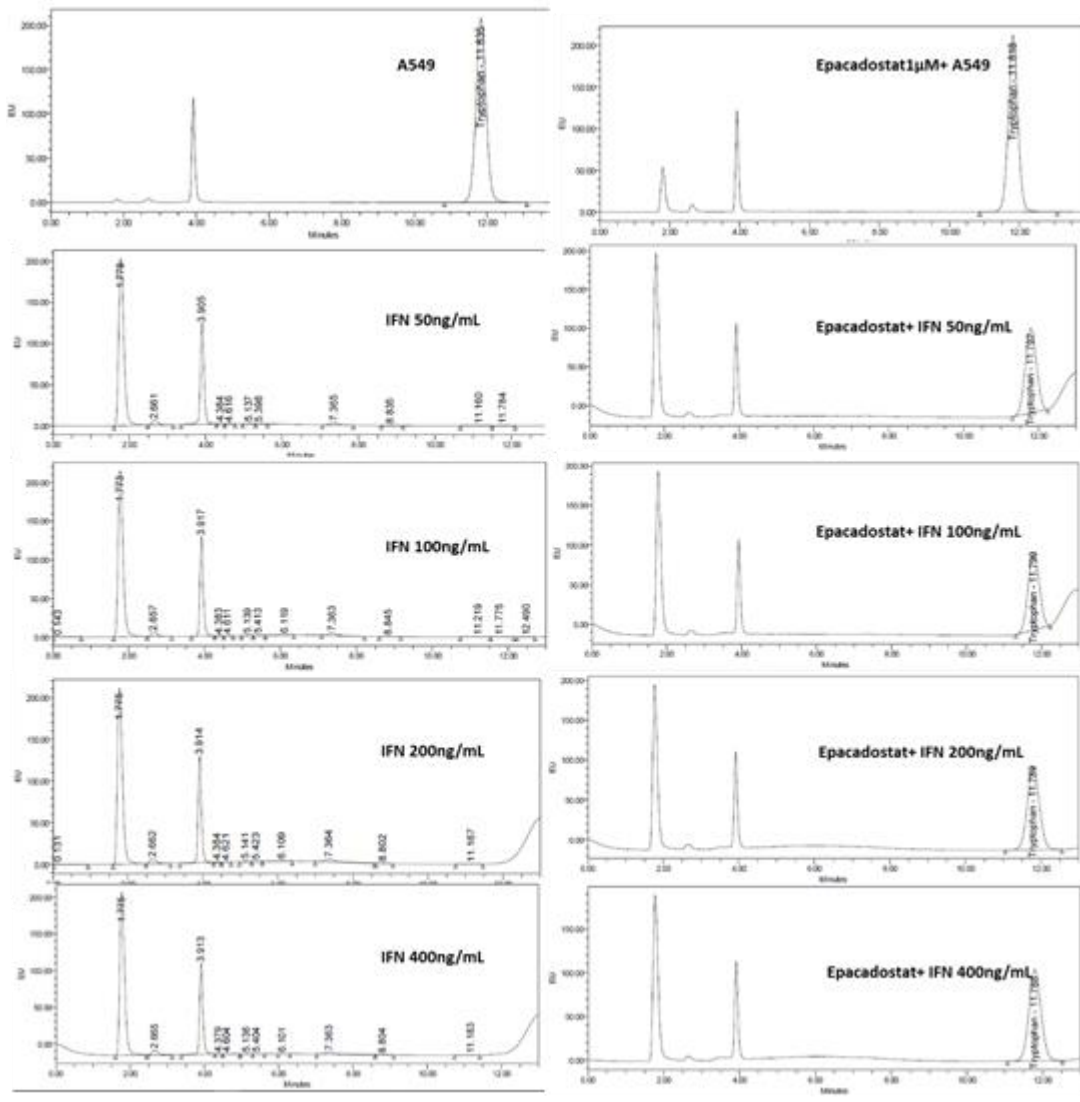


Figure 4-113: HPLC traces showing the effect of epacadostat 1µM on tryptophan in conditioned media from A549 cells treated with IFN-γ (50-400ng/mL)

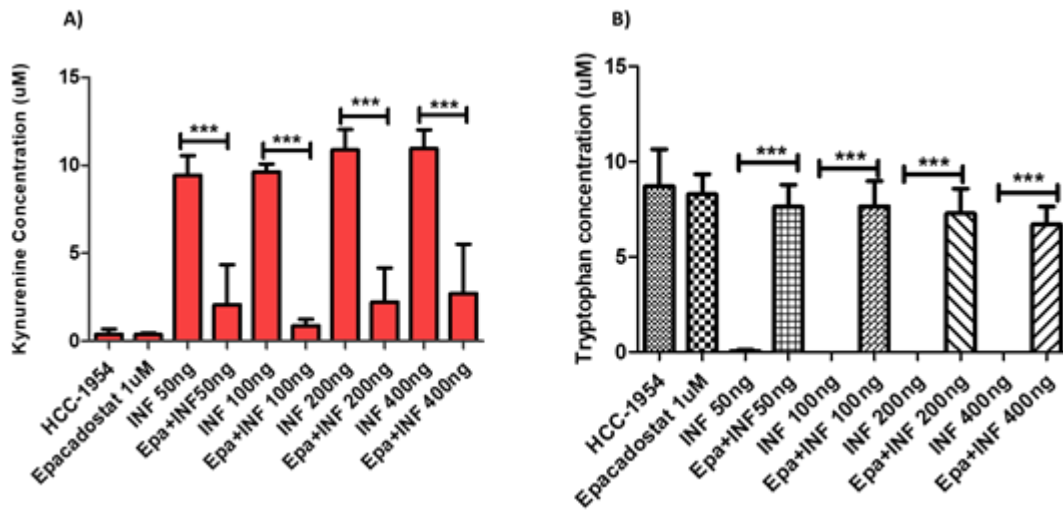


Figure 4-114: Effect of Epacadostat on kynurenine production and tryptophan consumption in IFN- γ treated HCC-1954 cells. (A) statistical analysis demonstrating the significant effect of epacadostat on kynurenine generation induced by IFN- γ on HCC-1954 cells. (B) Statistical analysis exhibiting the significant effect of epacadostat on tryptophan consumption in conditioned media of HCC-1954 cells incubated with IFN- γ . Data is represented as mean \pm SD; n=4; One-way ANOVA & Tukey's post-test. *** P < 0.001.

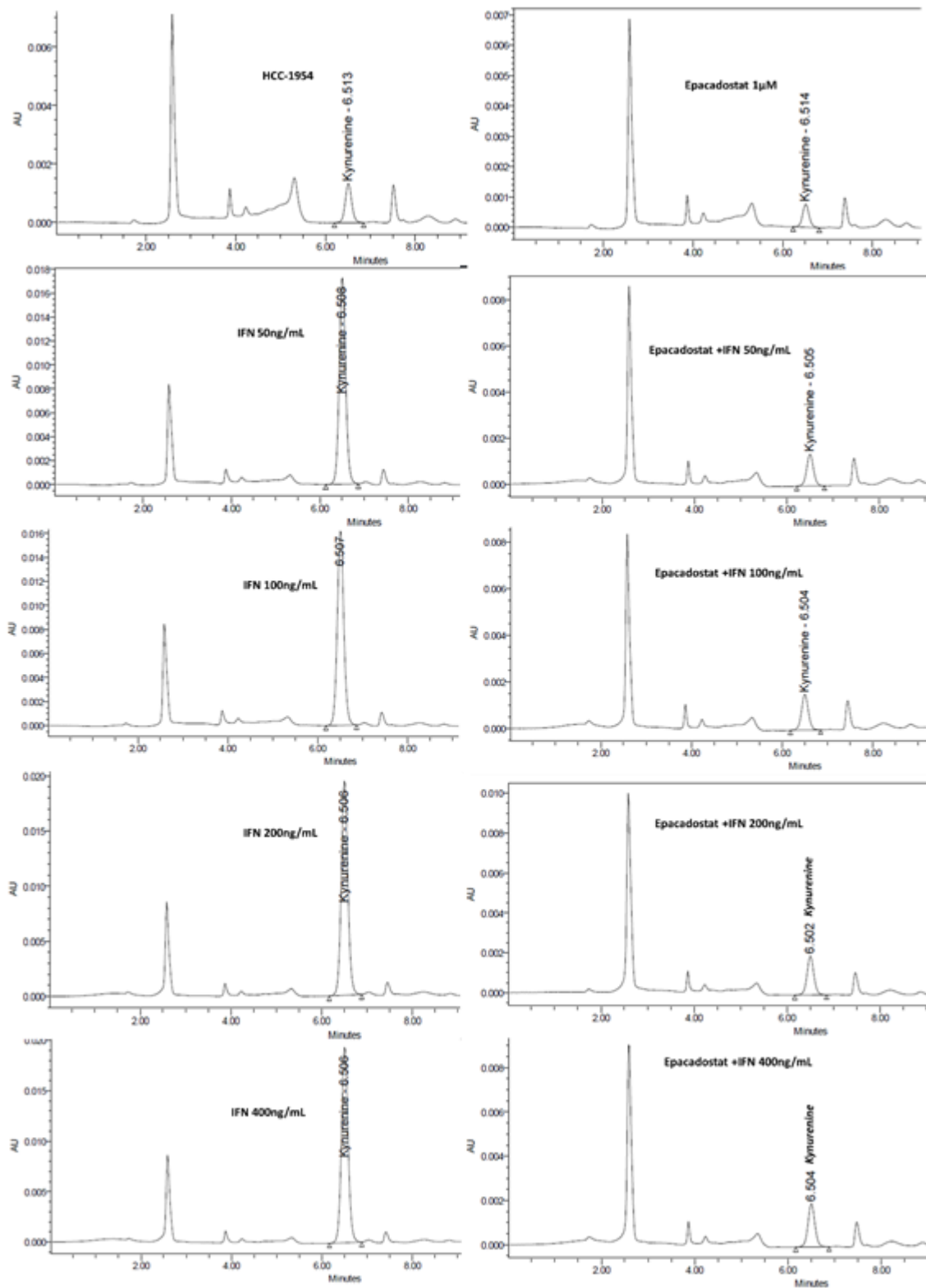


Figure 4-115: HPLC traces showing the effect of epacadostat 1 μ M kynurenine production by HCC-1954 cells incubated with IFN- γ (50-400 ng/mL).

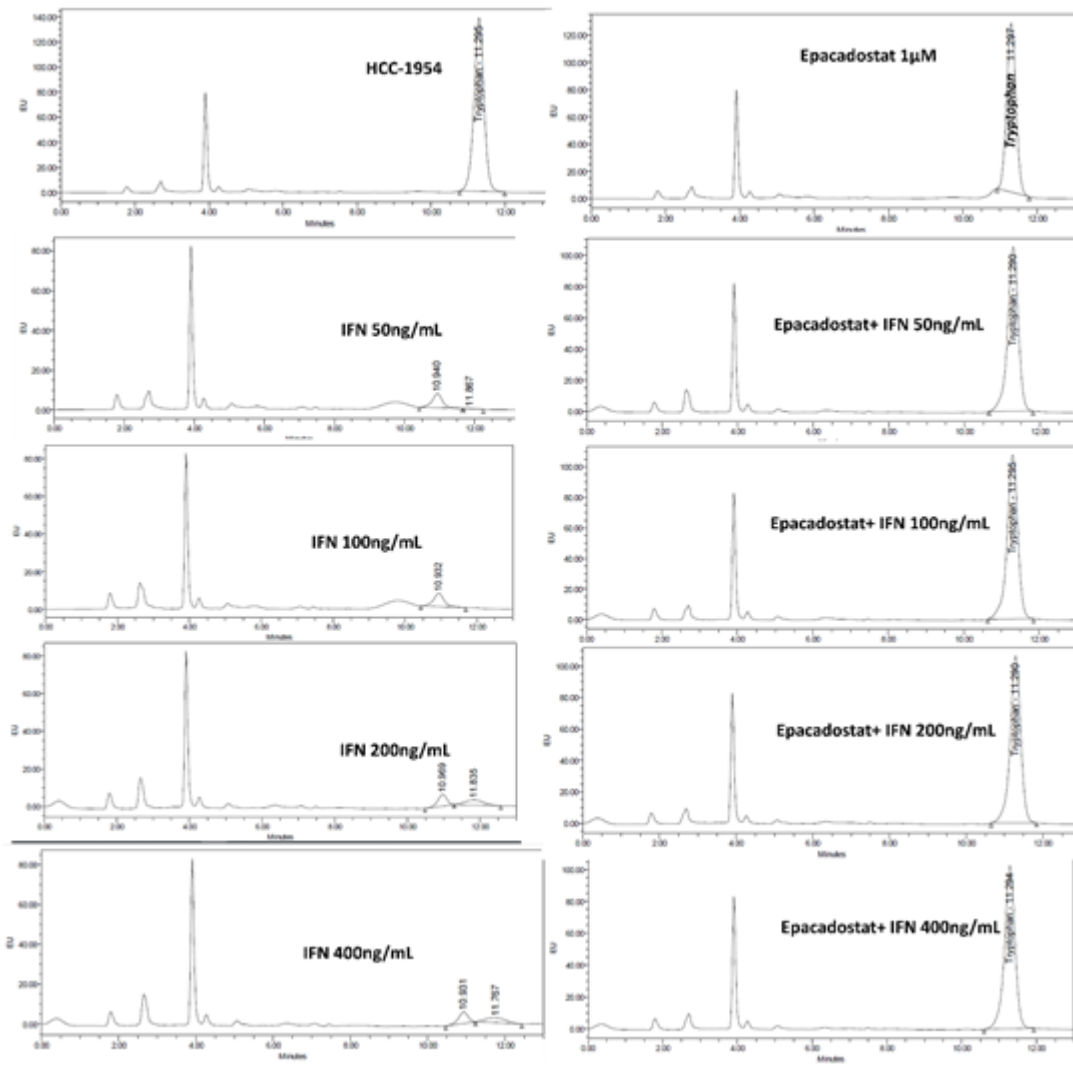


Figure 4-116: HPLC traces showing the effect of epacadostat 1 μ M on tryptophan in conditioned media from HCC-1954 cells treated with IFN- γ (50-400ng/mL).

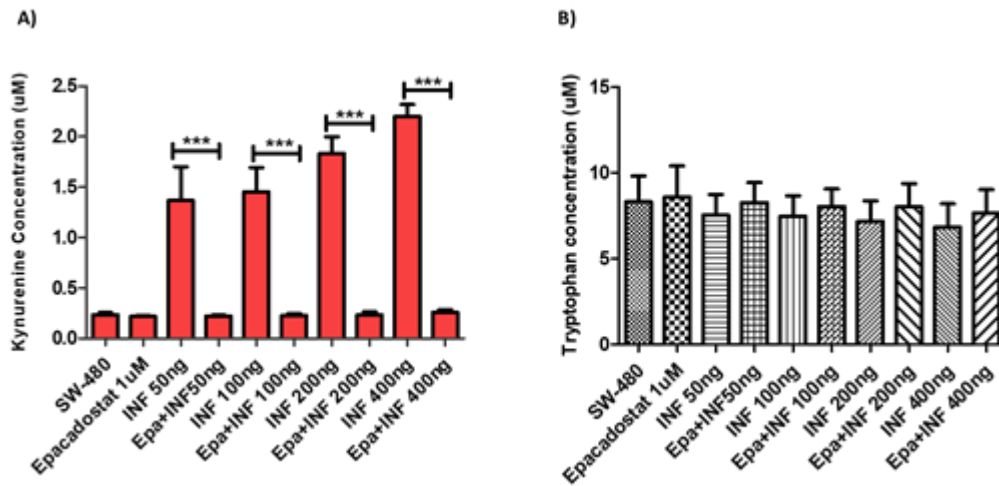


Figure 4-117: Effect of epacadostat on kynurenine production and tryptophan consumption in IFN- γ treated SW-180 cells. (A) statistical analysis demonstrating the significant effect of epacadostat on kynurenine generation induced by IFN- γ on SW-180 cells. (B) Statistical analysis exhibiting the absence of effect of Epacadostat on tryptophan consumption in conditioned media of Sw-180 cells incubated with IFN- γ . Data is represented as mean \pm SD; n=4; One-way ANOVA & Tukey's post-test. *** P < 0.001.

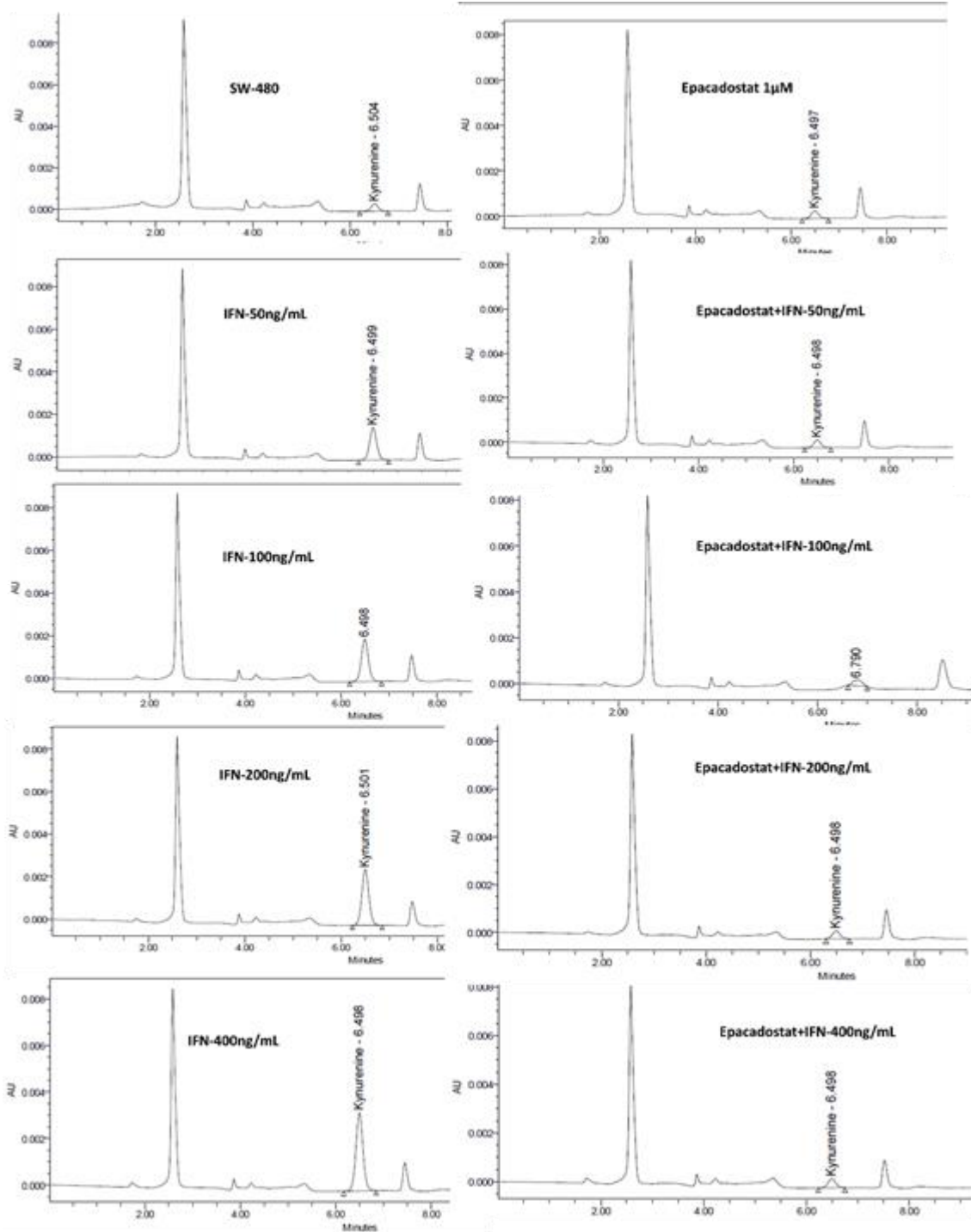


Figure 4-118: HPLC traces showing the effect of Epacadostat 1 μ M on kynurenine production by SW-480 cells incubated with IFN- γ (50-400ng/mL).

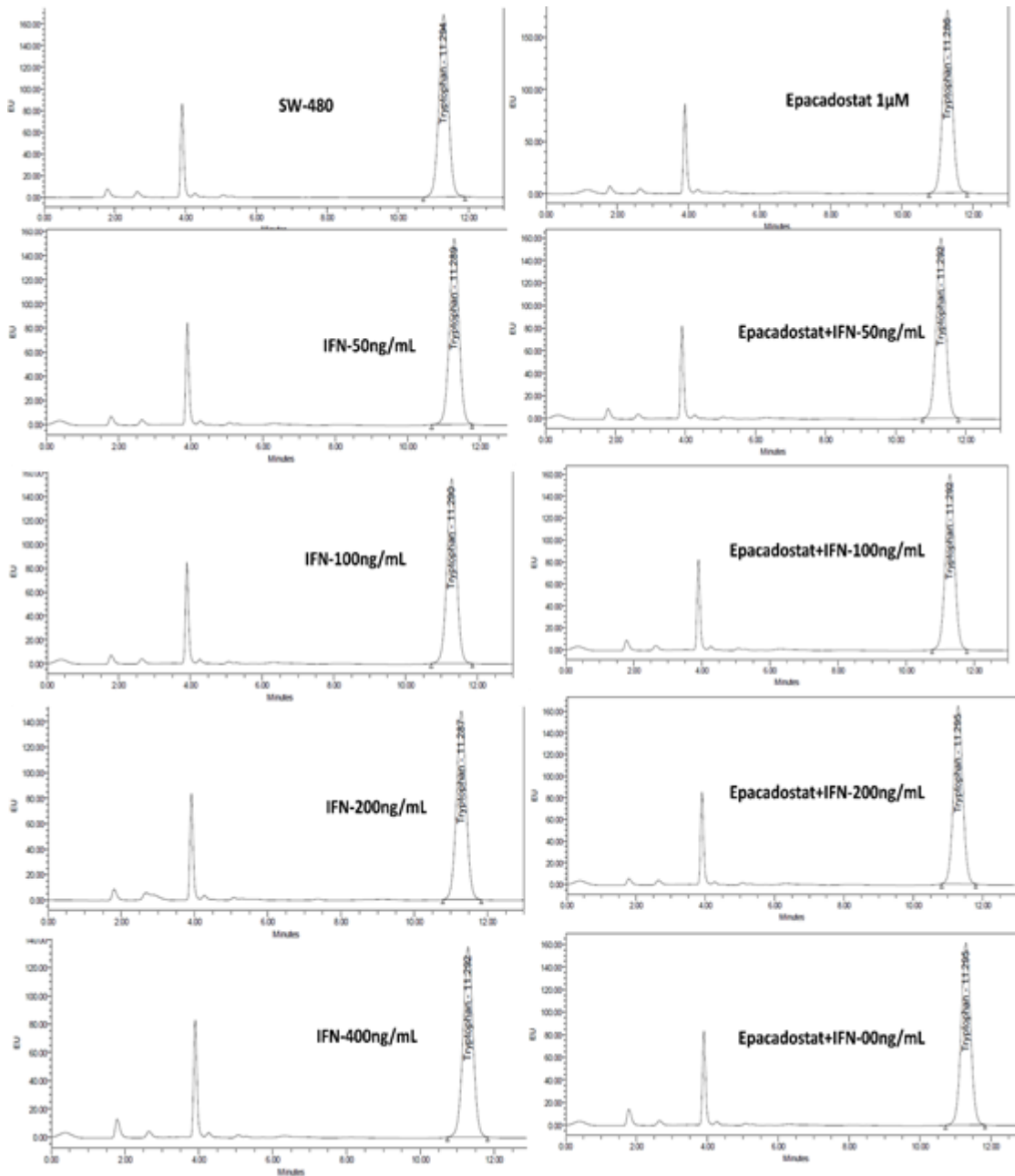


Figure 4-119: HPLC traces showing the effect of epacadostat 1 μ M on tryptophan in conditioned media from SW-180 cells treated with IFN- γ (50-400ng/mL).

The extent to which SW-480 could increase its kynurenine production induced by IFN- γ was lower to that of HCC-1954 and A549 cells. SW-480 showed a shorter lag phase than A549 and a higher basal production of kynurenine. HCC-1954 showed a shorter lag phase than SW-480 but a higher basal and IFN- γ induced kynurenine level. However, kynurenine concentration produced by A549 cells incubated with IFN- γ was much higher (about 10 times) than that of SW-480, that produced the lowest concentration of kynurenine (around 2.2 μ M). The highest kynurenine production induced by IFN- γ was achieved by A549 cells, although only around 18 μ M which is a much lower concentration than the minimum concentration used to inhibit TCIPA *in vitro* by LTA at the beginning of this research (100 μ M).

4.8.5. Effect of the pharmacological manipulation of IDO on HCC-1954 and A549 on TCIPA

A549 and HCC-1954 cell lines were chosen to examine the potential effect of the pharmacological manipulation of IDO on TCIPA induced by A549 and HCC-1954.

In this set of experiments, cells were first seeded on T-25 flask (0.8×10^6) and once they reached about 70% of confluency, incubated with IFN- γ (50-400 ng), epacadostat (1 μ M) or a combination of epacadostat (1 μ M) and IFN- γ (100-400 ng) in FBS free media. After 48 hours of incubation cells were detached by DPBS+EDTA and prepared as previously described (section 2.2) to test their ability to induce TCIPA in platelets re-suspended in FBS free media.

4.8.5.1. Effect of IFN- γ on A549 TCIPA

TCIPA induced by A549 cells (1000) incubated with IFN- γ (50-400ng) resulted in an elongation of the lag phase (figure 4-120A and figure 4-121). Epacadostat at 1 μ M could not reverse this effect as shown in figure 4-122A and figure 4-123. On the other hand, cells incubated with both agents(alone or in combination) did not exert any effect on maximal platelet aggregation induced by A549 as observed in figure 4-120B and figure 4-122B and represented in figure 4-121 and figure 4-123.

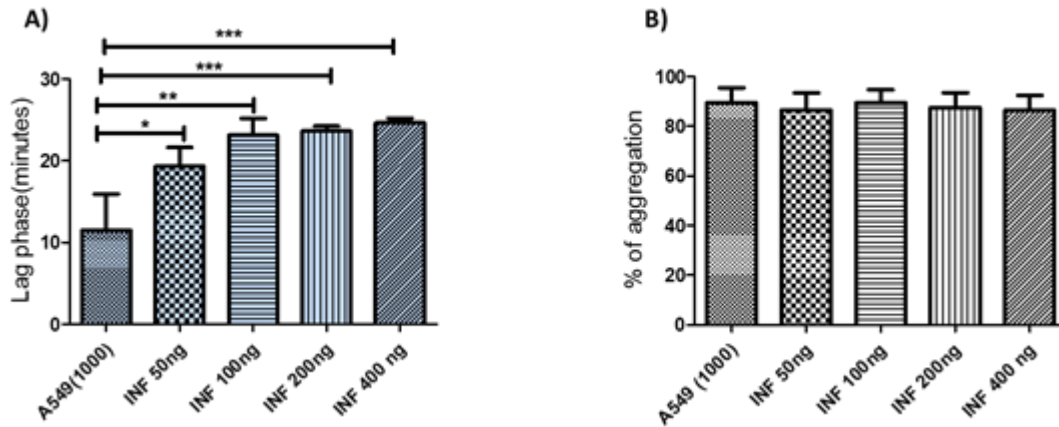


Figure 4-120: Effect of A549 cells incubated with INF- γ on platelet aggregation. (A) Statistical analysis exhibiting the significant increase in the duration of the lag phase induced by cells incubated with INF- γ for 48hr. (B) Statistical analysis showing that cells incubated with INF- γ (50-400) ng/mL induced maximal aggregation. Data is represented as mean \pm SD; n=4; One-way ANOVA & Tukey's post-test. * P < 0.05 **; P < 0.01; *** P < 0.001.

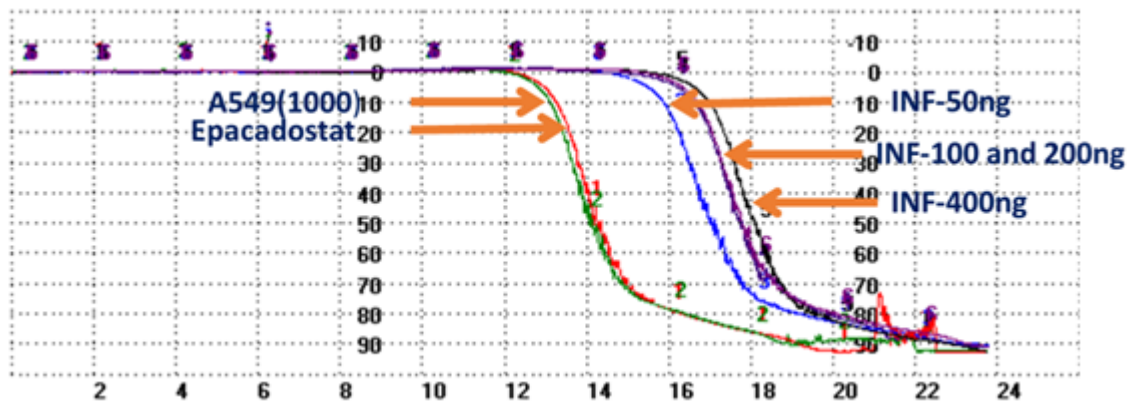


Figure 4-121: Representative traces from light transmission aggregometer showing the effect of INF- γ on A549 TCIPA. Cells incubated with INF- γ (50-400ng/mL) has significant increase in their lag phase but and A549 induced maximal aggregation not affected.

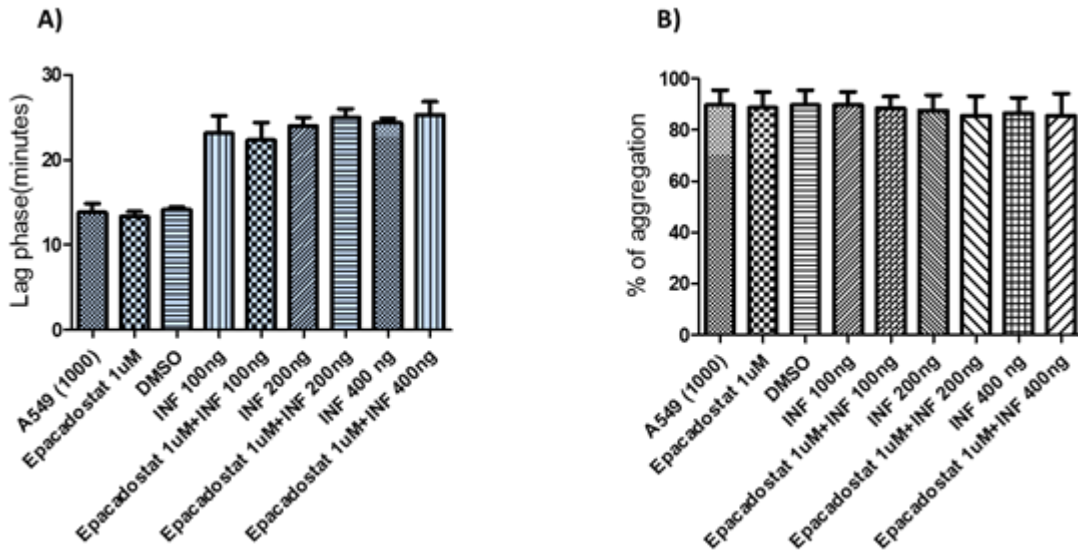


Figure 4-122: Effect of epacadostat on IFN- γ incubated A549 TCIPA. (A) and (B): Statistical analyses showing that epacadostat had no effect on A549 lag time and maximal aggregation; respectively. Data is represented as mean \pm SD; n=4; One-way ANOVA & Tukey's post-test.

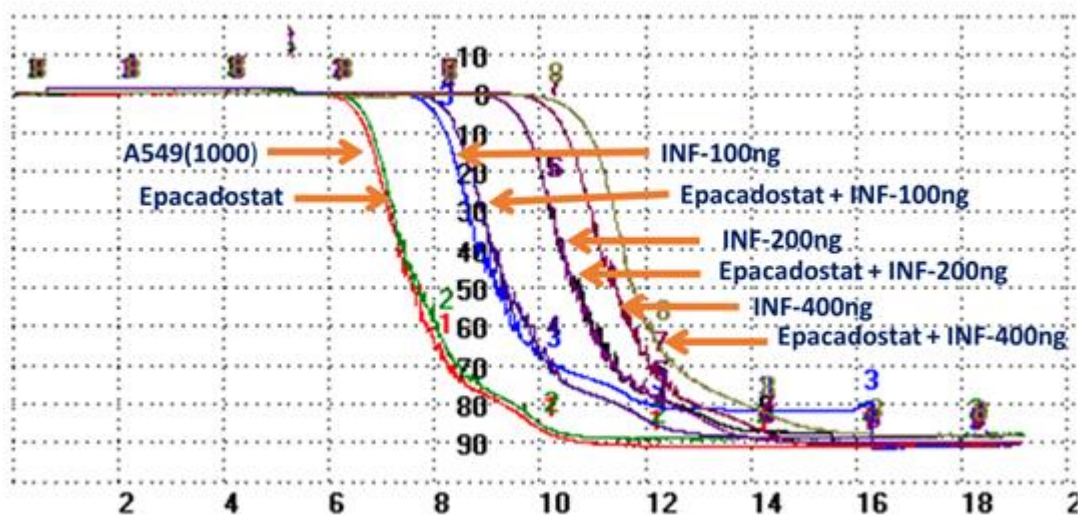


Figure 4-123: Representative traces from light transmission aggregometer showing that epacadostat had no effect neither on the increment in lag phase of A549 (1000 cells/500uL) induced by IFN(100-400ng/mL) nor on A549 induced maximal platelet aggregation.

IFN- γ had no effect on A549 TCIPA but caused a significant increase in lag phase. However, kynurenine seems to have no role in IFN- γ induced A549 lag phase increment since epacadostat which significantly reduced the increase in A549 kynurenine production could not reduce IFN- induced A549 lag time increment. IFN- γ can impair the release of inflammatory and pro-aggregatory cytokines from A549 like IL-8[419]. IL-8 was demonstrated to cause WP activation [420, 421] and therefore, A549 induced by IFN become less potent inducing platelet aggregation and having longer lag phase. IFN- γ induced A549 elongation could be due the presence of less active A549 cells that was used to induce TCIPA in IFN- γ treated A549 because IFN- γ found to inhibit A549 cell growth and to induce cell apoptosis due to depletion of tryptophan from the culture media and the enhancement of caspase-8 expression through IFN-response element[412, 422, 423].

It was reported that IFN- γ or IFN- γ plus lipopolysaccharide potently induces IDO activity but not nitric oxide synthase activity [424]while in murine macrophages IFN- γ or I IFN- γ plus lipopolysaccharide potently induces nitric oxide synthase but not IDO activity [425]. However, IFN- γ found to increase the expression of type II NOS and induced NO production in A549 cells [426-428]. NO is a potent inhibitor of platelet aggregation and concentration of NO produced by colorectal cell lines found to determine their potency toward TCIPA [251]. N-nitro-L-arginine methyl ester (L-NAME) is reversible non-selective inhibitor of NOS enzyme that was used in previous studies to inhibit all forms of NOS [429, 430].

4.8.5.2. Effect of L-NAME on A549 TCIPA

L-NAME at 100 μ M has been previously used to inhibit NO production by both, tumour cells and platelets, during TCIPA studies [240, 251]. Therefore, L-NAME was used in the next set of experiments to investigate the potential involvement of NO in the effect observed during the previous experimental procedure. However, L-NAME did not exert a significant effect on the lag phase duration during TCIPA induced by IFN- γ treated A549 cells (1000 cells) and had no effect on maximal platelet aggregation induced by the cells as shown in figures 4-124 and 4-125. Previous studies have reported a significant effect of L-NAME modulating of NO production induced by IFN- γ in A549 cells [428]. Park et al. have previously shown that the presence of L-NAME in a cytokine stimulated cell line could paradoxically increase the expression and activity of inducible NOS (iNOS) and NO production [431]. However, the level of basal and induced NO produced by A549 were not measured in our experiments to confirm the induction of NOS and therefore it is not known if IFN- γ induced NOS activity and if L-NAME inhibited its production. In addition, it could be that under our experimental conditions there are active concentrations of NO that could not be controlled by L-NAME only and required the presence of NO scavengers like haemoglobin which could inhibit the effect of the released NO on TCIPA induced by A549.

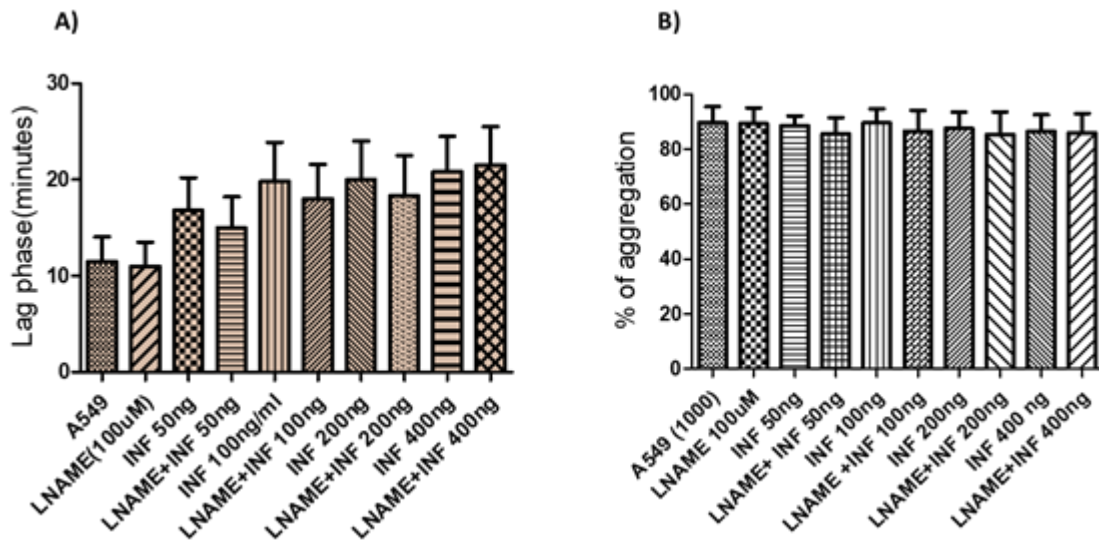


Figure 4-124: Effect of L-NAME on TCIPA induced by IFN- γ incubated A549 cells. (A) Statistical analyses showing no significant effect of L-NAME on the increment in lag phase induced by of IFN- γ treated A549 cells during TCIPA. (B) Statistical analysis exhibiting the effect of L-NAME on maximal platelet aggregation induced by IFN- γ treated A549cells. Data is represented as mean \pm SD; n=4; One-way ANOVA ($P > 0.05$)

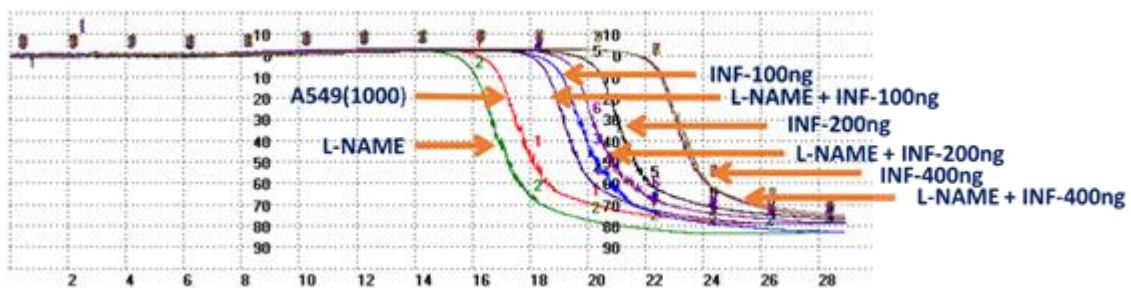


Figure 4-125: Representative traces from light transmission aggregometer showing that L-NAME could not modify neither the increment in lag phase nor maximal platelet aggregation induced by IFN- γ treated A549 cells.

There is no doubt that the use of IFN- γ to study TCIPA is challenging due to the lack of selectivity inducing IDO activity and the fact that the cytokine can interfere with several pathways that might affect tumour cells-platelets interactions. Therefore, further experiments involving HCC-1954 were not pursued.

Investigating the different ability of cancer cells to induce TCIPA, a new approach was used by resuspension of platelets in conditioned media from A549 and HCC-1954 cells and TCIPA was induced by A549 and HCC-1954 in LTA.

4.8.6. Effect of conditioned media on TCIPA

To investigate the effect of mediators released by HCC-1954 and A549 tumour cells on TCIPA, platelets were resuspended in serum free fresh and conditioned media from both cell lines and their function investigated by LTA.

HCC-1954 and A549 cells were first seeded in T-75 flask (1×10^6) and supplemented with complete media. Once cells reached about 50-60% of confluency, media was changed by fresh media containing 0% (free media), 2% (depleted media) or 10% (complete media) of FBS and incubated for further 48 hours. After 48 hours of incubation, conditioned media (free media and depleted media) were collected, filtered with 0.2 μm pore filters and used immediately to prepare WP (250,000 platelets/ μL). A549 and HCC-1954 cells grown in complete media were prepared as previously described (section 2.2) to induce TCIPA and their effects on platelets monitored by LTA.

4.8.6.1. Effect of HCC-1954 cells conditioned media

When platelets from three different blood donors were re-suspended in HCC-1954 serum free and depleted conditioned media, platelets spontaneously aggregated on resuspension. Although both, free and depleted conditioned media, induced platelet aggregation, the potential effect of FBS on platelet was evaluated by resuspending platelets in Tyrode's salt solution containing 1%, 0.5%, 0.25% and 0.125% FBS. FBS resulted in platelet aggregation at various stages of platelet preparation in intervals of time related to the percentage of FBS added to the Tyrode's salt solution.

It was concluded that HCC-1954 cells are able to produce pro-aggregatory mediator that resulted in platelet aggregation as even free conditioned media (0% FBS) collected after 48 hours of incubation with HCC-1954 cells primarily induced platelet aggregation on resuspension.

4.8.6.2. Effect of A549 cells conditioned media

4.8.6.3. Effect of A549 cells conditioned media on TCIPA induced by HCC-1954 cells

Interestingly, resuspension of platelets in depleted conditioned media from A549 cells (incubated with 2% FBS) resulted in inhibition of TCIPA induced by HCC-1954 as shown by the significant increase in the lag phase in figure 4-126B and figure 4-127. Nevertheless, free and depleted conditioned media had no effect on HCC-1954 induced maximal platelet aggregation as shown in figure 4-126A and figure 4-127. This inhibitory effect was also confirmed on platelet expression of GPIIb/IIIa activated and P-selectin induced by HCC-1954 as measured by flow cytometry (figure 4-128 and figure 4-129). In the presence of A549 depleted conditioned media platelet integrin (GPIIb/IIIa) expression was significantly lower when compared to platelet integrin expression induced by HCC-1954 in fresh media (figure 4-128A). P-selectin expression was also significantly lower in platelets re-suspended in A549 conditioned media than platelets re-suspended in fresh media when they were activated by HCC-1954 cells as shown in figure 4-128B.

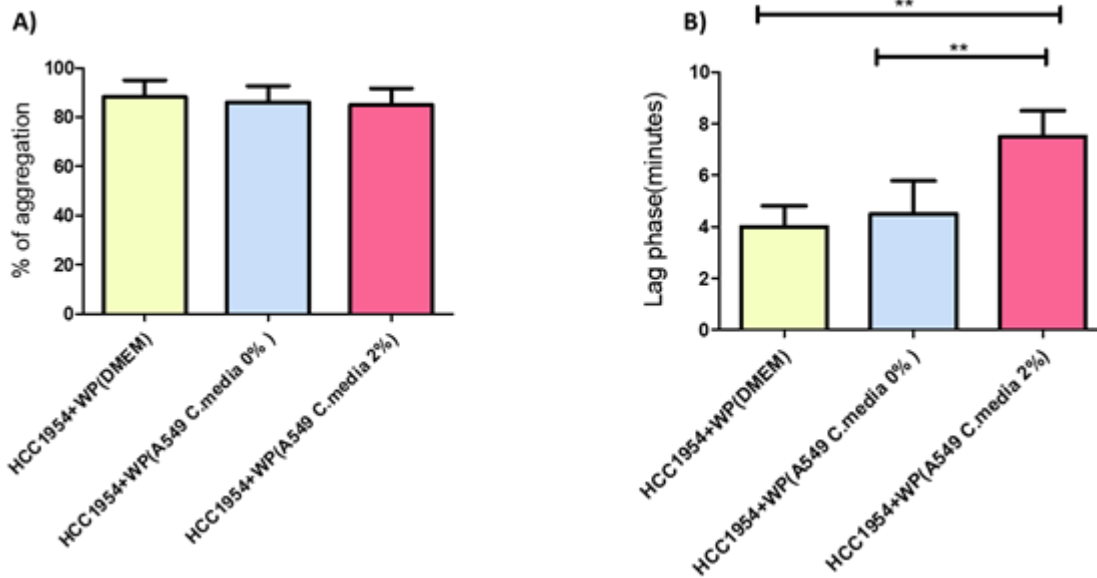


Figure 4-126: Effect of conditioned media from A549 on TCIPA induced by HCC-1954. Statistical analyses showing the effect of free (0% FBS) and depleted (2% FBS) A549 conditioned media (C.media) on HCC-1954 induced platelet aggregation (A) and lag phase (B). Data is represented as mean ± SD; n=4; One-way ANOVA & Tukey's post-test. ** P < 0.01

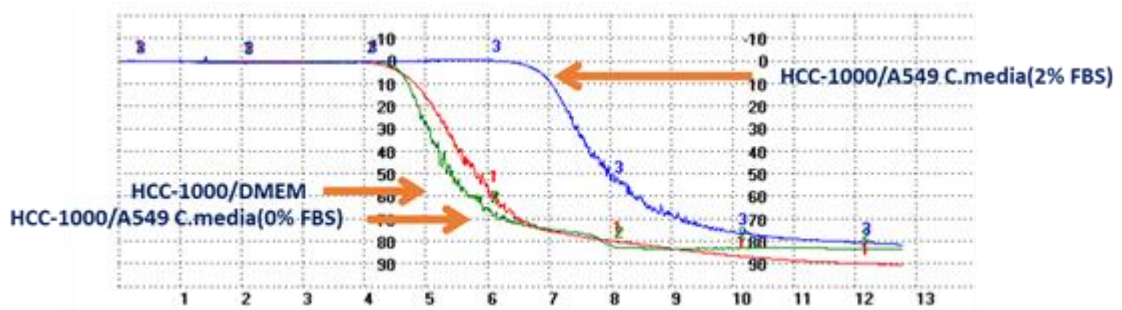


Figure 4-127: Representative traces from light transmission aggregometer showing the noticeable increase in the lag phase when platelet aggregation was induced by 1000 HCC-1954 cells on re-suspended in A549 depleted conditioned media [C.media 2% FBS] compared to platelet re-suspended in A549 free conditioned media [0% FBS] or fresh DMEM F12 media. No differences were observed on platelet maximal aggregation.

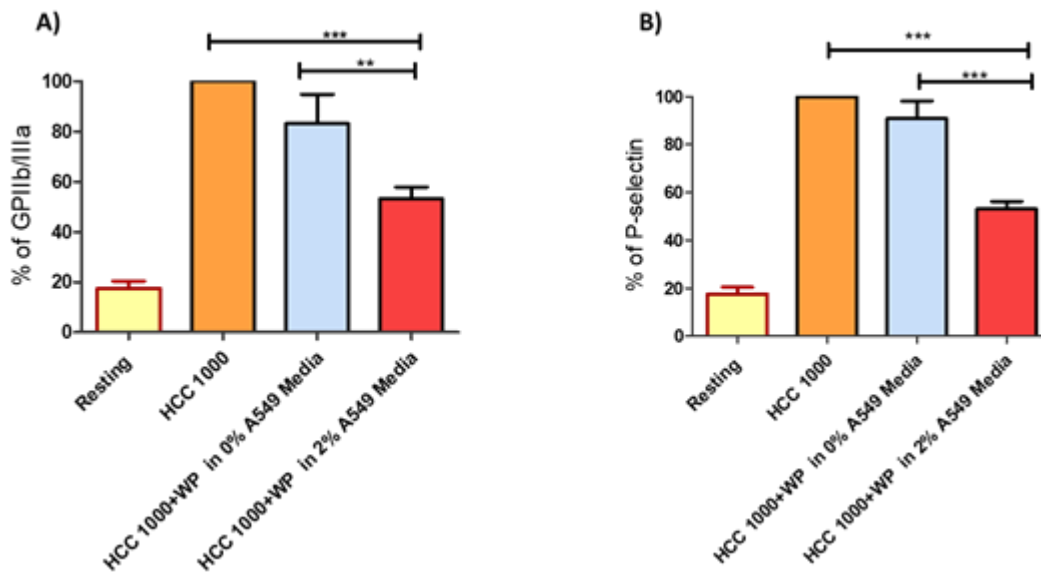


Figure 4-128: Effect of conditioned media from A549 on HCC-1954 induced platelet expression of GPIIb/IIIa and P-selectin. Statistical analyses of GPIIb/IIIa(A) and P-selectin(B) expression when TCIPA was induced by HCC-1954 (1000 cells) on platelets re-suspended in DMEM F12 fresh media (HCC-1000) and in A549 FBS free conditioned media (0% FBS) and A549 depleted conditioned media (2% FBS) [WP in 0% and 2% A549 media]. Data is represented as mean \pm SD; n=4; One-way ANOVA & Tukey's post-test. ** P < 0.01; *** P < 0.001.

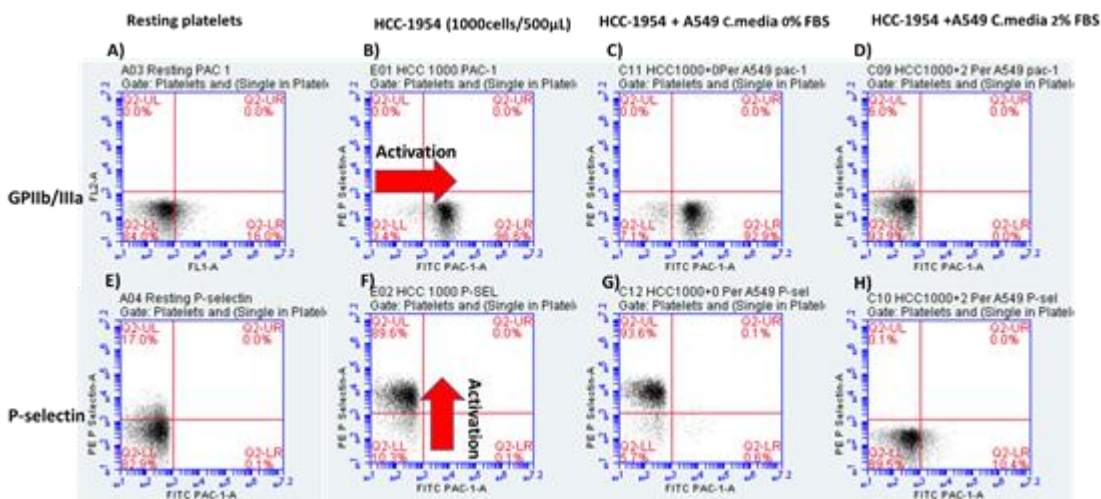


Figure 4-129: Representative gates from flow cytometry analysis for GPIIb/IIIa and P Selectin expression. Resting platelets (A), platelets activated with HCC-1954 cells re-suspended in fresh media (B), A549 FBS free conditioned media (0% FBS) (C) and A549 depleted conditioned media (2% FBS) (D). Activation of GPIIb/IIIa is represented by a rightward shifting of the platelet population from the lower left quarter (LL) to the lower right quarter (LR). Activation of P-selectin is represented by an upward shifting of the platelet population from lower left quarter (LL) to the upper left quarter (UL).

When 1000 A549 cells were used to induce platelet aggregation in platelets re-suspended under the same conditions a dramatic inhibition of TCIPA induced by A549 was observed. It can be demonstrated in figures 4-130 and 4-131 that when A549 cells were added to the suspension of platelets prepared in depleted conditioned media (2% FBS) platelets starting aggregating after 35 minutes for all the donors tested. Likewise, the percentage of maximal platelet aggregation was significantly reduced. Platelet expression of activated GPIIb/IIIa and P-selectin significantly downregulated in both FBS free conditioned media (0% FBS) and depleted media (2% FBS) when compared to platelets re-suspended in fresh media as shown in figure 4-132 and the represented flow cytometry gates in figure 4-133.

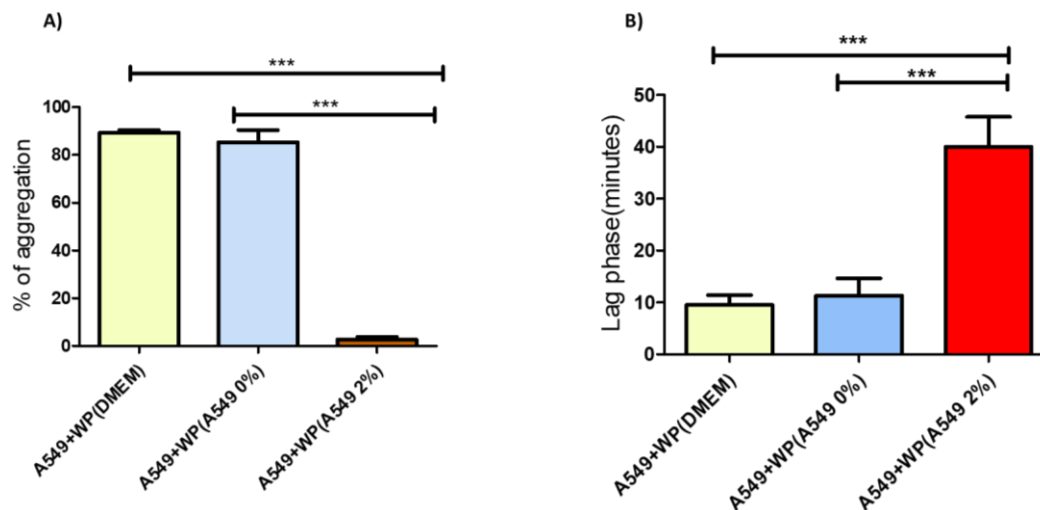


Figure 4-130: Effect of conditioned media from A549 on TCIPA induced by A549. Statistical analyses showing the significant inhibitory effect of A549 depleted conditioned media (C.media) primarily supplemented with 2% FBS (WP A549 2%) on A549 (1000 cells/500 μ L) induced maximal platelet aggregation (A) and lag phase (B) when compared to platelet re-suspended in DMEM/F12 fresh media and A549 free conditioned media (primarily free of FBS). Data is represented as mean \pm SD; n=4; One-way ANOVA & Tukey's post-test *** P < 0.001.

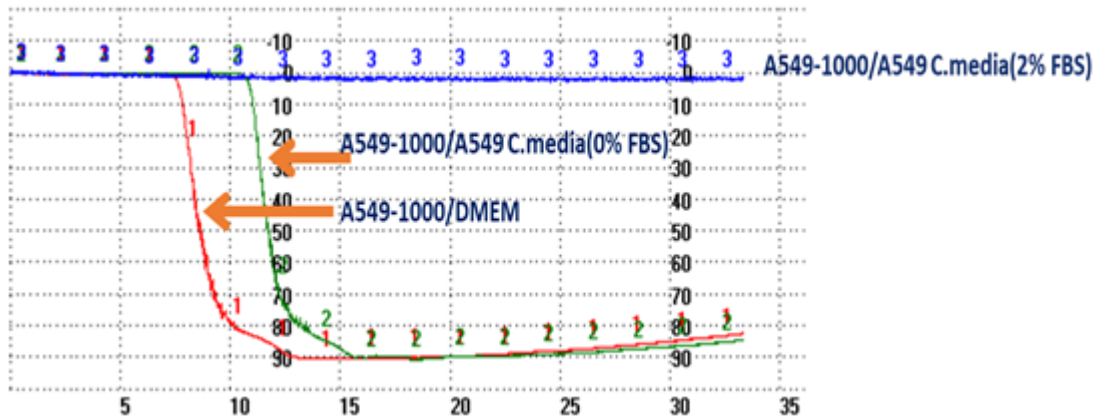


Figure 4-131: Representative traces from light transmission aggregometer showing that platelets re-suspended in free conditioned media from A549 [A549 C.media (0% FBS)] increased the lag phase but had no effect on maximal platelet aggregation. A549 failed to induce platelet aggregation when platelets were re-suspended in depleted conditioned media from A549 cells [A549 C.media 2% FBS].

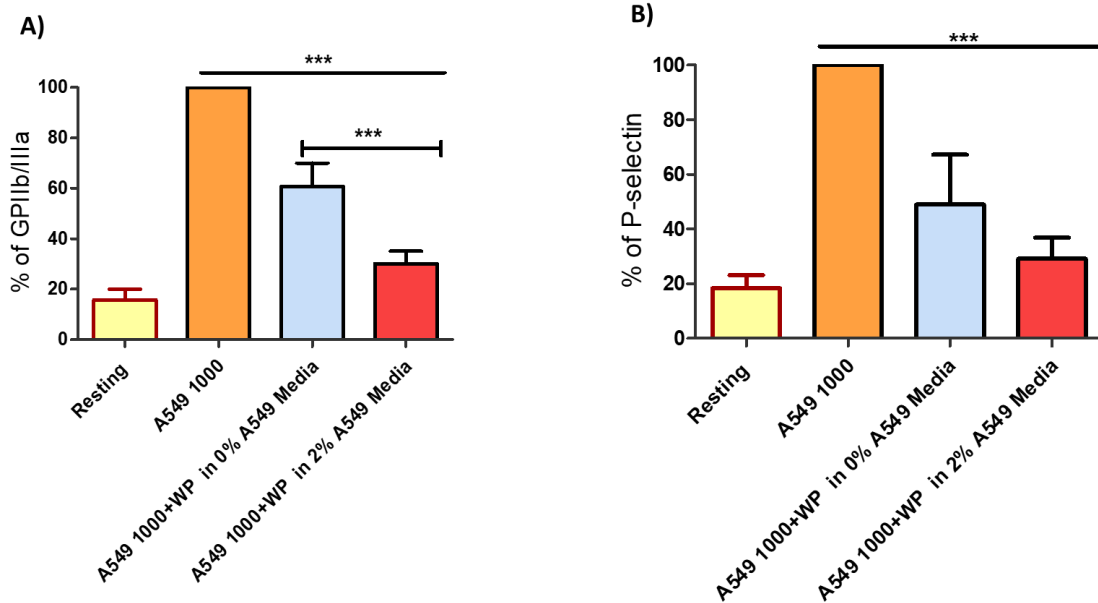


Figure 4-132: Effect of conditioned media from A549 on A549 induced platelet expression of GPIIb/IIIa and P-selectin. Statistical analysis showing the significant downregulation of the platelet surface expression of GPIIb/IIIa (A) and P-selectin (B) induced by A549 (1000) when platelets were re-suspended in free conditioned media from A549 and depleted conditioned media (WP in 0% and 2% A549 media) compared to platelets re-suspended in DMEM F12 fresh media. Data is represented as mean \pm SD; n=3; One-way ANOVA & Tukey's post-test. *** P < 0.001.

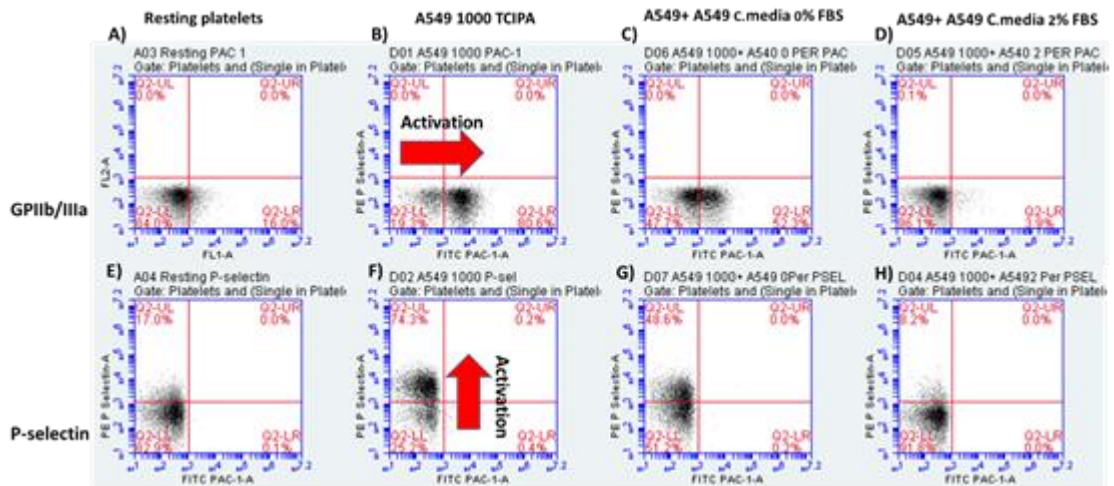


Figure 4-133: Representative gates from flow cytometry showing GPIIb/IIIa and P Selectin expression on resting platelets (A) and platelets activated with A549 cells re-suspended on fresh media (B); free conditioned media (0% FBS) (C) and depleted conditioned media (2% FBS) (D). Activation of GPIIb/IIIa is represented by a rightward shifting of the platelet population from lower left quarter (LL) to the lower right quarter (LR). Activation of platelet P-selectin expression is represented by an upward shifting of the platelet population from the lower left quarter (LL) to the upper left quarter (UL).

Platelets re-suspended on depleted conditioned media from A549 did not aggregate when 1000 A549 were used to induced platelet aggregation. Taking these results together, it can be concluded that although both cancer cell lines, HCC-1954 and A549 are able to produce pro-aggregatory mediator(s) during TCIPA as reported for other cell lines [207, 230, 231], A549 cells may be also able to generate inhibitory mediator(s) that are released to the media over time and may therefore have longer lag phase.

4.8.6.4. Effect of A549 conditioned media on collagen induced platelet aggregation

Next, free (0% FBS) and depleted (2% FBS) conditioned media from A549 was used to re-suspend platelets and their ability to aggregate in the presence of collagen tested by LTA. Once again, collagen 4 μ g/mL induced platelet aggregation when platelets were re-suspended in fresh media, but not in free and depleted conditioned media as shown in figure 4-134 and figure 4-135. These results were further corroborated by optical microscopy, as demonstrated in the micrographs in figure 4-136 where the aggregates induced by collagen are much

smaller when platelets were re-suspended in free conditioned media and completely vanished in the micrographs of platelets re-suspended in conditioned media from A549 (containing 2% FBS).

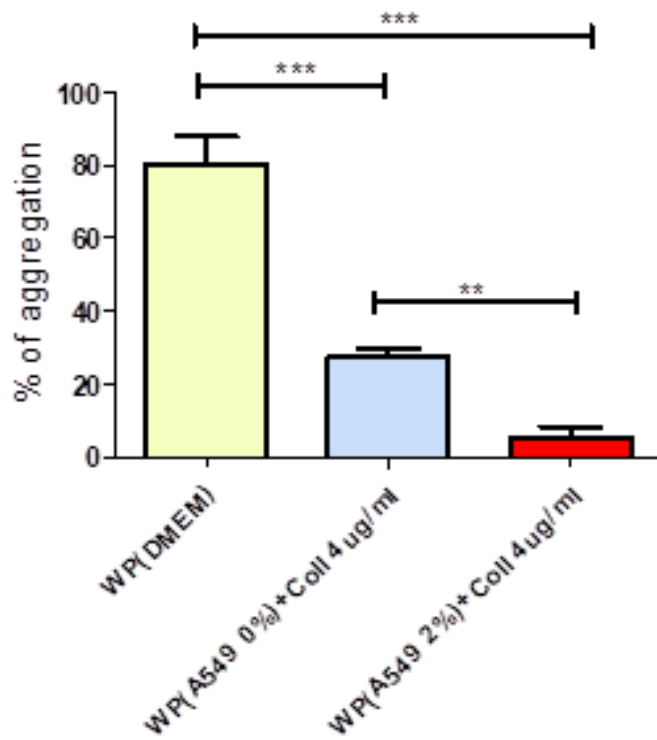


Figure 4-134: Effect of conditioned media from A549 cells on collagen-induced platelet aggregation. Statistical analysis exhibiting significant inhibition of collagen (4 $\mu\text{g}/\text{mL}$) induced platelet aggregation in the presence of A549 conditioned media primarily supplemented with 0% and 2% FBS (WP A549 0% and WP A549 2%). Data is represented as mean \pm SD; n=4; One-way ANOVA & Tukey's post-test. ** P < 0.01; *** P < 0.001.

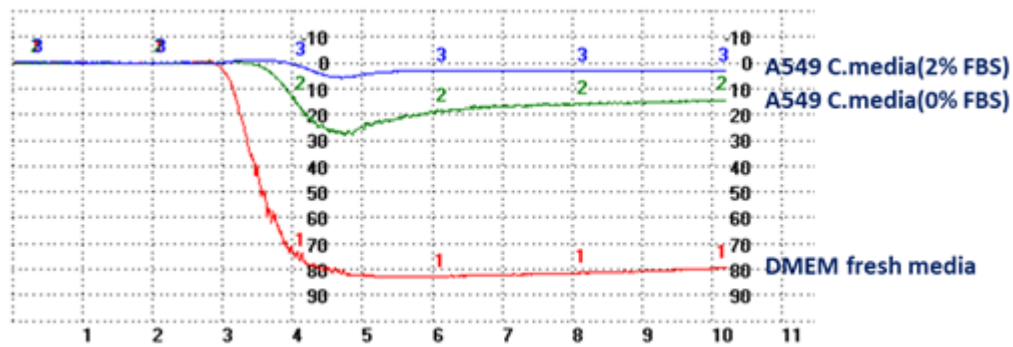


Figure 4-135: Representative traces from the light transmission aggregometer showing platelet aggregation induced by collagen 4µg/mL on platelets re-suspended in fresh media and conditioned media from A549.

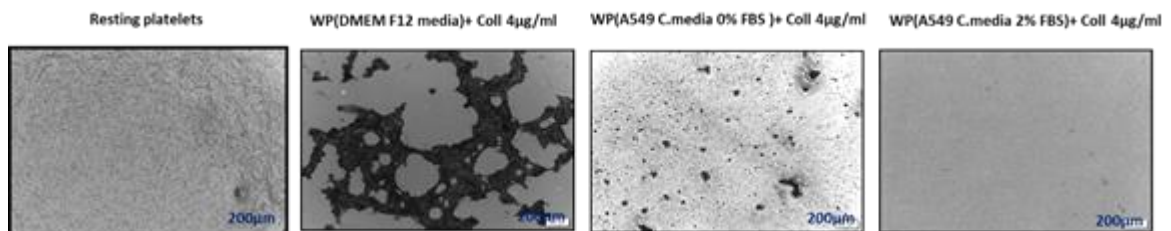


Figure 4-136: Optical microscopy: representative micrographs (5X objective) showing resting platelets and the effect of collagen on platelet aggregation: big aggregates are formed when platelets were re-suspended in fresh media; a significant decrease in the number and size of platelet aggregates (black areas) can be observed when platelets were prepared using free conditioned media from A549 cells (0% FBS) and absence of platelet aggregates when platelets were prepared using depleted conditioned media from A549 cells (2% FBS).

Finally, and to confirm the inhibitory effect of the conditioned media from A549 on collagen induced platelet aggregation, platelet expression of GPIIb/IIIa and P-selectin, in the presence collagen 4 µg/mL, was studied using flow cytometry. Although figures 4-137 and 4-138 are showing a significant downregulation of the expression of both platelet receptors (GPIIb/IIIa and P-selectin) on platelets re-suspended in depleted conditioned media from A549 (2% FBS), only GPIIb/IIIa activated was found to be significantly downregulated when platelets were re-suspended in free conditioned media from A549 (0% FBS) and stimulated with collagen.

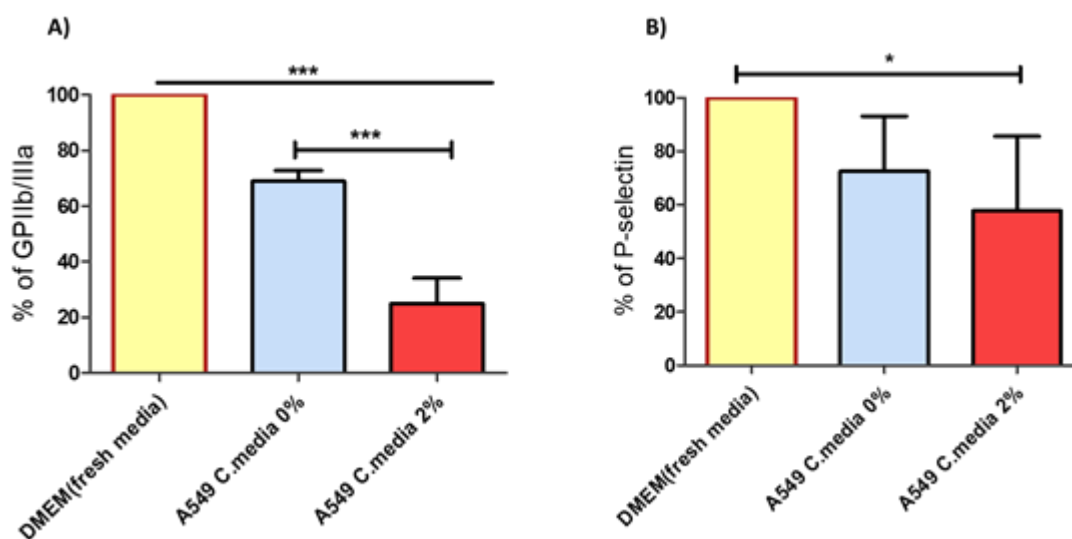


Figure 4-137: Effect of collagen on platelet expression of GPIIb/IIIa and P-selectin. (A) Statistical analysis showing the significant downregulation of platelet surface expression of integrin (GPIIb/IIIa) induced by collagen 4 μ g/mL on platelets re-suspended in conditioned media from A549 primarily supplemented with 0% and 2% FBS (A549 C. media 0% and 2%) when compared to platelets re-suspended in DMEM F12 fresh media (DMEM fresh media). (B) Statistical analysis showing downregulation of P-selectin translocation to platelet surface induced by collagen 4 μ g/ml in the presence of A549 conditioned media 2% FBS (A549 C. media 2%). Data is represented as mean \pm SD; n=3; One-way ANOVA & Tukey's post-test. * P < 0.05; *** P < 0.001.

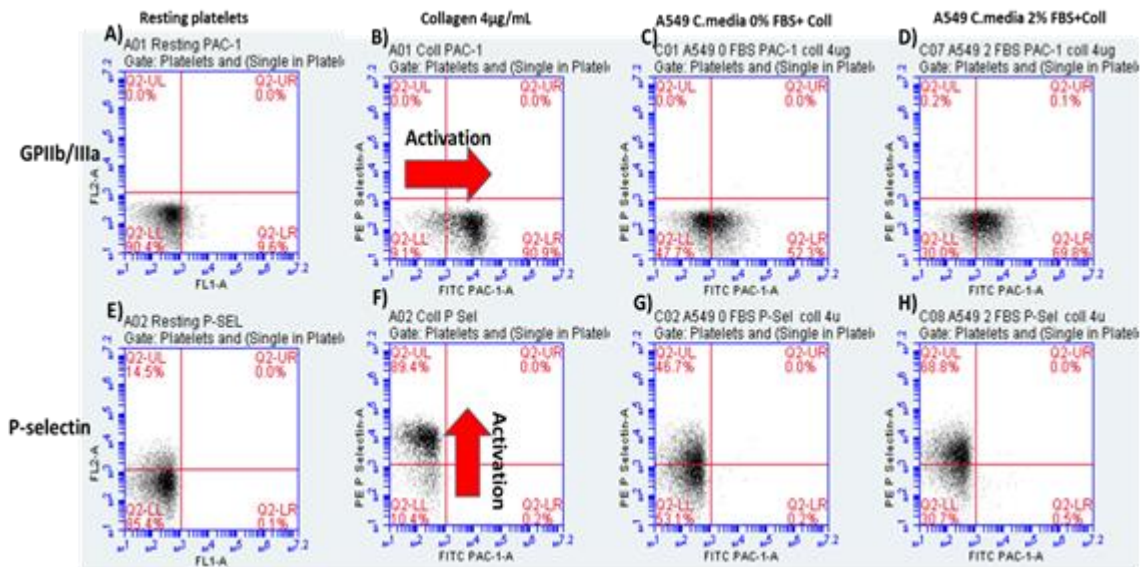


Figure 4-138: Representative flow cytometry gates showing GPIIb/IIIa and P Selectin expression on resting platelets (A) and platelets activated with collagen re-suspended on fresh media (B); free conditioned media (0% FBS) (C) and depleted conditioned media (2% FBS) (D). Activation of GPIIb/IIIa is represented by rightward shifting of the platelet population from lower left quarter (LL) to the lower right quarter (LR). Activation of P-selectin expression is represented by an upward shifting of the platelet population from the lower left quarter (LL) to the upper left quarter (UL)

It is known that cells metabolic activity can reduce the pH of the media and low pH can in turn affect platelet function and aggregation by reducing intraplatelet Ca^{+2} concentration which is essential for Ca^{+2} dependent enzymes and platelet shape change in response to platelet agonists during platelet aggregation [432, 433]. Therefore, it seemed reasonable the need of excluding the possibility that the pH of the conditioned media could be responsible for the platelet's response to collagen and cancer cells.

4.8.7. Effect of media pH on platelet aggregation

The effect of various pH on platelet aggregation was studied by LTA. First, cells were seeded and grown in complete media. Once cells reached around 70% of confluency, media was changed by free serum media and incubated with the cells for 72 hours. Conditioned media was collected from the flask and the pH measured after 24; 48 and 72 hours to examine the change in pH overtime. To exclude the possibility of low pH effect on platelet's reactivity, Tyrode's solution

was adjusted to the same values obtained from the media, used to re-suspended platelets and platelets response to collagen (4 $\mu\text{g}/\text{mL}$) investigated by LTA.

Platelets prepared in Tyrode's salt solution at the same ranges of pH observed in media over 72 hr (from pH 6.9 to pH 7.3), responded in similar way to collagen as platelets re-suspended in Tyrode's solution at physiological pH (pH 7.4) as shown in figure 4-139.

Previous studies have shown that pH as low as 6.8 affect the rate of platelet shape change by 10%; although it seems that ADP-induced platelet shape change and actin-myosin association with the cytoskeleton was mainly affected by cytosolic pH and not dependent on the external pH [432]. However, external pH can affect platelet aggregation due to the effect on Store-Operated Ca^{2+} entry [433].

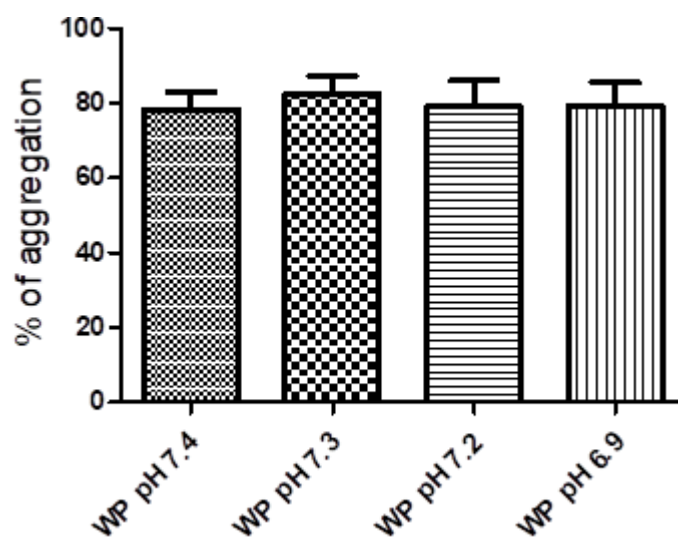


Figure 4-139: Effect of pH on collagen-induced platelet aggregation. Statistical analysis showing no significant effect of pH on platelet aggregation. Data is represented as mean \pm SD; n=4; One-way ANOVA ($P > 0.05$)

Based on these results, it can be excluded that the potential changes in the pH of the media overtime was responsible for the inhibitory effect observed when the conditioned media from A549 cells was used for preparing platelets suspensions. It could be then, that A549 cells generate and release 'mediators' that have the ability to inhibit platelet aggregation and to modify the platelet's response to HCC-1954 and A549 cells. The presence of this 'mediator' or its differential production by different cell lines may justify to some extent and in some cases the differences among cell lines to induce TCIPA. However, other possibilities are needed to be considered and to be excluded such as the measurement of Ca^{+2} concentration in media prior to getting the conclusion of A549 media having an inhibitory effect. There is no doubt that the effect of conditioned media on TCIPA and platelet aggregation is a very interesting finding and deserves more attention and effort to be further investigated. In fact, this novel approach has the potential to provide a better insight for looking at the effect of cell lines derived mediators that could inhibit or induce platelet aggregation within the tumour microenvironment.

5. Conclusions and future directions

This research focused on the effect of kynurenine on platelet function and tumour cell induced platelet aggregation and the potential mechanism by which kynurenine exerts its effects. First, it was found that kynurenine was able to inhibit platelet aggregation induced by a wide range of platelet agonists (collagen, ADP, TXA2 and arachidonic acid) at the concentrations tested *ex vivo*. Despite the different potencies and signalling pathways associated with those platelet agonists, kynurenine was able to prevent their effect in a concentration dependent manner.

Kynurenine is an AhR receptor agonist. Although platelets express the AhR receptor, the inhibitory effect of kynurenine on platelet function was not found to be mediated through the AhR receptor. In fact, the AhR receptor agonists tested during the course of this project did not exert a similar effect to kynurenine and AhR receptor antagonists could not attenuate the inhibitory effect of kynurenine on platelet function.

The large neutral amino acid transporter (LAT) can participate in kynurenine uptake by human platelets. However, the effect of high concentrations of kynurenine (1mM) was not modified when washed platelets were prepared in the presence of the LAT inhibitor BCH, suggesting that more than one mechanism may participate in kynurenine uptake by platelets. It is worth noting that the intraplatelet concentration of kynurenine was not measured after incubation with BCH to confirm the inhibition of kynurenine uptake. Attenuation of the inhibitory effect of kynurenine at lower concentrations on platelet aggregation induced by collagen was confirmed by light transmission aggregometry and used as indirect indicator of kynurenine uptake inhibition. However, it is not known if the interaction between kynurenine and BCH might play a role in this effect. More experiments are needed to unravel the mechanism by which kynurenine uptake by platelet takes place using a wider range of transporter inhibitors, fluorescent tagging of kynurenine and HPLC or LC-MS to measure the effective transported concentration of kynurenine.

The possibility that kynurenine can act through an interaction with the platelet surface cannot be excluded as 'platelet washing' abolished the inhibitory effect of kynurenine on platelet function. In addition, adenylyl cyclase (AC), which is

activated by kynurenine, is membrane bound and not a cytosolic enzyme. Kynurenine exerts its inhibitory effect on platelet acting on platelet's adenylyl cyclase and on the oxidised and the reduced forms of soluble guanylyl cyclase, causing a significant elevation in cAMP and cGMP; respectively. In addition to the central role of cAMP and cGMP in platelets and via cGMP and cAMP dependent mechanisms, kynurenine phosphorylates VASP which plays a key role in actin polymerization, platelet shape change and GPIIb/IIIa expression during platelet activation/aggregation.

Kynurenine acts mainly through the AC-cAMP pathway, although sGC-cGMP also plays an important role. Despite the use of ODQ to inhibit the sGC enzyme, kynurenine resulted in an increase in cGMP and VASP phosphorylation at serine 238. It was therefore not feasible to evaluate the role of sGC-cGMP pathway activation in the presence of kynurenine. Inhibition of PKG did not result in attenuation of the inhibitory effect of kynurenine on collagen- induced platelet aggregation. Although the inhibition of AC enzyme which is responsible for cAMP synthesis did not affect the inhibitory effect of kynurenine, the incubation of platelets with Rp-cAMP (PKA inhibitor) attenuated this effect. It is worth to mention that the inhibition of PDEIII by cGMP is independent of PKG and that it can lead to elevation of cAMP concentration and PKA activation. Therefore, it can be concluded that the inhibitory effect of kynurenine on platelet function requires activation of both sGC and AC enzymes that converge on cAMP and PKA activation. This conclusion was further supported by the observation that a group of selected compounds that activates sGC were not able to inhibit collagen induced platelet aggregation in a similar manner to kynurenine.

To exclude the possibility that the observed effect on platelets by kynurenine could be due to its metabolites, the effect of kynurenine metabolites on sGC activation and collagen induced platelet aggregation was also investigated. Kynurenine metabolites that activated sGC were not able to modulate collagen induced platelet aggregation indicating that the effect observed in platelets is likely due to kynurenine.

The results showed in the first part of this investigation demonstrate that Kynurenine represents a novel compound that can regulate platelet function in an independent way of NO and prostacyclin, the two major physiological platelet

inhibitors, and provides a molecule that may lead to the design of a safe, stable and effective analogue for preclinical studies.

This discovery, together with the well-known involvement of kynurenine in cancer biology, led to the second part of this project where the potential effect of kynurenine on TCIPA was investigated. TCIPA provides advantages to cancer cells for survival during cancer development and promotes the development of haematogenous metastasis. In fact, inhibition of TCIPA may reduce cancer cell survival, metastasis and ultimately cancer related deaths in patients suffering from this disease. A549 lung cancer, HeLa cervical cancer, HT-29 colon cancer, SW-480 colon cancer and HCC-1954 breast cancer cells show variable potencies to induce platelet aggregation. Based on the duration of their lag phase, A549 was the least aggressive and HCC-1954 the most aggressive cancer cell lines tested as they induced the longest and the shortest lag phase during TCIPA; respectively. Kynurenine, at the concentrations tested *ex vivo*, had the ability to inhibit A549, HeLa, HT-29, SW-480 and HCC-1954 TCIPA and to downregulate GPIIb/IIIa activation and translocation of P-selectin during this interaction. It is noteworthy that P-selectin also participates in pro-carcinogenic and cancer-related immunological mechanisms that contribute to tumour growth and metastasis.

When studying the possible involvement of kynurenine during TCIPA it was observed that the basal production of kynurenine by the tumour cells included in this project was inversely correlated with their ability to induce platelet aggregation. However, the concentrations of kynurenine generated by those cell lines were significantly lower than the concentrations required to modulate TCIPA *in vitro*.

IFN- γ was used to promote the generation of kynurenine by cancer cells to give a better insight to the role of kynurenine in cancer cell-platelet interactions. Induction of kynurenine production by A549 elongated the lag phase but the inhibition of kynurenine generation had no effect on the lag phase induced by IFN- γ . The induced kynurenine production from A549 following incubation with IFN- γ were at least 50 times less than the concentrations required to inhibit TCIPA *in vitro*. The non-selective induction of IDO by IFN- γ and the potential effect that IFN- γ can have on cell behaviour during TCIPA are factors that, among

others, limit the interpretation of the results obtained during these experimental procedures.

A novel approach was also used to study the effect of mediators released into conditioned media from cultured cancer cells on platelet function. Platelets re-suspended in conditioned media from HCC-1954 aggregated spontaneously. However, platelets re-suspended in conditioned media from A549 did not aggregate in the presence of A549-, HCC-1954 and collagen. It can be concluded that A549 cells secrete inhibitory mediator(s) that can modulate the platelet response to A549 while HCC-1954 generates pro-aggregatory agent(s) making HCC-1954 more aggressive at inducing platelet aggregation.

Nevertheless, fresh media incubated with cancer cells for a period of time can lead to changes on both, the composition and the characteristics of the media that could influence platelet response to various agonists. Although changes in pH were excluded, other factors such as Ca^{+2} concentration need to be further investigated.

Future studies investigating and comparing the composition of conditioned media from different cancer cell lines with variable potencies to induce platelet aggregation are warranted. In this regard, for instance, it has been found that breast-cancer cells produce extracellular vesicles that can induce platelet activation and aggregation by tissue factor-independent and -dependent mechanisms. Extracellular vehicles (EVs) can be isolated from conditioned media from cancer cell lines and their effect on TCIPA tested as one of the potential factors that determines the ability of cancer cells to influence platelet aggregation. Proteins produced by the cancer cell lines and released into conditioned media can be also identified as an initial step in studying why different cancer cells behave in different ways when they interact with platelets and why some of them have a greater potential to metastasis than others.

Appendix 1- Reagents

Reagent	Company	Catalogue number
1. Acetylsalicylic acid	Sigma	A5376
2. Acrylamide 30%	Sigma	A3574
3. ADP	Sigma	A5285
4. AhR Ab	Santacruz	Sc-5579
5. Anti-Mouse secondary Ab	Sigma	A0168
6. Anti-Rabbit secondary Ab	Sigma	A0545
7. Aracidonic acid and	Bio Data Corporation	101297
8. B-actin	Sigma	A1978
9. BCH	Sigma	A7902
10. Bovine serum albumin	Sigma	A8022
11. Bradford reagent	Biorad	5000006
12. cAMP ELISA kit	ELISAGenie	UNFI0047
13. cAMPS-Rp	TOCRIS	1337
14. CD62P Ab	BD pharmingen	555524
15. Cell lysis buffer	Invitrogen	FNN0011
16. cGMP ELISA kit	ELISAGenie	GEBY001
17. Collagen	Chronolog	P/N 385
18. Developer	Thermoscientific	34095
19. DMSO	Sigma	D8414
20. Extraction buffer	Life technologies	FNN0011
21. Epacadostat (INCB-024360)	Biosciences	ABE8768
22. FICZ	Tocris	5304
23. Forskolin	CAYMAN	11018
24. Glycin	BIO-RAD	161-0724
25. IDO anti body	Abcam	Ab55305
26. Kynuramine	Santa Cruz Biotechnology	Sc-207782
27. Kynurenic acid	Sigma	K3375-1G

28. Ladder	Bio-rad	1610374
29. L-Arginine	Sigma	A5006
30. L-Kynurenine	Sigma	K8625
31. LNAME	Sigma	N5751
32. Melatonin	Fluorochem Limited	M02088-5G
33. NADPH	Acros	328742500
34. ODQ	Sigma	O3636
35. PAC-1 Ab	BD pharmingen	340507
36. Paraformaldehyde 37%	Sigma	F1635
37. Phosphate buffer saline	Fisher chemical	1282-1680
38. Picolinic acid	Fluorochem Limited	321691-5G
39. Prostacyclin	Sigma	P6188
40. protease inhibitor cocktail	Thermo scientific	87786
41. Quinaldic acid	Sigma	160660-2.5G
42. Quinolinic acid	Fisher Scientific Ltd	10793275
43. Rp-8-pCPT-cGMP	TOCRIS	5524
44. Running buffer (10XTris/Glycin/SDS) Buffer	BIO-RAD	161-0732
45. Serotonin hydrochloride	Fluorochem Limited	169300-25G
46. Serotonin	Sigma	14927-25MG
47. SNAP	Sigma	N3398
48. Sodium Dodecyl Sulphate SDS	Fisher chemical	BP166-500
49. SQ-22,536	Santacruz, USA	Sc-201572
50. TheCytoTox-ONE™	Promega	G7890
51. Thromboxane analogue U1333961	Tocris	1932
52. Tris Base	Fisher bioreagents	BP152-1
53. Triton X-100	Fisher Bioreagents	BP151-500
54. Tween-20	Sigma	T2700
55. Tyrod's buffer	Sigma	T2397
56. P. VASP 157 Ab	LSBIO	LS-C117505

57. P. VASP 238 Ab	LSBIO	LS-C178002
58. VASP antibody	Santacruz	SC-46668
59. Xanthurenic acid	Sigma	D120804-1G
60. IBMX	Sigma	I5879-100MG

Appendix-2 Electrophoresis gel preparation reagents

Stacking Buffer	Tris base	6.05 g
	Water	300 ml
	Adjust to pH 6.8	
	Add water up to	500 ml
	Filter 0.45 μ m	
	Add SDS	0.4 g
	Store 4 °C	
Resolving buffer	Tris base	91 g
	Water	300 ml
	Adjust to pH 8.8	
	Add water up to	500 ml
	Filter 0.45 μ m	
	Add SDS	2 g
	Store 4 °C	
Stacking gel for (4 gels)	Acrylamide 30%	1300 μ l
	Stacking buffer	2500 μ l
	Water	6000 μ l
	Ammonium persulfate 10 %	50 μ l
	Tetramethylethylenediamine(TEMED)	10 μ l
Separating gel 10% (4 gels)	Acrylamide 30%	5 ml
	Resolving buffer	3.75 ml
	Water	6.25 ml
	APS 10 % (m/m)	50 μ l
	TEMED	10 μ l
Laemmli loading buffer (4X)	Stacking buffer	4ml
	Beta-mercaptoethanol	2ml
	Glycerol	6ml
	SDS	1g

	Bromophenol blue	50mg
Tank buffer (10x)	Tris base	30.2 g
	Glycine	144 g
	SDS	10 g
	Water	1000 ml
	pH 8.3	
Towbing transfer buffer	Tris base	12.12 g
	Glycine	57.6 g
	SDS	2 g
	Methanol	800 ml
	Water	4000 ml
Washing buffer	TBS + Tween 0.05 % (V/V), pH 7.4	

6. References

1. White, J.G., Platelet membrane ultrastructure and its changes during platelet activation. *Prog Clin Biol Res*, 1988. 283: p. 1-32.
2. Yan, M. and P. Jurasz, The role of platelets in the tumor microenvironment: From solid tumors to leukemia. *Biochim Biophys Acta*, 2016. 1863(3): p. 392-400.
3. Michelson, A.D., How platelets work: platelet function and dysfunction. *J Thromb Thrombolysis*, 2003. 16(1-2): p. 7-12.
4. Ma, Y.Q., J. Qin, and E.F. Plow, Platelet integrin alpha(IIb)beta(3): activation mechanisms. *J Thromb Haemost*, 2007. 5(7): p. 1345-52.
5. Offermanns, S., Activation of platelet function through G protein-coupled receptors. *Circ Res*, 2006. 99(12): p. 1293-304.
6. Reed, G.L., M.L. Fitzgerald, and J. Polgar, Molecular mechanisms of platelet exocytosis: insights into the "secreted" life of thrombocytes. *Blood*, 2000. 96(10): p. 3334-42.
7. Harrison, P. and E.M. Cramer, Platelet alpha-granules. *Blood Rev*, 1993. 7(1): p. 52-62.
8. Turitto, V.T. and C.L. Hall, Mechanical factors affecting hemostasis and thrombosis. *Thromb Res*, 1998. 92(6 Suppl 2): p. S25-31.
9. Ruggeri, Z.M., Platelets in atherothrombosis. *Nat Med*, 2002. 8(11): p. 1227-34.
10. Jackson, S.P., W.S. Nesbitt, and S. Kulkarni, Signaling events underlying thrombus formation. *J Thromb Haemost*, 2003. 1(7): p. 1602-12.

11. Rivera, J., et al., Platelet receptors and signaling in the dynamics of thrombus formation. *Haematologica*, 2009. 94(5): p. 700-11.
12. Li, Z., et al., Signaling during platelet adhesion and activation. *Arterioscler Thromb Vasc Biol*, 2010. 30(12): p. 2341-9.
13. Chen, J. and J.A. Lopez, Interactions of platelets with subendothelium and endothelium. *Microcirculation*, 2005. 12(3): p. 235-46.
14. Clemetson, K.J. and J.M. Clemetson, Platelet collagen receptors. *Thromb Haemost*, 2001. 86(1): p. 189-97.
15. Mu, F.T., et al., Functional association of phosphoinositide-3-kinase with platelet glycoprotein Iba α , the major ligand-binding subunit of the glycoprotein Ib-IX-V complex. *J Thromb Haemost*, 2010. 8(2): p. 324-30.
16. Nieswandt, B. and S.P. Watson, Platelet-collagen interaction: is GPVI the central receptor? *Blood*, 2003. 102(2): p. 449-61.
17. Gilio, K., et al., Non-redundant roles of phosphoinositide 3-kinase isoforms α and β in glycoprotein VI-induced platelet signaling and thrombus formation. *J Biol Chem*, 2009. 284(49): p. 33750-62.
18. Li, Z., et al., A stimulatory role for cGMP-dependent protein kinase in platelet activation. *Cell*, 2003. 112(1): p. 77-86.
19. Riba, R., et al., Von Willebrand factor activates endothelial nitric oxide synthase in blood platelets by a glycoprotein Ib-dependent mechanism. *J Thromb Haemost*, 2006. 4(12): p. 2636-44.
20. Li, Z., X. Xi, and X. Du, A mitogen-activated protein kinase-dependent signaling pathway in the activation of platelet

- integrin alpha IIb beta3. *J Biol Chem*, 2001. 276(45): p. 42226-32.
21. Li, Z., et al., Sequential activation of p38 and ERK pathways by cGMP-dependent protein kinase leading to activation of the platelet integrin alpha IIb beta3. *Blood*, 2006. 107(3): p. 965-72.
 22. Gambaryan, S., et al., NO-synthase-/NO-independent regulation of human and murine platelet soluble guanylyl cyclase activity. *J Thromb Haemost*, 2008. 6(8): p. 1376-84.
 23. Angiolillo, D.J., D. Capodanno, and S. Goto, Platelet thrombin receptor antagonism and atherothrombosis. *Eur Heart J*, 2010. 31(1): p. 17-28.
 24. Heemskerk, J.W., E.M. Bevers, and T. Lindhout, Platelet activation and blood coagulation. *Thromb Haemost*, 2002. 88(2): p. 186-93.
 25. Kahn, M.L., et al., A dual thrombin receptor system for platelet activation. *Nature*, 1998. 394(6694): p. 690-4.
 26. Kahn, M.L., et al., Protease-activated receptors 1 and 4 mediate activation of human platelets by thrombin. *J Clin Invest*, 1999. 103(6): p. 879-87.
 27. Offermanns, S., et al., G proteins of the G12 family are activated via thromboxane A2 and thrombin receptors in human platelets. *Proceedings of the National Academy of Sciences of the United States of America*, 1994. 91(2): p. 504-508.
 28. Klages, B., et al., Activation of G12/G13 results in shape change and Rho/Rho-kinase-mediated myosin light chain phosphorylation in mouse platelets. *J Cell Biol*, 1999. 144(4): p. 745-54.
 29. Murugappa, S. and S.P. Kunapuli, The role of ADP receptors in platelet function. *Front Biosci*, 2006. 11: p. 1977-86.

30. Gachet, C., Regulation of platelet functions by P2 receptors. *Annu Rev Pharmacol Toxicol*, 2006. 46: p. 277-300.
31. P. Savi, P.B., C. Labouret, M. Delfaud, V. Salel, M. Kaghad, J.M. Herbert, Role of P2Y1 purinoceptor in ADP-induced platelet activation. *FEBS Letters*, 1998. 19793(422): p. 291-295.
32. Be´ atrice Hechler, C.L.o., Catherine Vial, Paul Vigne, Christian Frelin, and a.C.G. Jean-Pierre Cazenave, The P2Y1 Receptor Is Necessary for Adenosine 58-Diphosphate–Induced Platelet Aggregation. *Blood Rev*, (July 1), 1998. 92(1): p. 152-159.
33. Ohlmann, P., et al., The human platelet ADP receptor activates Gi2 proteins. *Biochemical Journal*, 1995. 312(Pt 3): p. 775-779.
34. Quinn, M.J. and D.J. Fitzgerald, Ticlopidine and clopidogrel. *Circulation*, 1999. 100(15): p. 1667-72.
35. Bhatt, D.L. and E.J. Topol, Scientific and therapeutic advances in antiplatelet therapy. *Nat Rev Drug Discov*, 2003. 2(1): p. 15-28.
36. Radomski, M.W. and S. Moncada, Regulation of vascular homeostasis by nitric oxide. *Thromb Haemost*, 1993. 70(1): p. 36-41.
37. Bennett, J.S., Structure and function of the platelet integrin alphaIIb beta3. *J Clin Invest*, 2005. 115(12): p. 3363-9.
38. Tadokoro, S., et al., Talin binding to integrin beta tails: a final common step in integrin activation. *Science*, 2003. 302(5642): p. 103-6.
39. Needleman, P., et al., Identification of an enzyme in platelet microsomes which generates thromboxane A2 from

- prostaglandin endoperoxides. *Nature*, 1976. 261(5561): p. 558-60.
40. Born, G.V.R., Effects of Adenosine Diphosphate (ADP) and Related Substances on the Adhesiveness of Platelets in vitro and in vivo*. *British Journal of Haematology*, 1966. 12(1): p. 37-38.
 41. Sawicki, G., et al., Release of gelatinase A during platelet activation mediates aggregation. *Nature*, 1997. 386(6625): p. 616-9.
 42. Larsen, E., et al., PADGEM protein: a receptor that mediates the interaction of activated platelets with neutrophils and monocytes. *Cell*, 1989. 59(2): p. 305-12.
 43. Moore, K.L., Structure and function of P-selectin glycoprotein ligand-1. *Leuk Lymphoma*, 1998. 29(1-2): p. 1-15.
 44. Gong, H., et al., G protein subunit Galpha13 binds to integrin alphallbbeta3 and mediates integrin "outside-in" signaling. *Science*, 2010. 327(5963): p. 340-3.
 45. Arias-Salgado, E.G., et al., Src kinase activation by direct interaction with the integrin beta cytoplasmic domain. *Proc Natl Acad Sci U S A*, 2003. 100(23): p. 13298-302.
 46. Reddy, K.B., D.M. Smith, and E.F. Plow, Analysis of Fyn function in hemostasis and alphallbbeta3-integrin signaling. *J Cell Sci*, 2008. 121(Pt 10): p. 1641-8.
 47. Obergfell, A., et al., Coordinate interactions of Csk, Src, and Syk kinases with [alpha]IIB[beta]3 initiate integrin signaling to the cytoskeleton. *J Cell Biol*, 2002. 157(2): p. 265-75.
 48. Shattil, S.J. and P.J. Newman, Integrins: dynamic scaffolds for adhesion and signaling in platelets. *Blood*, 2004. 104(6): p. 1606-15.

49. Dutta-Roy, A.K. and A.K. Sinha, Purification and properties of prostaglandin E1/prostacyclin receptor of human blood platelets. *J Biol Chem*, 1987. 262(26): p. 12685-91.
50. Miller, S.B., Prostaglandins in health and disease: an overview. *Semin Arthritis Rheum*, 2006. 36(1): p. 37-49.
51. Smolenski, A., Novel roles of cAMP/cGMP-dependent signaling in platelets. *J Thromb Haemost*, 2012. 10(2): p. 167-76.
52. Halbrugge, M. and U. Walter, Purification of a vasodilator-regulated phosphoprotein from human platelets. *Eur J Biochem*, 1989. 185(1): p. 41-50.
53. Neal S. Kleiman, M., FACC, Will Measuring Vasodilator-Stimulated Phosphoprotein Phosphorylation Help Us Optimize the Loading Dose of Clopidogrel?*. *Journal of the American College of Cardiology*, 2008. Vol. 51(14): p. 1412-1414.
54. Eigenthaler, M., et al., Concentration and regulation of cyclic nucleotides, cyclic-nucleotide-dependent protein kinases and one of their major substrates in human platelets. Estimating the rate of cAMP-regulated and cGMP-regulated protein phosphorylation in intact cells. *Eur J Biochem*, 1992. 205(2): p. 471-81.
55. Laurent, V., et al., Role of Proteins of the Ena/VASP Family in Actin-based Motility of *Listeria monocytogenes*. *The Journal of Cell Biology*, 1999. 144(6): p. 1245-1258.
56. Sudo, T., H. Ito, and Y. Kimura, Phosphorylation of the vasodilator-stimulated phosphoprotein (VASP) by the anti-platelet drug, cilostazol, in platelets. *Platelets*, 2003. 14(6): p. 381-390.

57. Butt, E., et al., cAMP- and cGMP-dependent protein kinase phosphorylation sites of the focal adhesion vasodilator-stimulated phosphoprotein (VASP) in vitro and in intact human platelets. *J Biol Chem*, 1994. 269(20): p. 14509-17.
58. Smolenski, A., et al., Analysis and regulation of vasodilator-stimulated phosphoprotein serine 239 phosphorylation in vitro and in intact cells using a phosphospecific monoclonal antibody. *J Biol Chem*, 1998. 273(32): p. 20029-35.
59. Özüyan, B., et al., Endothelial nitric oxide synthase plays a minor role in inhibition of arterial thrombus formation. *Thrombosis and Haemostasis*, 2005. 93(6): p. 1161-1167.
60. Rowley, J.W., et al., Genome-wide RNA-seq analysis of human and mouse platelet transcriptomes. *Blood*, 2011. 118(14): p. e101-11.
61. Radomski, M.W., R.M. Palmer, and S. Moncada, An L-arginine/nitric oxide pathway present in human platelets regulates aggregation. *Proc Natl Acad Sci U S A*, 1990. 87(13): p. 5193-7.
62. Riba, R., et al., Regulation of platelet guanylyl cyclase by collagen: evidence that Glycoprotein VI mediates platelet nitric oxide synthesis in response to collagen. *Thromb Haemost*, 2005. 94(2): p. 395-403.
63. Stojanovic, A., et al., A phosphoinositide 3-kinase-AKT-nitric oxide-cGMP signaling pathway in stimulating platelet secretion and aggregation. *J Biol Chem*, 2006. 281(24): p. 16333-9.
64. Zhang, G., et al., Biphasic roles for soluble guanylyl cyclase (sGC) in platelet activation. *Blood*, 2011. 118(13): p. 3670-9.
65. Mellion B.T., I., L.,J. , Ohlstein, E.,H. et al, Evidence for the inhibitory role of guanosine 3',5' monophosphate in ADP -

- induced human platelet aggregation in the presence of nitric oxide and related nitrovasodilators. *Blood* 1981. 57: p. 946-955.
66. Stasch, J.P., et al., NO- and haem-independent activation of soluble guanylyl cyclase: molecular basis and cardiovascular implications of a new pharmacological principle. *Br J Pharmacol*, 2002. 136(5): p. 773-83.
 67. Walter, U., Physiological role of cGMP and cGMP-dependent protein kinase in the cardiovascular system. *Rev Physiol Biochem Pharmacol*, 1989. 113: p. 41-88.
 68. Jang, E.K., et al., Roles for both cyclic GMP and cyclic AMP in the inhibition of collagen-induced platelet aggregation by nitroprusside. *Br J Haematol*, 2002. 117(3): p. 664-75.
 69. Jensen BO, S.F., Doskeland SO, Gear AR, Holmsen H. , Protein kinase A mediates inhibition of the thrombin-induced platelet shape change by nitric oxide. *Blood* 2004; 104: 2775–82. *Blood* 2004. 2775: p. 82.
 70. Launay, J.M., et al., Increase of human platelet serotonin uptake by atypical histamine receptors. *Am J Physiol*, 1994. 266(2 Pt 2): p. R526-36.
 71. Haynes., J.S.J.D.H., Cyclic GMP increases the rate of the calcium extrusion pump in intact human platelets but has no direct effect on the dense tubular calcium accumulation system. *Elsevier*, 1992. 1105(1): p. 40-50.
 72. Nozawa, S.N.T.T.H.H.Y.O.Y., Inhibitory action of cyclic GMP on secretion, polyphosphoinositide hydrolysis and calcium mobilization in thrombin-stimulated human platelets. *Elsevier*, 1986 28 March. 135(3): p. 1099-1104.

73. Paul Jurasz, a.r., Grzegorz Sawicki, ilvin Mayer and Marek Radomeski, nitric oxide and platelets function in nitric oxide biology and pathobiology I.j. ignarro, editor. 30 nov 2009, academic presss: los angeles , california. p. 823-839.
74. Du, X., A new mechanism for nitric oxide– and cGMP-mediated platelet inhibition. *Blood*, 2007. 109(2): p. 392-393.
75. Salas, E., et al., Comparative pharmacology of analogues of S-nitroso-N-acetyl-dl-penicillamine on human platelets. *British Journal of Pharmacology*, 1994. 112(4): p. 1071-1076.
76. Murohara, T., et al., Inhibition of nitric oxide biosynthesis promotes P-selectin expression in platelets. Role of protein kinase C. *Arterioscler Thromb Vasc Biol*, 1995. 15(11): p. 2068-75.
77. Michelson, A.D., et al., Effects of nitric oxide/EDRF on platelet surface glycoproteins. *Am J Physiol*, 1996. 270(5 Pt 2): p. H1640-8.
78. Mendelsohn, M.E., et al., Inhibition of fibrinogen binding to human platelets by S-nitroso-N-acetylcysteine. *J Biol Chem*, 1990. 265(31): p. 19028-34.
79. Schwarcz, R., The kynurenine pathway of tryptophan degradation as a drug target. *Curr Opin Pharmacol*, 2004. 4(1): p. 12-7.
80. Xu, K., et al., Redox Properties of Tryptophan Metabolism and the Concept of Tryptophan Use in Pregnancy. *International Journal of Molecular Sciences*, 2017. 18(7): p. 1595.
81. Stokes, A.H., et al., p-ethynylphenylalanine: a potent inhibitor of tryptophan hydroxylase. *J Neurochem*, 2000. 74(5): p. 2067-73.

82. Fukami, M.H., et al., An improved method for the isolation of dense storage granules from human platelets. *J Cell Biol*, 1978. 77(2): p. 389-99.
83. Ni, W. and S.W. Watts, 5-hydroxytryptamine in the cardiovascular system: focus on the serotonin transporter (SERT). *Clin Exp Pharmacol Physiol*, 2006. 33(7): p. 575-83.
84. Stahl, S.M., The human platelet. A diagnostic and research tool for the study of biogenic amines in psychiatric and neurologic disorders. *Arch Gen Psychiatry*, 1977. 34(5): p. 509-16.
85. Richard, D.M., et al., L-Tryptophan: Basic Metabolic Functions, Behavioral Research and Therapeutic Indications. *Int J Tryptophan Res*, 2009. 2: p. 45-60.
86. Li, N., et al., Effects of serotonin on platelet activation in whole blood. *Blood Coagul Fibrinolysis*, 1997. 8(8): p. 517-23.
87. Vanhoutte, P.M., et al., Endothelial dysfunction and vascular disease. *Acta Physiol (Oxf)*, 2009. 196(2): p. 193-222.
88. Leon-Ponte, M., G.P. Ahern, and P.J. O'Connell, Serotonin provides an accessory signal to enhance T-cell activation by signaling through the 5-HT₇ receptor. *Blood*, 2007. 109(8): p. 3139-46.
89. Cloutier, N., et al., Platelets can enhance vascular permeability. *Blood*, 2012. 120(6): p. 1334-43.
90. Eloranta, M.L., et al., Regulation of the interferon-alpha production induced by RNA-containing immune complexes in plasmacytoid dendritic cells. *Arthritis Rheum*, 2009. 60(8): p. 2418-27.
91. Shajib, M.S., et al., Interleukin 13 and serotonin: linking the immune and endocrine systems in murine models of intestinal inflammation. *PLoS One*, 2013. 8(8): p. e72774.

92. Kim, J.J., et al., Targeted inhibition of serotonin type 7 (5-HT₇) receptor function modulates immune responses and reduces the severity of intestinal inflammation. *J Immunol*, 2013. 190(9): p. 4795-804.
93. Shajib, M.S. and W.I. Khan, The role of serotonin and its receptors in activation of immune responses and inflammation. *Acta Physiol (Oxf)*, 2015. 213(3): p. 561-74.
94. Sarac, H., et al., Platelet serotonin in primary Sjogren's syndrome: level and relation with disease activity. *J Neuroimmunol*, 2012. 251(1-2): p. 87-9.
95. Opitz, C.A., et al., An endogenous tumour-promoting ligand of the human aryl hydrocarbon receptor. *Nature*, 2011. 478(7368): p. 197-203.
96. Widner, B., et al., Enhanced tryptophan degradation in systemic lupus erythematosus. *Immunobiology*, 2000. 201(5): p. 621-30.
97. Schäfer A, S.M., Seufert J, Keicher C, Weissbrich B, Rieger P, et al. , Platelet serotonin (5-HT) levels in interferon-treated patients with hepatitis C and its possible association with interferon-induced depression. *J Hepatol*, 2010. 52(1).
98. Mellor, A.L. and D.H. Munn, IDO expression by dendritic cells: tolerance and tryptophan catabolism. *Nat Rev Immunol*, 2004. 4(10): p. 762-74.
99. Ohnishi, T., F. Hirata, and O. Hayaishi, Indoleamine 2,3-dioxygenase. Potassium superoxide as substrate. *J Biol Chem*, 1977. 252(13): p. 4643-7.
100. Hayaishi, O., et al., Indoleamine 2,3-dioxygenase: incorporation of 18O₂-- and 18O₂ into the reaction products. *J Biol Chem*, 1977. 252(10): p. 3548-50.

101. Theate, I., et al., Extensive profiling of the expression of the indoleamine 2,3-dioxygenase 1 protein in normal and tumoral human tissues. *Cancer Immunol Res*, 2015. 3(2): p. 161-72.
102. Wang, Y., et al., Kynurenine is an endothelium-derived relaxing factor produced during inflammation. *Nat Med*, 2010. 16(3): p. 279-85.
103. Yasui, H., et al., Interferon enhances tryptophan metabolism by inducing pulmonary indoleamine 2,3-dioxygenase: its possible occurrence in cancer patients. *Proc Natl Acad Sci U S A*, 1986. 83(17): p. 6622-6.
104. Daubener W, M.C., IFN-gamma activated indoleamine 2,3-dioxygenase activity in human cells is an antiparasitic and an antibacterial effector mechanism. *Adv Exp Med Biol*, 1999. 467: p. 517-524.
105. Mellor, A.L., et al., Tryptophan catabolism and T cell responses. *Adv Exp Med Biol*, 2003. 527: p. 27-35.
106. Munn, D.H., et al., Prevention of allogeneic fetal rejection by tryptophan catabolism. *Science*, 1998. 281(5380): p. 1191-3.
107. Munn, D.H., et al., Inhibition of T cell proliferation by macrophage tryptophan catabolism. *J Exp Med*, 1999. 189(9): p. 1363-72.
108. Lee, G.K., et al., Tryptophan deprivation sensitizes activated T cells to apoptosis prior to cell division. *Immunology*, 2002. 107(4): p. 452-60.
109. Frumento, G., et al., Tryptophan-derived catabolites are responsible for inhibition of T and natural killer cell proliferation induced by indoleamine 2,3-dioxygenase. *J Exp Med*, 2002. 196(4): p. 459-68.

110. Fallarino, F., et al., T cell apoptosis by kynurenines. *Adv Exp Med Biol*, 2003. 527: p. 183-90.
111. Terness, P., et al., Inhibition of allogeneic T cell proliferation by indoleamine 2,3-dioxygenase-expressing dendritic cells: mediation of suppression by tryptophan metabolites. *J Exp Med*, 2002. 196(4): p. 447-57.
112. Ball, H.J., et al., Indoleamine 2,3-dioxygenase-2; a new enzyme in the kynurenine pathway. *Int J Biochem Cell Biol*, 2009. 41(3): p. 467-71.
113. Nguyen, N.T., et al., Aryl hydrocarbon receptor and kynurenine: recent advances in autoimmune disease research. *Front Immunol*, 2014. 5: p. 551.
114. Mellor, A.L. and D.H. Munn, Tryptophan catabolism and regulation of adaptive immunity. *J Immunol*, 2003. 170(12): p. 5809-13.
115. Sakurai, K., et al., Effect of indoleamine 2,3-dioxygenase on induction of experimental autoimmune encephalomyelitis. *J Neuroimmunol*, 2002. 129(1-2): p. 186-96.
116. Szanto, S., et al., Inhibition of indoleamine 2,3-dioxygenase-mediated tryptophan catabolism accelerates collagen-induced arthritis in mice. *Arthritis Res Ther*, 2007. 9(3): p. R50.
117. Yousef A. Taher, M., et al., Indoleamine 2,3-dioxygenase-dependent tryptophan metabolites contribute to tolerance induction during allergen immunotherapy in a mouse model. *J Allergy Clin Immunol* 2008. 121: p. 983-991.
118. Gurtner, G.J., et al., Inhibition of indoleamine 2,3-dioxygenase augments trinitrobenzene sulfonic acid colitis in mice. *Gastroenterology*, 2003. 125(6): p. 1762-73.

119. Changsirivathanathamrong, D., et al., Tryptophan metabolism to kynurenine is a potential novel contributor to hypotension in human sepsis. *Crit Care Med*, 2011. 39(12): p. 2678-83.
120. Lunow, D., et al., Tryptophan-containing dipeptides are C-domain selective inhibitors of angiotensin converting enzyme. *Food chemistry*, 2015. 166: p. 596-602.
121. Sakakibara, K., et al., Kynurenine causes vasodilation and hypotension induced by activation of KCNQ-encoded voltage-dependent K(+) channels. *J Pharmacol Sci*, 2015. 129(1): p. 31-7.
122. Pedersen, E.R., et al., Urinary excretion of kynurenine and tryptophan, cardiovascular events, and mortality after elective coronary angiography. *Eur Heart J*, 2013. 34(34): p. 2689-96.
123. Pawlak, K., M. Mysliwiec, and D. Pawlak, Kynurenine pathway - a new link between endothelial dysfunction and carotid atherosclerosis in chronic kidney disease patients. *Adv Med Sci*, 2010. 55(2): p. 196-203.
124. Bartosiewicz, J., et al., The activation of the kynurenine pathway in a rat model with renovascular hypertension. *Exp Biol Med (Maywood)*, 2017. 242(7): p. 750-761.
125. Kalev-Zylinska, M.L., et al., N-methyl-D-aspartate receptors amplify activation and aggregation of human platelets. *Thromb Res*, 2014. 133(5): p. 837-47.
126. Bessede, A., et al., Aryl hydrocarbon receptor control of a disease tolerance defence pathway. *Nature*, 2014. 511: p. 184.
127. Denison, M.S. and S.R. Nagy, Activation of the aryl hydrocarbon receptor by structurally diverse exogenous and endogenous chemicals. *Annu Rev Pharmacol Toxicol*, 2003. 43: p. 309-34.

128. Carlstedt-Duke, J.M., Tissue distribution of the receptor for 2,3,7,8-tetrachlorodibenzo-p-dioxin in the rat. *Cancer Res*, 1979. 39(8): p. 3172-6.
129. Johansson, G., et al., The TCDD receptor in rat intestinal mucosa and its possible dietary ligands. *Nutr Cancer*, 1982. 3(3): p. 134-44.
130. Sogawa, K. and Y. Fujii-Kuriyama, Ah receptor, a novel ligand-activated transcription factor. *J Biochem*, 1997. 122(6): p. 1075-9.
131. Tomita, S., et al., T cell-specific disruption of arylhydrocarbon receptor nuclear translocator (Arnt) gene causes resistance to 2,3,7,8-tetrachlorodibenzo-p-dioxin-induced thymic involution. *J Immunol*, 2003. 171(8): p. 4113-20.
132. Sugiyama, T., et al., Grape Seed Extract from Koshu Cultivar Antagonizes Dioxin-Induced Aryl Hydrocarbon Receptor Activation. *American Journal of Enology and Viticulture*, 2013. 64(1): p. 146-151.
133. Matsumura, F., The significance of the nongenomic pathway in mediating inflammatory signaling of the dioxin-activated Ah receptor to cause toxic effects. *Biochem Pharmacol*, 2009. 77(4): p. 608-26.
134. Gerbal-Chaloin, S., et al., Role of CYP3A4 in the regulation of the aryl hydrocarbon receptor by omeprazole sulphide. *Cell Signal*, 2006. 18(5): p. 740-50.
135. Wilhelmsson, A., et al., Agonistic and antagonistic effects of alpha-naphthoflavone on dioxin receptor function. Role of the basic region helix-loop-helix dioxin receptor partner factor Arnt. *J Biol Chem*, 1994. 269(29): p. 19028-33.

136. Murray, I.A., et al., Antagonism of aryl hydrocarbon receptor signaling by 6,2',4'-trimethoxyflavone. *J Pharmacol Exp Ther*, 2010. 332(1): p. 135-44.
137. Lu, Y.F., et al., Identification of 3'-methoxy-4'-nitroflavone as a pure aryl hydrocarbon (Ah) receptor antagonist and evidence for more than one form of the nuclear Ah receptor in MCF-7 human breast cancer cells. *Arch Biochem Biophys*, 1995. 316(1): p. 470-7.
138. Harris, M., et al., Partial antagonism of 2,3,7,8-tetrachlorodibenzo-p-dioxin-mediated induction of aryl hydrocarbon hydroxylase by 6-methyl-1,3,8-trichlorodibenzofuran: mechanistic studies. *Mol Pharmacol*, 1989. 35(5): p. 729-35.
139. Thomas, S.R., D. Mohr, and R. Stocker, Nitric oxide inhibits indoleamine 2,3-dioxygenase activity in interferon-gamma primed mononuclear phagocytes. *J Biol Chem*, 1994. 269(20): p. 14457-64.
140. YutangWang¹, D.C., Gavin McKenzie², Sanjay Patel³, David S. Celermajer³, Roland Stocker¹, tryptophanmetabolismtokynurenineregulates vascular tone in atherosclerosis. *heart, lung and circulation*, 2009. 18s: p. 285.
141. Trousseau, a., phlegmasia alba dolens., in *clinique medicale de l'hotel-dieu paris*. 1865, new sydenham society,: london. p. 94–96.
142. Gasic, G.J., T.B. Gasic, and C.C. Stewart, Antimetastatic effects associated with platelet reduction. *Proc Natl Acad Sci U S A*, 1968. 61(1): p. 46-52.

143. Karpatkin, S. and E. Pearlstein, Role of platelets in tumor cell metastases. *Ann Intern Med*, 1981. 95(5): p. 636-41.
144. Gasic, G.J., et al., Platelet-tumor-cell interactions in mice. The role of platelets in the spread of malignant disease. *Int J Cancer*, 1973. 11(3): p. 704-18.
145. Jurasz, P., D. Alonso-Escolano, and M.W. Radomski, Platelet--cancer interactions: mechanisms and pharmacology of tumour cell-induced platelet aggregation. *Br J Pharmacol*, 2004. 143(7): p. 819-26.
146. Shau, H., M.D. Roth, and S.H. Golub, Regulation of natural killer function by nonlymphoid cells. *Nat Immun*, 1993. 12(4-5): p. 235-49.
147. Philippe, C., et al., Protection from tumor necrosis factor-mediated cytotoxicity by platelets. *Am J Pathol*, 1993. 143(6): p. 1713-23.
148. Kopp, H.G., T. Placke, and H.R. Salih, Platelet-derived transforming growth factor-beta down-regulates NKG2D thereby inhibiting natural killer cell antitumor reactivity. *Cancer Res*, 2009. 69(19): p. 7775-83.
149. Placke, T., et al., Platelet-derived MHC class I confers a pseudonormal phenotype to cancer cells that subverts the antitumor reactivity of natural killer immune cells. *Cancer Res*, 2012. 72(2): p. 440-8.
150. Timar, J., et al., Platelet-mimicry of cancer cells: epiphenomenon with clinical significance. *Oncology*, 2005. 69(3): p. 185-201.
151. RICKLES, F.R., LEVINE, M.N. & DVORAK, H.F. , Abnormalities of hemostasis in malignancy. *Hemostasis and Thrombosis Basic Principles and Clinical practice*, ed. R.F.

Colman, Hirsh, J., Marder, and C. V.J., A.W. & George, J.N..
2001, Philadelphia:: Lippincott Williams & Wilkins.

152. Honn, K.V. and D. Tang, Hemostasis and malignancy: an overview. *Cancer Metastasis Rev*, 1992. 11(3-4): p. 223-6.
153. Honn, K.V., D.G. Tang, and Y.Q. Chen, Platelets and cancer metastasis: more than an epiphenomenon. *Semin Thromb Hemost*, 1992. 18(4): p. 392-415.
154. Lou, X.L., et al., Interaction between circulating cancer cells and platelets: clinical implication. *Chin J Cancer Res*, 2015. 27(5): p. 450-60.
155. Lewalle, J.M., et al., Malignant cell attachment to endothelium of ex vivo perfused human umbilical vein. Modulation by platelets, plasma and fibronectin. *Thromb Res*, 1991. 62(4): p. 287-98.
156. Jones, D.S., A.C. Wallace, and E.E. Fraser, Sequence of events in experimental metastases of Walker 256 tumor: light, immunofluorescent, and electron microscopic observations. *J Natl Cancer Inst*, 1971. 46(3): p. 493-504.
157. Sarach, M.A., R.A. Rovasio, and A.R. Eynard, Platelet factors induce chemotactic migration of murine mammary adenocarcinoma cells with different metastatic capabilities. *Int J Exp Pathol*, 1993. 74(5): p. 511-7.
158. Belloc, C., et al., The effect of platelets on invasiveness and protease production of human mammary tumor cells. *Int J Cancer*, 1995. 60(3): p. 413-7.
159. Francis, J.L., J. Biggerstaff, and A. Amirkhosravi, Hemostasis and malignancy. *Semin Thromb Hemost*, 1998. 24(2): p. 93-109.

160. Sierko, E. and M.Z. Wojtukiewicz, Platelets and angiogenesis in malignancy. *Semin Thromb Hemost*, 2004. 30(1): p. 95-108.
161. Noble, S. and J. Pasi, Epidemiology and pathophysiology of cancer-associated thrombosis. *Br J Cancer*, 2010. 102 Suppl 1: p. S2-9.
162. Blom, J.W., et al., Malignancies, prothrombotic mutations, and the risk of venous thrombosis. *Jama*, 2005. 293(6): p. 715-22.
163. Heit, J.A., et al., Risk factors for deep vein thrombosis and pulmonary embolism: a population-based case-control study. *Arch Intern Med*, 2000. 160(6): p. 809-15.
164. Alonso-Escolano, D., et al., Membrane type-1 matrix metalloproteinase stimulates tumour cell-induced platelet aggregation: role of receptor glycoproteins. *Br J Pharmacol*, 2004. 141(2): p. 241-52.
165. Honn, K.V., et al., Alpha IIb beta 3 integrin expression and function in subpopulations of murine tumors. *Exp Cell Res*, 1992. 201(1): p. 23-32.
166. Berndt, M.C., et al., Purification and preliminary characterization of the glycoprotein Ib complex in the human platelet membrane. *Eur J Biochem*, 1985. 151(3): p. 637-49.
167. Du, X., et al., Glycoprotein Ib and glycoprotein IX are fully complexed in the intact platelet membrane. *Blood*, 1987. 69(5): p. 1524-7.
168. Hagen, I., et al., Further studies on the interaction between thrombin and GP Ib using crossed immunoelectrophoresis. Effect of thrombin inhibitors. *Thromb Res*, 1982. 27(5): p. 549-54.

169. Romo, G.M., et al., The glycoprotein Ib-IX-V complex is a platelet counterreceptor for P-selectin. *J Exp Med*, 1999. 190(6): p. 803-14.
170. Simon, D.I., et al., Platelet glycoprotein Iba α is a counterreceptor for the leukocyte integrin Mac-1 (CD11b/CD18). *J Exp Med*, 2000. 192(2): p. 193-204.
171. Bradford, H.N., R.A. Pixley, and R.W. Colman, Human factor XII binding to the glycoprotein Ib-IX-V complex inhibits thrombin-induced platelet aggregation. *J Biol Chem*, 2000. 275(30): p. 22756-63.
172. Baglia, F.A., et al., Factor XI binding to the platelet glycoprotein Ib-IX-V complex promotes factor XI activation by thrombin. *J Biol Chem*, 2002. 277(3): p. 1662-8.
173. Berndt, M.C., et al., The vascular biology of the glycoprotein Ib-IX-V complex. *Thromb Haemost*, 2001. 86(1): p. 178-88.
174. Canobbio, I., C. Balduini, and M. Torti, Signalling through the platelet glycoprotein Ib-V-IX complex. *Cell Signal*, 2004. 16(12): p. 1329-44.
175. Oleksowicz, L. and J.P. Dutcher, Adhesive receptors expressed by tumor cells and platelets: novel targets for therapeutic anti-metastatic strategies. *Medical Oncology*, 1995. 12(2): p. 95-102.
176. Jurasz, P., et al., Role of von Willebrand factor in tumour cell-induced platelet aggregation: differential regulation by NO and prostacyclin. *Br J Pharmacol*, 2001. 134(5): p. 1104-12.
177. Grossi, I.M., et al., Inhibition of human tumor cell induced platelet aggregation by antibodies to platelet glycoproteins Ib and IIb/IIIa. *Proc Soc Exp Biol Med*, 1987. 186(3): p. 378-83.

178. Bastida, E., L. Almirall, and A. Ordinas, Tumor-cell-induced platelet aggregation is a glycoprotein-dependent and lipoxygenase-associated process. *Int J Cancer*, 1987. 39(6): p. 760-3.
179. Lian, L., et al., Inhibition of MCF-7 breast cancer cell-induced platelet aggregation using a combination of antiplatelet drugs. *Oncol Lett*, 2013. 5(2): p. 675-680.
180. JURASZ, P., SAWICKI, G., DUSZYK, M., SAWICKA, J., MIRANDA, C., and I.R. MAYERS, M.W., Matrix metalloproteinase- 2 in tumor cell-induced platelet aggregation: regulation by nitric oxide. *Cancer Res.*, 2001a. 61: p. 376–382.
181. Clezardin, P., et al., Role of platelet membrane glycoproteins Ib/IX and IIb/IIIa, and of platelet alpha-granule proteins in platelet aggregation induced by human osteosarcoma cells. *Cancer Res*, 1993. 53(19): p. 4695-700.
182. TRIKHA, M., ZHOU, Z., TIMAR, J., RASO, E., KENNEL, M., and E.N. EMMELL, M.T., Multiple roles for platelet GPIIb/IIIa and avb3 integrins in tumor growth, angiogenesis, and metastasis. *Cancer Res.*, 2002. 62: p. 2824–2833.
183. AMIRKHOSRAVI, A., MOUSA, S.A., AMAYA, M., BLAYDES, S., and H. DESAI, MEYER, T. & FRANCIS, J.L. , Inhibition of tumor cell-induced platelet aggregation and lung metastasis by the oral GpIIb/IIIa antagonist XV454. *Thromb. Haemost*, 2003. 90: p. 549–554.
184. Boukerche H, B.-V.O., Tabone E, Doré JF, Leung LL, McGregor Platelet-melanoma cell interaction is mediated by the glycoprotein IIb-IIIa complex. *Blood Cells Mol Dis*, 1989. 74: p. 658–663.

185. Amirkhosravi, A., et al., Blockade of GpIIb/IIIa inhibits the release of vascular endothelial growth factor (VEGF) from tumor cell-activated platelets and experimental metastasis. *Platelets*, 1999. 10(5): p. 285-92.
186. Engebraaten, O., et al., Inhibition of in vivo tumour growth by the blocking of host alpha(v)beta3 and alphaII(b)beta3 integrins. *Anticancer Res*, 2009. 29(1): p. 131-7.
187. Felding-Habermann, B., et al., Integrin activation controls metastasis in human breast cancer. *Proc Natl Acad Sci U S A*, 2001. 98(4): p. 1853-8.
188. Lonsdorf, A.S., et al., Engagement of alphaIIb beta3 (GPIIb/IIIa) with alpha5 beta3 integrin mediates interaction of melanoma cells with platelets: a connection to hematogenous metastasis. *J Biol Chem*, 2012. 287(3): p. 2168-78.
189. Crockett-Torabi, E., Selectins and mechanisms of signal transduction. *J Leukoc Biol*, 1998. 63(1): p. 1-14.
190. Kansas, G.S., Selectins and their ligands: current concepts and controversies. *Blood*, 1996. 88(9): p. 3259-87.
191. McEver, R.P., Selectin-carbohydrate interactions during inflammation and metastasis. *Glycoconj J*, 1997. 14(5): p. 585-91.
192. Kim, Y.J., et al., P-selectin deficiency attenuates tumor growth and metastasis. *Proc Natl Acad Sci U S A*, 1998. 95(16): p. 9325-30.
193. Laubli, H. and L. Borsig, Selectins as mediators of lung metastasis. *Cancer Microenviron*, 2010. 3(1): p. 97-105.
194. Mannori, G., et al., Differential colon cancer cell adhesion to E-, P-, and L-selectin: role of mucin-type glycoproteins. *Cancer Res*, 1995. 55(19): p. 4425-31.

195. Qi, C., et al., P-selectin-mediated platelet adhesion promotes tumor growth. *Oncotarget*, 2015. 6(9): p. 6584-96.
196. Laubli, H., K.S. Spanaus, and L. Borsig, Selectin-mediated activation of endothelial cells induces expression of CCL5 and promotes metastasis through recruitment of monocytes. *Blood*, 2009. 114(20): p. 4583-91.
197. Shao, B., et al., Carcinoma mucins trigger reciprocal activation of platelets and neutrophils in a murine model of Trousseau syndrome. *Blood*, 2011. 118(15): p. 4015-23.
198. Schlesinger, M., Role of platelets and platelet receptors in cancer metastasis. *J Hematol Oncol*, 2018. 11(1): p. 125.
199. Bastida, E., et al., Differentiation of platelet-aggregating effects of human tumor cell lines based on inhibition studies with apyrase, hirudin, and phospholipase. *Cancer Res*, 1982. 42(11): p. 4348-52.
200. Grignani, G., et al., Mechanisms of platelet activation by cultured human cancer cells and cells freshly isolated from tumor tissues. *Invasion Metastasis*, 1989. 9(5): p. 298-309.
201. Pinto, S., et al., Increased thromboxane A2 production at primary tumor site in metastasizing squamous cell carcinoma of the larynx. *Prostaglandins Leukot Essent Fatty Acids*, 1993. 49(1): p. 527-30.
202. Zucchella, M., et al., Human tumor cells cultured "in vitro" activate platelet function by producing ADP or thrombin. *Haematologica*, 1989. 74(6): p. 541-5.
203. Yu, L.X., et al., Platelets promote tumour metastasis via interaction between TLR4 and tumour cell-released high-mobility group box1 protein. *Nat Commun*, 2014. 5: p. 5256.

204. Yan, M. and P. Jurasz, The role of platelets in the tumor microenvironment: From solid tumors to leukemia. *Biochimica et Biophysica Acta (BBA) - Molecular Cell Research*, 2016. 1863(3): p. 392-400.
205. Liu, Y., et al., Tissue factor-activated coagulation cascade in the tumor microenvironment is critical for tumor progression and an effective target for therapy. *Cancer Res*, 2011. 71(20): p. 6492-502.
206. Ruf, W., N. Yokota, and F. Schaffner, Tissue factor in cancer progression and angiogenesis. *Thromb Res*, 2010. 125 Suppl 2: p. S36-8.
207. BASTIDA, E., ESCOLAR, G., ALMIRALL, L. & ORDINAS, A. , Platelet activation induced by a human neuroblastoma tumor cell line is reduced by prior administration of ticlopidine. *Thromb.Haemost.*, 1986a. 55: p. 333–337.
208. Heinmoller, E., et al., Studies on tumor-cell-induced platelet aggregation in human lung cancer cell lines. *J Cancer Res Clin Oncol*, 1996. 122(12): p. 735-44.
209. Boukerche, H., et al., Human melanoma cell lines differ in their capacity to release ADP and aggregate platelets. *Br J Haematol*, 1994. 87(4): p. 763-72.
210. alonso-escolano, d., strongin, a.y., chung, a.w., and e.i.r. deryugina, m.w., Membrane type-1 matrix metalloproteinase stimulates tumour cell-induced platelet aggregation: role of receptor glycoproteins. *Br. J. Pharmacol.*, 2004. 141 p. 241–252.

211. Wu, C.C., et al., Antipsychotic Drugs Inhibit Platelet Aggregation via P2Y 1 and P2Y 12 Receptors. *Biomed Res Int*, 2016. 2016: p. 2532371.
212. Dorsam, R.T. and S.P. Kunapuli, Central role of the P2Y12 receptor in platelet activation. *J Clin Invest*, 2004. 113(3): p. 340-5.
213. Cho, M.S., et al., Role of ADP receptors on platelets in the growth of ovarian cancer. *Blood*, 2017. 130(10): p. 1235-1242.
214. Holmes, C.E., et al., Platelet phenotype changes associated with breast cancer and its treatment. *Platelets*, 2016. 27(7): p. 703-711.
215. Honn, K.V., Inhibition of tumor cell metastasis by modulation of the vascular prostacyclin/thromboxane A₂ system. *Clin Exp Metastasis*, 1983. 1(2): p. 103-14.
216. Sakai, H., et al., Upregulation of thromboxane synthase in human colorectal carcinoma and the cancer cell proliferation by thromboxane A₂. *FEBS Lett*, 2006. 580(14): p. 3368-74.
217. Cathcart, M.C., et al., Examination of thromboxane synthase as a prognostic factor and therapeutic target in non-small cell lung cancer. *Mol Cancer*, 2011. 10: p. 25.
218. Kajita, S., et al., Role of COX-2, thromboxane A₂ synthase, and prostaglandin I₂ synthase in papillary thyroid carcinoma growth. *Mod Pathol*, 2005. 18(2): p. 221-7.
219. Moussa, O., et al., Prognostic and functional significance of thromboxane synthase gene overexpression in invasive bladder cancer. *Cancer Res*, 2005. 65(24): p. 11581-7.
220. Nie, D., et al., Differential expression of thromboxane synthase in prostate carcinoma: role in tumor cell motility. *Am J Pathol*, 2004. 164(2): p. 429-39.

221. Grignani, g., Pacchiarini, L., Almasio, P., Pagliarino, M., And G. Gamba, Rizzo, S.C. & Ascari, E., Characterization of the platelet-aggregating activity of cancer cells with different metastatic potential. *Int. J. Cancer*, 1986. 38: p. 237-244.
222. Pacchiarini, L., Zucchella, M., Milanese, G., Tacconi, F., And E. Bonomi, Canevari, A. & Grignani, G., Thromboxane production by platelets during tumor cell-induced platelet activation. *Invasion Metast*, 1991. 11: p. 102-109.
223. Tzanakakis, G.N., et al., The preventive effect of ketoconazole on experimental metastasis from a human pancreatic carcinoma may be related to its effect on prostaglandin synthesis. *Int J Gastrointest Cancer*, 2002. 32(1): p. 23-30.
224. De Leval, X., et al., Pharmacological evaluation of the novel thromboxane modulator BM-567 (II/II). Effects of BM-567 on osteogenic sarcoma-cell-induced platelet aggregation. *Prostaglandins Leukot Essent Fatty Acids*, 2003. 68(1): p. 55-9.
225. Steinert, B.W., et al., Studies on the role of platelet eicosanoid metabolism and integrin alpha IIb beta 3 in tumor-cell-induced platelet aggregation. *Int J Cancer*, 1993. 54(1): p. 92-101.
226. Nie, D., et al., Thromboxane A(2) regulation of endothelial cell migration, angiogenesis, and tumor metastasis. *Biochem Biophys Res Commun*, 2000. 267(1): p. 245-51.
227. Coughlin, S.R., Thrombin signalling and protease-activated receptors. *Nature*, 2000. 407(6801): p. 258-64.
228. Chung, A.W., Jurasz, P., Hollenberg, M.D. & Radomski, and M.W., Mechanisms of action of proteinase-activated receptor agonists on human platelets. *Br. J. Pharmacol.*, 2002. 135: p. 1123-1132.

229. Bastida, E., et al., Morphometric evaluation of thrombogenesis by microvesicles from human tumor cell lines with thrombin-dependent (U87MG) and adenosine diphosphate-dependent (SKNMC) platelet-activating mechanisms. *Translational Research*. 108(6): p. 622-627.
230. Esumi, N., S. Todo, and S. Imashuku, Platelet aggregating activity mediated by thrombin generation in the NCG human neuroblastoma cell line. *Cancer Res*, 1987. 47(8): p. 2129-35.
231. Heinmoller, E., et al., Tumor cell-induced platelet aggregation in vitro by human pancreatic cancer cell lines. *Scand J Gastroenterol*, 1995. 30(10): p. 1008-16.
232. Adams, G.N., et al., Colon Cancer Growth and Dissemination Relies upon Thrombin, Stromal PAR-1, and Fibrinogen. *Cancer Res*, 2015. 75(19): p. 4235-43.
233. Plantureux, L., et al., Impacts of Cancer on Platelet Production, Activation and Education and Mechanisms of Cancer-Associated Thrombosis. *Cancers (Basel)*, 2018. 10(11).
234. HONN, K.V., CAVANAUGH, P., EVENS, C., TAYLOR, J.D. & SLOANE, and B.F., Tumor cell-platelet aggregation: induced by cathepsin B-like proteinase and inhibited by prostacyclin. *Science*, 1982. 217: p. 540-542.
235. Falanga, A. and S.G. Gordon, Isolation and characterization of cancer procoagulant: a cysteine proteinase from malignant tissue. *Biochemistry*, 1985. 24(20): p. 5558-67.
236. DONATI, M.B., GAMBACORTI-PASSERINI, C., CASALI, B., FALANGA, and V. A., P., FOSSATI, G., SEMERARO, N. & GORDON, S.G., Cancer procoagulant in human tumor cells:

- evidence from melanoma patients. *Cancer Res*, 1986. 46: p. 6471-6474.
237. OLAS, B., WACHOWICZ, B., MIELICKI, W.P. & BUCZYNSKI, A., Free radicals are involved in cancer procoagulant-induced platelet activation. *Thromb. Res.*, 2000. 97: p. 169-175.
238. Andrade, S.S., et al., Cathepsin K induces platelet dysfunction and affects cell signaling in breast cancer - molecularly distinct behavior of cathepsin K in breast cancer. *BMC Cancer*, 2016. 16: p. 173.
239. Paul Jurasz, A.W.Y.C., Anna Radomski and Marek W. Radomski, Nonremodeling Properties of Matrix Metalloproteinases The Platelet Connection. *Circ Res.*, 2002. 90: p. 1041-1043.
240. Jurasz, P., et al., Matrix metalloproteinase 2 in tumor cell-induced platelet aggregation: regulation by nitric oxide. *Cancer Res*, 2001. 61(1): p. 376-82.
241. Jurasz, P., et al., Matrix metalloproteinase-2 contributes to increased platelet reactivity in patients with metastatic prostate cancer: a preliminary study. *Thromb Res*, 2003. 112(1-2): p. 59-64.
242. Medina, C., et al., Platelet aggregation-induced by caco-2 cells: regulation by matrix metalloproteinase-2 and adenosine diphosphate. *J Pharmacol Exp Ther*, 2006. 317(2): p. 739-45.
243. Ahmed, H. and D.M. AlSadek, Galectin-3 as a Potential Target to Prevent Cancer Metastasis. *Clin Med Insights Oncol*, 2015. 9: p. 113-21.

244. Kuo, H.Y., et al., Galectin-3 modulates the EGFR signalling-mediated regulation of Sox2 expression via c-Myc in lung cancer. *Glycobiology*, 2016. 26(2): p. 155-65.
245. Dovizio, M., et al., Pharmacological inhibition of platelet-tumor cell cross-talk prevents platelet-induced overexpression of cyclooxygenase-2 in HT29 human colon carcinoma cells. *Mol Pharmacol*, 2013. 84(1): p. 25-40.
246. Barnes, N.L., et al., Cyclooxygenase-2 inhibition: effects on tumour growth, cell cycling and lymphangiogenesis in a xenograft model of breast cancer. *Br J Cancer*, 2007. 96(4): p. 575-82.
247. Honn, K.V., R.S. Bockman, and L.J. Marnett, Prostaglandins and cancer: a review of tumor initiation through tumor metastasis. *Prostaglandins*, 1981. 21(5): p. 833-64.
248. Honn, K.V., B. Cicone, and A. Skoff, Prostacyclin: a potent antimetastatic agent. *Science*, 1981. 212(4500): p. 1270-2.
249. Lerner, W.A., et al., A new mechanism for tumor induced platelet aggregation. Comparison with mechanisms shared by other tumor with possible pharmacologic strategy toward prevention of metastases. *Int J Cancer*, 1983. 31(4): p. 463-9.
250. Schirner, M. and M.R. Schneider, The prostacyclin analogue cicaprost inhibits metastasis of tumours of R 3327 MAT Lu prostate carcinoma and SMT 2A mammary carcinoma. *J Cancer Res Clin Oncol*, 1992. 118(7): p. 497-501.
251. Radomski, M.W., et al., Human Colorectal Adenocarcinoma Cells: Differential Nitric Oxide Synthesis Determines Their Ability to Aggregate Platelets. *Cancer Research*, 1991. 51(22): p. 6073-6078.

252. Bazou, D., et al., Elucidation of flow-mediated tumour cell-induced platelet aggregation using an ultrasound standing wave trap. *British journal of pharmacology*, 2011. 162(7): p. 1577-1589.
253. Vane, J.R., Y.S. Bakhle, and R.M. Botting, Cyclooxygenases 1 and 2. *Annu Rev Pharmacol Toxicol*, 1998. 38: p. 97-120.
254. Algra, A.M. and P.M. Rothwell, Effects of regular aspirin on long-term cancer incidence and metastasis: a systematic comparison of evidence from observational studies versus randomised trials. *Lancet Oncol*, 2012. 13(5): p. 518-27.
255. Langley, R.E., et al., Aspirin and cancer: has aspirin been overlooked as an adjuvant therapy? *British journal of cancer*, 2011. 105(8): p. 1107-1113.
256. Sandler, R.S., et al., A randomized trial of aspirin to prevent colorectal adenomas in patients with previous colorectal cancer. *N Engl J Med*, 2003. 348(10): p. 883-90.
257. Lipton, A., et al., Adjuvant antiplatelet therapy with aspirin in colo-rectal cancer. *J Med*, 1982. 13(5-6): p. 419-29.
258. Lebeau B1, C.C., Muir JF, Vincent J, Massin F, Fabre C, No effect of an antiaggregant treatment with aspirin in small cell lung cancer treated with CCAVP16 chemotherapy. Results from a randomized clinical trial of 303 patients. The "Petites Cellules" Group. *Cancer Immunol Res*, 1993 Mar 71(5): p. 1741-1745.
259. HAMILTON, J., SUBBARAO, V., GRANACK, K. & TSAO, C., Platelet interaction with a pancreatic ascites tumor. *Am. J. Pathol.*, 1986. 122: p. 160-168.
260. Bastida, E., L. Almirall, and A. Ordinas, Tumor-cell-induced platelet aggregation is a glycoprotein-dependent and

- lipoygenase-associated process. *International Journal of Cancer*, 1987. 39(6): p. 760-763.
261. BRADLEY, C.J., DAUER, R.J., THURLOW, P.J. & CONNELLAN, J.M., Characterization of platelet aggregation induced by the human carcinosarcoma Colo 526: role of platelet activation, tumor cell cytoskeleton and tumor cell plasma membrane. *Pathology*, 1997. 29: p. 189-195.
262. Zarà, M., et al., Molecular mechanisms of platelet activation and aggregation induced by breast cancer cells. *Cellular Signalling*, 2018. 48: p. 45-53.
263. Medina, C., et al., Differential inhibition of tumour cell-induced platelet aggregation by the nicotinate aspirin prodrug (ST0702) and aspirin. *Br J Pharmacol*, 2012. 166(3): p. 938-49.
264. Mehta, P., Lawson, D., Ward, M.B., Lee-Ambrose, L. & and A. Kimura, Effects of thromboxane A₂ inhibition on osteogenic sarcoma cell-induced platelet aggregation. *Cancer Res.*, 1986. 46: p. 5061–5063.
265. JURASZ, P., et al., *Nitric Oxide Biology and Pathobiology*. 2000.
266. Jenkins, D.C., et al., Human colon cancer cell lines show a diverse pattern of nitric oxide synthase gene expression and nitric oxide generation. *Br J Cancer*, 1994. 70(5): p. 847-9.
267. Rigas, B. and J.L. Williams, NO-donating NSAIDs and cancer: an overview with a note on whether NO is required for their action. *Nitric oxide : biology and chemistry*, 2008. 19(2): p. 199-204.

268. Palmer, R.M., D.S. Ashton, and S. Moncada, Vascular endothelial cells synthesize nitric oxide from L-arginine. *Nature*, 1988. 333(6174): p. 664-6.
269. Radomski, M.W., R.M. Palmer, and S. Moncada, The role of nitric oxide and cGMP in platelet adhesion to vascular endothelium. *Biochem Biophys Res Commun*, 1987. 148(3): p. 1482-9.
270. Lepoivre, M., et al., Inactivation of ribonucleotide reductase by nitric oxide. *Biochem Biophys Res Commun*, 1991. 179(1): p. 442-8.
271. Goligorsky, M.S., et al., Co-operation between endothelin and nitric oxide in promoting endothelial cell migration and angiogenesis. *Clin Exp Pharmacol Physiol*, 1999. 26(3): p. 269-71.
272. Schini-Kerth, V.B., Dual effects of insulin-like growth factor-I on the constitutive and inducible nitric oxide (NO) synthase-dependent formation of NO in vascular cells. *J Endocrinol Invest*, 1999. 22(5 Suppl): p. 82-8.
273. Bando, H., T. Yamashita, and E. Tsubura, Effects of antiplatelet agents on pulmonary metastases. *Gan*, 1984. 75(3): p. 284-91.
274. Mezouar, S., et al., Inhibition of platelet activation prevents the P-selectin and integrin-dependent accumulation of cancer cell microparticles and reduces tumor growth and metastasis in vivo. *Int J Cancer*, 2015. 136(2): p. 462-75.
275. Gebremeskel, S., et al., The reversible P2Y₁₂ inhibitor ticagrelor inhibits metastasis and improves survival in mouse models of cancer. *Int J Cancer*, 2015. 136(1): p. 234-40.

276. Radomski, A., et al., Identification, regulation and role of tissue inhibitor of metalloproteinases-4 (TIMP-4) in human platelets. *Br J Pharmacol*, 2002. 137(8): p. 1330-8.
277. Overall, C.M. and C. Lopez-Otin, Strategies for MMP inhibition in cancer: innovations for the post-trial era. *Nat Rev Cancer*, 2002. 2(9): p. 657-72.
278. Karpatkin, S., et al., Role of adhesive proteins in platelet tumor interaction in vitro and metastasis formation in vivo. *J Clin Invest*, 1988. 81(4): p. 1012-9.
279. Cohen, S.A., M. Trikha, and M.A. Mascelli, Potential future clinical applications for the GPIIb/IIIa antagonist, abciximab in thrombosis, vascular and oncological indications. *Pathol Oncol Res*, 2000. 6(3): p. 163-74.
280. Bakewell, S.J., et al., Platelet and osteoclast beta3 integrins are critical for bone metastasis. *Proc Natl Acad Sci U S A*, 2003. 100(24): p. 14205-10.
281. Pinedo, H.M., et al., Involvement of platelets in tumour angiogenesis? *Lancet*, 1998. 352(9142): p. 1775-7.
282. PINEDO, H.M.S., D.J. , translational research: the role of VEGF in tumor angiogenesis. *Oncologist*, 2000. 5: p. 1-2.
283. Jurasz, P., et al., Generation and role of angiostatin in human platelets. *Blood*, 2003. 102(9): p. 3217-23.
284. Burkholder, B., et al., Tumor-induced perturbations of cytokines and immune cell networks. *Biochim Biophys Acta*, 2014. 1845(2): p. 182-201.
285. Lu, B. and O.J. Finn, T-cell death and cancer immune tolerance. *Cell Death Differ*, 2008. 15(1): p. 70-9.

286. Okamoto, A., et al., Indoleamine 2,3-dioxygenase serves as a marker of poor prognosis in gene expression profiles of serous ovarian cancer cells. *Clin Cancer Res*, 2005. 11(16): p. 6030-9.
287. Brandacher, G., et al., Prognostic value of indoleamine 2,3-dioxygenase expression in colorectal cancer: effect on tumor-infiltrating T cells. *Clin Cancer Res*, 2006. 12(4): p. 1144-51.
288. Smith, C., et al., IDO is a nodal pathogenic driver of lung cancer and metastasis development. *Cancer Discov*, 2012. 2(8): p. 722-35.
289. Suzuki, Y., et al., Increased serum kynurenine/tryptophan ratio correlates with disease progression in lung cancer. *Lung Cancer*, 2010. 67(3): p. 361-5.
290. Zhai, L., et al., The kynurenine to tryptophan ratio as a prognostic tool for glioblastoma patients enrolling in immunotherapy. *J Clin Neurosci*, 2015. 22(12): p. 1964-8.
291. Ferns, D.M., et al., Indoleamine-2,3-dioxygenase (IDO) metabolic activity is detrimental for cervical cancer patient survival. *Oncol Immunology*, 2015. 4(2): p. e981457.
292. Ogawa, K., et al., (-)-Epigallocatechin gallate inhibits the expression of indoleamine 2,3-dioxygenase in human colorectal cancer cells. *Oncol Lett*, 2012. 4(3): p. 546-550.
293. Labadie, B.W., R. Bao, and J.J. Luke, Reimagining IDO Pathway Inhibition in Cancer Immunotherapy via Downstream Focus on the Tryptophan-Kynurenine-Aryl Hydrocarbon Axis. *Clin Cancer Res*, 2019. 25(5): p. 1462-1471.
294. Cattaneo, M., et al., Recommendations for the Standardization of Light Transmission Aggregometry: A Consensus of the Working Party from the Platelet Physiology Subcommittee of SSC/ISTH. *J Thromb Haemost*, 2013.

295. Harrison, P.a.D.K., platelets 2ed. Platelets, ed. A.D. Michelson. 2007: Canada: Academic Pres.
296. Born, G.V., Aggregation of blood platelets by adenosine diphosphate and its reversal. *Nature*, 1962. 194: p. 927-9.
297. Chitale, K., et al., Vasodilator-stimulated phosphoprotein is a substrate for protein kinase C. *FEBS Letters*, 2004. 556(1): p. 211-215.
298. Darcy, C.J., et al., An Observational Cohort Study of the Kynurenine to Tryptophan Ratio in Sepsis: Association with Impaired Immune and Microvascular Function. *PLOS ONE*, 2011. 6(6): p. e21185.
299. Paul, B.Z., J. Jin, and S.P. Kunapuli, Molecular mechanism of thromboxane A₂-induced platelet aggregation. Essential role for p2t(ac) and alpha(2a) receptors. *J Biol Chem*, 1999. 274(41): p. 29108-14.
300. Ju-Ye Ro¹, Hui-Jin Lee^{1,§}, Jin-Hyeob Ryu², Hwa-Jin Park³ and Hyun-Jeong Cho^{1,†}, Anti-platelet Effects of Dimethyl Sulfoxide via Down-regulation of COX-1 and TXA₂ Synthase Activity in Rat Platelets. *Biomedical Science Letters*, 2014. 20(2): p. 70-76.
301. Vane, J.R. and R.M. Botting, The mechanism of action of aspirin. *Thromb Res*, 2003. 110(5-6): p. 255-8.
302. Schafer, A., et al., Platelet serotonin (5-HT) levels in interferon-treated patients with hepatitis C and its possible association with interferon-induced depression. *J Hepatol*, 2010. 52(1): p. 10-5.
303. D.M. Vanags, S.E.R., *E.M. Duncan, ',*J.V. Lloyd & F. Bochner, Potentiation of ADP-induced aggregation in human platelet-rich

- plasma by 5-hydroxytryptamine and adrenaline. *Br. J. Pharmacol.*, 1992. 106: p. 917-923.
304. Okuma, M., et al., Antagonism of 5-hydroxykynurenamine against serotonin action on platelet aggregation. *Proc Natl Acad Sci U S A*, 1976. 73(2): p. 643-5.
305. Lopez-Vilchez, I., et al., Serotonin enhances platelet procoagulant properties and their activation induced during platelet tissue factor uptake. *Cardiovasc Res*, 2009. 84(2): p. 309-16.
306. Pombo, M., et al., TCDD and omeprazole prime platelets through the aryl hydrocarbon receptor (AhR) non-genomic pathway. *Toxicol Lett*, 2015. 235(1): p. 28-36.
307. Lindsey, S., et al., Platelets from mice lacking the aryl hydrocarbon receptor exhibit defective collagen-dependent signaling. *J Thromb Haemost*, 2014. 12(3): p. 383-94.
308. Bunaciu, R.P. and A. Yen, 6-Formylindolo (3,2-b)carbazole (FICZ) enhances retinoic acid (RA)-induced differentiation of HL-60 myeloblastic leukemia cells. *Mol Cancer*, 2013. 12: p. 39.
309. Woulfe, D., et al., Activation of Rap1B by G(i) family members in platelets. *J Biol Chem*, 2002. 277(26): p. 23382-90.
310. Kim, S., H. Sundaramoorthi, and P. Jagadeeswaran, Dioxin-induced thrombocyte aggregation in zebrafish. *Blood Cells, Molecules, and Diseases*, 2015. 54(1): p. 116-122.
311. Asmis, L., et al., DMSO inhibits human platelet activation through cyclooxygenase-1 inhibition. A novel agent for drug eluting stents? *Biochem Biophys Res Commun*, 2010. 391(4): p. 1629-33.

312. Rainesalo, S., et al., GABA and glutamate transporters are expressed in human platelets. *Brain Res Mol Brain Res*, 2005. 141(2): p. 161-5.
313. Jedlitschky, G., A. Greinacher, and H.K. Kroemer, Transporters in human platelets: physiologic function and impact for pharmacotherapy. *Blood*, 2012. 119(15): p. 3394-402.
314. Sekine, A., et al., Amino acids inhibit kynurenic acid formation via suppression of kynurenine uptake or kynurenic acid synthesis in rat brain in vitro. *Springerplus*, 2015. 4: p. 48.
315. Jedlitschky, G., A. Greinacher, and H.K. Kroemer, Transporters in human platelets: physiologic function and impact for pharmacotherapy. *Blood*, 2012. 119(15): p. 3394-3402.
316. Sinclair, L.V., et al., Single cell analysis of kynurenine and System L amino acid transport in T cells. *Nature communications*, 2018. 9(1): p. 1981-1981.
317. Speciale, C., et al., High-affinity uptake of L-kynurenine by a Na⁺-independent transporter of neutral amino acids in astrocytes. *J Neurosci*, 1989. 9(6): p. 2066-72.
318. Christensen, H.N., On the meaning of effects of substrate structure on biological transport. *J Bioenerg*, 1973. 4(1): p. 31-61.
319. Alberati-Giani, D., et al., Differential regulation of indoleamine 2,3-dioxygenase expression by nitric oxide and inflammatory mediators in IFN-gamma-activated murine macrophages and microglial cells. *J Immunol*, 1997. 159(1): p. 419-26.
320. Oh, G.S., et al., 3-Hydroxyanthranilic acid, one of metabolites of tryptophan via indoleamine 2,3-dioxygenase pathway, suppresses inducible nitric oxide synthase expression by

- enhancing heme oxygenase-1 expression. *Biochem Biophys Res Commun*, 2004. 320(4): p. 1156-62.
321. Schubert, P. and D.V. Devine, De novo protein synthesis in mature platelets: a consideration for transfusion medicine. *Vox Sang*, 2010. 99(2): p. 112-22.
322. Yin, H., et al., The role of Akt in the signaling pathway of the glycoprotein Ib-IX induced platelet activation. *Blood*, 2008. 111(2): p. 658-65.
323. Moro, M.A., et al., cGMP mediates the vascular and platelet actions of nitric oxide: confirmation using an inhibitor of the soluble guanylyl cyclase. *Proc Natl Acad Sci U S A*, 1996. 93(4): p. 1480-5.
324. Garbers, D.L., D. Koesling, and G. Schultz, Guanylyl cyclase receptors. *Mol Biol Cell*, 1994. 5(1): p. 1-5.
325. Ignarro, L.J., Signal transduction mechanisms involving nitric oxide. *Biochem Pharmacol*, 1991. 41(4): p. 485-90.
326. Montfort, W.R., J.A. Wales, and A. Weichsel, Structure and Activation of Soluble Guanylyl Cyclase, the Nitric Oxide Sensor. *Antioxid Redox Signal*, 2017. 26(3): p. 107-121.
327. Friebe, A. and D. Koesling, Regulation of Nitric Oxide-Sensitive Guanylyl Cyclase. *Circulation Research*, 2003. 93(2): p. 96-105.
328. Priviero, F.B. and R.C. Webb, Heme-dependent and independent soluble guanylate cyclase activators and vasodilation. *J Cardiovasc Pharmacol*, 2010. 56(3): p. 229-33.
329. Lucas, K.A., et al., Guanylyl cyclases and signaling by cyclic GMP. *Pharmacol Rev*, 2000. 52(3): p. 375-414.

330. Roger, S., et al., The anti-aggregating effect of BAY 41-2272, a stimulator of soluble guanylyl cyclase, requires the presence of nitric oxide. *Br J Pharmacol*, 2010. 161(5): p. 1044-58.
331. Schrammel, A., et al., Characterization of 1H-[1,2,4]oxadiazolo[4,3-a]quinoxalin-1-one as a heme-site inhibitor of nitric oxide-sensitive guanylyl cyclase. *Mol Pharmacol*, 1996. 50(1): p. 1-5.
332. Stasch, J.P., et al., Targeting the heme-oxidized nitric oxide receptor for selective vasodilatation of diseased blood vessels. *J Clin Invest*, 2006. 116(9): p. 2552-61.
333. Hwang, T.L., C.C. Wu, and C.M. Teng, Comparison of two soluble guanylyl cyclase inhibitors, methylene blue and ODQ, on sodium nitroprusside-induced relaxation in guinea-pig trachea. *Br J Pharmacol*, 1998. 125(6): p. 1158-63.
334. Gerassimou, C., et al., Regulation of the expression of soluble guanylyl cyclase by reactive oxygen species. *Br J Pharmacol*, 2007. 150(8): p. 1084-91.
335. Stasch, J.P., P. Pacher, and O.V. Evgenov, Soluble guanylate cyclase as an emerging therapeutic target in cardiopulmonary disease. *Circulation*, 2011. 123(20): p. 2263-73.
336. Schmidt, P.M., et al., Identification of residues crucially involved in the binding of the heme moiety of soluble guanylate cyclase. *J Biol Chem*, 2004. 279(4): p. 3025-32.
337. Jensen, B.O., et al., Protein kinase A mediates inhibition of the thrombin-induced platelet shape change by nitric oxide. *Blood*, 2004. 104(9): p. 2775-82.
338. Wentworth, J.K., G. Pula, and A.W. Poole, Vasodilator-stimulated phosphoprotein (VASP) is phosphorylated on Ser157 by protein kinase C-dependent and -independent

- mechanisms in thrombin-stimulated human platelets. *Biochem J*, 2006. 393(Pt 2): p. 555-64.
339. Butt, E., M. Eigenthaler, and H.G. Genieser, (Rp)-8-pCPT-cGMPS, a novel cGMP-dependent protein kinase inhibitor. *Eur J Pharmacol*, 1994. 269(2): p. 265-8.
340. Fritsch, R.M., et al., InsP3R-associated cGMP Kinase Substrate (IRAG) Is Essential for Nitric Oxide-induced Inhibition of Calcium Signaling in Human Colonic Smooth Muscle. *Journal of Biological Chemistry*, 2004. 279(13): p. 12551-12559.
341. Bertele, V., et al., SQ 22536, an adenylate-cyclase inhibitor, prevents the antiplatelet effect of dazoxiben, a thromboxane-synthetase inhibitor. *Thromb Haemost*, 1984. 51(1): p. 125-8.
342. Rukoyatkina, N., et al., Protein kinase A activation by the anti-cancer drugs ABT-737 and thymoquinone is caspase-3-dependent and correlates with platelet inhibition and apoptosis. *Cell Death Dis*, 2017. 8(6): p. e2898-.
343. Rukoyatkina, N., et al., Differentiation of cGMP-dependent and -independent nitric oxide effects on platelet apoptosis and reactive oxygen species production using platelets lacking soluble guanylyl cyclase. *Thrombosis and Haemostasis*, 2011. 106(11): p. 922-933.
344. Schwarz, U.R., U. Walter, and M. Eigenthaler, Taming platelets with cyclic nucleotides. *Biochem Pharmacol*, 2001. 62(9): p. 1153-61.
345. El-Daher, S.S., et al., Distinct localization and function of (1,4,5)IP(3) receptor subtypes and the (1,3,4,5)IP(4) receptor GAP1(IP4BP) in highly purified human platelet membranes. *Blood*, 2000. 95(11): p. 3412-22.

346. Schinner, E., K. Salb, and J. Schlossmann, Signaling via IRAG is essential for NO/cGMP-dependent inhibition of platelet activation. *Platelets*, 2011. 22(3): p. 217-27.
347. Antl, M., et al., IRAG mediates NO/cGMP-dependent inhibition of platelet aggregation and thrombus formation. *Blood*, 2007. 109(2): p. 552-9.
348. Buys, E.S., et al., Discovery and development of next generation sGC stimulators with diverse multidimensional pharmacology and broad therapeutic potential. *Nitric Oxide*, 2018. 78: p. 72-80.
349. Ehara, T., et al., The Discovery of (S)-1-(6-(3-((4-(1-(Cyclopropanecarbonyl)piperidin-4-yl)-2-methylphenyl)amino)-2,3-dihydro-1H-inden-4-yl)pyridin-2-yl)-5-methyl-1H-pyrazole-4-carboxylic Acid, a Soluble Guanylate Cyclase Activator Specifically Designed for Topical Ocular Delivery as a Therapy for Glaucoma. *J Med Chem*, 2018. 61(6): p. 2552-2570.
350. Martin, F., et al., Structure of cinaciguat (BAY 58-2667) bound to Nostoc H-NOX domain reveals insights into heme-mimetic activation of the soluble guanylyl cyclase. *J Biol Chem*, 2010. 285(29): p. 22651-7.
351. Melillo, G., et al., Picolinic acid, a catabolite of L-tryptophan, is a costimulus for the induction of reactive nitrogen intermediate production in murine macrophages. *J Immunol*, 1993. 150(9): p. 4031-40.
352. Kornblihtt, L.I., L. Finocchiaro, and F.C. Molinas, Inhibitory effect of melatonin on platelet activation induced by collagen and arachidonic acid. *J Pineal Res*, 1993. 14(4): p. 184-91.

353. Vacas, M.I., et al., Inhibition of human platelet aggregation and thromboxane B2 production by melatonin. Correlation with plasma melatonin levels. *J Pineal Res*, 1991. 11(3-4): p. 135-9.
354. Cardinali, D.P., M.M. Del Zar, and M.I. Vacas, The effects of melatonin in human platelets. *Acta Physiol Pharmacol Ther Latinoam*, 1993. 43(1-2): p. 1-13.
355. Martinuzzo, M., et al., Melatonin effect on arachidonic acid metabolism to cyclooxygenase derivatives in human platelets. *J Pineal Res*, 1991. 11(3-4): p. 111-5.
356. DEL ZAR, M.D.L.M., et al., Inhibition of Human Platelet Aggregation and Thromboxane-B2 Production by Melatonin: Evidence for a Diurnal Variation*. *The Journal of Clinical Endocrinology & Metabolism*, 1990. 70(1): p. 246-251.
357. Ho-Tin-Noé, B., et al., Platelet granule secretion continuously prevents intratumor hemorrhage. *Cancer Res*, 2008. 68(16): p. 6851-8.
358. Mitrugno, A., et al., A novel and essential role for FcγRIIIa in cancer cell-induced platelet activation. *Blood*, 2014. 123(2): p. 249-60.
359. Jurasz, P., et al., Matrix Metalloproteinase 2 in Tumor Cell-induced Platelet Aggregation: Regulation by Nitric Oxide. *Cancer Research*, 2001. 61(1): p. 376-382.
360. Sheu, J.R., et al., Triflavin, an Arg-Gly-Asp-containing peptide, inhibits tumor cell-induced platelet aggregation. *Jpn J Cancer Res*, 1993. 84(10): p. 1062-71.
361. Guillem-Llobat, P., et al., Aspirin prevents colorectal cancer metastasis in mice by splitting the crosstalk between platelets and tumor cells. *Oncotarget*, 2016. 7(22): p. 32462-77.

362. Chiang, H.S., M.W. Swaim, and T.F. Huang, Characterization of platelet aggregation induced by human colon adenocarcinoma cells and its inhibition by snake venom peptides, trigramin and rhodostomin. *Br J Haematol*, 1994. 87(2): p. 325-31.
363. Santos-Martínez, M.J., et al., Role of metalloproteinases in platelet function. *Thrombosis Research*, 2008. 121(4): p. 535-542.
364. Martinez, A., et al., Matrix metalloproteinase-2 in platelet adhesion to fibrinogen: interactions with nitric oxide. *Med Sci Monit*, 2001. 7(4): p. 646-51.
365. Choi, W.S., et al., MMP-2 regulates human platelet activation by interacting with integrin α IIb β 3. *J Thromb Haemost*, 2008. 6(3): p. 517-23.
366. Zhiqiang Fu, H.W., Yi Zhou, Qi Zhou, Inhibition of platelet-tumour cell interaction with ibrutinib reduces proliferation, migration and invasion of lung cancer cells *Tropical Journal of Pharmaceutical Research*, April 2018. 17(4): p. 589-596.
367. Atkinson, B.T., W. Ellmeier, and S.P. Watson, Tec regulates platelet activation by GPVI in the absence of Btk. *Blood*, 2003. 102(10): p. 3592-9.
368. Stone, J.P. and D.D. Wagner, P-selectin mediates adhesion of platelets to neuroblastoma and small cell lung cancer. *Journal of Clinical Investigation*, 1993. 92(2): p. 804-813.
369. Maione, T.E., et al., Inhibition of angiogenesis by recombinant human platelet factor-4 and related peptides. *Science*, 1990. 247(4938): p. 77-9.

370. McLaren, K.M., Immunohistochemical localisation of thrombospondin in human megakaryocytes and platelets. *J Clin Pathol*, 1983. 36(2): p. 197-9.
371. Ruf, W. and B.M. Mueller, Thrombin generation and the pathogenesis of cancer. *Semin Thromb Hemost*, 2006. 32 Suppl 1: p. 61-8.
372. Coughlin, S.R., Protease-activated receptors in hemostasis, thrombosis and vascular biology. *J Thromb Haemost*, 2005. 3(8): p. 1800-14.
373. Leger, A.J., L. Covic, and A. Kuliopulos, Protease-Activated Receptors in Cardiovascular Diseases. *Circulation*, 2006. 114(10): p. 1070-1077.
374. Dörmann, D., K.J. Clemetson, and B.E. Kehrel, The GPIb thrombin-binding site is essential for thrombin-induced platelet procoagulant activity. *Blood*, 2000. 96(7): p. 2469-2478.
375. Woulfe, D.S., Platelet G protein-coupled receptors in hemostasis and thrombosis. *J Thromb Haemost*, 2005. 3(10): p. 2193-200.
376. Hassock, S.R., et al., Expression and role of TRPC proteins in human platelets: evidence that TRPC6 forms the store-independent calcium entry channel. *Blood*, 2002. 100(8): p. 2801-11.
377. Redondo, P.C., et al., Intracellular Ca²⁺ store depletion induces the formation of macromolecular complexes involving hTRPC1, hTRPC6, the type II IP₃ receptor and SERCA3 in human platelets. *Biochim Biophys Acta*, 2008. 1783(6): p. 1163-76.
378. Franke, B., J.W. Akkerman, and J.L. Bos, Rapid Ca²⁺-mediated activation of Rap1 in human platelets. *Embo j*, 1997. 16(2): p. 252-9.

379. Danielewski, O., J. Schultess, and A. Smolenski, The NO/cGMP pathway inhibits Rap 1 activation in human platelets via cGMP-dependent protein kinase I. *Thromb Haemost*, 2005. 93(2): p. 319-25.
380. Kato, M., et al., Direct binding and regulation of RhoA protein by cyclic GMP-dependent protein kinase I α . *J Biol Chem*, 2012. 287(49): p. 41342-51.
381. Dovizio, M., et al., Pharmacological Inhibition of Platelet-Tumor Cell Cross-Talk Prevents Platelet-Induced Overexpression of Cyclooxygenase-2 in HT29 Human Colon Carcinoma Cells. *Molecular Pharmacology*, 2013. 84(1): p. 25-40.
382. Dovizio, M., et al., Novel insights into the regulation of cyclooxygenase-2 expression by platelet-cancer cell cross-talk. *Biochemical Society Transactions*, 2015. 43(4): p. 707-714.
383. Dovizio, M., et al., Effects of celecoxib on prostanoid biosynthesis and circulating angiogenesis proteins in familial adenomatous polyposis. *J Pharmacol Exp Ther*, 2012. 341(1): p. 242-50.
384. Radziwon-Balicka, A., et al., Mechanisms of platelet-stimulated colon cancer invasion: role of clusterin and thrombospondin 1 in regulation of the P38MAPK-MMP-9 pathway. *Carcinogenesis*, 2014. 35(2): p. 324-32.
385. Reid, H.M. and B.T. Kinsella, The α , but not the β , isoform of the human thromboxane A₂ receptor is a target for nitric oxide-mediated desensitization. INDEPENDENT MODULATION OF TP α SIGNALING BY NITRIC OXIDE AND PROSTACYCLIN. *J Biol Chem*, 2016. 291(37): p. 19260.
386. Chiang, H.S., M.W. Swaim, and T.F. Huang, Characterization of platelet aggregation induced by human colon

- adenocarcinoma cells and its inhibition by snake venom peptides, trigramin and rhodostomin. *British Journal Of Haematology*, 1994. 87(2): p. 325-331.
387. Chiang, H.-S., H.-C. Peng, and T.-F. Huang, Characterization of integrin expression and regulation on SW-480 human colon adenocarcinoma cells and the effect of rhodostomin on basal and upregulated tumor cell adhesion. *Biochimica et Biophysica Acta (BBA) - Molecular Cell Research*, 1994. 1224(3): p. 506-516.
388. Singh-Ranger, G., M. Salhab, and K. Mokbel, The role of cyclooxygenase-2 in breast cancer: review. *Breast Cancer Res Treat*, 2008. 109(2): p. 189-98.
389. Howe, L.R., Inflammation and breast cancer. *Cyclooxygenase/prostaglandin signaling and breast cancer. Breast Cancer Res*, 2007. 9(4): p. 210.
390. Hou, Z., et al., Macrophages induce COX-2 expression in breast cancer cells: role of IL-1beta autoamplification. *Carcinogenesis*, 2011. 32(5): p. 695-702.
391. Senis, Y.A., A. Mazharian, and J. Mori, Src family kinases: at the forefront of platelet activation. *Blood*, 2014. 124(13): p. 2013-24.
392. Saklatvala, J., et al., Role for p38 mitogen-activated protein kinase in platelet aggregation caused by collagen or a thromboxane analogue. *J Biol Chem*, 1996. 271(12): p. 6586-9.
393. Bugaud, F., et al., Regulation of c-jun-NH2 terminal kinase and extracellular-signal regulated kinase in human platelets. *Blood*, 1999. 94(11): p. 3800-5.
394. Begonja, A.J., et al., Thrombin stimulation of p38 MAP kinase in human platelets is mediated by ADP and thromboxane A2

- and inhibited by cGMP/cGMP-dependent protein kinase. *Blood*, 2007. 109(2): p. 616-8.
395. Jackson, E.C. and A. McNicol, Cyclic nucleotides inhibit MAP kinase activity in low-dose collagen-stimulated platelets. *Thromb Res*, 2010. 125(2): p. 147-51.
 396. Greco, F., et al., Activation of the small GTPase Rap2B in agonist-stimulated human platelets. *J Thromb Haemost*, 2004. 2(12): p. 2223-30.
 397. Munn, D.H. and A.L. Mellor, Indoleamine 2,3-dioxygenase and tumor-induced tolerance. *J Clin Invest*, 2007. 117(5): p. 1147-54.
 398. Platten, M., W. Wick, and B.J. Van den Eynde, Tryptophan catabolism in cancer: beyond IDO and tryptophan depletion. *Cancer Res*, 2012. 72(21): p. 5435-40.
 399. Balachandran, V.P., et al., Imatinib potentiates antitumor T cell responses in gastrointestinal stromal tumor through the inhibition of Ido. *Nat Med*, 2011. 17(9): p. 1094-100.
 400. Brody, J.R., et al., Expression of indoleamine 2,3-dioxygenase in metastatic malignant melanoma recruits regulatory T cells to avoid immune detection and affects survival. *Cell Cycle*, 2009. 8(12): p. 1930-4.
 401. Flaumenhaft, R., et al., The actin cytoskeleton differentially regulates platelet α -granule and dense-granule secretion. *Blood*, 2005. 105(10): p. 3879-3887.
 402. Pagel, O., et al., Taking the stock of granule cargo: Platelet releasate proteomics. *Platelets*, 2017. 28(2): p. 119-128.
 403. Strandberg, G., et al., Standardizing the freeze-thaw preparation of growth factors from platelet lysate. *Transfusion*, 2017. 57(4): p. 1058-1065.

404. Heldin, C.H., B. Westermark, and A. Wasteson, Platelet-derived growth factor. Isolation by a large-scale procedure and analysis of subunit composition. *Biochem J*, 1981. 193(3): p. 907-13.
405. Mohle, R., et al., Constitutive production and thrombin-induced release of vascular endothelial growth factor by human megakaryocytes and platelets. *Proc Natl Acad Sci U S A*, 1997. 94(2): p. 663-8.
406. Brunner, G., et al., Basic fibroblast growth factor expression in human bone marrow and peripheral blood cells. *Blood*, 1993. 81(3): p. 631-8.
407. Marti, L.C., et al., Vascular endothelial growth factor-A enhances indoleamine 2,3-dioxygenase expression by dendritic cells and subsequently impacts lymphocyte proliferation. *Mem Inst Oswaldo Cruz*, 2014. 109(1): p. 70-9.
408. Sarkar, S.A., et al., Induction of Indoleamine 2,3-Dioxygenase by Interferon- γ in Human Islets. *Diabetes*, 2007. 56(1): p. 72-79.
409. Juhász, C., et al., Tryptophan metabolism in breast cancers: molecular imaging and immunohistochemistry studies. *Nucl Med Biol*, 2012. 39(7): p. 926-32.
410. Gwynne, W.D., et al., Serotonergic system antagonists target breast tumor initiating cells and synergize with chemotherapy to shrink human breast tumor xenografts. *Oncotarget*, 2017. 8(19): p. 32101-32116.
411. Taylor, M.W. and G.S. Feng, Relationship between interferon-gamma, indoleamine 2,3-dioxygenase, and tryptophan catabolism. *Faseb j*, 1991. 5(11): p. 2516-22.
412. Takikawa, O., et al., Mechanism of interferon-gamma action. Characterization of indoleamine 2,3-dioxygenase in cultured

- human cells induced by interferon-gamma and evaluation of the enzyme-mediated tryptophan degradation in its anticellular activity. *J Biol Chem*, 1988. 263(4): p. 2041-8.
413. Jochems, C., et al., The IDO1 selective inhibitor epacadostat enhances dendritic cell immunogenicity and lytic ability of tumor antigen-specific T cells. *Oncotarget*, 2016. 7(25): p. 37762-37772.
414. Dewi, D.L., et al., Suppression of indoleamine-2,3-dioxygenase 1 expression by promoter hypermethylation in ER-positive breast cancer. *Oncoimmunology*, 2017. 6(2): p. e1274477.
415. Heseler, K., et al., Antimicrobial and immunoregulatory effects mediated by human lung cells: role of IFN-gamma-induced tryptophan degradation. *FEMS Immunol Med Microbiol*, 2008. 52(2): p. 273-81.
416. Ozaki, Y., M.P. Edelstein, and D.S. Duch, Induction of indoleamine 2,3-dioxygenase: a mechanism of the antitumor activity of interferon gamma. *Proc Natl Acad Sci U S A*, 1988. 85(4): p. 1242-6.
417. Chon, S.Y., H.H. Hassanain, and S.L. Gupta, Cooperative role of interferon regulatory factor 1 and p91 (STAT1) response elements in interferon-gamma-inducible expression of human indoleamine 2,3-dioxygenase gene. *J Biol Chem*, 1996. 271(29): p. 17247-52.
418. Richards, T. and E. Brin, Cell based functional assays for IDO1 inhibitor screening and characterization. *Oncotarget*, 2018. 9(56): p. 30814-30820.
419. Boost, K.A., et al., IFN-gamma impairs release of IL-8 by IL-1beta-stimulated A549 lung carcinoma cells. *BMC Cancer*, 2008. 8: p. 265.

420. Regnault, V., et al., Platelet activation induced by human antibodies to interleukin-8. *Blood*, 2003. 101(4): p. 1419-1421.
421. Bester, J. and E. Pretorius, Effects of IL-1 β , IL-6 and IL-8 on erythrocytes, platelets and clot viscoelasticity. *Scientific Reports*, 2016. 6: p. 32188.
422. Kim, K.-B., et al., Potentiation of Fas- and TRAIL-mediated apoptosis by IFN-gamma in A549 lung epithelial cells: enhancement of caspase-8 expression through IFN-response element. *Cytokine*, 2002. 20(6): p. 283-288.
423. Oh, Y.M., et al., The Mechanism of Interferon-gamma Induced Cytotoxicity on the Lung Cancer Cell Line, A549. *Tuberc Respir Dis*, 1996. 43(1): p. 63-68.
424. Padgett, E.L. and S.B. Pruetz, Evaluation of nitrite production by human monocyte-derived macrophages. *Biochem Biophys Res Commun*, 1992. 186(2): p. 775-81.
425. Murray, H.W., et al., Role of tryptophan degradation in respiratory burst-independent antimicrobial activity of gamma interferon-stimulated human macrophages. *Infect Immun*, 1989. 57(3): p. 845-9.
426. Roy, S., et al., Induction of nitric oxide release from the human alveolar epithelial cell line A549: an in vitro correlate of innate immune response to *Mycobacterium tuberculosis*. *Immunology*, 2004. 112(3): p. 471-80.
427. Pechkovsky, D.V., et al., Human alveolar epithelial cells induce nitric oxide synthase-2 expression in alveolar macrophages. *European Respiratory Journal*, 2002. 19(4): p. 672-683.
428. Kwon, S. and S.C. George, Synergistic cytokine-induced nitric oxide production in human alveolar epithelial cells. *Nitric Oxide*, 1999. 3(4): p. 348-57.

429. Luszczki, J.J., et al., 7-Nitroindazole, but not NG-nitro-L-arginine, enhances the anticonvulsant activity of pregabalin in the mouse maximal electroshock-induced seizure model. *Pharmacol Rep*, 2011. 63(1): p. 169-75.
430. Talarek, S., J. Listos, and S. Fidecka, Effect of nitric oxide synthase inhibitors on benzodiazepine withdrawal in mice and rats. *Pharmacol Rep*, 2011. 63(3): p. 680-9.
431. Park, S.K., H.L. Lin, and S. Murphy, Nitric oxide limits transcriptional induction of nitric oxide synthase in CNS glial cells. *Biochem Biophys Res Commun*, 1994. 201(2): p. 762-8.
432. Nachmias, V.T., K. Yoshida, and M.C. Glennon, Lowering pH in blood platelets dissociates myosin phosphorylation from shape change and myosin association with the cytoskeleton. *J Cell Biol*, 1987. 105(4): p. 1761-9.
433. Marumo, M., et al., Extracellular pH affects platelet aggregation associated with modulation of store-operated Ca(2+) entry. *Thromb Res*, 2001. 104(5): p. 353-60.